TIME VARIATION OF COSMIC RAYS

SANTOSH KUMAR
M. Sc., M. Phil.

THESIS SUBMITTED FOR THE PARTIAL FULFILMENT OF THE REQUIREMENTS FOR THE AWARD OF THE DEGREE OF

DOCTOR OF PHILOSOPHY

IN

PHYSICS

OF

THE ALIGARH MUSLIM UNIVERSITY,
ALIGARH-202001
INDIA

1978

Certified that the work presented in this thesis is the original work of Mr. Santosh Kumar, done under my supervision.

(R.S. Yadav)

Department of Physics,
Aligarh Muslim University,
Aligarh (U.P.) - 202 001.
INDIA.

ABSTRACT

The author presents, in this thesis, the results on time variation of cosmic rays derived after having a detailed and systematic analysis of ground based cosmic ray intensity data. The isotropic nature of the galactic cosmic rays is changed by the interplanetary magnetic field when they enter in the solar system. As a consequence of it, significant variations in the cosmic ray intensity are observed with time and space with the ground based instruments. These variations are used as a tool to infer the electromagnetic state of the entire interplanetary medium.

Even though, lot of informations on both long term and short term variations are presently available, the low counting rate and the associated poor statistics have prevented a better understanding, particularly of anisotropic variations of small amplitude (< 1%), e.g., diurnal and semi-diurnal variations. Since International Quiet Sun Year (1964) this lacuna has been overcome to a considerable extent with the availability of a large number of high counting rate super neutron monitors and large area scintillation telescopes.

A ground based monitor looks only into a small region of the sky at any given time, but it scans the entire sky during the course of a day, as the Earth spins on its axis. With a longitudinally well distributed set of high counting rate neutron

monitoring stations, it has now become possible to keep a continuous watch of the interplanetary medium, both in time and space, by studying the observed variations in the cosmic ray intensity at Earth to understand the interplanetary physics. Inspite of the fact that a large number of 'in situ' direct space observations are now available, the ground based cosmic ray observations are still of great importance since the former refers to the conditions only at a particular point in the space, whereas the later are affected by the electromagnetic conditions in the entire interplanetary medium.

Even though a number of high counting rate neutron monitors are in existence in longitudinal zones corresponding to Canada, Europe and U.S.A., there are very few reliable monitoring stations in the Asian zone. Having realised the importance of the high counting rate neutron monitor in the Asian zone, the author took a leading part in setting up the high counting rate neutron monitor at Aligarh (27.7°N, 355°E) which is at the equatorial location with a vertical cutoff rigidity $\sim$ 15 GV. The author was intimately involved in the fabrication and assembly of the neutron monitor pile and its transistorised circuits. The author was also involved in the design and fabrication of the photographic arrangement for recording the cosmic ray intensity data. The author collected the neutron monitor data together with pressure and temperature data for a feasible period at Aligarh.

The author has performed a detailed and systematic study of the characteristics of the diurnal and semi-diurnal anisotropies on different types of days and periods of solar activity using the data from world wide network of neutron and meson monitors for the period 1957-76. It has been observed that the nature of the long term daily variation of cosmic ray intensity, particularly on Q^D, is comparable to the results on yearly average basis where all the days in a year are considered.

The thesis is divided into six chapters. The first chapter briefly reviews the subject of time variation of cosmic ray intensity, in particular, the present understanding of the daily variation. The second chapter deals with the experimental set up of the high counting rate neutron monitor at Aligarh and a brief account of the data recording system. The third chapter gives an account of the analytical methods employed for processing the data from various neutron and meson monitors. In the fourth chapter, the observational results and the detailed characteristics of the diurnal anisotropy on different types of days, e.g. quiet days (QD), magnetic storms days (MSD), disturbed days (DD) and disturbed days without magnetic storms (DDWMS), with a particular emphasis on their association with the available solar and geophysical parameters have been discussed in detail. Also, the earlier observations from both the neutron as well as the meson detectors have been considered with a view to understand the changing behaviour of the interplanetary

medium. The author has satisfactorily proposed a composite model for the explanation of the long term variation of the daily variation and to account for the various changes recently observed in the daily variation of cosmic ray intensity. The detailed characteristics of the semi-diurnal anisotropy of cosmic ray intensity derived from data from a number of monitors and their theoretical interpretations are discussed in the fifth chapter. The results based on neutron and meson monitor observations for the solar flare location effect on daily variation of cosmic ray intensity are presented in the sixth chapter.

The study has revealed that the earlier notion of the time invariance of the diurnal anisotropy is not valid even at the neutron monitor energies. The nature of the diurnal anisotropy, particularly on QD, is also found to be very much different from that reported earlier. The results obtained for the diurnal anisotropy on QD (considering 60 most quiet days in a year) are as much informative as the results obtained on an yearly average basis (considering all the days in a year) for examining the nature of the diurnal anisotropy. Therefore, the present investigation is of relevance with regard to the understanding of the detailed characteristics of the daily variation and its relationship with various solar and geophysical parameters representing the inter-planetary conditions during different phases of solar activity

and has indicated further scope for investigation in this direction.

Some of the important conclusions that have emerged from the present investigation are briefly summarized below

1. the yearly average diurnal anisotropy of cosmic ray intensity on QD has been determined as rigidity independent ($\beta \simeq 0$) with the upper limiting rigidity $R_{max} \simeq 100$ GV, the amplitude ($\simeq 0.4$ % in space) and phase corresponding to azimuthal direction in space are observed practically invariant during the period 1957-70. The small but significant change in the diurnal amplitude on QD during solar minimum period 1964-65 may be understood in terms of the variation of upper cutoff rigidity, beyond which cosmic ray particles do not corotate. Thus, the characteristics of the diurnal anisotropy on QD, during the period 1957-70, are in complete agreement with the predictions of convection-diffusion theory.

2. during 1971-74, the rigidity exponent β has been estimated to be $\simeq -0.4$ for the upper limiting rigidity $\simeq 100$ GV.

3. during 1971-72, a small decrease in the amplitude of the diurnal anisotropy on QD is observed on all the latitudes.

4. again, during 1975-76, the period of minimum solar activity, the decrease in the diurnal amplitude on QD (A_η^Q) is more pronounced. This variation in A_η^Q is not accountable by a reasonable change in the value of rigidity spectrum or R_{max}. Further, the diurnal amplitude on QD is very low during

July - September 1976.

5. the phase of the diurnal anisotropy has been continuously shifting to earlier hours as we go back from 1957 to 1954. Also, in 1954, the year of minimum solar activity (22-years ago than 1976) the diurnal phase is observed in the $\simeq$ 03 hour direction and the diurnal amplitude is observed almost insignificant associated with constantly 'away' interplanetary magnetic field (I.M.F.).

6. again, during the declining phase of the present solar cycle 20, the phase of the diurnal anisotropy on QD has steadily advanced to earlier hours since 1971. The phase shift during 1971 is found to be larger at equatorial stations as compared to other stations.

7. the phase shift to earlier hours is more pronounced in the years 1971, 1973, 1975 and 1976. The phase of the diurnal anisotropy on QD, on monthly average basis, has been observed in the early morning hours ($\simeq$ 03 hour) during July - September 1976, during this period the I.M.F. is almost pointing 'away' leaving aside the mixed polarity days.

8. thus, the variation in the diurnal anisotropy on QD as observed by neutron monitors for the minimum solar activity period 1975-76 is exactly similar to that occurred during the minimum solar activity period 1953-54. Hence, it is quite apparent from these observations that there is 22-year

periodicity in the diurnal anisotropy which is clearly observable particularly on QD, when a systematic and detailed analysis on long term variation of diurnal anisotropy during different types of days has been performed by the author.

9. the phase of the diurnal anisotropy on MSD where the value of A_p-index is higher, is found to shift towards earlier hours in comparison to the phase of the diurnal anisotropy on QD where the value of A_p-index is lower, on all the stations except Ahmedabad and Mt. Norikura for the period from 1965-72, which is normally expected. For the period from 1973-75, this relationship has become completely opposite on all the stations, i.e., the phase of the diurnal anisotropy on MSD where A_p is higher, has shifted towards later hours in comparison to the phase of the diurnal anisotropy on QD where A_p is lower. However, Ahmedabad and Mt. Norikura neutron monitoring equatorial stations have shown this opposite relationship between A_p - β_1 starting from 1971 onwards. Therefore, the relationship between the A_p-index and the diurnal anisotropy is not invariant during the entire period 1965-75.

10. the diurnal anisotropy on QD, when studied on a day-to-day basis, shows variability both in amplitude and in phase and this variability is larger on MSD.

11. the observed variations in the amplitude and phase of the diurnal anisotropy on QD during 1971-76 are not explained by the simple convection-diffusion model due to the probable

significant contribution of the perpendicular diffusion and the density gradient terms. Therefore, the knowledge of their relative contribution is of great importance.

12. from the discussion of the presently available theoretical models it is concluded that Levy's theoretical model suggested to explain the 22-year periodicity in the diurnal anisotropy has been found to be satisfactory for understanding the changing behaviour of the interplanetary medium and to explain the neutron monitor observations on QD for the entire period under consideration.

13. the semi-diurnal amplitude in space on QD (A_2^Q) for cosmic ray intensity in the range 1 - 200 GV is $\simeq 0.08 \pm 0.01\%$ and is invariant during the period 1964-70. But A_2^Q has increased by a factor of 2 in all the stations during 1970-71. A_2^Q also shows a significant increase during 1973-74.

14. the phase of the semi-diurnal anisotropy on QD (ϕ_2^Q) is $\simeq 3.3 \pm 0.5$ hours and remains statistically constant during the entire period 1964-76. Thus, ϕ_2^Q is essentially along a direction perpendicular to the I.M.F. direction.

15. the characteristics of the semi-diurnal anisotropy of cosmic ray intensity on QD in the rigidity range 1 - 200 GV are found to be rigidity dependent with the spectral exponent $\simeq + 0.6$

The semi-diurnal anisotropy on QD depends on R with $R^{+1.4}$

upto 60 GV above which the value of the exponent decreases.

16. inspite of a slight random variation, an increasing trend of the semi-diurnal amplitude is observable on MSD in comparison to that observed on QD during 1964-70.

The semi-diurnal amplitude on MSD during 1970-71 has decreased and during 1972-73 it has increased at most of the neutron monitoring stations.

17. the phase of the semi-diurnal anisotropy on MSD shows no definite trend for the entire period 1964-76.

18. the systematic behaviour as observed on QD is neither observed for the diurnal anisotropy nor for semi-diurnal anisotropy on DD and DDWMS during the entire period 1964-76.

19. the amplitude of the diurnal anisotropy for western limb solar flare days is larger than the eastern limb solar flare days, during 1957-58 (period of maximum solar activity). This relationship between the amplitude of the diurnal anisotropy for western limb and for eastern limb solar flare days is opposite during 1973 (period of declining solar activity).

20. the phase of the diurnal anisotropy for western as well as eastern limb solar flare days shows a shift towards earlier hours by about three hours in comparison to the phase of the diurnal anisotropy on QD during 1957-58. Whereas, during 1973, the phase of the diurnal anisotropy for western as well as eastern limb solar flare days remains almost in the same

direction as it is observed on QD.

In future, it may be possible through more refined cosmic ray observations to obtain the upper limiting rigidity beyond which the diurnal modulation ceases. The lower limiting rigidity is also undetermined. Therefore, it is necessary to extend the range of the observations of the cosmic ray daily variation both by using the space-craft data as well as the data from under ground monitors for understanding the present behaviour of the diurnal anisotropy and establishing the validity of the proposed model. The future emphasis may also be given in determining the local time dependence of the 'asymptotic direction of viewing' and the cutoff rigidity of a particular station, and their influence on the daily variation of cosmic rays. The recent observations of the shift in the diurnal phase on QD during 1971 and onwards to earlier hours are still unexplained.

In contrast to above, very little is understood about the day-to-day changes in the diurnal and semi-diurnal anisotropy. Therefore, investigations of these day-to-day changes in relation to varying solar-interplanetary and geophysical parameters need a further study in detail.

Santosh Kumar.

(Santosh Kumar)

17. 10. 78.

LIST OF PUBLICATIONS

1. Instrumentation for continuous monitoring of low energy cosmic ray intensity -

   S. Kumar, R. Prasad, R.S. Yadav, T.H. Naqvi and Rais Ahmed.

   J. of the Inst. of Elec. and Telecom. Engrs., 1975, Vol. 21, No. 12, p. 653.

2. The study of the diurnal variation of cosmic ray intensity during the magnetically quiet and disturbed days and days of magnetic storms -

   Santosh Kumar and R.S. Yadav.

   Abstract published in the proceedings of the symposium on 'Earth's Near Space Environment', held at N.P.L., New Delhi, 1975, No. 10.18, p. 304.

3. Modulation of cosmic rays -

   Santosh Kumar

   M.Phil. Dissertation (Unpub.), A.M.U., Aligarh, 1975.

4. Spectral characteristics of the diurnal anisotropy during different types of days -

   Santosh Kumar and R.S. Yadav,

   Abstract published in the proceedings of the 'Space Sciences Symposium-1977', held at Vikram Sarabhai Space Centre, Trivandrum, 1977, p. 260.

5. Solar flare location effect on the spectral characteristics of the diurnal anisotropy of cosmic ray intensity-I -

   R.S. Yadava, Santosh Kumar and T.H. Naqvi.

Abstract published in the proceedings of the 'Space Sciences Symposium-1977', held at Vikram Sarabhai Space Centre, Trivandrum, 1977, p. 347.

6. Solar flare location effect on the spectral characteristics of the diurnal anisotropy of cosmic ray intensity-II -

R.S. Yadava, Santosh Kumar and T.H. Naqvi.

Published in the proceedings of the Forty Sixth Annual Session of the National Academy of Sciences, India, held at Delhi University, Delhi, 1977, Vol. 47A, Part II, p.87.

7. Daily variation of cosmic ray intensity -

Santosh Kumar and R.S. Yadava.

Published in the proceedings of the Forty Sixth Annual Session of the National Academy of Sciences, India, held at Delhi University, Delhi, 1977, Vol. 47A, Part IV, p.235.

8. The study of the diurnal anisotropy of cosmic ray intensity during solar flare days-I -

R.S. Yadava, Santosh Kumar, Badruddin, D.S. Rana and T.H. Naqvi.

Abstract published in the proceedings of the 'Space Sciences Symposium-1978', held at Andhra University, Waltair, 1978, No. 2.6.6, p. 18.

9. Variation of the semi-diurnal anisotropy of cosmic ray intensity during solar flare days -

Santosh Kumar, R.S. Yadava and Badruddin.

Published in the proceedings of the Forty Seventh Annual Session of the National Academy of Sciences, India, held at Bhopal University, 1978, No. 53/110, p. 17/38.

A C K N O W L E D G E M E N T S

I acknowledge with deep gratitude my indebtedness to Dr. R.S. Yadav, my supervisor, for his inspiring guidance, constant encouragement and generous support throughout the course of the present investigation. I am grateful to him for many valuable suggestions and exceedingly helpful discussions during the critical checking of the thesis. I am extremely grateful to Prof. M.Z. Rahman Khan, Head, Department of Physics, A.M.U., Aligarh for extending to me the valuable research facilities in the Department. At this moment, when I am submitting my Ph.D. Thesis, I remember Prof. Rais Ahmed whose kind permission could make it possible for me to join the research group in the Department, I am highly obliged to him.

The author gratefully acknowledges the fruitful discussions and the encouraging interest taken by Profs. M.S. Swami and T.H. Naqvi. I feel deeply indebted to Prof. S.P. Agrawal, Vikram Space Physics Centre, A.P.S.U., Rewa; for his inspiring and stimulating discussions. The author expresses his sincere thanks to Drs. G. Subramanian and A.G. Ananth, P.R.L., Ahmedabad for many valuable suggestions and to Dr. R.L. Singh, Govt. Science College, Rewa for promptly supplying some of the informations.

The author expresses his indebtedness to the World Data Centres and to all the investigators who have supplied the data and in particular, to Prof. R.P. Kane, P.R.L., Ahmedabad;

Prof. A.P. Mitra, N.P.L., New Delhi and Prof. V. Rampu, I.I.A., Kodaikanal for providing the solar geophysical data etc.

The author is very much thankful to Prof. Aslam Qadeer, Director, Computer Center, A.M.U., Aligarh; for making the computer facilities available to us and to Sri D.C. Tomar for his help in the preparation of various computer programmes.

The author expresses his sincere appreciation to his colleagues who have helped him in all matters big or small and much more by their encouraging friendship. Amongst these mention should be made of Messrs Badruddin and R.C. Verma for their enthusiastic help extended to him.

Mr. Nasim Ahmad receives the special thanks for the painstaking and excellent job of typing the thesis.

The financial support received from D.A.E., Govt. of India, and U.G.C., New Delhi, are gratefully acknowledged.

Finally, I am deeply indebted to my parents for their moral support and encouragement.

Santosh Kumar.

(Santosh Kumar)

17.10.78.

CONTENTS

CHAPTER - I

INTRODUCTION

1.1 General survey of cosmic rays

Since the discovery of cosmic rays in 1912 by Victor F. Hess, the cosmic ray research has offered the number of problems for investigation in Astrophysics, Solar-physics, Geophysics, High-energy physics and Elementary particle physics. At present, we have the cosmic ray observations from a number of ground based monitors well distributed in longitude and latitude and the large amount of 'in situ' space-craft observations of the interplanetary plasma and magnetic field parameters. This provides the research workers an opportunity to develop physical understanding of the Earth's near environmental and the electromagnetic processes which operate in the interplanetary medium.

It is observed that during solar flares, Sun locally produces a large number of cosmic ray particles, normally with energies $\lesssim$ 100 MeV, but sometimes extending even to energies $\gtrsim$ 1 GeV, producing a detectable enhancement in the counting rate registered by the ground based detectors (Pomerantz and Petnis, 1960; Pomerantz et al., 1960). In fact, the first inference on the Archimedean spiral nature of the interplanetary magnetic field was actually obtained from

these indirect ground based observations of solar flare increases (McCracken, 1962). Direct 'in situ' measurements carried out onboard Pioneers and IMP space-crafts (Ness et al., 1964; McCracken and Ness, 1966) have confirmed the spiral nature of the interplanetary magnetic field and associated small scale irregularities.

The solar magnetic field is known to extend over very large regions in space ($\sim$100 AU) and has high energy density ($\gtrsim$ 10 times) compared to galactic magnetic field. Consequently, the propagation of the cosmic radiation in the interplanetary space is very much affected by the characteristics of the magnetic field in the solar system. Therefore, the galactic cosmic radiation which is largely isotropic outside the solar system shows time variations ranging in periodicities from a few minutes (Dhanju and Sarabhai, 1967) to eleven year.

A number of space-crafts are continuously monitoring the behaviour of particles and fields in the interplanetary space, the observations are mainly limited to low energies ($\lesssim$ 100 MeV) and are also confined to near Earth region. Therefore, the ground based detectors are essential to provide a continuous index of cosmic radiation for investigating the variation of high energy galactic cosmic ray particles ($\gtrsim$ 1 GeV). Such a study provides the information on the long term basis of the electromagnetic conditions of the interplanetary space and also

'inaccessible' regions at large distances away from the orbit of the Earth. Thus the study of the modulation of cosmic rays is essentially a complementary study to the 'in situ' measurements for providing a complete understanding of the interplanetary processes. The various aspects of modulation of cosmic rays have been recently reviewed in a very comprehensive manner by Lockwood (1971), Pomerantz and Duggal (1971, 1974) and Rao (1972).

1.11 Atmospheric effects on primary cosmic rays

The primary cosmic rays consist of protons (83 - 89 %), α-particles (10 - 15 %) and heavy nuclei (1 - 2 %) (Singer, 1958). Isotopes of different nuclei in cosmic rays have also been observed. Although, there is no definite evidence about the presence of anti-nuclei among primary cosmic rays but an upper limit on their fluxes has been placed at 0.1 to 1.0 % of the proton flux. Proportion of electrons and γ-rays is about 1 % and they mainly constitute the low energy part of cosmic ray flux. Neutrinos are also expected to be present in primary cosmic rays but their proportion is uncertain and their detection is rather difficult. Upto iron the composition is well established. The evidence for the existence of nuclei upto about uranium is reported in literature by various authors (Blanford et al., 1973). As far as, modulation of cosmic rays is concerned nuclei with $Z \geq 5$ are unimportant.

The property of cosmic rays that sets them apart from all other kinds of radiations is the very large individual energies of cosmic ray particles. The energy of the primary cosmic ray particles vary from a few hundred MeV to about 10^{20} eV (Suga et al., 1971; Ryan et al., 1972) and possibly higher. However, in any case particles of energies greater than 10^{21} eV are not expected in the primary cosmic rays as they undergo severe energy losses through Bremsstrahlung process.

Such a primary cosmic ray nuclei, when traverse the Earth's atmosphere, collide at or near the top of the Earth's atmosphere with air nuclei (N, O or O) and produce secondary cosmic rays, depending on the energy of the incident particle, by nuclear disintegration, as shown in Figure-1.1 (Simpson et al., 1953). The behaviour of the primary cosmic rays is reflected into the secondary cosmic rays which are being studied later on by the ground based detectors. Practically all the study of the modulation of cosmic rays has been conducted from ground based observations using neutron and meson monitors. It must be remembered that all these monitors respond to a wide range of energies. At ground these monitors respond from an energy of $\sim$1.3 GeV (Limited by the atmosphere) to a few hundred GeV.

It is very essential to have a clear understanding of the cumulative effect of Earth's atmosphere and the geomagnetic field

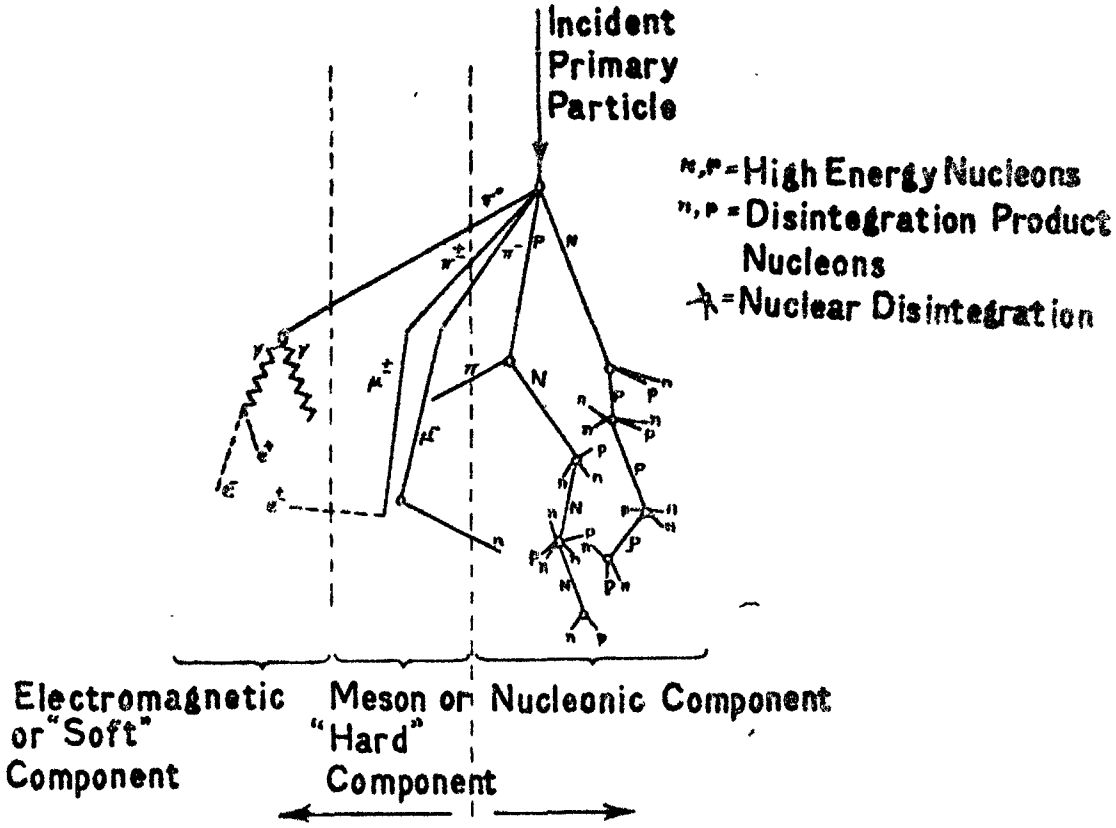

Fig. 1.1 - Schematic representation of a nuclear cascade in the atmosphere (after Simpson et al., 1953).

on the incident primary particles, before interpreting the ground based cosmic ray observations in terms of primary cosmic ray variations in the interplanetary medium. Essentially there are two important effects; the first being the generic relationship between the primaries and the secondary they produce through their interactions in the Earth's atmosphere, the second relates to the motion of the primary particles in the geomagnetic field. A number of theoretical attempts (Dorman, 1957; Wainio et al., 1968; De Brunner and Flueckiger, 1971) have been made to relate the secondary cosmic ray production to the primary intensity at the top of the atmosphere. However, it is observed that deriving a multiplicity or specific yield function from observed latitude effects is found very useful in interpreting the secondary cosmic ray variations in terms of the primary cosmic ray variations at the top of the atmosphere. Dorman (1957) has expressed 'coupling constant' or 'the differential response function' to estimate the contribution of a primary particle of energy E to the secondary component of type i at a atmospheric depth h as follows

$$W_\lambda^i (E, h) = \frac{m^i(E, h)\, D(E)}{I_\lambda(h)} \qquad \ldots 1.1$$

where $m^i(E, h)$ is the multiplicity function, D(E) is the primary differential energy spectrum which is expressed as $AE^{-\gamma}$ where A is a constant and $\gamma \approx 2.6$ and $I_\lambda^i(h)$ is the observed intensity of the secondary component i at latitude γ and at atmospheric depth h.

Thus, a number of authors (Neher, 1952; Treiman, 1952; Dorman, 1957; Webber and Quenby, 1959; Lockwood and Webber, 1967) have obtained the appropriate multiplicity function applicable to the studies of modulation of cosmic rays. Following Dorman (1974), the modulation of cosmic rays observed at any ground based detector may be expressed as follows

$$\frac{\delta I_\lambda^i(h)}{I_\lambda^i(h)} = - \delta E_\lambda^0 \, W_\lambda^i(E_\lambda^0, h) + \int_{E^0}^{\infty} \frac{\delta m^i(E, h)}{m^i(E, h)} W_\lambda^i(E, h) \, dE +$$

$$\int_{E^0}^{\infty} \frac{\delta D(E)}{D(E)} W_\lambda^i(E, h) \, dE \qquad \ldots 1.2$$

where E_λ^0 is the cutoff energy at latitude λ.

The first term on the right hand side of Equation-1.2, represents the variation due to the changes in the cutoff energy, which is usually very small except for days associated with magnetic storms and only recently it has become possible to detect this in the presence of the larger variations of different origin. The second term is due to the changes in the terrestrial atmospheric parameters (meteorological effects) such as pressure and temperature. The third term includes the variation due to changes in the primary energy spectrum, which may be due to acceleration or retardation of cosmic electromagnetic fields, additional generating processes, scattering of particles, changes of the spectrum with changing direction of incidence in connection with a possible anisotropy of the

flux of cosmic rays in space. However, the Equation-1.2 does not include the effects of the asymmetric magnetosphere, which may be significant in the studies of the daily variation at energies $\lesssim$ 1 GeV, though negligible at higher energies.

The geomagnetic field acts as a spectrum analyser to the incoming particles at any location 'λ'. Thus, only those particles whose energy exceeds the minimum or cutoff energy (E^{o}_{λ}) are allowed to reach the detector. The latitude effect observed in the cosmic ray intensity indicates that the cut-off energy is maximum at the equator and minimum at the pole. The trajectory of the particles, even at energies much higher than E^{o}_{λ}, is strongly influenced by geomagnetic field. Though there are extensive calculations on cosmic ray particle trajectories in the geomagnetic field are available (Bland, 1962; Hedgecock, 1965), the concept of 'Asymptotic cone of acceptance' developed by Rao et al. (1963) is found extremely useful for deriving particle trajectories prior to their entry into the geomagnetic field. They have demonstrated, by tracing the actual trajectories of the particles in the geomagnetic field, that even though, any given neutron monitor has a large opening angle at the ground, it essentially scans only a very narrow region in the celestial sky. The 'Asymptotic cone of acceptance' of a detector is defined

as the cone in the celestial sphere which includes all those asymptotic directions which makes a significant contribution to the counting rate of a detector. As the Earth spins on its axis, the asymptotic cone of acceptance of the detector corotates with the Earth, thus scanning a narrow belt in the celestial sky in a period of one day.

1.2 Interplanetary medium

The magnetic irregularities which act as effective scatterers are carried away from the Sun by radially moving solar plasma with supersonic velocities 300 to 1000 kms/sec. Therefore, to interpret theoretically the modulation of galactic cosmic ray intensity, it is very essential to have a clear understanding of both the continuously blowing solar wind and the motion of the cosmic ray particles in the disordered interplanetary magnetic field (I.M.F.).

1.21 Solar wind

The emission of particles (solar plasma) by the Sun was inferred long ago to explain the geomagnetic disturbance and Auroras. The first evidence for a constant emission of the corpuscular radiation from the Sun was pointed out by Biermann (1951, 1957) in his explanation of the tails of the comets pointing away from the Sun. Later, Chapman gave the idea that the heating of the upper atmosphere is caused by the

extension of the solar corona. Working on this, Parker (1958a) formulated theory of continuous hydrodynamical expansion of the solar corona and showed that the inner corona with observed temperatures of $\sim 10^6$ °K is too hot to be held static by the Sun's gravitational field. Thus, in the steady state the corona must expand continuously and this results in the formation of the solar wind. The gross properties of the radially blowing solar wind, predicted by the theory have been verified since then by a number of direct space-craft observations e.g.; Luna, Vela, Mariner, Explorer and Pioneer space-crafts. A number of comprehensive reviews dealing with experimental and theoretical models of solar wind are available in literature (Dessler, 1967; Lust, 1967; Hess, 1967; Axford, 1968; Hundhausen, 1968, 1970, 1972; Parker, 1969; Burlaga, 1971).

Some of the average properties of the solar wind plasma and their variability at the orbit of the Earth (1AU) are summarised in the Table-1.1 which indicates that the solar wind plasma on an average is characterized by a velocity $\sim$ 400 km/sec and density $\sim$ 8 particles per cm^3 and is in good agreement with the theoretical predictions. A large variability in the solar wind parameters such as velocity, density and temperature (Snyder et al., 1963) has been well established from a large number of space-craft observations.

The flux due to solar wind is not constant but varies from day-to-day. On a long term basis contrary to the theoretical

TABLE - 1.1

The observed average solar wind plasma parameters and its variability at the orbit of the Earth (1AU).

Solar wind plasma parameters	Average Characteristics	Variability
Velocity	400 km/sec	200 - 1000 km/sec
Flow direction	1.6^{0} of the Sun-Earth line	8^{0} E to 8^{0} W of the Sun-Earth line
Proton and Electron density	8 particles/cm^{3}	1 - 50 particles/cm^{3}
Proton temperature	4×10^{4} ^{0}K	3×10^{4} to 5×10^{5} ^{0}K
Electron temperature	1.5×10^{5} ^{0}K	1 to 2×10^{5} ^{0}K
Ratio of Helium to Hydrogen (n_{α}/n_{p})	0.05	0.01 to 0.20
Magnetic field	5 γ	0.25 to 40 γ

predictions, earlier it was reported that the solar wind speed has remained practically invariant over the current solar cycle since 1964 (Gosling et al., 1971; Mathews et al., 1971; Hedgecock et al., 1972). Also the frequency of occurrence and amount of energy in streams has not changed much since 1965 (Montgomery, 1975). However, very recently on the basis of the observations of the solar wind by Pioneer and Vela spacecrafts, Intriligator (1974, 1975) found that frequency of high speed streams and their duration vary over the solar cycle. There are more days associated with high speed streams during solar maximum than solar minimum and the yearly average of the solar wind speed varies over the solar cycle and is highest at solar maximum. There is no correlation between the solar wind velocity and the solar activity, measured in terms of the sunspot number or the intensity of the 10.7 radiation from the Sun. But there is found to be a very strong correlation between solar wind velocity and K_p index, the index of geomagnetic field disturbance, by many investigators (Snyder et al., 1963).

$$V(\text{km/sec}) = 8.44 \Sigma K_p + 330 \qquad \ldots 1.3$$

The pronounced 27-day recurrence tendency both in high ΣK_p and enhanced solar wind velocity has also been noted, which are probably related to M-region storms.

The solar wind flow though largely radial, occasionally shows a significant component ($\pm 5^{0}$) perpendicular to the ecliptic plane (Wolfe et al., 1966; Strong et al., 1967). For a clear understanding of the observed properties of the solar wind, Burlaga and Ness (1968) and Burlaga (1971) introduced an idea of scale length (time). They have pointed out, as shown in Figure-1.2, that the Macro and Meso-scale properties ($f \sim 3 \times 10^{-4}$ to 3×10^{-8} sec^{-1}) of the solar wind are important to the study of high energy cosmic rays ($\geq$ 2 GeV) in a field of $\sim 5\gamma$, whereas only Micro-scale properties (3×10^{-2} to 3×10^{-4} sec^{-1}) are most relevant to the study of low energy cosmic rays ($\leq$ 1 GeV). The microstructure corresponds to shock waves and the contact discontinuities and act as scattering centres for cosmic rays. The mesostructure corresponding to filaments or kinks in the field structure, the origin of this scale of structure may be in the solar supergranmulations are known as 'flux tubes' which are responsible for channeling of cosmic rays. The macrostructure manifests itself as a longitudinal variation in the magnetic fields in the form of sector structure, the boundaries of which are sharp ($< 10^{5}$ km) and stable in time. However, changes do occur in magnetic field magnitude, solar wind velocity, K_p index and electron density (N_e) in the individual sectors.

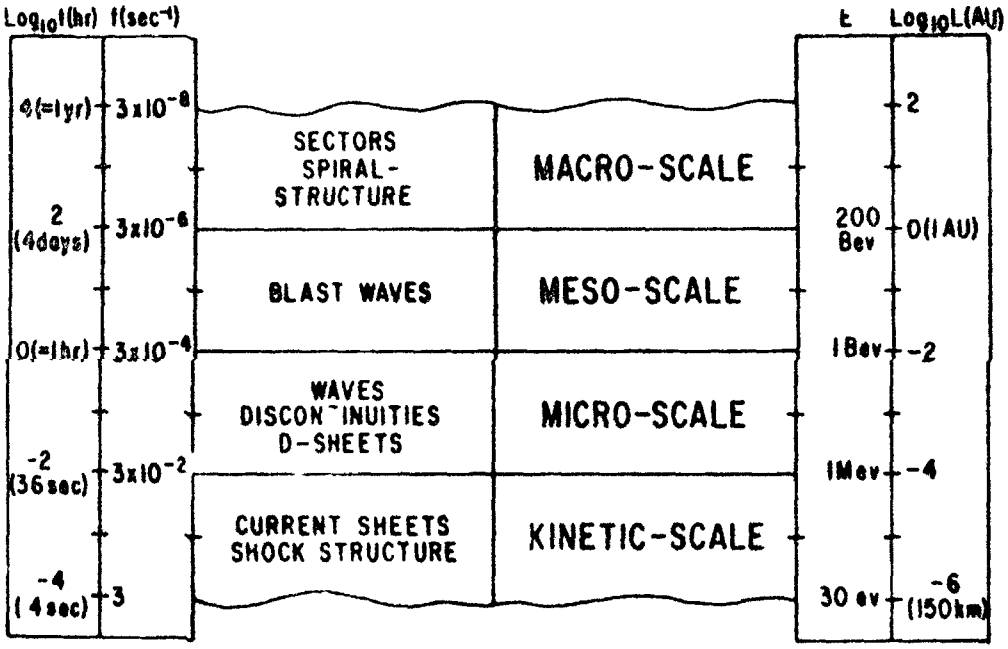

Fig. 1.2 - Defines the scales in terms of characteristic times, frequencies and lengths. Some characteristic features seen on the different scales are shown. E is the energy of a proton whose gyro radius is the scale length in a 5γ field (after Burlaga, 1971).

1.22 Interplanetary magnetic field (I.M.F.)

Parker (1958b) showed that the conductivity of the matter in the corona is very high and the heat flow is proportional to T^4, where $T(^0K)$ is the temperature of the corona. From this mode he showed that the solar wind plasma freely expands continuously in the interplanetary space. Due to high conductivity, the I.M.F. lines are frozen into the solar wind plasma and they are constrained to move alongwith the moving plasma (Alfven, 1950), and therefore they are stretched out in the form of an Archimedes spiral by the supersonic solar wind, as the Sun rotates (Parker, 1958a; Ahluwalia and Dessler, 1962). The angle θ between the normal to the spiral field line and the Sun-Earth line, as shown in Figure-1.3, is given by the relation

$$\theta = \tan^{-1} \left(\frac{V_s}{\omega r}\right) \qquad \ldots 1.4$$

where V_s is the average velocity of the solar wind, ω is the angular velocity of rotation of the Sun and r is the heliocentric distance from the Sun (i.e., the Sun-Earth distance). The angle ψ (i.e., $\pi/2 - \theta$) is normally referred to as the 'garden-hose angle'. At the orbit of the Earth, r = 1AU = 1.5×10^8 km, taking Ω = 1 rev/27 days = 2.7×10^{-6} rad/sec, and V = 400 km/sec; we have $\psi \approx 45^0$.

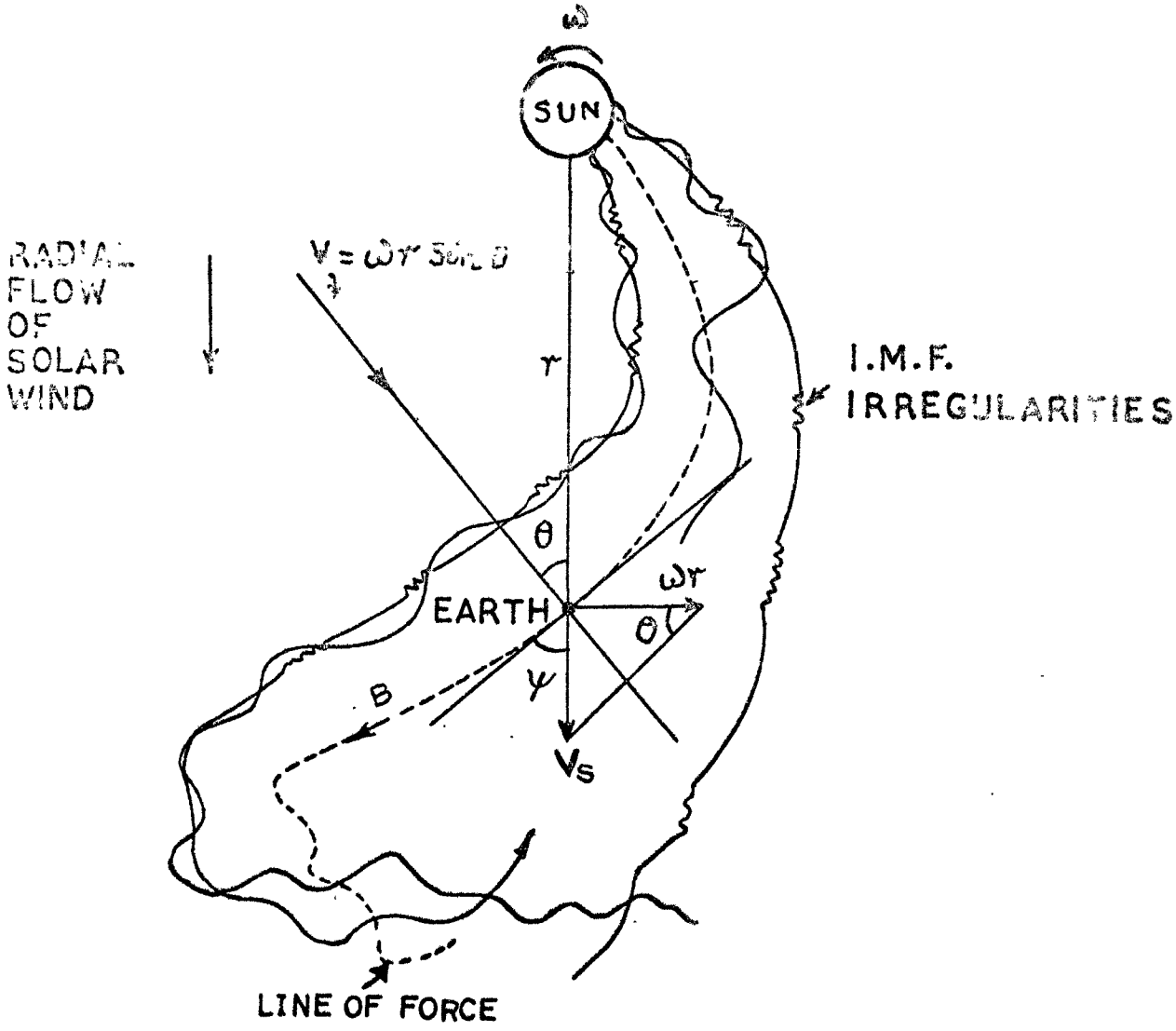

Fig. 1.3 - Interplanetary magnetic field configuration.

From the solar flare observations, McCracken (1962) for the first time confirmed experimentally the spiral structure of the I.M.F. The recent measurements of the I.M.F. from a number of space-crafts e.g., Pioneer-10 and Pioneer-11 have now conclusively proved that even at a distance as large as $\simeq$ 4AU (at the orbit of the Jupiter), where the garden-hose angle changes from 45° to 67°, the large scale structure of the field is in a very good agreement with the predicted Archimedean spiral configuration and is distributed in the form of a well defined sector structure with I.M.F. being alternatively positive (away from the Sun) and negative (towards the Sun). This sector pattern, which corotates with the Sun, is found to exist throughout the solar cycle (Wilcox and Ness, 1965; Wilcox and Colburn, 1972). The existence of sector structure in the I.M.F., even during the period of maximum solar activity, has been well established (Coleman et al., 1966; Wilcox and Colburn, 1969, 1970). During 1963-64, the Archimedes spiral structure showed a four sector structure having unidirectional field, alternatively away or towards the Sun. However, in the later course number of sectors have not always remained four and the spiral structure with alternate sectors having opposite polarities has also been observed (Wilcox and Colburn, 1972; Fairfield and Ness, 1974) also a semi-annual and solar cycle variation of the sector structure is reported by Sawyer (1974).

When the I.M.F. structure is studied with time scales of $\sim$ 1 day or less than one day (i.e., microstructure), it is found that the properties of the field show considerable departure from the average spiral structure of the field due to presence of a continuous distribution of small scale irregularities or kinks which are essentially frozen into the solar wind and hence corotate with it. The origin of these irregularities of different scale size has been attributed to the motion of prominent photospheric features such as granulations ($\sim 10^3$ km diameter) and super-granulations (2 X 10^4 km diameter) on the photosphere (Michel, 1967; Parker, 1969). In addition the turbulent motion of the solar plasma makes the field line stochastic (executing a random motion) even if they were symmetrical to start with. An important contribution of the random-walk is to increase the value of perpendicular diffusion ($K_\perp$) in contrast to the much smaller effect that is expected from the usual resonant scattering by small scale irregularities.

Recently, it has been suggested that low energy coronal transient events occur more frequently than solar flares and eject material and magnetic fields in the form of closed bubbles (blobs) into interplanetary space (Barouch and Burlaga, 1975). These blobs are the large scale scattering centres for cosmic ray particles. The frequency of occurrence of these blobs being more than the frequency of interplanetary shocks and Forbush

decreases, and maximum at solar activity maximum thereby decreasing the interplanetary diffusion coefficient which is an important parameter responsible for the propagation of cosmic rays inside the solar system.

1.3 Modulation of galactic cosmic rays

The extra-terrestrial nature of the cosmic radiation was discovered from the manned balloon flights using ionisation chambers. This discovery started the search for the influence of the Sun on the modulation of its intensity as observed by the ground based instrumentation. Even though, the continuous and systematic registration of the cosmic ray flux started as early as 1936 with the establishment of a network of ionisation chambers by the Carnegie Institute of Washington, the detailed investigations of the interplanetary space from the study of modulation of cosmic rays, became possible only after the establishment of a world-wide network of neutron and meson monitors during International Geophysical Year (IGY) period (1957-58). The encouraging results obtained from the analysis of the data collected during IGY period and earlier, finally led to the establishment of very high counting rate super neutron monitors and large area scintillation telescopes (meson monitors) during International Quiet Sun Year (IQSY) period (1964). The data now obtained from these high counting rate monitors have sufficient statistical accuracy, so as to

permit the study of the short term variations such as diurnal and semi-diurnal variation even on a day-to-day basis. The observed modulation of cosmic ray intensity at ground based monitors may be classified as follows

A. Modulation by solar plasma, which may be broadly divided into two classes: (a) isotropic time variations; (b) anisotropic (spatial) variations.

(a) Isotropic time variations are

(i) 11-year modulation (or variation)

(ii) 27-day modulation (or variation)

(iii) Forbush decrease

(iv) Increase before Forbush decrease

(b) Anisotropic (spatial) variations such as solar daily variation -diurnal, semi-diurnal and tri-diurnal variation.

B. Generation of free particles on the Sun

(i) Large increases of intensity related with powerful solar flares

(ii) Small increases of intensity connected with small solar flares

C. Anisotropy within galactic cosmic rays

(i) Sidereal variation of high energy particles

(ii) 22-year variation of the diurnal variation which is

anomalous behaviour of the solar daily variation at minimum solar activity.

To explain these experimentally observed modulations of cosmic ray intensity, various theoretical models have been proposed, the radial density gradient, the anisotropies and their interconnection, in terms of either the electric fields in the interplanetary space or the I.M.F. structure, including solar wind. There are mainly two groups of all the models and processes that have been advanced to explain the modulation of galactic cosmic rays, e.g., (1) Electric field model and (2) Convection-diffusion model. However, since the convection-diffusion theory incorporating the energy loss term, leads to the most satisfactory explanation of the observed long term modulation, the radial density gradient and anisotropies (Gleeson, 1971). In the following sections we have briefly discussed this model and its predictions for the radial density gradient.

1.31 Convection-diffusion model (isotropic diffusion)

The establishment of a positive radial density gradient of cosmic rays in the solar system due to solar wind implies the presence of an outward convection (UV) and an inward diffusion ($-K\frac{\partial U}{\partial r}$) which in the steady state condition must balance each other (Parker, 1958a, 1963). Therefore, we may write

$$UV = -K\frac{\delta U}{\delta r} \qquad \ldots 1.5$$

which for a spherical symmetric system yields

$$U(r, E) = U_{\infty}(E) \exp\left(-\int_{r}^{D} \frac{V}{K}\, dr\right) \qquad \ldots 1.6$$

where $U(r, E)$ and $U_{\infty}(E)$ are the flux of particles of kinetic energy E at a distance r from the Sun and at an outer boundary $r = D$ respectively and K is the isotropic diffusion coefficient which is an important term related to the power spectra of the I.M.F. The simple convection-diffusion theory has been modified by a number of workers (Gleeson and Axford, 1967; Jokipii and Parker, 1967, 1970), taking into account

(a) Adiabatic energy changes due to non-zero divergence of solar wind velocity (Parker, 1965; Gleeson and Axford, 1967)

(b) Anisotropic diffusion due to average (non-fluctuating) interplanetary magnetic field (Parker, 1965; Axford, 1965a) and

(c) The relationship between diffusion tensor and the magnetic field power spectrum (Jokipii, 1966, 1967; Roelof, 1968).

The differential number density $U(r, E, t)$ and differential current density $S(r, E, t)$ in an isotropic velocity distribution at kinetic energy E and heliocentric distance r from the Sun, is given by the equation of transport and streaming (Parker,

1965; Gleeson and Axford, 1967; Fisk and Axford, 1969, 1970; Gleeson, 1973) as follows

$$\frac{\partial U}{\partial t} + \frac{1}{r^2}\frac{\partial}{\partial r}(r^2 UV - r^2 K \frac{\partial U}{\partial r}) - \frac{1}{3r^2}\frac{\partial}{\partial r}(r^2 V)\frac{\partial}{\partial E}(\alpha E U) = 0 \qquad \ldots 1.7$$

$$S(r, E, t) = CUV - K\frac{\partial U}{\partial r} \qquad \ldots 1.8$$

where the Compton-Getting factor C, that was originally derived to transform the differential streaming of cosmic rays between frames of reference moving relative to each other at constant velocity (Compton and Getting, 1935), is given by

$$C(r, E, t) = 1 - \frac{1}{3U}\frac{\partial}{\partial E}(\alpha E U) \qquad \ldots 1.9$$

and $$\alpha(E) = \frac{E + 2E_o}{E + E_o} \qquad \ldots 1.10$$

where V(r, t) is the solar wind speed, K(r, E, t) is the diffusion coefficient, E is the kinetic energy of the particle with rest mass E_o and r is the heliocentric radial distance.

The Equation-1.7 may be solved for U by specifying the galactic spectrum and the diffusion coefficient within the cavity. The result for U is substituted in Equation-1.8 for determining the flow or anisotropy of the particles. Though there is no exact general analytical solution of the Equation-1.7

various approximate numerical solutions have been obtained and are used very extensively to explore the physics of the modulation of cosmic rays. Among them the force field approximation is most successful at high energies (> 200 MeV/nucleon) (Gleeson and Axford, 1968a; Gleeson and Urch, 1973) in which instead of using Equation-1.7, one can drop the term S in Equation-1.8 since at sufficiently high energies the streaming S is small and may be approximated to zero so that a simpler streaming equation becomes

$$CUV - K \frac{\partial U}{\partial r} = 0 \qquad \ldots 1.11$$

The diffusion coefficient (K) is assumed to be a separable function of distance (r) and rigidity (R) and is of the form

$$K = K_1(r, t)\, K_2(R, t)\, \beta \qquad \ldots 1.12$$

where $\beta = \frac{V}{c}$ and v is the particle velocity. To obtain the force field solution (Gleeson and Axford, 1968b), the Equation-1.11 is integrated. At kinetic energies $\gtrsim$ 2 GeV/nucleon the spectral slop of the intensity of cosmic rays is fairly constant (C = 1.5) so that Equation-1.11 with C = 1.5, yields the modified convection-diffusion equation.

From Equation-1.11, the radial density gradient of the cosmic rays is given by

$$G = \frac{1}{U} \frac{\partial U}{\partial r} = \frac{V}{K} C(r, E) \qquad \ldots 1.13$$

For $K = 9.3 \times 10^{21}$ cm^2 sec^{-1} at 5 GeV, it works out to be $\approx +9$ %/AU which is quite comparable with the experimental observations (O'Gallagher, 1967).

The radial anisotropy ξ is given as (Fisk and Axford, 1970)

$$\xi = -\gamma a \left(\frac{V}{2v}\right) \left(\frac{r}{U} \frac{\partial U}{\partial r}\right) \qquad \ldots 1.14$$

for the cosmic ray spectrum of the type T^{γ}. The radial anisotropy at high energies ($\gtrsim 2$ GeV) is $\lesssim 0.02$ % and is consistent with the observations (McCracken and Rao, 1965).

1.32 Convection-diffusion model (anisotropic diffusion)

Axford (1965b) showed that the diffusion of cosmic rays into the solar system is in general, highly anisotropic with $K_{\parallel} > K_{\perp}$, where $K_{\parallel}$ and $K_{\perp}$ are the diffusion coefficients parallel and perpendicular to field lines. For an idealised spiral I.M.F., the cosmic ray density U at a radial distance r and colatitude θ is given by (Parker, 1965)

$$U(r, \theta) = U_{\infty} \exp\left\{-\frac{V(D - r)}{K_{\parallel}}\left[1 + \frac{1}{3}\left(\frac{\Omega \sin\theta}{V}\right)^2 (D^2 + Dr + r^2)\right]\right\} \qquad \ldots 1.15$$

where Ω is the angular velocity of the Sun. Since the term in the square bracket of Equation-1.15 is greater than 1, the density reduction will be larger than that expected for the case of the isotropic diffusion. The radial gradient for the

anisotropic diffusion at the orbit of the Earth ($\Omega r = V$, $\theta = 90^{0}$) is approximately given by

$$G = \frac{1}{U}\frac{\partial U}{\partial r} \approx \frac{2V}{K_{\parallel}} \qquad \ldots 1.16$$

Both the Equations-1.16 and 1.15 show that the cosmic ray particle density at a distance r from the Sun would increase with increase in diffusion coefficient K and with decrease in solar wind velocity V and depth of modulating boundary D.

1.33 <u>The 11-year and long term solar modulation of cosmic rays</u>

Observations over several decades have revealed that the cosmic ray flux is modulated by the 11-year solar cycle of sunspot activity, reaching a maximum during the quiet period of the solar cycle and a minimum near the peak of solar activity; thus establishing an inverse relationship between the solar activity and the galactic cosmic ray intensity (Forbush, 1954; Pomerantz et al., 1958a,b). During the active period of the solar cycle, more solar events pull more of the solar magnetic field into the interplanetary space to prevent the galactic cosmic rays from reaching the Earth and therefore the cosmic ray intensity at the Earth is depressed. The intensity variation observed which is approximately of ~ 20 % at neutron monitors and of ~ 5 % at meson monitors from solar minimum to solar maximum is found to be

strongly energy dependent. The results, from a large amount of data concerning the rigidity dependence of the long term modulation, indicate that the low energy component of the cosmic rays shows the highest solar cycle modulation, while the particles with rigidities higher than 15 GV seem to remain relatively unaffected and even during minimum solar activity there exists a residual modulation of cosmic ray intensity.

On the basis of the convection-diffusion theory proposed by Morrison (1956), either of the three parameters, e.g., the diffusion coefficient (K), solar wind velocity (V) and the depth of modulating boundary (D), should vary with 11-year periodicity. However, the systematic variation in either K, V or D as measured by satellite detectors (Mathews et al., 1971; Hedgecock et al., 1972) has not been detected, so that the 11-year variation may be explained fully. The diffusion coefficients $K_{\perp}$ and $K_{\parallel}$ are functions of particle rigidity and for energies > 2 GeV the variational spectrum of 11-year modulation is R^{-1} (O'Gallagher and Simpson, 1967; Hatton et al., 1968; Lockwood and Webber, 1968; Ormes and Webber, 1968). However, the spectral exponent ranging from -0.5 to -2.0 has been quoted for different phases of 11-year cycle (Stozhkov and Charakhchyan, 1968; Steker et al., 1971; Kane, 1972). Many authors have pointed out the steplike alterations in the spectral form of the eleven year modulation which may be

on account of the sudden changes in the radius of the modulating region (Kane, 1972).

The observed time lag between the maximum cosmic ray intensity and the minimum solar activity may be utilised to estimate the size of the modulating region (Pulkkinen, 1975). Using sunspot number as the parameter to define solar activity, a time lag of 9 to 12 months is found (Forbush, 1958) which corresponds to the extent of the corona i.e., the distance upto which the solar wind has not been broken up by the I.M.F., $D \approx 100$ AU, a value which is an order of magnitude greater than that obtained from many other evidences. Moreover the value is found to be different for different periods of the solar cycle. Quenby (1965) has, however, pointed out that consideration of sunspot number close to the solar equator ($\lambda \pm 10^0$) substantially reduces the time lag. Subsequent studies have shown that coronal green line intensity (λ 5303) from the equatorial region of the sun ($\pm 10^0$) is a better index of the solar activity (Hatton et al., 1968). Comparison with both ΣK_p and λ 5303 intensity shows that the time lag between the solar activity and cosmic ray intensity is of the order of $\sim$ 1 month which corresponds to $D \approx 7$AU (Pathak and Sarabhai, 1970). The solar flare data have also been often interpreted in terms of small modulating region of less than 10AU. However, the solar cosmic ray studies have yielded the dimension of the modulating region

to be $\sim$ 3-5AU (Burlaga, 1967; Jokipii, 1971). But, the recent measurement by instrument on board, Pioneer-10 and 11 no longer allow such a choice. Therefore, the question of the solar modulating region remains unsolved.

A number of authors (Barouch, 1974; Wibberenz, 1974; Barouch and Burlaga, 1975) have recently suggested that the cause of solar modulation and low radial gradient of cosmic rays could be accounted by assuming that a small number of magnetic blobs or bubbles or the large angle scattering centres exist in the interplanetary space and the origin of these scattering centres might be the coronal transients (Newkirk Jr., 1975). These scattering centres provide an explanation for the solar cycle modulation of cosmic rays as well as for the low radial gradients.

1.34 Forbush decrease and 27-day modulation

The cosmic ray intensity at ground based monitors was found to abruptly decrease almost simultaneously with geomagnetic storms following a day or two after a solar flare, which was demonstrated by Forbush (1938) to be of worldwide character. Simpson (1954) suggested that these worldwide decreases are caused by a sudden and drastic change in the electromagnetic condition of the interplanetary medium due to the flare occurring on the Sun. These decreases range in ground based neutron monitors from a few percent to more than

15 % of the integrated relativistic spectrum of the cosmic rays extending to particles with rigidities beyond 50 GV and are found to be energy dependent. Forbush decreases are normally characterised by a sudden decrease of cosmic ray intensity simultaneously from all the directions with a recovery period of several days.

Various models (Alfven, 1954; Dorman, 1957) have been suggested from time to time, who attributed the Forbush decrease to the energy losses produced by the electric field associated with the solar plasma beam. The two most successful models which have been proposed to explain the Forbush decrease, are due to Gold (1959) and Parker (1963). According to Gold (1959), a plasma cloud ejected by a large flare event can draw out the magnetic field of the Sun forming a large 'magnetic bottle' under certain geometric conditions this 'magnetic bottle' can engulf the Earth and provide the additional shielding which explains the Forbush decrease in the cosmic ray flux. According to the model proposed by Parker (1963), following the eruption of a large flare a blast wave (magnetic shock front) develops which propagates in the interplanetary space causing a sharp local increase of I.M.F. This shell of higher field intensity provides the extra protection against cosmic rays which attributes the Forbush decrease. Several space probes, such as Mariner-2 and Explorer-3 and 4, have observed this type of an abrupt

increase shock wave. An enhancement in the cosmic ray flux which is occasionally observed after a large flare and before the on set of the Forbush decrease, is produced by solar cosmic rays which are emitted during certain flare events. A brief increase which sometimes occur before the beginning of a Forbush decrease is probably related to the arrival of the shock wave from the Sun which in this case contains a relatively large number of semi-trapped solar cosmic rays.

More recently, Agrawal et al. (1974) have proposed a qualitative model to explain the various aspects of the observed characteristics of the Forbush decrease which occurred on August 4-5, 1972. The model is based on the convection by a transient modulating region containing very high tangled magnetic fields behind the shock front which is followed by a Gold/Parker (Gold, 1959; Parker, 1963) type cavity containing fairly well ordered magnetic fields and depressed cosmic ray intensity. It is concluded that the large Forbush decrease is mainly due to the depressed cosmic ray intensity in the region of tangled magnetic field behind the shock.

The Forbush decreases corotating with a strong 27-day recurrence tendency have also been detected in addition to Forbush decreases initiated by solar flares. The corotating Forbush decreases observed at low energies ($\sim$10 MeV) may manifest themselves as the enhanced diurnal wave trains at high energies ($\sim$1 GeV) (McCracken et al., 1966; Dukata et al.,

1968; Rao et al., 1972). At present, it is not very clear that Forbush decreases are associated solely to 27-day recurrent solar corotating streams or to transient plasma cloud or the shock waves from solar flares. Probably, more than one mechanism is operating simultaneously in the Sun-Earth region in a complicated manner to cause the recurrent Forbush decreases.

There is also 27-day modulation of the cosmic ray flux because the I.M.F. corotates with the active region on the Sun from which it stems. The 27-day cycle is due to intrinsic rotation of the Sun and is associated with central meridian passage of active coronal regions and unipolar magnetic regions on the solar disc. This cycle is especially noticeable during periods of high solar activity when a very active region might last for more than one rotation of the Sun. Detailed reviews are available in the literature on the subject (Webber, 1962) and since this does not directly form the main part of the thesis, we have made only a brief reference to this subject of cosmic ray modulation.

1.33 Spatial anisotropies and the daily variation

As the Earth spins on its axis with a period of 24-hours, a ground based detector on Earth scans the spatial anisotropies in the interplanetary space once each day as their 'asymptotic cone of acceptance' sweeps through the

directions containing the spatial anisotropies. Therefore, a spatial anisotropy in the sky manifests itself as a time variation at ground, giving rise to daily variation. The daily variation of cosmic ray intensity has been studied using ground based observations mainly from neutron and meson monitors during the period of IGY. In the recent years, these variations have been studied not only by using more sophisticated high counting rate ground based detectors, such as super neutron monitors and large area meson telescopes but also by using the data from low energy detectors flown in high altitude balloons, rockets and space probes and also by underground detectors responding to high energies. On an average basis only three frequencies, e.g., 1 cycle per day or diurnal variation, 2 cycles per day or semi-diurnal variation and 3 cycles per day or tri-diurnal variation, are generally observed as is shown in Figure-1.4, which shows the plot of the power spectrum density distribution at different frequencies (Girgis et al., 1977). In fact, practically, the harmonic component higher than 3 cycles per day in cosmic ray neutron and meson data has not been reported so far. The diurnal variation is found to be most dominant in comparison to other two components of the daily variation. The occurrence of semi-diurnal variation has been confirmed much earlier (Nicolson and Sarabhai, 1948; Elliot and Dolbear, 1951; Rao and Sarabhai, 1964) and its characteristics have been discussed

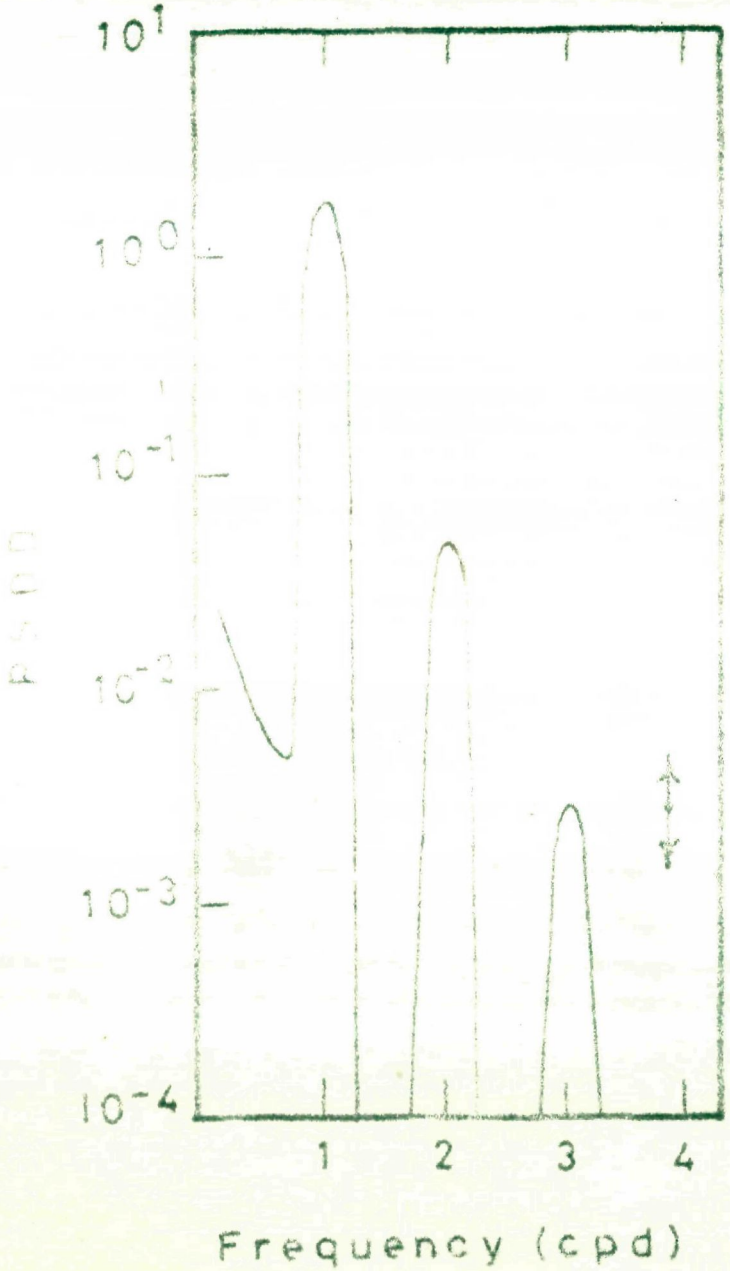

Fig. 1.4 - The power spectrum density distribution derived from the cosmic ray intensity measurement at Deep River is plotted against frequencies (after Girgis et al., 1977).

by many workers (Ables et al., 1965; Patel et al., 1968; Lietti and Quenby, 1968; Fujii et al., 1970; Rao and Agrawal, 1970). The tri-diurnal variation has been reported very recently (Mori et al., 1971; Ahluwalia and Singh, 1973). The subject has been reviewed in the literature from time to time (Sarabhai and Nerurkar, 1956; Dorman, 1957, 1963; Sandstrom, 1965; Pomerants and Duggal, 1971; Rao, 1972).

1.4 Characteristics of diurnal variation and experimental observations

From an extensive and systematic analysis of ground based neutron monitor observations, Rao et al. (1963) and McCracken and Rao (1965) have shown that the average diurnal anisotropy $\delta J(R)/J(R)$ of cosmic ray intensity observed at relativistic energies ($\geq$ 1 GeV) may be expressed by

$$\left.\begin{aligned} \frac{\delta J(R)}{J(R)} &= A\, R^{\beta}\, \mathrm{Cos}(\psi - \psi_0)\, \mathrm{Cos}\Lambda \qquad \text{for } R < R_{max} \\ &= 0 \qquad\qquad\qquad\qquad\qquad\quad \text{for } R > R_{max} \end{aligned}\right\} \quad \ldots\ 1.17$$

where R is the rigidity measured in GV, A is a constant equal to $(0.38 \pm 0.02) \times 10^{-2}$, $\beta = 0$, $\psi_0 = (89 \pm 1.6)^{\circ}$ measured anti-clockwise from the noon-meridian and Λ is the declination, R_{max} is the upper cutoff rigidity beyond which the diurnal anisotropy does not exist and is usually of the order of 100 GV. In other words, the average diurnal anisotropy of

cosmic radiation

(i) has a time invariant amplitude in space of 0.38 ± 0.02%;

(ii) is rigidity independent in the rigidity range 1-100 GV;

(iii) has a maximum flux incident from 89° ± 1.6° East of the Sun-Earth line, that is 1800 hours local time; and

(iv) varies as cosine of declination.

These characteristics of the diurnal variation has been derived by using the variational coefficients (Rao et al., 1963) which include particles of rigidities upto 500 GV (McCracken et al., 1965). An extensive theoretical computational calculation of the diurnal variation of cosmic ray intensity has also been performed by Nagashima et al. (1961). However, Parker (1964) and Axford (1965b) have theoretically predicted the amplitude of the diurnal variation $\approx$ 0.6 % instead of $\approx$ 0.4 % as observed experimentally. This controversy has invoked large and unobserved perpendicular gradients (Parker, 1964; Axford, 1965b; Gleeson, 1969) or a significant random walk contribution to transverse diffusion ($K_\perp$) (Jokipii and Parker, 1969). However, Subramanian (1971a) considering $R_{max} \approx$ 90 GV has estimated the effect of small but certain cumulative errors that should be considered and from which he concluded that the observed amplitude for Deep River neutron monitor during most of the periods, is in reasonably good agreement with the amplitude $\approx$ 0.6 % expected from

theoretical consideration.

It may be mentioned here that considerable deviations from the average picture exists in both amplitude and phase of the diurnal anisotropy on a day-to-day basis. A significant fraction of days in each year have either amplitudes much higher (> 0.6 %) than predicted by the theory or phase significantly different from the 1800 hour direction. These transient variations in the diurnal anisotropy have been explained to a large extent by using the convection-diffusion theory (Hashim et al., 1972; Rao et al., 1972; Ananth et al., 1974; Kane, 1974).

1.41 Long term anisotropic modulation

The yearly mean diurnal amplitude and phase are found to be practically constant during the period 1957-70 (McCracken and Rao, 1965; Fuller and Marsden, 1965; Rao, 1972), except for the small though significant decrease in amplitude in the years of the minimum solar activity (Duggal et al., 1967). The mean amplitude of the diurnal variation of the muleonic component in 1965 for example was $\approx$ 20 % less than in 1958. The decrease in diurnal amplitude in 1965 is now understood as due to a significant reduction of the upper cutoff rigidity (R_{max}). The change of R_{max} has been investigated by a large number of workers (Rao et al., 1963). Using the ratio of diurnal vectors observed at neutron and underground meson

telescopes at Hobart R_{max} is estimated to be $\sim$ 100 GV. Later using similar methods a number of authors (Agrawal et al., 1972) have concluded that R_{max} < 100 GV and varies with solar cycle, attains a lowest value of $\sim$ 40 to 50 GV during solar minimum and a highest value of $\sim$ 100 GV during solar maximum.

From the rigorous analysis of ion-chamber and meson monitor data, Forbush (1967, 1969) concluded that the average diurnal variation is composed of two distinct components W and V. The component W has its maximum (or minimum) in the direction 128° East of the Sun-Earth line, which is roughly the average I.M.F. direction, and varies simusoidally with a periodicity of 20 years and passes through its zero amplitude when the Sun's polar magnetic field is reversed (Forbush, 1973). The other component V has its maximum along 90° East of the Sun-Earth line and varies with solar activity, showing a solar cycle dependence. The spectral nature of both the components seems to be alike namely they are both energy independent (Duggal et al., 1970).

Forbush and Venkatesan (1960) carried out a rigorous statistical analysis which revealed that significant variations both in the amplitude and phase of the diurnal anisotropy occurred during the period 1957-59. Eventhough, the neutron moniter results for the period 1957-70 have not indicated any significant long term changes in the diurnal anisotropy of cosmic radiation, the observations from other detectors

responding to higher energies such as meson monitors and underground detectors have always indicated a significant change both in the diurnal phase and the amplitude from year to year (Duggal et al., 1970). Moreover, the recent observations have indicated that even the diurnal variation derived from neutron monitor observations is not invariant from 1971 (Agrawal and Ananth, 1975). However, their detailed characteristics and explanations have not been provided. Therefore, the work presented in this thesis mainly deals with the behaviour of the diurnal and semi-diurnal anisotropy during the period 1957-76 on magnetically quiet, magnetic storms and disturbed days, and disturbed days without magnetic storms with a view to find their detailed characteristics and their physical significance with possible explanations.

1.42 Short term anisotropic modulation

In the recent past, the average behaviour of the daily variation of cosmic rays is fairly well understood. However, in contrast to the average properties, the understanding of the short term modulation of diurnal and semi-diurnal anisotropies and the large variability observed on a day-to-day basis, which is essentially caused by significant variations in the electromagnetic properties of the interplanetary medium, is relatively very less. Several investigators (Rao and Sarabhai, 1961, 1964; Patel et al., 1968; Pomerants and

Duggal, 1971; Rao, 1972) have shown that both the amplitude and phase of the diurnal and semi-diurnal vectors vary considerably on a day-to-day basis. The fluctuation in both diurnal and semi-diurnal components is far more than that expected from a statistical behaviour. Further, it is also seen that the variability in the amplitude and the phase of the semi-diurnal component is much larger than that observed in the diurnal component. Sarabhai and Subramanian (1965) and Patel et al. (1968), using the method of variational coefficient (Rao et al., 1963), have further shown that the energy spectrum of diurnal and semi-diurnal variation on a day-to-day basis shows large variability from its average value even during relatively quiet period e.g., 1964-65. Therefore, the large variability in the spectral characteristics and the phase may not be understood in terms of corotation theory alone.

During geomagnetic storm days, the characteristics of the diurnal anisotropy is usually changed. However, no general relationship between the intensity and the nature of the storm has been established so far. There have been some reports that the amplitude of the diurnal variation increases and the phase shifts to earlier hours during the period of geomagnetic storms (Sekido and Yoshida, 1950; Yoshida, 1955; Dorman, 1957, 1963; Tanskanen, 1968). However, these conclusions have not been supported by others (Crowden and Marsden, 1962; Kane, 1962). Many workers have confirmed an initial

anisotropy aligned along a direction 30° - 50° West of the Sun-Earth line during the onset of Forbush decrease. The anisotropy sometimes also develops even before the onset of the sudden commencement (Fenton et al., 1959; Ables et al., 1967; Mathews et al., 1968; Mercer and Wilson, 1968). McCracken (1962) has explained the observed initial anisotropy as due to the sampling of the inner region of plasma cloud emitted from the Sun containing the observed cosmic ray intensity which becomes accessible to detectors looking along this direction. Recently, Lindgren (1970) and Rasdan and Bemalkhedkar (1971) have shown that the 27-day recurrent Forbush decreases in their recovery phase are usually associated with enhanced diurnal amplitudes with the direction of maxima in the 9 - 10 hour direction.

The occurrence of trains of consecutive days having abnormally high diurnal amplitude (> 0.6 %) with the phase shift towards later hours ($\sim$21 hour) have been reported by Mathews et al. (1969) and Hashim and Thambyahpillai (1969) both during quiet as well as disturbed days. These authors have shown that these are caused by a large decrease of the cosmic ray intensity along the garden-hose direction rather than the streaming along the antigarden-hose direction. The possible existence of sinks in the garden-hose direction was inferred much earlier by Rao and Sarabhai (1964), from the study of the distribution of time of maxima and minima of the daily variation. However, in certain cases, the diurnal

variation has its time of maximum along the garden-hose direction, i.e., 09 hour (Rasdan and Bemalkhedkar, 1971, 1972; Bemalkhedkar, 1974). This is found to occur both during the recovery phase of Forbush decreases as well as during quiet periods and usually has 27-day recurrent tendency. The large amplitude diurnal wave trains studied by Duggal and Pomerants (1962) showed a systematic anti-clockwise shift in the diurnal anisotropy for $\sim$ 8 days. The diurnal phase shift towards later hours ($\sim$21 hours) caused by enhanced radial gradients is studied by Rao et al., (1972). Like-wise trains of days with negligibly small diurnal amplitudes are also found to occur (Agrawal, 1973).

Recently, a number of investigators have made an attempt to show the association of the diurnal anisotropy on individual days or groups of days with I.M.F. sector structure. A north-south gradient in the cosmic ray intensity, intensity increasing southward i.e., below the equatorial plane of the Sun (Barker and Hatton, 1970, 1971; Subramanian, 1971b, Hashim and Berecviteh, 1972) is assumed to exist so that the diurnal amplitude is expected to be larger and phase shifted to earlier hours for positive I.M.F. direction (away from the Sun) in comparison to days having negative polarity I.M.F.(towards the Sun). It has been shown that during IMP-1 period the days of enhanced diurnal variation were observed corresponding to the sectors pointing away from the Sun (Patel et al., 1968;

Venkatesan and Mathews, 1968; Ryder and Patton, 1968), confirming the above effect. However, from these observations Washim and Bercovitch (1972) have estimated the density gradient perpendicular to ecliptic plane, being 5.5 $R^{-0.6}$ % / AU, which differ both in magnitude and rigidity dependence from the radial gradient. When the results of the diurnal variation are examined for the period 1968-1969 (Parthra, 1972), it has been found that while the observed diurnal amplitude and phase for 1968 are consistent with the earlier findings, the results for 1969 are opposite i.e., for the positive polarity days the amplitude is small and phase shifts to later hours.

The characteristics of the diurnal anisotropy has also been associated with geomagnetic conditions (Sekido et al., 1952; Sandstrom, 1955, 1965). It has been shown from these early studies that the phase of the diurnal anisotropy shifts to earlier hours with increasing geomagnetic activity. Therefore, whenever the geomagnetic field variation indices e.g., K_p or A_p will be high, the time of maximum will be earlier as compared to average value. Further, the diurnal amplitude was shown to increase with increasing geomagnetic activity, though this is not true for all the stations even for the same period. The analysis has been extended by the author to find, if any correlation between, $A_p - \beta_1$ exists and thereafter examine the results with those reported above. This is essential to explain and/or to understand the long term changes in the diurnal anisotropy.

1.43 Theoretical models

Brunberg and Dattner (1954), for the first time, proposed that the diurnal variation of galactic cosmic rays as observed by the ground based instrumentation is due to an excess of cosmic ray flux incident from the 1800 hour local asymptotic time. They pointed out that the galactic cosmic rays in the vicinity of the Sun corotates with the Sun, and producing an increase in the cosmic ray intensity in a direction opposite to the Earth's orbital motion. A rapid progress in exploring the cause and mechanism of the diurnal anisotropy could be made only after the discovery of the solar wind (solar corpuscular stream) by Parker (1958a) and its interaction with the I.M.F. Starting with the concept that the solar magnetic field is twisted into an Archimedes spiral, which on the average, corotates with the Sun (Parker, 1958a), Ahluwalia and Dessler (1962) proposed a simple model to explain the average behaviour of the diurnal anisotropy, according to which the diurnal anisotropy is due to those cosmic ray particles that fully or partially take part in the corotation motion of the solar magnetic field. From an elaboration of the model they predicted that

(i) the source of the diurnal variation lies in the ecliptic plane and the diurnal anisotropy is energy independent ($\beta = 0$);

(ii) all particles whose rigidity is below an upper cutoff rigidity ($R_{max} \approx 100$ GV) undergo diurnal variation;

(iii) the direction of the diurnal anisotropy is perpendicular to the I.M.F. direction; and

(iv) the amplitude and the direction of the diurnal anisotropy is a strong function of solar wind velocity.

Whereas the first two predictions were in agreement with the observed characteristics of the average diurnal variation, the observed direction and the amplitude of anisotropy did not agree with theoretical predictions (Bercovitch, 1963; Rao et al., 1963; Snyder et al., 1963).

At the same time Stern (1964) raised a fundamental objection that in a highly conducting plasma an electric field induced by the relative motion between the solar magnetic field and the Earth $\bar{E} = -\bar{V} \times \bar{B}$ can exist where V ($=\omega r \sin\theta$, as shown in Figure-1.3) is the velocity of solar magnetic field lines relative to an observer on Earth and B is the solar magnetic field strength at a heliocentric distance r from the Sun. For a magnetic field which is axisymmetric around the axis, $\nabla \times \bar{E} = -\delta\bar{B}/\delta t \approx 0$, and the electric field will be conservative. According to Lieuville's theorem, the cosmic ray density is preserved in any conservative system (Lemaitre and Vallarta, 1933; Swann, 1933), thus if the cosmic ray intensity is same in all the directions at any point outside the solar system then it must be so at any accessible point inside the solar system. The electric field $\bar{E}$ in turn produces a density gradient and

the streaming produced by this density gradient will exactly cancel the streaming produced by the electric drift and no time independent magnetic field can produce an anisotropy such as diurnal anisotropy in the solar system.

In order to overcome this difficulty Parker (1964) suggested that the assumption of fields in the interplanetary space being conservative is not completely correct, that is $(\partial \bar{B}/\partial t) \neq 0$ and in fact one may expect a large number of small scale irregularities to be present in the magnetic field which are convected out along with the solar wind. The scattering of particles by these irregularities wipes out a major portion of the perpendicular density gradient established by the electric field $\bar{E}$ and the density gradient does not cancel the electric drift proposed by Ahluwalia and Dessler (1962), resulting in a net streaming of cosmic ray particles in the interplanetary medium. While Parker (1964) assumed the presence of irregularities beyond the orbit of the Earth, Axford (1965a) assuming the presence of scattering centres over the entire modulating region arrived at the same conclusion. The basic assumptions are as follows

(1) the I.M.F. is quite regular across the orbit of the Earth, so that the particles are constrained to move along the lines of force of the general spiral field, that is the diffusion perpendicular to the magnetic field lines is negligible ($K_{\parallel} \gg K_{\perp}$);

(ii) there are sufficient irregularities in the magnetic field beyond the orbit of the Earth to wipe out most of the density gradient produced in the incoming particles by the electric field, that is there is no density gradient perpendicular to the ecliptic plane ($(\delta U/\delta r)_{\perp} \approx 0$); and

(iii) there is no net radial streaming of cosmic ray particles in the solar system, that is Sun is neither a source nor a sink of cosmic rays.

Under these conditions the cosmic ray particles undergo a rigid corotation with the Sun and will give rise to a net streaming in the azimuthal direction and this rigid corotation of cosmic ray particles in the interplanetary medium is the origin of diurnal variation. The amplitude of the average diurnal or corotational anisotropy produced at any distance 'r' from the Sun is given by (Compton and Getting, 1935)

$$\xi = \frac{3G\, V_{ec}}{v} \qquad \ldots 1.18$$

where $G = \frac{(2+\gamma)}{3}$ ... 1.19

and $V_{ec} = \Omega r$, is the corotational streaming velocity, v is the particle velocity and Ω is the angular rotation velocity of the Sun (as shown in Figure-1.3). For particles of energy $\geq$ 1 GeV ($v \approx c$, the velocity of light) and at the orbit of the Earth (r = 1AU) where $V_{ec} \approx$ 400 kms/sec, γ = 2.65 for the

solar minimum period, the expected amplitude of the diurnal anisotropy, ξ would be ≈ 0.6 %. It is seen that the theory predicts an energy independent diurnal anisotropy at relativistic energies with the phase at around 1800 hours local time (90^0E of the Sun-Earth line) and an amplitude $\approx$ 0.6 %. Though the theoretical predictions were found to be in good agreement with the experimentally observed average diurnal variation characteristics (McCracken and Rao, 1965; Rao, 1972), the observed average diurnal amplitude $\approx$0.4 % was found less by $\sim$50 % during solar minimum and $\sim$ 30 % during solar maximum compared to the theoretically predicted amplitude.

Parker (1967) and Jokipii and Parker (1967) suggested that the discrepancy in the observed and calculated diurnal amplitude may be attributed to a finite diffusion coefficient perpendicular to the magnetic field ($K_\perp \neq 0$). A reduction in the observed diurnal amplitude may be produced when

(i) $K_\perp$ is very small beyond the orbit of the Earth, that is, the magnetic field is very smooth throughout the modulating region, therefore, the cosmic ray density gradients perpendicular to the ecliptic plane are not completely wiped off and the partial neutralisation of cosmic ray gradients perpendicular to the ecliptic plane will reduce the diurnal amplitude. A typical value of $K_\perp/K_{11} \approx 10^{-2}$ (or more) beyond the orbit of the Earth may be an order of magnitude, to account for the reduction in

(Jokipii and Coleman, 1968). The observed isotropy of 10 MeV protons (Rao et al., 1967) may be explained if $(K_\perp/K_{||}) \approx 1$ at low energies due to the random walk or meandering of field lines and azimuthal streaming at these energies is found to be almost zero (Jokipii and Parker, 1969).

With a careful analysis of the extra-atmospheric factors affecting the anisotropy observed by the neutron monitors, Subramanian (1971a) concluded that if due allowance is made to the four cumulative effects which includes the use of variable γ_g (the exponent of the energy spectrum of the primary radiation) ranging from 1.5 to 2.5 corresponding to rigidity range 2 to 15 GV, and the normalisation of the variational coefficient at much higher rigidity than 500 GV, then during solar maximum the observed average diurnal amplitude is in good agreement with the theoretically expected amplitude indicating that the transverse diffusion near Earth ($K_\perp$) is negligible at relativistic energies. Such a conclusion is essentially in agreement with that obtained by McCracken et al. (1968, 1971) from the low energy flare particle observations.

It may be mentioned that considerable deviations from the average picture exists in both amplitude and phase of the diurnal anisotropy on a day-to-day basis. A significant fraction of days in each year have either amplitudes much higher (> 0.6 %) than predicted by the theory or phase significantly different from the 1800 hour (corotational) direction, both of

which can not be explained with the simple theory of corotation. This suggests that the basic assumptions inherent in the corotational model (e.g., equilibrium conditions) may only provide an explanation for the gross average behaviour of the diurnal variation. Therefore, the short term and day-to-day variations of diurnal anisotropy have to be understood in terms of changing electromagnetic parameters of the interplanetary medium.

1.44 Modified theory of diurnal variation

For a spherically symmetric system, starting with the relativistic Boltzman hydromagnetic equation, Gleeson (1969) obtained a general expression for the differential current density S of cosmic ray particles in presence of magnetic field $\bar{B}$ and electric field $\bar{E}$, as follows

$$S = U\bar{V} = \phi_{\parallel} - \frac{1}{1+\eta^2}\phi_{\perp} + \frac{\eta}{1+\eta^2}(\phi_{\perp} \times \frac{\bar{B}}{B}) \qquad \ldots 1.21$$

where

$$\phi = C(r, E)\, U\bar{V} - K(\frac{\delta U}{\delta r}) + C(r, E)\frac{\eta\, U\bar{E}}{B} \qquad \ldots 1.22$$

and U is the differential number density of cosmic ray particles, $\bar{V}$ is the solar wind velocity, $\eta = \omega\tau$, $\omega = eB/m$ is the proton gyro-frequency, τ is the average time between the collisions, $K = v^2\tau/3$ is the isotropic diffusion coefficient which in the presence of magnetic field $\bar{B}$ has components $K_{\parallel} = K$ and $K_{\perp} = K/(1+\eta^2)$, v is the particle velocity and C(r, E) is the

Compton-Getting factor given by Equation-1.9 or 1.19. Due to high electrical conductivity of solar wind plasma, the magnetic field $\bar{B}$ is convected along with it, which induces an electric field $\bar{E} = -\bar{V} \times \bar{B}$. Therefore, the Equation-1.21 may be expressed in terms of electric field $\bar{E}$ (Forman and Gleeson, 1970, 1975) as follows

$$S = CU\bar{V}_{||} - K\left(\frac{\delta U}{\delta r}\right)_{||} - \frac{K}{1+\eta^2}\left(\frac{\delta U}{\delta r}\right)_{\perp} - \frac{\eta K}{1+\eta^2}\left(\frac{\delta U}{\delta r} \times \frac{\bar{B}}{B}\right) + CU\left(\frac{\bar{E} \times \bar{B}}{B^2}\right) \quad \ldots 1.23$$

while in terms of solar wind velocity,

$$S = CU\bar{V} - K\left(\frac{\delta U}{\delta r}\right)_{||} - \frac{K}{1+\eta^2}\left(\frac{\delta U}{\delta r}\right)_{\perp} - \frac{\eta K}{1+\eta^2}\left(\frac{\delta U}{\delta r} \times \frac{\bar{B}}{B}\right) \quad \ldots 1.24$$

In Equation-1.23, the convective term $CU\bar{V}_{||}$ is parallel to the magnetic field and the electric field drift $\bar{E} \times \bar{B}$ is displayed explicitly while Equation-1.24, combines these two terms into a simple convective flow of particles with the solar wind, $CU\bar{V}$. The other two terms represent the diffusive and gradient drift effects. The Equations-1.23 and 1.24 are vectorially represented in Figure-1.5.

Including the effects of random walk of the field lines on the cosmic ray particles (Jokipii and Parker, 1969) the modified streaming equation is given by

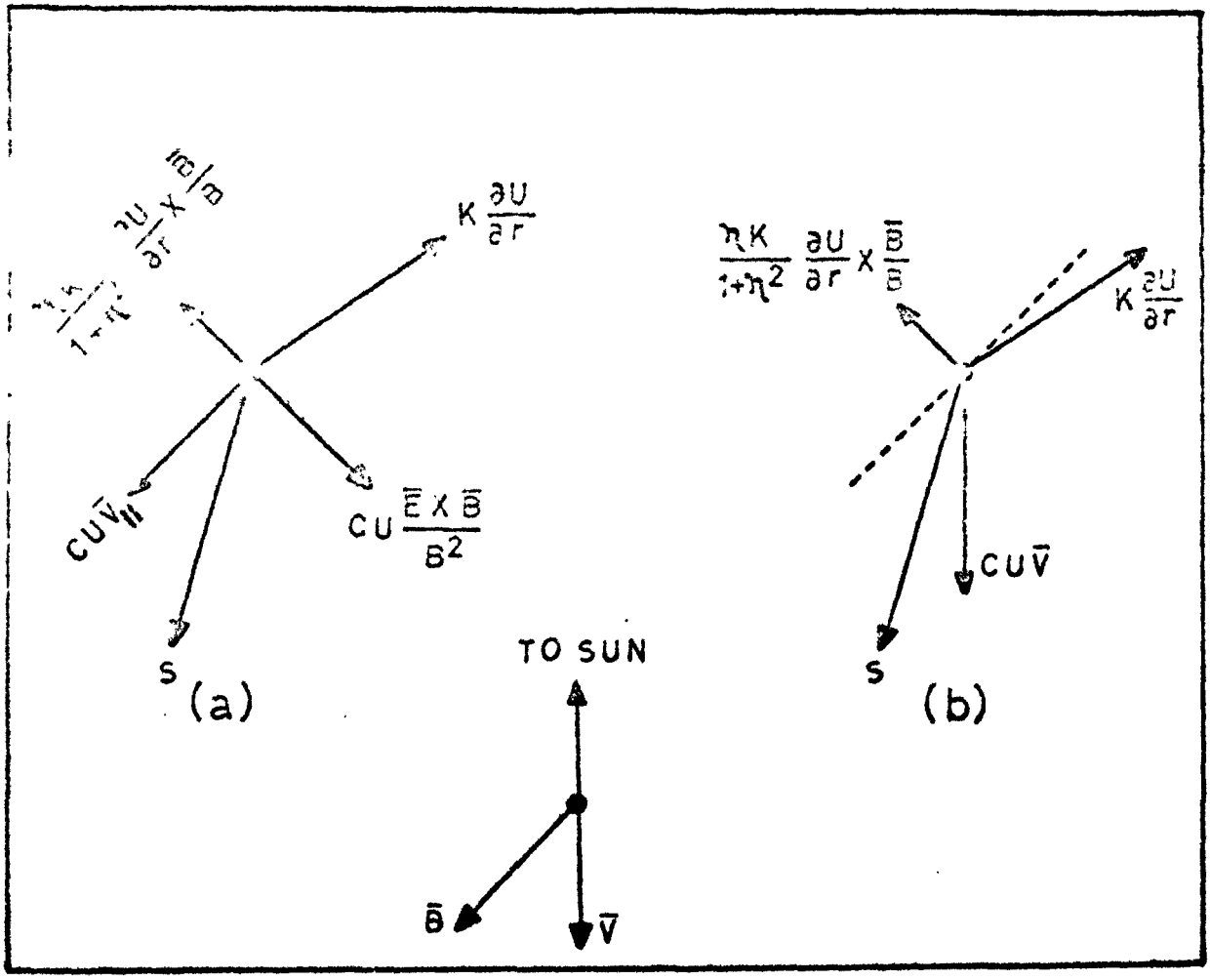

Fig. 1.5 - The differential current density S is described in terms of its components. In (a) the electric field is emphasised and in (b) the convective component $CU\bar{V}$.

$$S = S_c + K_{\parallel}\left(\frac{\delta U}{\delta r}\right)_{\parallel} - K_{\perp}\left(\frac{\delta U}{\delta r}\right)_{\perp} - \frac{V^2}{3\omega}\frac{\eta^2}{1+\eta^2}\left(\frac{\delta U}{\delta r} \times \frac{\bar{B}}{B}\right) \quad \ldots 1.25$$

where $S_c = C\bar{U}\bar{V}$ is the convection current density,

$$K_{\perp} = K_{\perp}'(\bar{B}, t, r) + \frac{K_{\parallel}}{1+\eta^2} \quad \ldots 1.26$$

and

$$F\left(\frac{\delta U}{\delta r}\right) = K_{\parallel}\left(\frac{\delta U}{\delta r}\right)_{\parallel} + K_{\perp}\left(\frac{\delta U}{\delta r}\right)_{\perp} \quad \ldots 1.27$$

The Equation-1.25 physically interprets that the net streaming of cosmic ray particles in the interplanetary space is essentially due to (i) the convection of particle radially away from the Sun, (ii) the diffusion of particles parallel to the magnetic field, (iii) the diffusion of particles perpendicular to the magnetic field, and (iv) the streaming produced by the density gradient perpendicular to the ecliptic plane.

The observed diurnal variation may be obtained from the Equation-1.25 with the assumptions that (a) the radial component is zero (i.e., $S_r = 0$), (b) the diffusion coefficient perpendicular to the magnetic field is negligible (i.e., $K_{\perp} \approx 0$), and (c) the transverse gradient current is zero (i.e., $\delta U/\delta r \times \bar{B}/B \approx 0$) (Subramanian, 1971a). Under such circumstances the radial convective component $S_c = C\bar{U}\bar{V}$ is balanced by the inward diffusive component $K_{\parallel}(\delta U/\delta r)_{\parallel}$ and since the field lines are inclined to the radial direction by an angle ψ (garden-hose angle) results in a net azimuthal streaming given by $C\bar{U}\bar{V}\tan\psi$, which

leads to the particles corotating with a velocity $V_{co} = \bar{V} \tan \chi$ and give rise to a diurnal anisotropy given by

$$\xi = \frac{3C\, V_{co}}{v} = \frac{3C\, \bar{V} \tan \chi}{v} \qquad \ldots 1.28$$

At relativistic energies ($v \approx c$), the amplitude of diurnal anisotropy is $\xi \approx 0.6\ \%$ for a $\bar{V} \approx 400$ kms/sec and $\chi \approx 45^{\circ}$.

Recently, a detailed study (McCracken et al., 1968, 1971; Rao et al., 1971; Allum et al., 1974) of the low energy solar particle observations made simultaneously at different helio-longitudes with widely spaced Pioneer space-crafts have clearly indicated that the azimuthal anisotropy at energies $\lesssim$ 100 MeV is quite negligible and that the particle population is largely determined by the balance between radial convection and field aligned diffusion. Extending these arguments to relativistic energies ($\gtrsim$ 1 GeV), McCracken et al. (1968) suggested that the diurnal anisotropy observed in the galactic cosmic radiation may also be understood as a superposition of simple convection and diffusion, that is in terms of a simple concept of an outward radial convection and inward field aligned diffusion of cosmic radiation. On an yearly average basis, using the cosmic ray intensity data from a number of neutron monitoring stations, this simple mechanism is able to explain successfully the observed diurnal anisotropy characteristics. Furthermore, this

mechanism is able to explain the diurnal anisotropy characteristics for nearly 80 percent of days on a day-to-day basis whereas for rest of the days it has been suggested that the transverse diffusion $K_{\perp}/K_{\parallel} \approx 0.2$ is operative at the orbit of the Earth (Ananth et al., 1974; Ananth, 1975; Fane, 1974, 1975).

1.5 Characteristics of the semi-diurnal variation

The harmonic analysis of the ionization chamber data has shown the existence of a semi-diurnal (12-hourly) wave in addition to the diurnal (24-hourly) component in the cosmic ray intensity (Rau, 1939; Elliot and Dolbear, 1950, 1951). However, due to its possible atmospheric origin, the extra-terrestrial nature of the semi-diurnal variation was not firmly established till recently (Elliot, 1952; Dorman, 1957; Fatsman and Venkatesan 1960). Rao and Sarabhai (1961) gave a reasonable evidence for the existence of the semi-diurnal wave from the observations made by east and west pointing telescope inclined at the same angle to zenith where the changes of meteorological origin may be cancelled to a first approximation (Elliot and Rothwell, 1956). However, they expressed some doubt as to whether it was of extraterrestrial origin in view of their suspicion that, it might have arisen due to the presence of large amplitude of semi-diurnal pressure wave, which may introduce a pressure induced variation, the poor statistical accuracy due to the low counting rate of the large variability of the observed semi-diurnal variation on a day-to-day basis (Rao and Sarabhai, 1961;

Ahluwalia, 1962).

Ables et al. (1965) were able to give the first conclusive experimental evidence for the presence of a significant semi-diurnal anisotropy of cosmic rays, with its maximum aligned in a direction perpendicular to the direction of the I.M.F., because the new techniques for observing the nucleonic component, coupled with improved pressure recorders, have greatly reduced the uncertainties in the meteorological corrections. Subsequent analysis by other investigators (Kane, 1966; Rao and Agrawal, 1970) have not only confirmed the existence of the semi-diurnal anisotropy but have also provided its detailed characteristics, which on an average basis may be summarised as follows

(1) The average free space semi-diurnal amplitude for cosmic ray particles has a value $\approx$ 0.11 $\pm$ 0.02 % during the period 1958-1970 with slight random variation between 0.13 $\pm$ 0.03 in 1965 to 0.08 $\pm$ 0.03 in 1967 (Agrawal, 1973). The time of maximum $\beta_2 \approx 135^0$ West of the Sun-Earth line (or at 0300 hour LST), essentially perpendicular to the direction of average I.M.F.

(2) The maximum cutoff rigidity upto which semi-diurnal variation exists has not been estimated unambiguously, though R_{max} = 200 GV may be the best choice, beyond which complete isotropy prevails.

(3) The anisotropy is rigidity dependent with a positive spectral exponent of $\approx$ + 1.0, as compared to $\gamma \approx 0.0$ for the

diurnal variation.

(4) In contrast with the $\mathrm{Cos}\lambda$ dependence of the diurnal variation, the semi-diurnal amplitude varies as $\mathrm{Cos}^2\lambda$, where λ is the mean asymptotic latitude of response.

To understand the origin of the semi-diurnal variation, both Subramanian and Sarabhai (1967) and Quenby and Lietti (1968) proposed the model independently and showed that the existence of a symmetrical latitudinal cosmic ray particle density gradient perpendicular to the equatorial plane produces diamagnetic drift which gives rise to a flux of cosmic ray particles in the plane of ecliptic perpendicular to the direction of the local I.M.F. For an Archimedes spiral configuration of the I.M.F., it is clear that the particles arriving along the Sun's polar field lines suffer much less modulation as compared to those arriving in the ecliptic plane, thus giving rise to a cosmic ray density gradient, with the intensity increasing away from the plane of ecliptic. Therefore, a ground based detector, due to spinning of the Earth, would observe an excess flux coming from directions 45^0 East and 135^0 West of the Sun-Earth line. This would appear as the semi-diurnal variation in the counting rate recorded by the detector. Both the theories, predict that the semi-diurnal anisotropy as observed in space (1) has a maximum flux in a direction perpendicular to the I.M.F.; (2) has an exponent of $R^{+1.0}$, where R is rigidity; and (3) varies

as $\mathrm{Cos}^2\lambda$. The positive spectral exponent predicted by the theory is consistent with the much larger semi-diurnal variation observed at equatorial latitudes.

In the model proposed by Lietti and Quenby (1968), the perpendicular gradient of the cosmic ray flux is a consequence of the random scattering of particles by scattering centers superimposed on the quiet time Archimedean spiral. The galactic particles that arrive over the poles experience easy access, since they diffuse along almost straight field lines, whereas those entering in the solar equatorial plane are constrained to follow many spiral loops. Consequently, the cosmic ray density should rise on each side of the solar equatorial plane. Subramanian and Sarabhai (1967), on the other hand, inferred the perpendicular cosmic ray density gradient from λ 5303 index measurements, based on their finding of the inverse relationship between λ 5303 green coronal line and the cosmic ray intensity. However, for a given cosmic ray density distribution, both the theories predict practically same results. The cosmic ray density in the vicinity of the Earth (Quenby and Lietti, 1968) is approximately given as follows

$$N_a = N_D \exp\left[\frac{-VD^3}{3K_{\parallel} a^2} \sin^2\theta\right] \qquad \ldots 1.29$$

where N_D is the density at the boundary D of the modulating region, V is the solar wind velocity, $K_{\parallel}$ is the diffusion

coefficient for cosmic rays moving in a direction parallel to the field at the Earth and θ is the polar angle with respect to the Sun's rotational axis. The peak-to-peak amplitude of the second harmonic wave derived from the above expression is

$$\left.\begin{aligned} r_2 = 0.005\, R(1 - \cos^2\chi\cos^2\lambda)^{3/2} \left[1 + \frac{\tan^2\lambda}{\sin^2\chi}\right]^{-1} \\ \text{for } R < R_{max} \end{aligned}\right\} \quad \ldots 1.30$$

$$\left.\begin{aligned} \text{and } r_2 = 0 \\ \text{for } R > R_{max} \end{aligned}\right\}$$

where R is in GV, λ represents asymptotic latitude with respect to the solar equatorial plane, χ is asymptotic longitude measured from the spiral field direction and R_{max} is the maximum rigidity upto which the semi-diurnal anisotropy exists.

The essential requirement of both the model described above is the existence of cosmic ray density gradient perpendicular to the solar equatorial plane. However, the results obtained from the neutron monitor observations, though not conclusive (Kane, 1968; Barker and Hatton, 1970; Subramanian, 1971b) have not generally supported the existence of required gradients. It has been felt for a long time, that the 'pitch angle distribution' of the particles in the I.M.F. (Sarabhai et al., 1965) may cause the semi-diurnal anisotropy. Nagashima et al., (1972a,b) have also proposed the loss cone model employing three dimensional propagation. Recently, Barnden

(1973) has introduced the idea of 'origin of scatter' technique to explain the semi-diurnal variation, However, none of these theories have been widely accepted for the explanation of the semi-diurnal variation of cosmic rays.

CHAPTER - II

INSTRUMENTATION

2.1 Introduction

An incoming primary cosmic ray particle collides with the air nuclei (Oxygen or Nitrogen) at the top of the atmosphere and produces a cascade of secondary particles, including the evaporation neutrons which are proportional to the nucleonic component intensity. The evaporation neutrons are associated with lower energy part of the spectrum of the primary cosmic rays (Simpson, 1948). Thus, the primary cosmic rays loose their identity when they penetrate the atmosphere surrounding the Earth, the direct observations are being carried out by the instruments on board balloons, rockets, satallites and space probes. Cloudchambers, photographic emulsions and spark chambers are the instruments generally used for seeing the particles and ionisation chambers, Geiger-Muller counters, Scintillators, solid state detectors and Cerenkov counters are used in various combinations to obtain the information about the flux and the energy spectra of the various components of primary cosmic rays.

The ground based instrumentation is very essential for continuous monitoring of high energy particles, however, there are various other modes as well for recording the cosmic ray particles at a wide range of energies both directly and indirectly. The conversion of primary energy to different modes depend upon

the energy of the incident particle. Therefore, for various components, three types of cosmic ray detectors have been developed to measure their intensity. These are:

(a) Neutron Monitor,

(b) Ionisation chamber and Meson telescope, and

(c) Extensive air shower arrays, in the increasing energy range.

A neutron monitor has low mean rigidity response as compared to that of a meson telescope. Thus, these detectors are complementary to each other in the study of cosmic ray intensity variations, as they cover a large energy range, when taken together. The mean rigidity response of the neutron monitor varies from $\approx$ 10 GV at the geomagnetic latitude $\approx$ 55° to $\approx$ 40 GV near the geomagnetic equator, whereas the surface meson monitor and the underground meson monitors have mean rigidity response $\approx$ 50 GV and $\gtrsim$ 80-100 GV respectively.

The neutron monitors have been found to be most suitable for the study of solar modulation of cosmic ray intensity among all the above mentioned ground based cosmic ray detectors since the neutron monitors response to low rigidity range at which the most of solar modulation are effective and also due to the fact that the correction for atmospheric effects may be done easily. Therefore, a large number of neutron monitors at various geographic coordinates on the surface of the Earth

have been installed during IGY, IQSY period and later on (Figure-2.1). The general principle and the design of the neutron monitor and its data recording units are therefore described in detail with particular reference to the neutron monitor at A.M.U., Aligarh (India), which has been partially designed and fabricated by the author.

2.2 Principle of the neutron monitor

For continuous monitoring of cosmic ray intensity, Simpson et al. (1953) suggested that for detecting the atmospheric evaporation neutrons, a simple neutron detector using BF_3 filled proportional counter is not suitable due to (i) a slow neutron detector using a bare BF_3 counter with the atmosphere as moderator will be greatly affected by the changes in the climatic conditions of the atmosphere and (ii) the fast neutron detector using a BF_3 counter surrounded by a local moderating medium will readily respond to changes of ambient neutron production near the detector resulting from movement of heavy materials. Therefore, the continuous monitoring of the nucleonic component by detecting the evaporation neutrons produced by its interactions in a target or 'producer' of high atomic mass (A) was preferred (production rate per gm $\propto A^{+0.4}$). Thus the use of lead, as a target of high atomic mass (A), for local production of evaporation neutrons has not only removed the above discussed short coming but also

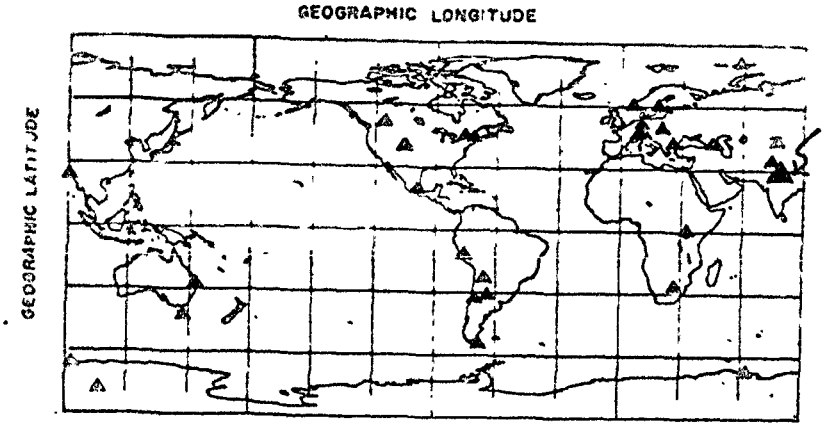

IGY NEUTRON MONITORS

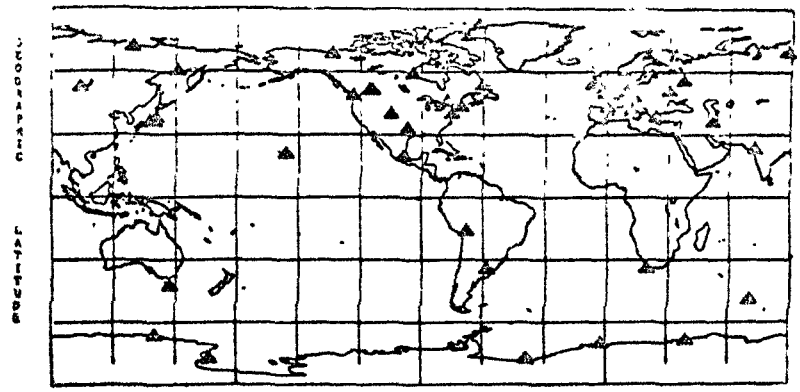

IQSY NEUTRON MONITORS

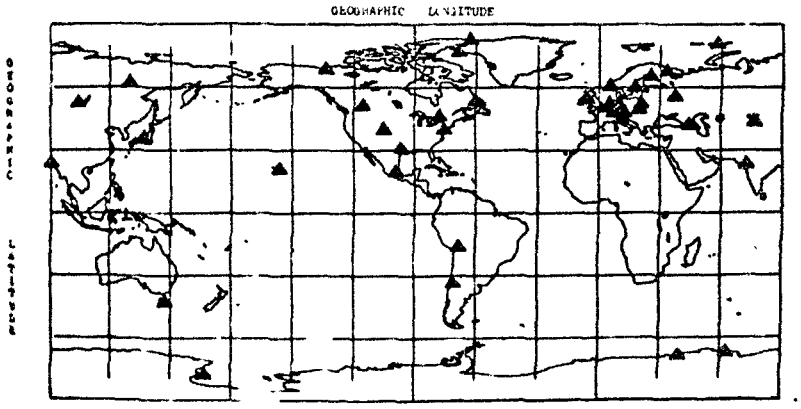

MESON MONITOR TELESCOPES

Fig. 2.1 – Showing the positioning of the presently [illegible] type and IGY-64(10%) type neutron monitoring [illegible] location of Aligarh [illegible] at the operating meson [illegible] (after Shea, 1972).

increased the counting rate of the detector, thus improving the statistical accuracy.

Simpson in 1952 installed the first Neutron Monitor at Chicago, Climax, Huancayo and Jungfraujoch, which consisted of BF_3 proportional counters surrounded by paraffin moderator, lead producer and a shield of hydrogenous material. Such an arrangement is referred to as a 'pile'. A nucleon incident on such a pile has got a high probability of causing a nuclear interaction in the lead and produces a multiplicity of low-energy neutrons. These neutrons are slowed down to thermal velocities by elastic collisions in the moderator when they diffuse into the pile. The thermal neutrons are captured by the B^{10} nucleus in the BF_3 counter and an electric pulse of amplitude $\approx$ 1 millivolt is observed at the output of the counter. This pulse is amplified and counted by the use of suitable electronic circuits.

Later, Simpson (1957) recommended a standard design of Neutron Monitor to be installed at various geographical locations during IGY period for continuous monitoring of nucleonic component of cosmic ray intensity. Lot of valuable information regarding many aspects such as large enhancements of solar origin and through them the interplanetary field configuration was derived from the data recorded by these monitors during 1957-58 and later. However, it was felt that their counting

rate were too low to study some of the aspects of modulation of cosmic rays such as daily variation on short term basis could not be established unambiguously. Carmichael (1964) designed the Super Neutron Monitor (NM-64) making use of large size BF_3 proportional counters developed at Chalk River by Fowler (1963) in order to improve the statistical accuracy of the neutron monitor data. The counting rate of a full size NM-64 super neutron monitor, consisting of 18 counters in three independent units each containing six counters, is about a million per hour at a sea level station having cutoff rigidity $\lesssim$ 2 GV.

A large number of neutron monitors of IGY type and of NM-64 type are in operation at various geographical locations in different countries, however, there are very few neutron monitors operating nearer to the equator. Therefore, the high counting rate neutron monitor at Aligarh has due consideration because of its geographical situation which is nearer to the equator, thereby recording only high energy ($\approx$15 GeV) cosmic ray particles. Thus a wide band of energy spectrum will be provided from the data of this station together with the continuous data from other stations.

2.3 Neutron Monitor at Aligarh

The neutron monitor at Aligarh closely follows the design recommended by Simpson during IGY. One module of the

neutron monitor (it is planned to fabricate four such modules at Physics Department, A.M.U., Aligarh) as shown in Figures-2.2, 2.3 and 2.4, consists of 12 BF_3 counters sensitive to thermal neutrons. Around each counter there is an 'inner moderator', i.e., paraffin, the function of which is to slow down or moderate the locally produced neutrons to near thermal energies to facilitate their capture in BF_3 gas. The counter assembly consisting of the inner moderator and counter is surrounded by lead 'producer' of purity greater than 99.9 percent in which evaporation neutrons are produced by the interaction of the nucleonic component. This arrangement is completely shielded by paraffin 'reflector' which prevents the escape of neutrons that would otherwise fail to be detected. This reflector also excludes the low energy neutrons produced in the vicinity of the monitor. The output from 12 counters is divided into two sections each containing six counters. Each section is associated with its own independent electronic circuits. The block diagram of the whole electronic arrangement is shown in Figure-2.5. The division of counters into two half sections provides a check on the performance of the detecting system by comparing the counting rate from two half sections.

2.31 BF_3 proportional counter

The proportional counters filled with pure Boron trifluoride (BF_3) gas enriched to more than 90 % B^{10} isotope

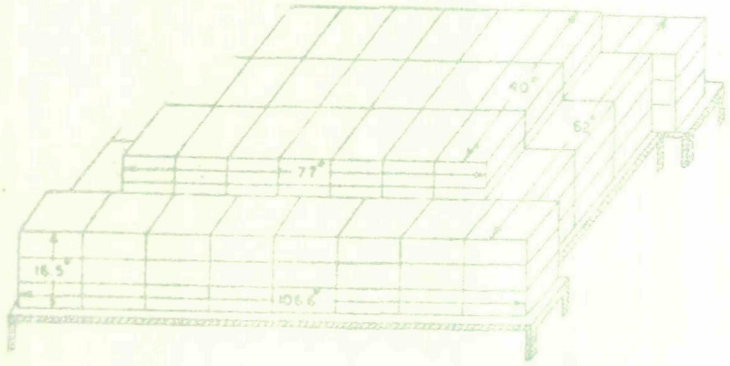

Fig. 2.2 - Exterior view of the neutron monitor.

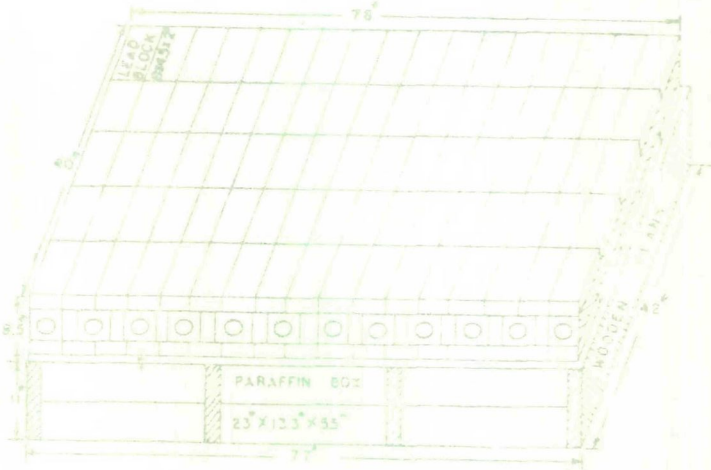

Fig. 2.3 - Interior view of the neutron monitor.

Fig. 2.4 - Lateral view of the neutron monitor

Fig. 2.5 - Block diagram of the electronic apparatus.

at a pressure of 60 cm Hg are used for the detection of thermal neutrons. The counters have a plateau in the proportional region for over a range of 300-400 V, with a slope less than 1 % per 100 volts. The thermal neutron which is captured by a B^{10} nucleus induces the following exothermic reaction

$$_5B^{10} + _0n^1 \rightarrow _3Li^7 + _2He^4 + 2.78 \text{ MeV} \qquad \ldots 2.1$$

The cross-section of this reaction follows a 1/v dependence (v is the velocity of the captured neutron) and is $\approx$ 3820 barns at thermal energies (1/40 eV). In 94 % of the reactions Li^{7*} nucleus is left in a 0.48 MeV excited state, 2.30 MeV being shared by the Li^7 and He^4 nuclei. In the remaining 6 % the Li^7 nucleus is left in the ground state and Li^7 and He^4 nuclei have a total K.E. of 2.78 MeV. The Li^7 nucleus may give a gamma ray photon by its transition into ground state. This photon may induce beta rays either by photoelectric effect or Compton effect. To discriminate the genuine pulses against relatively small pulses produced by the passage of muons, electrons etc. through the counter, the counter is operated in proportional region. Commercially prepared BF_3 gas is composed of B^{10} ($\sim$18.8 %) and B^{11} ($\sim$81.2 %) isotopes. Above reaction responds only to the B^{10} isotope and the B^{11} isotope performs no useful function. Therefore, proportional counters filled with BF_3 gas enriched in B^{10} isotope to more than 90 % are used for the detection of thermal neutrons.

2.32 Production of thermal neutrons in the neutron monitor

The choice of the geometry and quantity of the reflector, lead producer and moderator must be optimised to obtain maximum efficiency (Table-2.1).

Simple rectangular wooden boxes containing low density paraffin wax of 1½ inch thick layer surrounding the lead blocks and the counter assembly is used as a reflector and it establishes the full albedo of neutrons from the lead producer inside the monitor. It also diminishes the proportion of unwanted low energy neutrons arriving at the detector from outside.

The local neutron producer i.e., lead of purity greater than 99.9 % in the form of blocks of thickness 2 inch is placed above, below and in between the counter assembly (Figure-2.3).

The inner moderator which consists of 1.25 inch thick layer of paraffin wax is contained in the wooden box as shown in Figure-2.4. Inside this wooden box lies the BF_3 counter and its outer edge is fitted closely with the layer of lead blocks. The capture cross-section of the BF_3 filled proportional counter is maximum for thermal energy neutrons.

TABLE - 2.1

Dimensions and counting rate of IGY type standard neutron monitor and MM-64 type super neutron monitor.

Specification	Standard IGY Monitor	MM-64 Monitor
Number of counters per tray	6	6
Number of trays in one unit	2	3
Counters		
Active length (cm)	86.4	191
Diameter (cm)	3.8	14.8
Pressure (cm Hg)	45	20
Inner moderator		
Average thickness (cm)	3.2	2.0
Producer		
Average depth (g cm^{-2})	153	156
Area per tray (m^2)	0.94	6.21
Length parallel to counters (cm)	102	207
Reflector		
Average thickness (cm)	28	7.5
Counting rate (typical) of a high latitude sea-level station		
per tray per hour	$\sim$ 12,000	$\sim$ 250,000
per m^2 of producer	$\sim$ 12,800	$\sim$ 40,000

The nucleonic component interacting in the lead produces several associated evaporation neutrons, the number of these evaporation neutrons in general, being proportional to the energy of the interacting particle. Typically, a parent particle of energy 200 to 300 MeV produces on an average of about 10 evaporation neutrons. These evaporation neutrons are quickly slowed down to thermal energies by inelastic collisions with the modulating material and most of them are subsequently captured by B^{10} atoms of the counter gas. A small portion may be slowed down to the extent that they are lost in the moderator or counter walls.

2.4 Total counting rate

A number of authors have estimated the contributions to the counting rate made by various secondary components, using different methods, for both IGY and NM-64 monitors (Simpson et al., 1953; Hughes and Marsden, 1966; Harman and Hatton, 1968). A summary of the relative contributions of different primary components by Hatton (1971) for Leeds-IGY and NM-64 monitors, which is also applicable to any high latitude neutron monitor is given in Table-2.2.

A slight increase in the neutron contribution in NM-64 monitor as compared to IGY monitor has been attributed to the smaller thickness of the reflector in the NM-64 monitor. This

TABLE - 2.2

The percentage contributions made by various secondary components to the counting rate of the IGY and NM-64 monitors.

Component	IGY Monitor	NM-64 Monitor
Neutrons	83.6 ± 2.0	85.2 ± 2.0
Protons	7.4 ± 1.0	7.2 ± 1.0
Pions	1.2 ± 0.3	1.0 ± 0.3
Stopping muons	4.4 ± 0.8	3.6 ± 0.7
Interacting muons	2.4 ± 0.4	2.0 ± 0.4
Background	1.0	1.0

increase occurs, preferentially, in the neutron contribution due to the low energy neutrons (< 100 MeV) having a smaller absorption mean free path in the paraffin wax, than the other components.

2.41 Neutron production by nucleons

Nucleon-nucleus interactions are usually described in terms of a two stage process. During the first phase, the so called 'cascade' phase, knock-on nucleons and created pions are emitted with a broad energy spectrum extending upto energies comparable with the incident nucleon energy and with an angular distribution peaked in the direction of motion of the incident nucleon. At the end of first phase the nucleus is left in an excited state and further emission of particles, predominantly evaporation neutrons, follows during the second phase, the de-excitation or evaporation phase. The evaporation neutrons are characterised by an isotopic angular distribution and an energy spectrum peaked around a few MeV. Both theoretically (Shen, 1968) and experimentally (Hughes et al., 1964) it is known that the average number of evaporation neutrons produced, increases both with the increase in the energy of the incident particle and with the increase in the producer thickness. A more detailed discussion of the neutron production by various secondary components is reviewed by Hatton (1971).

2.5 Zenith angle dependence of the neutron monitor

The relative contribution to the counting rate from the secondary nucleons at zenith angle varying between θ and $\theta + d\theta$ of a detector is given by (Hatton, 1971)

$$N(\theta)\, d\theta \propto J(\theta)\, S(\theta)\, \sin\theta\, d\theta \qquad \ldots 2.2$$

where $J(\theta)$ is the zenith angle distribution of the nucleonic component and $S(\theta)$ is the sensitivity of the monitor to this component as a function of zenith angle.

It is found that $S(\theta)$ is approximately constant indicating that the neutron monitor behaves as an omnidirectional detector. The smaller area presented to the incident nucleons at large zenith angles is compensated by the greater probability of the nucleons interacting and the larger number of evaporation neutrons produced following these interactions.

Phillips and Parsons (1962) using a mobile IGY monitor has determined the zenith angle dependence of the nucleonic component contributing to the counting rate which is consistent with $J(\theta) \propto \cos^5\theta$ over the range 0 to 40°, but for $\theta > 40^\circ$ the function falls off more slowly. Further, they determined the variation of the counting rate with zenith angle (Figure-2.6, curve C) and found that the greatest contribution to the counting rate was from zenith angle $\approx 25^\circ$ whereas the contribution to the counting rate for zenith angles $> 60^\circ$ is only

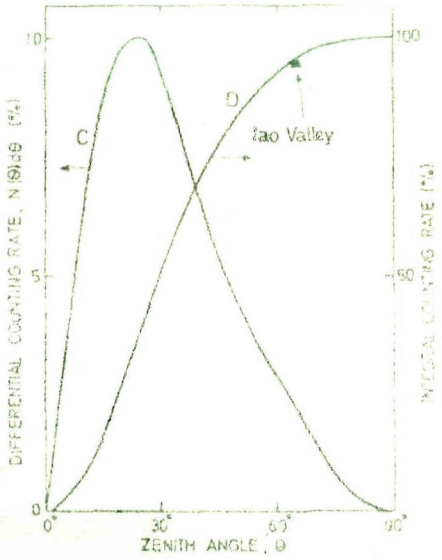

Fig. 2.6 - The differential (curve C) and integral (curve D) counting rates of a neutron monitor as a function of zenith angle as deduced by Phillips and Parsons (1962). Also shown is a point determined from the mobile NM-64 monitor survey of Carmichael et al. (1969) when the monitor was situated in the Iao Valley, Hawaii (after Hatton, 1971).

$\approx$7 %, as shown in Figure-2.6, curve D (which is the integral of Equation-2.2). The results of Carmichael et al. (1969) for Iao Valley, Hawaii, are also shown in the same Figure-2.6 and consistent with the earlier results obtained by Phillips and Parsons. Therefore, it is very essential for the long term stability of the neutron monitor that the effect of demolition or construction of a building if any, adjacent to the fixed neutron monitor should be taken into consideration. These changes will not only affect the attenuation of the nucleonic beam from low zenith angles, but they will also alter the low-energy environmental background which is quite important in the case of the high counting rate neutron monitor.

2.6 Electronic circuitry

The amplitude of the output α-pulses from BF_3 counters is of the order of a millivolt. These pulses are amplified by a pre-amplifier whose gain is $\approx$ 10. In each section, the output of two counters is connected to the input of a pre-amplifier. The output of 3 pre-amplifiers in each section is fed to a mixer and the output of the mixer is fed to a linear amplifier (ECIL Model No. 521). After sufficient amplification, the α-pulses are separated from much smaller background pulses by adding a discriminator in the output of the linear amplifier. The genuine α-pulses, thus obtained from the output of the discriminator circuit, are scaled down with the help of a

scaler and registered by an electromechanical recorder. Finally, the reading of the electromechanical recorder is photographed on 35 mm film at an hourly interval by an automatic photographic arrangement.

The details of the pre-amplifier, pulse mixer, discriminator, scaler and recorder driving circuits are given below.

2.61 Pre-amplifier

The detailed diagram of the pre-amplifier with typical values of components used is shown in Figure-2.7. The first two stages of this circuit have a feed-back bias arrangement for current stabilisation of both the stages. Resistance R_2 provides DC current feed-back from emitter of transistor T_2 to the base of transistor T_1. The AC negative current feed-back from the emitter of transistor T_3 to the emitter of transistor T_1 provides wide frequency response and low distortion. We have used a fixed resistance R of value 6.8 K in the emitter follower at the last stage. This value of the resistance R provides minimum noise and distortion in the circuit.

2.62 Pulse mixer unit

The circuit diagram of the pulse mixer unit with the values of components used is shown in Figure-2.8. Transistor

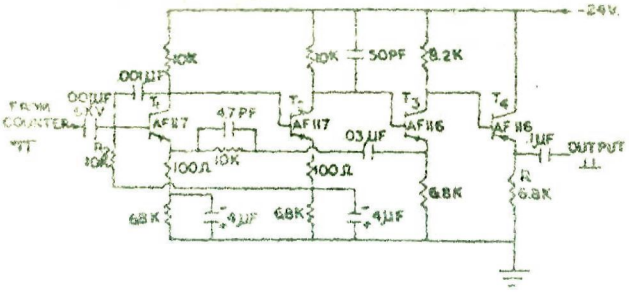

Fig. 2.7 - Pre-amplifier

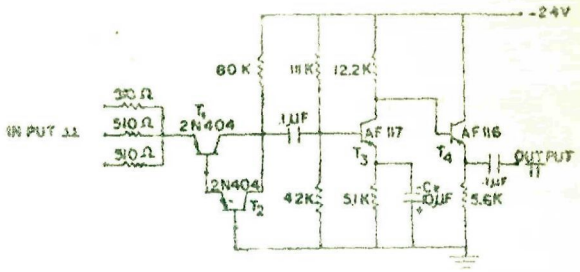

Fig. 2.8 - Pulse mixer unit

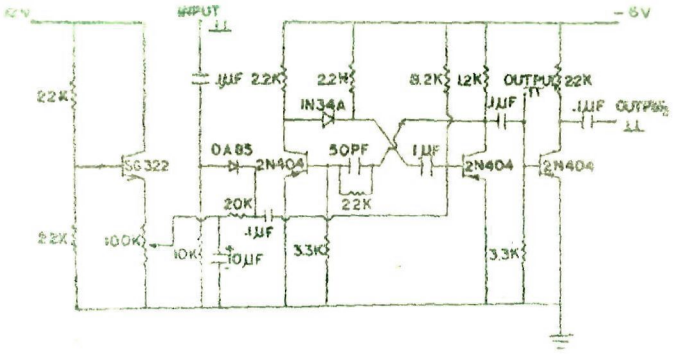

Fig. 2.9 - Discriminator unit

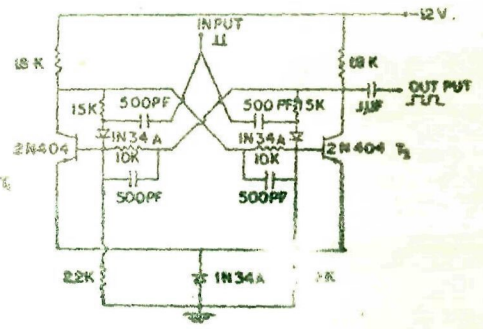

Fig. 2.10 - Scaling binary

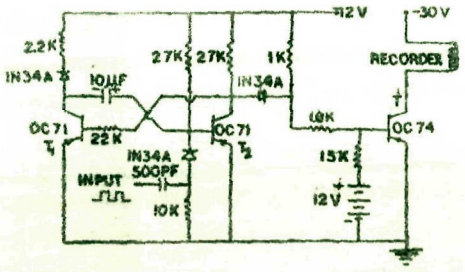

Fig.2.11 - Recorder driving unit

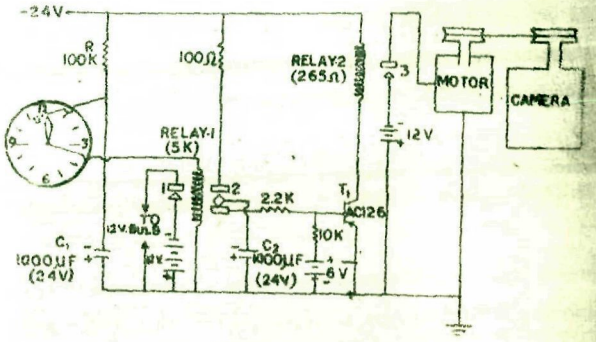

Fig. 2.12 - Automatic photographic recording system.

T_1 and T_2 form an OR-gate with three inputs and one output. When a pulse of positive polarity exists at one or more of the inputs of the OR-gate, an output of the same polarity is obtained. This output pulse of the OR-gate is amplified through a one stage common emitter amplifier T_3. The output stage T_4 is an emitter follower.

2.63 Discriminator unit

Discriminator unit, shown in Figure-2.9, is employed to cutoff the pulses having height less than a preset discriminator bias voltage. It gives positive pulses at the output for all input pulses of positive polarity exceeding the present discriminator bias. The bias may be varied from 0.6 to 5.0 volts, by means of a panel mounted helical potentiometer.

2.64 Scaling unit

It consists of eight binaries, which are identical. The detailed circuit diagram of a binary with typical values of the components used is shown in Figure-2.10. The binary has facility of symmetric triggering by positive pulses at the bases of transistor T_1 and T_2.

All components in this scaling unit are very critical. The components which are to be given extra special consideration are the collector resistors which have to be within 5 % of each

other and the base and feed-back resistors which have to be within less than 5 % of each other.

The circuit can handle approximately 10^6 evenly spaced pulses per second.

2.65 Recorder driving unit

The circuit diagram of the recorder driving unit is shown in Figure-2.11. In this, the output pulses of the last stage of the scaling unit is first fed to a monostable multivibrator (T_1 and T_2). The output pulses of the monostable multivibrator are used to operate the relay of electromechanical recorder connected in the collector arm of the power amplifier.

2.66 Automatic photographic recording system

The automatic photographic recording system is shown in Figure-2.12. It consists of a transistorised wall clock, an electronic circuit, a 1/20 HP motor and a 35 mm camera. The transistorised clock gives regular contacts after each hour. When the clock makes the contact 3, the condenser C_1, which is initially charged, gets discharged through relay-1 making contacts 1 and 2. Contact 1 lights the bulbs (12 V DC) for 5 seconds and during this time the contact 2 charges the condenser C_2. 5 seconds is the discharge time of the condenser C_1. When the condenser C_1 has been fully discharged, the contacts

1 and 2 break and the condenser C_2, now gets discharged giving negative pulse to the transistor T_1. This takes the transistor into conduction activating relay-2 and making the contact 3 which runs the motor for 12 seconds, which is the discharge time of the condenser C_2.

When the bulbs light for 5 seconds a photograph of the reading of the electromechanical recorder showing the number of counts of the cosmic ray intensity, time and date is taken by the 35 mm camera. After taking photograph, the motor runs for 12 seconds to roll the exposed part of the film and brings a fresh frame of the film in its position for the next exposure. The whole process is repeated at hourly intervals and thus the hourly data is preserved on the 35 mm films.

2.7 Auxiliary recording equipments

Barometric pressure and atmospheric temperature at the station are continuously recorded by means of standard Barograph (M.22) and Thermograph (M.16) respectively. Barograph records atmospheric pressure changes within the range of 100 mb, from 950 mb to 1050 mb. The instrumental error in recording pressure changes at ambient air temperature of 20° C does not exceed ± 0.7 mbs per every 10 millibars of atmospheric pressure change. Thermograph records air temperature changes, ranging from -25°C to +55°C accurate to ±1°C.

2.8 Long term stability of the neutron monitor

While studying the modulation of cosmic rays, the time scales involved vary appreciably from few seconds (Dhanju and Sarabhai, 1967) to the 11-years or more. The study of very short term time variations with scales $\leq$ 1 day is almost entirely limited due to the statistical significance of the counting rate. On the other hand, the study of time variations with time scales $\geq$ 1 day depend mainly upon the long term stability of the neutron monitor and the correctness with which corrections for meteorological effects are applied.

The neutron monitor is divided into two electronically independent sections in the IGY monitor. Since at any given location their response to primary as well as to meteorological variations is identical, a reliable internal check of the stability of the neutron monitor may be accomplished by monitoring the relative constancy of the ratio of the counting rate of different sections. Thus when the monitor is functioning properly, the ratio of the counting rates of two sections should remain constant with time apart from statistical fluctuations. However, the pulse height calibration on a long term basis is essential (McCracken et al., 1966) for keeping a completely reliable check of the total system particularly because of the monitors susceptibility to abrupt changes in efficiency. This method of testing counters also has the advantage that it may be

undertaken without the interruption of the normal operation of the monitor. The abrupt changes may occur due to a number of factors such as follows:

(i) Replacement of the counter,

(ii) Variation in the applied voltage of the counter,

(iii) Changes in the counter position relative to the producer,

(iv) Drift in the discriminator levels,

(v) Change in the amplifier dead time (pulse width), etc.

C H A P T E R - III

METHODS FOR ANALYSING THE COSMIC RAY DATA

3.1 Atmospheric effects

The primary cosmic ray particles, in their nuclear interactions with the air nuclei in the Earth's atmosphere produce secondary particles which are being registered by the ground based detectors. These secondary particles are very sensitive to the meteorological variations. Therefore, the knowledge of the atmospheric transition effects of cosmic ray particles, which includes (i) the cascade processes responsible for the production of secondary cosmic ray at different levels in the atmosphere and (ii) the effects of the variation of the meteorological conditions such as pressure and temperature throughout the atmosphere on the intensity fluctuations at different levels, is very essential to relate the observed secondary variation to variation in the primary cosmic ray intensity.

The effect of the changing meteorological conditions on cosmic ray variation has been studied quite extensively both theoretically and by employing well known correlation techniques between the observed cosmic ray intensity variations and the meteorological parameters. A very comprehensive review of the atmospheric effects has been given by Berezovitch (1967). Essentially, two major corrections are to be applied

to cosmic ray data; the first one is to correct for barometric or absorption effect and the second is to correct for temperature effect. The barometric effect is simply the change in the mass of the absorber, overlying the detector. The cosmic ray intensity measured at the ground is negatively correlated with the barometric pressure.

The mesonic component is quite sensitive for the temperature variations. Any increase in the atmospheric temperature, increases the height of the μ-meson production layer thereby increasing the path length for μ-mesons reaching the detector, so that the probability of μ-meson decay in the longer path increases. Thus, the cosmic ray intensity will decrease with the increase in temperature. In addition to this negative temperature effect, a small positive temperature effect is also operative due to competitive process between π-meson interaction with air nuclei and π-μ decay which depends on the variation of the differential density of upper atmosphere. Thus, the temperature effect is more complicated for mesonic component since for exact calculation of the effect, the temperature at different isobaric levels of the atmosphere should be correctly known.

The temperature effect is particularly, important when the cascade processes producing the secondary component involves particles with life-time that are comparable with

the time of flight from their point of origin to the detector. Earlier observations have clearly indicated that the neutron intensity at the ground is significantly affected by pressure variation, whereas the temperature effect for nucleonic component is very small. However, it may not always be negligible, since the neutron intensity as measured by neutron monitors, results due to neutron production in the monitor by nucleons as well as meson, with μ-meson contribution of $\approx 8 - 9$ % of the total counting rate of the neutron monitor for cutoff rigidity ≈ 6.4 GV. The temperature effect for neutron component has been worked out by Kaminer et al. (1964). The atmospheric effects related to neutron monitor have been recently reviewed by Hatton (1971).

3.11 Pressure correction of neutron monitor data

The neutron intensity N at any atmospheric pressure P may be expressed by the relation

$$N(P) = \exp(-P/L)$$

where L is the absorption mean free path of the nucleonic component, which depends on the mean energy of the recorded nucleonic component. Differentiating above equation with respect to P we have

$$\alpha = -\frac{1}{N}\frac{dN}{dP}$$

where $\alpha = 1/L$ is known as the barometric attenuation coefficient or pressure coefficient.

Extensive investigations have shown that the attenuation coefficient (α) of a neutron monitor is a function of both altitude and latitude (Bachelet et al., 1965, 1972a; Carmichael et al., 1968; Carmichael and Peterson, 1971) and at a given location varies during a solar cycle, being maximum at minimum solar activity (Bachelet et al., 1967). The attenuation coefficients obtained for various sea level neutron monitoring stations having different cutoff rigidities for the period 1964-65 (Bachelet et al., 1972b) and those obtained for 1965 by Carmichael and Bercovitch (1969) from latitude surveys, with a mobile monitor, show that there is a good agreement in the values of the attenuation coefficient derived for low latitude stations having cutoff rigidities $\geq$ 8 GV. Similar agreement is also found for latitude survey results by Kodama and Inoue (1970).

The attenuation coefficient (α) may be simply estimated by using straight forward regression analysis of the logarithm of the intensity, $I = Ln\ (N)$, with the atmospheric pressure P for short period intervals of three months each. Following well established methods, the attenuation coefficient (α) for a particular neutron monitor may be estimated by performing a more rigorous regression analysis of successive differences

(Lapointe and Rose, 1962) of the logarithm of the daily mean intensity (N) and the daily mean pressure (P). In this method, the change in counting rate from one day to next is correlated with the corresponding change in the pressure. Let the mean counting rates corresponding to mean pressures P_1 and P_2 be N_1 and N_2 respectively, then we write

$$N_1 = N\, e^{-(P_1-P)\alpha}$$

$$N_2 = N\, e^{-(P_2-P)\alpha}$$

$$\log\frac{N_2}{N_1} = -(P_2-P_1)\alpha$$

$$\log N_2 - \log N_1 = -(P_2-P_1)\alpha \qquad \ldots 3.1$$

Knowing all the parameters N_2, N_1 and P_2, P_1, the attenuation coefficient may be evaluated both graphically and analytically.

The day-to-day variation of pressure P at equatorial stations like Aligarh (Geomag. Lat. $\lambda = 23.7^{\circ}N$; Geomag. Long. = $355^{\circ}E$; Altitude H = 185.93 m; Cutoff Rigidity R = 14.85 GV) is very small of the order of 1 mm and seldom increases beyond 3 mm.

The pressure corrected neutron intensity N_p may be derived using the relationship

$$N_p = N \exp(\Delta_p \alpha)$$

where N is the observed neutron intensity (count rate) at pressure P and $\Delta_p = (P-P_o)$ is the difference between the observed pressure (P) and the standard pressure (P_o) which is basically chosen as the yearly average pressure at a particular station. Thus, the hourly pressure corrected data for neutrons reduced to a standard pressure (P_o) as described above forms the basic data for all further analysis.

3.2 Trend correction

While studying daily variation, sometimes the variation is not strictly periodic. Thus, if the numbers to be analysed represent bihourly (or hourly) mean of cosmic ray intensity, the mean for 0^{th} hour will not, in general, be the same as the mean for 24^{th} hour. This difference which is on account of secular changes etc., is allowed for in practice by applying a correction, generally referred as the trend correction (Yadava and Naqvi, 1973), to each of the terms (that is, 12 or 24 ordinates) except that forenoon.

To correct the data, let us consider the function $Y = F(t)$. Let Y_o is the value of the ordinate at $t = 0$ (0^{th} hour) and Y_{12} is the value of the ordinate at $t = 2\pi$ (24^{th} hour) in case of a bihourly data. It is found that sometimes the value of Y_o is not equal to Y_{12} due to the secular changes etc. Therefore, if $\bar{Y}_k$ or $\bar{Y}_{k'}$ represents the trend corrected values at $t = 2\pi k/12$ ($k = 0, 1, 2, \ldots, 12$)

or at $t = 2\pi(k' - 1)/12$ $(k' = 1, 2, 3, \ldots, 13)$ respectively, then the trend corrected values for any hour is given by the expressions

$$\bar{Y}_k = Y_k - \frac{\pm\Delta_Y \, k}{12} \qquad \ldots 3.2$$

where $k = 0, 1, 2, \ldots, 12$ and $\pm\Delta_Y = Y_{12} - Y_0$.

$$\bar{Y}_{k'} = Y_{k'} - \frac{\pm\Delta_{Y'} (k' - 1)}{12} \qquad \ldots 3.3$$

where $k' = 1, 2, 3, \ldots, 13$ and $\pm\Delta_{Y'} = Y_{13} - Y_1$. Y_k or $Y_{k'}$ represents the uncorrected value. Similarly, the trend correction for hourly data may also be applied.

3.3 Solar daily variation (anisotropies)

Even though the solar daily variation may be studied using different methods (Rao and Sarabhai, 1964; Kane, 1966), most of the qualitative information on the cosmic ray daily variation has been obtained through the study of the diurnal (I-Harmonic) and semidiurnal (II-Harmonic) components. The amplitude and phase of the harmonic components are usually derived by Fourier analysis (Chapman and Bartels, 1940) of the cosmic ray intensity data observed over a period of 24-hours, where it is implicitly assumed that the anisotropy remains constant for at least 24-hours. However, an indirect check of short term variation (< 24-hours) may be accomplished by comparing the amplitude and phase of the diurnal variation

observed at different stations having similar characteristics, but well distributed in longitude. A large discrepancy in either the amplitude or the phase indicates that either the anisotropy is changing within 24-hours or the universal time effects are predominant. Thus, the data obtained after applying the correction for secular changes is subjected to Harmonic analysis.

3.31 Harmonic analysis

Any single valued periodic function F(t), over a finite interval t = 0 to t = 2π, with 24 equidistant points within the interval, may be expressed in terms of a Fourier's series as follows,

$$F(t) = A_0 + \sum_{n=1}^{24} (A_n \text{ Cos } nt + B_n \text{ Sin } nt) \qquad \ldots 3.4$$

where A_0 is the mean value of F(t) in the interval 0 to 2π and A_n, B_n are coefficients of the n^{th} harmonic. These coefficients are given by

$$\left.\begin{aligned} A_0 &= \frac{1}{2\pi}\int_0^{2\pi} F(t)\,dt \\ A_n &= \frac{1}{\pi}\int_0^{2\pi} F(t) \text{ Cos } nt\,dt \\ B_n &= \frac{1}{\pi}\int_0^{2\pi} F(t) \text{ Sin } nt\,dt \end{aligned}\right\} \qquad \ldots 3.5$$

For 24-hourly cosmic ray intensity, these coefficients may also be expressed as follows

$$\left.\begin{aligned} A_0 &= \frac{1}{24} \sum_{i=1}^{24} R_i \\ A_n &= \frac{1}{12} \sum_{i=1}^{24} R_i \cos nt_i \\ B_n &= \frac{1}{12} \sum_{i=1}^{24} R_i \sin nt_i \end{aligned}\right\} \quad \ldots 3.6$$

The amplitude R_n and phase β_n of the n^{th} harmonic may be obtained from the expression

$$R_n \cos(nt - \beta_n) = A_n \cos nt + B_n \sin nt \quad \ldots 3.7$$

where

$$\left.\begin{aligned} R_n &= (A_n^2 + B_n^2)^{1/2} \\ \text{and} \quad \beta_n &= \text{Arc Tan } \left(\frac{B_n}{A_n}\right) \end{aligned}\right\} \quad \ldots 3.8$$

Since, the daily variation of the cosmic ray intensity may be adequately represented by the first two harmonics, it is customary to reconstruct the daily variation curve using these two harmonics for further study.

The Fourier coefficients for either 12-ordinates or 24-ordinates may conveniently be determined, without making use of computer, with the help of grouped terms method, as discussed by Yadava and Naqvi (1973). The 24-hourly cosmic ray intensity values, e.g., Y_0, Y_1, Y_2, ..., Y_{23} recorded at one hour interval, are grouped as shown in Table-3.1. From the Table-3.1, the harmonic coefficients are calculated as follows

TABLE - 3.1

	Y_0	Y_1	Y_2	Y_3	Y_4	Y_5	Y_6	Y_7	Y_8	Y_9	Y_{10}	Y_{11}	Y_{12}
		Y_{23}	Y_{22}	Y_{21}	Y_{20}	Y_{19}	Y_{18}	Y_{17}	Y_{16}	Y_{15}	Y_{14}	Y_{13}	
Sum	u_0	u_1	u_2	u_3	u_4	u_5	u_6	u_7	u_8	u_9	u_{10}	u_{11}	u_{12}
Diff.		v_1	v_2	v_3	v_4	v_5	v_6	v_7	v_8	v_9	v_{10}	v_{11}	

These sums and differences are again arranged as follows,

		u_0	u_1	u_2	u_3	u_4	u_5	u_6
		u_{12}	u_{11}	u_{10}	u_9	u_8	u_7	
	Sum	s_0	s_1	s_2	s_3	s_4	s_5	s_6
	Diff.	h_0	h_1	h_2	h_3	h_4	h_5	

and

		v_1	v_2	v_3	v_4	v_5	v_6	
		v_{11}	v_{10}	v_9	v_8	v_7		
	Sum	r_1	r_2	r_3	r_4	r_5	r_6	
	Diff.	s_1	s_2	s_3	s_4	s_5		

$$\left.\begin{aligned} A_0 &= \frac{1}{12}\sum_{m=0}^{6} g_m \\ A_1 &= \frac{1}{12}\sum_{m=0}^{5} h_m \cos\left(\frac{m\pi}{12}\right) \\ B_1 &= \frac{1}{12}\sum_{m=1}^{6} r_m \sin\left(\frac{m\pi}{12}\right) \\ A_2 &= \frac{1}{12}\sum_{m=0}^{6} g_m \cos\left(\frac{m\pi}{6}\right) \\ B_2 &= \frac{1}{12}\sum_{m=1}^{5} s_m \sin\left(\frac{m\pi}{6}\right) \end{aligned}\right\} \quad \ldots 3.9$$

The amplitude and phase of the diurnal and semidiurnal anisotropy are obtained by substituting the value obtained from expression 3.9 in expression 3.8. In determining the value of the phase β_n, it is necessary that the correct quadrant is determined. Let the phase angle γ_n be defined in terms of β_n depending on the sign of A_n and B_n as given below

A_n	B_n	γ_n
+	+	β_n
+	-	$180^\circ - \beta_n$
-	-	$180^\circ + \beta_n$
-	+	$360^\circ - \beta_n$

The standard errors of the harmonic coefficients for long period depend upon the distribution of 'cloud of points'. We assume that the hourly counts follow a standard Gaussian

distribution. The mean and standard deviation are obtained from the individual values of A and B, by calculating the harmonic coefficients for each day during any length of period.

$$\left.\begin{aligned} \bar{A} &= \frac{1}{N}\sum_{i=1}^{N} A_i \\ \bar{B} &= \frac{1}{N}\sum_{i=1}^{N} B_i \end{aligned}\right\} \quad \ldots 3.10$$

$$\left.\begin{aligned} \sigma_A^2 &= \frac{1}{N-1}\sum_{i=1}^{N} (A_i - \bar{A})^2 \\ \sigma_B^2 &= \frac{1}{N-1}\sum_{i=1}^{N} (B_i - \bar{B})^2 \end{aligned}\right\} \quad \ldots 3.11$$

where N denotes for the number of days used in the analysis. The standard error of the mean is given by

$$\left.\begin{aligned} \sigma_{\bar{A}} &= \frac{\sigma_A}{N} \\ \sigma_{\bar{B}} &= \frac{\sigma_B}{N} \end{aligned}\right\} \quad \ldots 3.12$$

Thus, the standard error in the mean amplitude will be

$$\sigma_R^2 = \frac{A^2}{(A^2 + B^2)}\sigma_{\bar{A}}^2 + \frac{B^2}{(A^2 + B^2)}\sigma_{\bar{B}}^2 \quad \ldots 3.13$$

if $\sigma_{\bar{A}} = \sigma_{\bar{B}}$; we have

$$\sigma_R = \sigma_{\bar{A}} = \sigma_{\bar{B}}$$

Similarly, the standard error in the determination of the phase will be

$$\sigma_{\phi}^2 = \frac{B^2}{(A^2 + B^2)^2}\sigma_{\bar{A}}^2 + \frac{A^2}{(A^2 + B^2)^2}\sigma_{\bar{B}}^2 \qquad \ldots 3.14$$

if $\sigma_{\bar{A}} = \sigma_{\bar{B}}$, we have

$$\sigma_{\phi} = \frac{\sigma_R}{R}$$

3.32 Graphical representation of daily variation

The amplitude and phase of both the harmonics may be represented graphically in a harmonic dial or clock diagram either as a (i) vector addition diagram with vectors starting at the end point of the previous vector, or as a (ii) cloud of points having their origin at a fixed point. In the study of the daily variation of cosmic rays, both of these representations are very commonly used.

3.4 Asymptotic cone of acceptance of a detector

The knowledge of the dependence of the counting rate on the asymptotic direction is essential for studying the time variation of cosmic rays. The asymptotic direction of approach of any particle incident at a given point on the surface of the Earth is defined as the direction prior to its entry into the geomagnetic field. Evaluation of the asymptotic directions has been performed either through model experiments in which a small model of the Earth and its field is used to simulate or through numerical methods. The asymptotic directions of

approach of different rigidities have been evaluated through numerical integration of the equation of motion of the particle in the six degree simulation of the geomagnetic field (McCracken et al., 1962). The asymptotic direction of approach for a number of neutron monitoring stations for different rigidities and incident directions have been published by McCracken et al., 1965; Shea et al., 1968.

In all such studies, Rao et al. (1963) have shown that it is very convenient to use the concept of the 'asymptotic cone of acceptance of a detector'; this may be defined as the solid angle containing those asymptotic directions of approach which make a significant contribution to the counting rate of the detector. Figure-3.1 shows plots of the asymptotic directions of approach of particles of selected rigidities between 2 and 100 GV and directions of approach into the atmosphere with zenith angles of 0°, 16° and 32° in the north-south and east-west geomagnetic planes, for four locations. It is quite clear from the Figure-3.1 that the geomagnetic field has the effect of causing the phase, and amplitude of a time variation that is due to any anisotropy in the cosmic radiation to vary from station to station and also to a lesser extent, from detector to detector at any one station.

3.41 Cosmic ray variational coefficient

For an arbitrary anisotropy of cosmic radiation in space, the counting rate of a ground based detector is given by

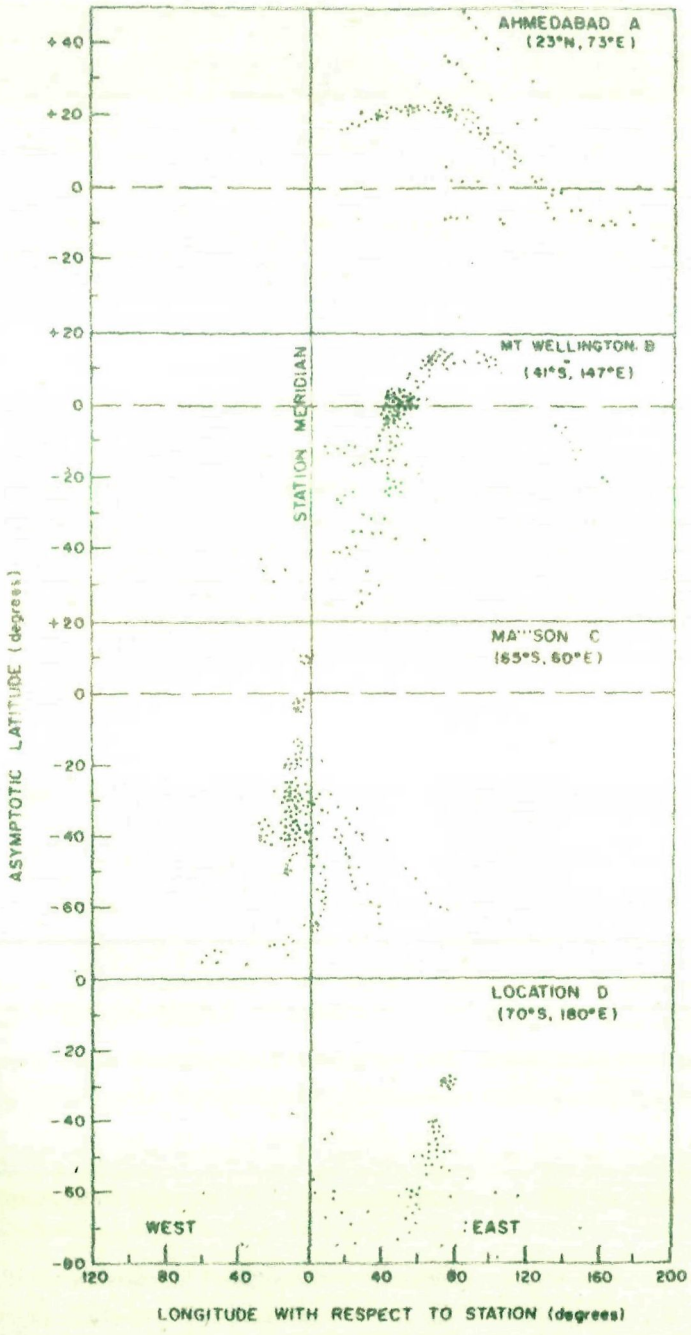

Fig. 3.1 - The asymptotic direction of approach for particles arriving at four different locations. Location 'D' has the same geomagnetic latitude as Mawson (after Rao et al. 1963).

$$dC_i = J_i(R)\, T(R, \theta, \phi)\, d\omega\, dR$$

$$= J_i(R)\, S(R)\, Z(\theta, \phi)\, d\omega\, dR \qquad \ldots 3.15$$

where $J_i(R)$ is the differential cosmic ray intensity from all directions within the i^{th} solid angle Ω_i, $T(R, \theta, \phi)$ is a characteristics of the atmosphere and is assumed to be a separable function of rigidity and direction, viz. the product of $S(R)$ and $Z(\theta, \phi)$, $d\omega$ is the solid angle subtended by the particle flux at the top of the atmosphere. Integrating over all directions θ, ϕ which are accessible to the monitor from Ω_i, we have

$$\Delta C(\Omega_i, R) = J_i(R)\, S(R)\, Y(\Omega_i, R)\, dR \qquad \ldots 3.16$$

For isotropic cosmic radiation, that is, the intensity from all asymptotic directions is $J_o(R)$, the total counting rate due to rigidities between R and R + dR is given by

$$\Delta C(4\pi, R) = J_o(R)\ S(R)\ Y(4\pi, R)\ dR \qquad \ldots 3.17$$

Dorman (1957) has defined the coupling constant $W(R)$ of a detector as

$$W(R) = \frac{1}{N} \frac{dC}{dR} \qquad \ldots 3.18$$

where dC is the counting rate due to the radiation in the rigidity range R to R + dR, and N is the total counting rate corresponding to the cosmic ray spectrum, $J_o(R)$. From the

above definitions, it is seen that $\Delta C(4\pi, R)$ in Equation-3.17 is identical to dC in Equation-3.18, and hence, equating these two quantities we have

$$S(R) = \frac{N\, W(R)}{J_0(R)\, Y(4\pi, R)} \qquad \ldots 3.19$$

and substituting in Equation-3.16, we get

$$\Delta C(\Omega_i, R) = N\, W(R)\, \frac{J_i(R)}{J_0(R)}\, \frac{Y(\Omega_i, R)}{Y(4\pi, R)}\, dR \qquad \ldots 3.20$$

We write $J_i(R) = J_0(R) + \Delta J_i(R)$, where $\Delta J_i(R)$ differs from one Ω_i to the next. Equation-3.20, after integration over R, becomes

$$C(\Omega_i) = N \int W(R) \left[1 + \frac{\Delta J_i(R)}{J_0(R)}\right] \frac{Y(\Omega_i, R)}{Y(4\pi, R)}\, dR$$

$$\frac{dN(\Omega_i)}{N} = \frac{C(\Omega_i) - C_0(\Omega_i)}{N}$$

$$= \int W(R)\, \frac{\Delta J_i(R)}{J_0(R)}\, \frac{Y(\Omega_i, R)}{Y(4\pi, R)}\, dR \qquad \ldots 3.21$$

where $C(\Omega_i)$ and $C_0(\Omega_i)$ are the counting rates due to particle fluxes $J_i(R)$ and $J_0(R)$ arriving from within the solid angle Ω_i. The quantity $dN(\Omega_i)/N$ is the fractional change in total counting rate produced by the cosmic ray intensity from Ω_i deviating from $J_0(R)$ by an amount $\Delta J_i(R)$. Let us assume that $\Delta J_i(R)/J_0(R)$ is a power law in rigidity, written as AR^{β} where A is a function of asymptotic direction. Thus,

the observed anisotropy may be given by

$$\frac{dN(\Omega_i)}{N} = A\, v(\Omega_i, \beta) \qquad \ldots 3.22$$

where $v(\Omega_i, \beta)$ is called the variational coefficient of the detector corresponding to the solid angle Ω_i and spectral exponent β. If the cosmic ray intensity from within solid angle Ω_i is $J_o(1 + A_i R^{\beta})$ and from all other directions is J_o, then the counting rate of an instrument will differ by an amount ΔN from the counting rate N, given by

$$\frac{\Delta N}{N} = v(\Omega_i, \beta)\, A_i$$

$J_o A_i R^{\beta}$ is the anisotropic component of the radiation that arrives from all directions within the solid angle Ω_i.

3.42 Evaluation of the variational coefficient

The elementary solid angle Ω_i is defined by planes of constant geographic longitudes spaced 5° apart and by surfaces of constant geographic latitude space every 5° on either side of the equator. For evaluating variational coefficients, cosmic ray particles of various rigidities arriving from nine specific directions, viz., vertical, geomagnetic north, south, east and west at zenith angles of 16° and 32° are used. The approximate summation for $v(\Omega_i, \beta)$ is given by the expression

$$v(\Omega_i, \beta) = \sum_k W(R_k)\, R_k^{\beta}\, \frac{Y(\Omega_i, R_k)}{Y(4\pi, R_k)}\, \frac{R_{k+1} - R_{k-1}}{2} \qquad \ldots 3.23$$

where the summation extends from near cutoff rigidity to a value R_{max}.

Expressing the anisotropy as a power law in rigidity, we have

$$\frac{\Delta J_i(R)}{J_o(R)} = A\, R^{\beta} = f(\chi)\, \cos\Lambda\, R^{\beta} \qquad \ldots 3.24$$

where A is the amplitude of the anisotropy, which is a separable function of the asymptotic latitude Λ and longitude χ and varies as cosine of declination. The fractional change in the total counting rate produced by the radiation from Ω_i may be written as

$$\frac{dN(\Omega_i)}{N} = f(\chi)\, v(\Omega_i, \beta)\, \cos\Lambda \qquad \ldots 3.25$$

Summing over all Ω_i, Equation-3.25 gives

$$\frac{dN(\chi_j)}{N} = f(\chi_j) \sum v(\Omega_i, \beta)\, \cos\Lambda$$

$$= f(\chi_j)\, V(\chi_j, \beta) \qquad \ldots 3.26$$

where $dN(\chi_j)$ is the solid angle defined by the two meridional planes 2.5° on either side of the meridional plane at geographic longitude χ_j. The modified variational coefficients, $V(\chi_j, \beta)$ have been evaluated for a number of stations for ten

values of β ranging from -1.5 to +0.6 by McCracken et al. (1965) and Shea et al. (1968). The calculations for values of β going upto +2.0 and for varying values of upper cutoff rigidity (R_{max}) have been extended by Agrawal (1973). It is interesting to note that the variational coefficients for $\beta = 0.0$ represent the manner in which the cosmic ray particles from different asymptotic longitudes contribute to the total counting rate of a detector.

3.43 Application to daily variation

The amplitude and phase of any anisotropy of cosmic radiation in space may be predicted from the knowledge of variational coefficients and observations at various stations. Let us consider an anisotropy that is an arbitrary function of direction η and that may be expanded as a Fourier series

$$f(\eta) = J_0(R) \sum_{m=1} a_m \cos m(\eta - \alpha_m) \qquad \ldots 3.27$$

where a_m and α_m are arbitrary amplitude and phase constants, and α_m is the direction of viewing from which a maximum of the m^{th} harmonic is seen. From the Figure-3.2, $\eta = \chi + 15T - 180^\circ$ and the intensity from asymptotic longitude χ may be written as

$$f(\chi) = J_0(R) \sum_{m=1}^{\infty} a_m \cos m(\chi + 15T - 180^\circ - \alpha_m) \qquad \ldots 3.28$$

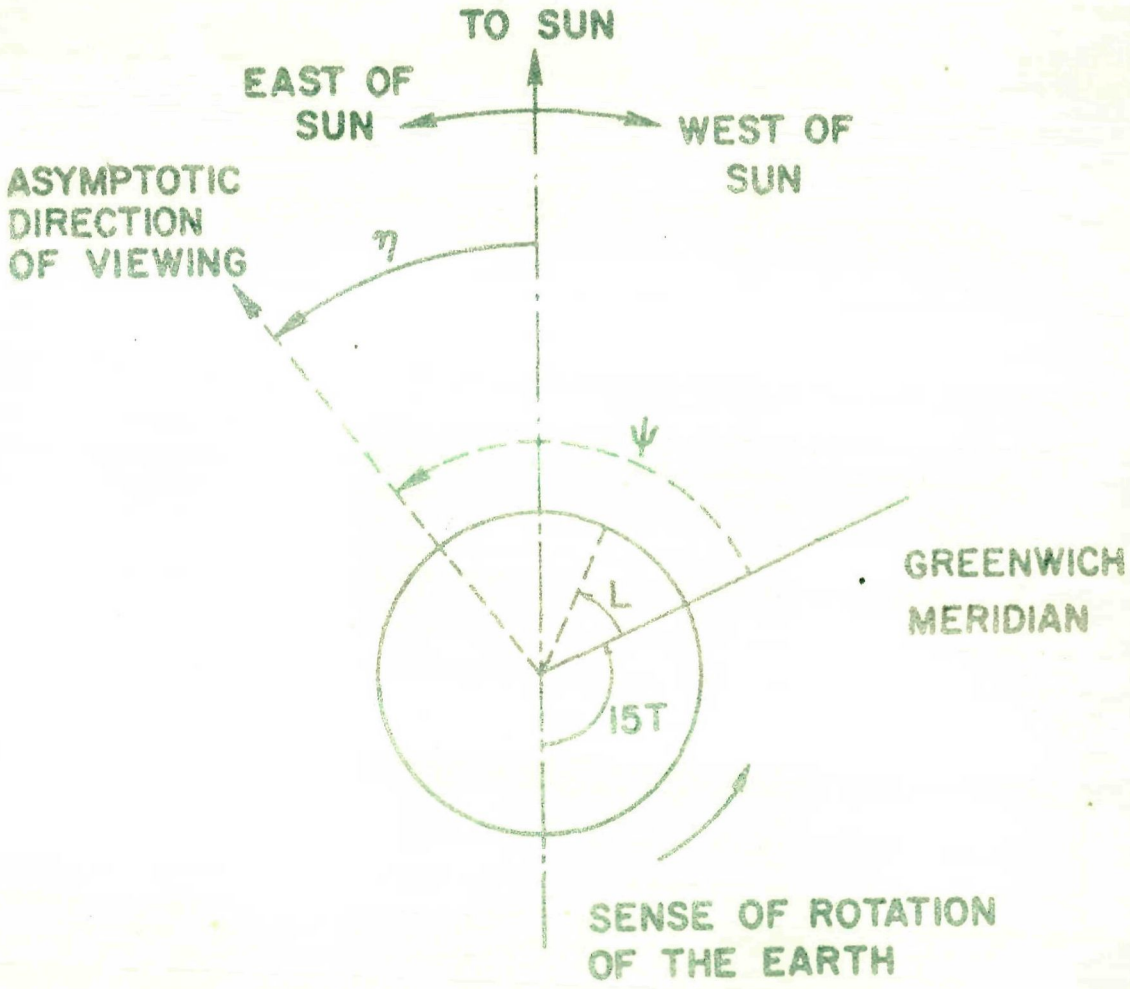

Fig. 3.2 - Defining the angles employed to specify the asymptotic direction of viewing of an arbitrary station (after Rao et al. 1963).

where asymptotic longitude $\chi_i = (5i + 2.5)^\circ$, the mean longitude of all the particles arriving from the solid angles lying between $\chi_i = 5i^\circ$ and $\chi_i = 5(i+1)^\circ$.

Substituting the value of $f(\chi_i)$ in Equation-3.26 and summing over i, the deviation, $N(T)$, from the mean value N of the counting rate of a detector at time T becomes

$$\frac{\Delta N(T)}{N} = \sum_{i=0}^{71} V(\chi_i, \beta) \sum_{m=1}^{\infty} a_m \cos m(5i + 2.5 + 15T - 180^\circ - \alpha_m)$$

$$= \sum_{m=1}^{\infty} a_m B_m \cos \left[m(15T - 180^\circ - \alpha_m) + \gamma_m \right] \quad \ldots 3.29$$

where

$$B_m^2 = \left[\sum_{i=0}^{71} V(\chi_i, \beta) \sin m(5i + 2.5)\right]^2 +$$

$$\left[\sum_{i=0}^{71} V(\chi_i, \beta) \cos m(5i + 2.5)\right]^2$$

and

$$\tan \gamma_m = \frac{\sum_{i=0}^{71} V(\chi_i, \beta) \sin m(5i + 2.5)}{\sum_{i=0}^{71} V(\chi_i, \beta) \cos m(5i + 2.5)}$$

where a_m B_m and $(-m\alpha_m + \gamma_m)$ represent the amplitude and phase constants of the m^{th} harmonic. The universal time at which the maximum intensity is observed is given by

$$T_m = \frac{180\,m + m\alpha_m - \gamma_m}{15\,m} \text{ hours}$$

and the local time of maximum intensity is $t_m = T_m + (L/15)$ where L is the geographic longitude of the station. The quantity $(\gamma_m - mL)/15\ m$ is named as the 'geomagnetic bending' of the cosmic ray flux.

3.5 Estimation of rigidity exponent (β) and upper cutoff rigidity (R_{max})

If the observed daily variation is due to a spatial anisotropy in interplanetary medium, the direction and amplitude of the anisotropy as determined by different stations should be the same within the limits of statistical error. Therefore, the best estimate of the value of rigidity exponent and the upper cutoff rigidity upto which the daily variation exists, may be estimated with the data observed at a number of stations, imposing the condition that there must be a minimum variance among the observations as determined from χ^2 statistics. Let us consider that $A_i(\beta, R_{max})$ and $\phi_i(\beta, R_{max})$ are the amplitudes and phases in space obtained for the i^{th} station after correction for the geomagnetic effects and $\bar{A}(\beta, R_{max})$ and $\bar{\phi}(\beta, R_{max})$ are the corresponding mean values in space obtained for N stations, the normalised variance χ^2 for each value of β and R_{max} is given by

$$\chi^2 = \frac{1}{N} \sum_{i=1}^{N} \left[\frac{\{A_i(\beta, R_{max}) - \bar{A}(\beta, R_{max})\}^2}{\bar{A}^2(\beta, R_{max})} + \frac{\{\phi_i(\beta, R_{max}) - \bar{\phi}(\beta, R_{max})\}^2}{\bar{\phi}^2(\beta, R_{max})} \right] \quad \ldots 3.30$$

If the values of χ^2, corresponding to various sets of β and R_{max}, are plotted, the minimum value of the variance χ^2 gives the most probable value of β, R_{max}, $\bar{A}$ and $\bar{\beta}$.

C H A P T E R - IV

CHARACTERISTICS OF THE DIURNAL ANISOTROPY

4.1 Introduction

The characteristics of the diurnal anisotropy of cosmic ray intensity, on yearly average basis as determined by neutron and meson monitor observations, were generally found as time invariant for the period earlier to 1970. This was particularly true in case of neutron monitor observations for the period from the International Geophysical Year (IGY) to 1970 (Rao, 1972). The time invariant hypothesis was generally accepted, because no systematic neutron observations were available before IGY period and also there is an ambiguity in the temperature correction for meson observations for which the data exists for a much longer period. On the basis of the observations presented in this chapter, it is observed that the diurnal anisotropy is time invariant on quiet days also for the period 1964-70 at all the latitudes in accordance with the observations found on yearly average basis. In this chapter, therefore, an entirely maiden approach has been made to study the long term variations in the diurnal anisotropy of cosmic ray intensity using the observational data from all the available neutron monitoring stations for the period 1964-76 on various types of days, namely-quiet days, magnetic storms days, disturbed days and disturbed days

without magnetic storms.

The large variations in the diurnal anisotropy of cosmic ray intensity indicate that continuous and large variations occur in interplanetary space, affecting the spatial distribution of cosmic ray intensity as well as producing geomagnetic variations. Ballif et al. (1969) observed that daily geomagnetic index represented by ΣK_p or A_p correlates well with genuine interplanetary measurements of the mean fluctuation in amplitude of the interplanetary magnetic field (I.M.F.) which is related with the diffusive component of the simple convection-diffusion theory. A_p is also found to be positively correlated with the solar wind velocity which is related with the convective component of the simple convection-diffusion theory. Thus, the variation of A_p-index may affect both the components (e.g., diffusive and convective components as discussed above), the degree of influence to each component is not known at present. In general, A_p is related with I.M.F., its gradient and solar wind velocity by a functional relationship $A_p = F(\bar{B}, \nabla \times \bar{B}, V)$. A_p may also be affected with some other unknown parameters in and out of the ecliptic plane.

The variation of A_p-index on quiet, magnetic storms and disturbed days and disturbed days without magnetic storms has been plotted in Figure-4.1 which illustrates that on quiet days the changes in A_p-index are minimum whereas the values of A_p-index on magnetic storms days are maximum. Therefore, to know the influence of varying A_p-index on the observed diurnal and

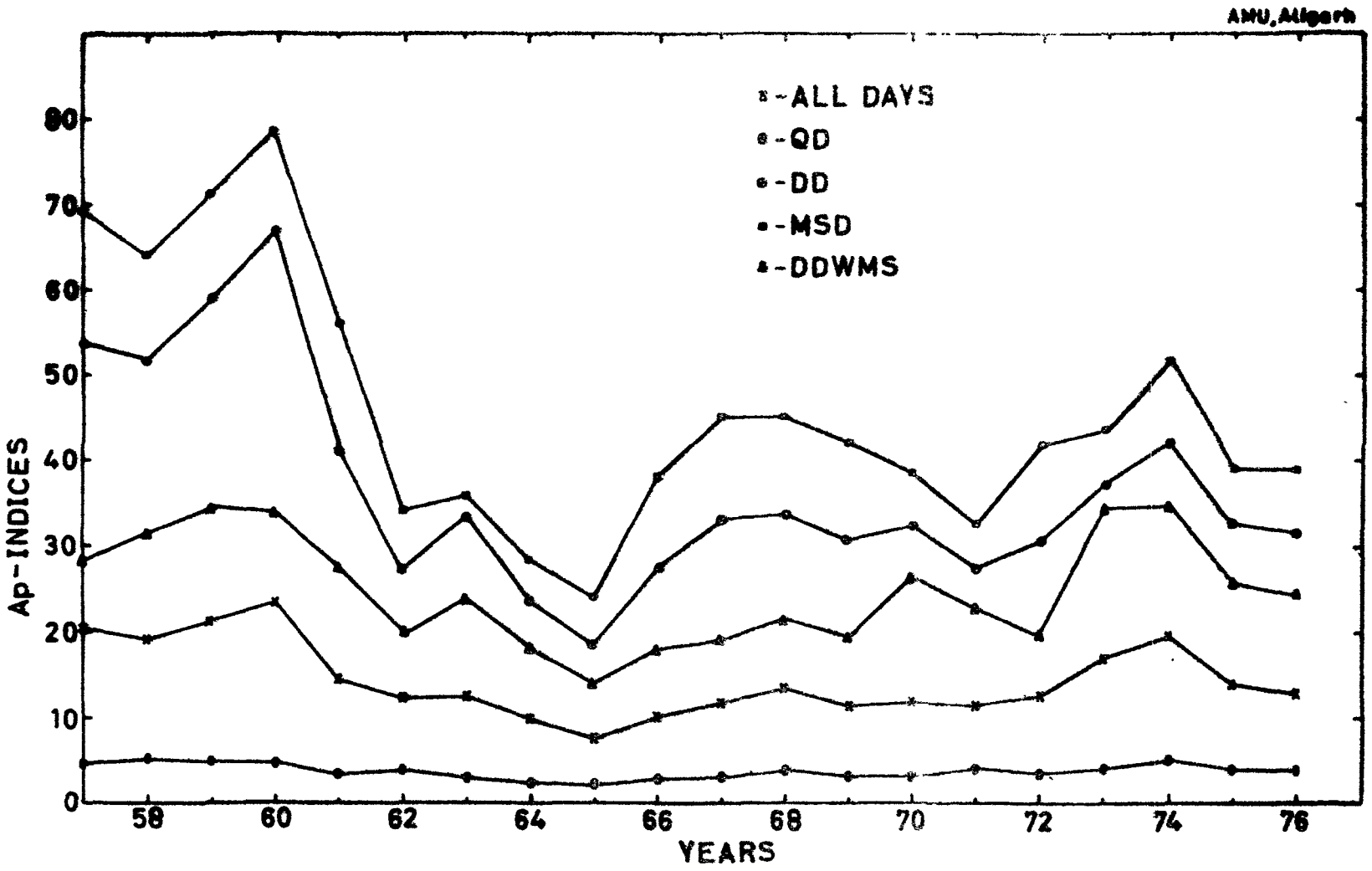

Fig. 4.1 - Variation of A_p-index during the period 1957-76 on all days, QD, DD, MSD and DDWMS.

semi-diurnal anisotropy, we have determined the statistical distribution of the diurnal and semi-diurnal anisotropy with varying values of A_p-index for the period 1964-76 making four groups e.g., (i) quiet days (QD), (ii) magnetic storms days (MSD), (iii) disturbed days (DD), and (iv) disturbed days without magnetic storms (DDWMS). It has been observed that the nature of the long term daily variation of cosmic ray intensity, particularly on QD, is comparable to the results on yearly average basis where all the days in a year are considered.

Furthermore, an attempt has been made to determine the detailed characteristics of the diurnal anisotropy and to compare them with the earlier observations, so as to define the long term variability of the diurnal anisotropy. Attempt has also been made for understanding these variations in terms of the existing theoretical models and with the changing interplanetary conditions. Wherever necessary, the results from other detectors have also been used to confirm our results and also to find additional information regarding energy spectrum and upper cutoff rigidity to supplement the neutron monitor observations. For investigating the detailed nature of the diurnal anisotropy variation and for finding the clue for its occurrence, the changes in a number of geophysical, interplanetary and solar parameters are investigated and their relationships have been determined. Thus, the analytical results

presented in this chapter may provide the gross as well as fine structure of the diurnal anisotropy and the plausible explanations for each of them. At the end, a composite model has been presented alongwith the possibility of further investigation in this direction.

4.2 Observational results

The pressure corrected hourly neutron monitor data, after applying trend correction (Yadava and Naqvi, 1973), is harmonically analysed to have the amplitude and phase of the diurnal anisotropy for each day. Such an analysis of the cosmic ray intensity data has been performed separately on QD, MSD, DD and DDWMS for the neutron monitoring stations listed in Table-4.1 and are also diagrammatically shown in Figure-4.2 to show a wide coverage both in latitude and longitude. The total number of days used for the analysis on different types of days and for the period 1964-76 are given in Table-4.2. The yearly average amplitude and phase are then calculated from the daily vectors separately on different types of days. The days with large Forbush decrease or sharp increase type, if any, are excluded from the analysis.

4.21 Spectral component of diurnal anisotropy

The average diurnal anisotropy of cosmic ray intensity may be represented by the spectrum of the type given by

TABLE - 4.1

Geographic coordinates for the neutron monitoring stations, whose data have been utilised for studying the daily variation of cosmic ray intensity on quiet, disturbed and magnetic storms days and disturbed days without magnetic storms.

S.No.	Station Name	Code	Vertical Cutoff Rigidity** (in GV)	Geographic Coordinates Latitude (in deg)	Geographic Coordinates E.Longitude (in deg)	Altitude (meters)	Hourly Counting Rate ($\times 10^5$)	Standard Error*** in B_1 (%)	Standard Error*** in B_2 (%)
1	Ahmedabad, India	AHM	15.94	23.01	72.61	0	1.87	.045	.005
2	Aligarh*, India	ALI	14.85	27.95	78.07	186	-	-	-
3	Tokyo-Kokushi, Japan	TOK	11.61	35.75	139.72	20	4.53	.010	.003
4	Mt.Norikura, Japan	NOR	11.39	36.12	137.56	2770	6.68	.008	.002
5	Seoul, Korea	SEO	10.79	37.58	127.05	50	1.01	.015	.005
6	Athens, Greece	ATH	8.72	37.97	23.72	110	8.89	.006	.001
7	Alma-Ata, USSR	ALM	6.69	43.25	76.92	806	0.35	.018	.006
8	Rome, Italy	ROM	6.32	41.90	12.52	60	2.95	.012	.004
9	Pic-du-Midi, France	PIC	5.36	42.93	0.25	2860	2.50	.012	.004
10	Dallas, USA	DAL	4.35	32.78	263.20	208	7.56	.008	.002
11	Climax, USA	CLI	3.05	39.37	253.83	3400	3.97	.010	.003
12	Kiel, FRG	KIE	2.29	54.35	10.13	54	6.28	.008	.002
13	Leeds, England	LEE	2.20	53.83	358.42	100	6.72	.008	.002
14	Chicago, USA	CHI	1.72	41.83	272.33	0	0.24	.018	.006
15	Uppsala, Sweden	UPP	1.43	59.85	17.58	0	0.58	.018	.006
16	Mt.Washington, USA	WAS	1.24	44.28	288.70	1909	1.45	.015	.005
17	Sulphur Mt., Canada	SUL	1.14	51.20	244.39	2283	8.82	.006	.001
18	Calgary, Canada	CAL	1.09	51.08	245.91	1130	1.18	.015	.005
19	Ottawa, Canada	OTT	1.08	45.40	284.40	57	1.95	.015	.005
20	Deep River, Canada	DEE	1.02	46.10	282.50	145	20.85	.006	.001
21	Goose Bay, Canada	GOO	0.52	53.33	299.58	46	7.00	.008	.002
22	Churchill, Canada	CHU	0.21	58.75	265.91	39	7.35	.008	.002
23	Inuvik, Canada	INU	0.18	68.35	226.27	21	6.92	.008	.002
24	Resolute, Canada	RES	0.05	74.69	265.09	17	2.16	.012	.004
25	Alert, Canada	ALE	0.00	82.50	297.67	66	7.08	.008	.002

* The Cosmic Ray Intensity Data is under Study.
** Ground-based Cosmic Ray Instrumentation Catalog-AFCRL-72-0411. No. 243 - Shea, M.A. (1972)
***Standard error in harmonic coefficient (Each day).

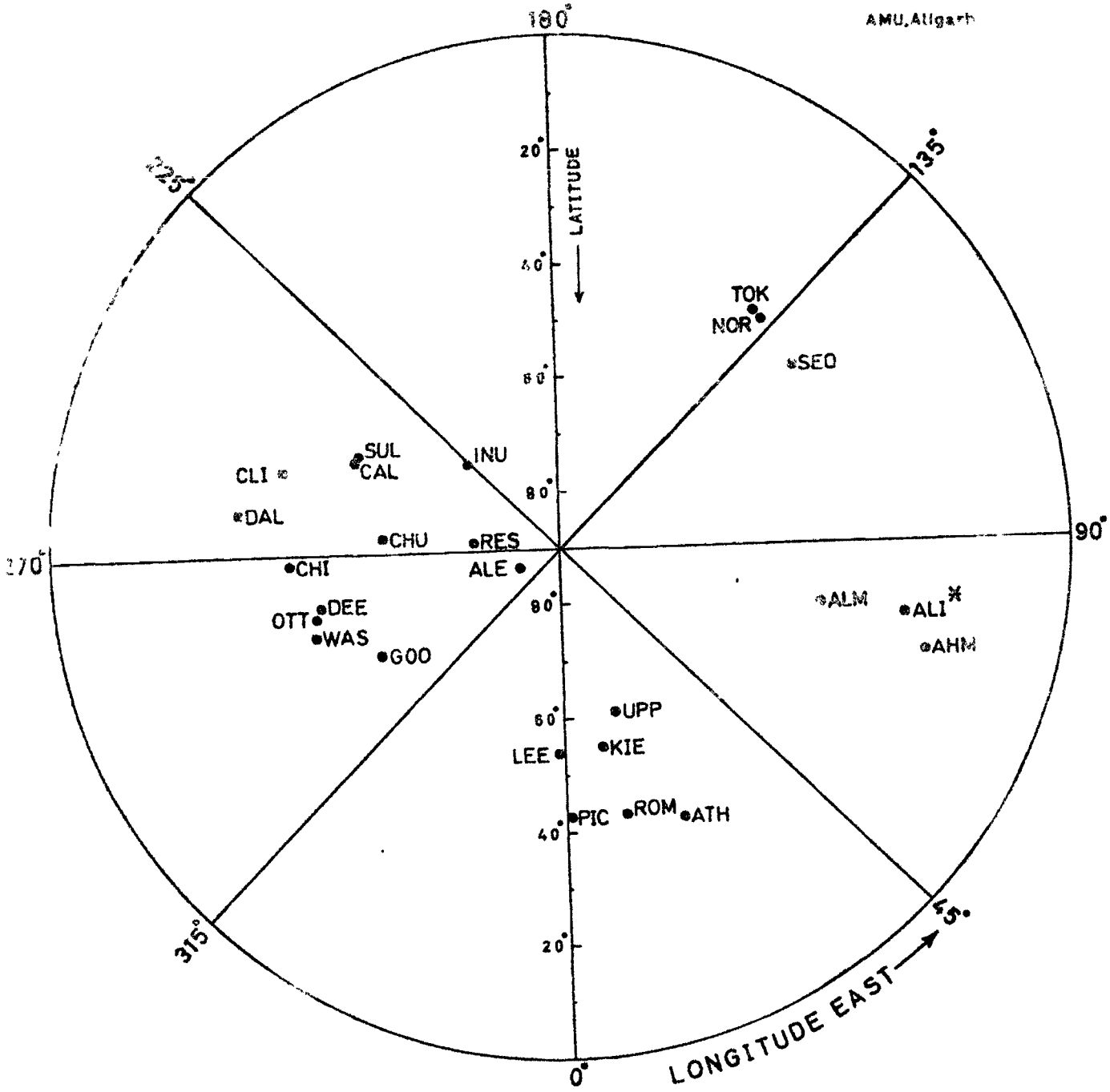

Fig. 4.2 - Illustrates the geographical latitudes and longitudes of the neutron monitoring stations used in the analysis. Mark * shows the location of Aligarh Neutron Monitor.

TABLE - 4.2

Number of days used for analysis on quiet-, disturbed-, magnetic storms-days and disturbed days without magnetic storms.

Year	Quiet Days	Disturbed Days	Magnetic Storms Days	Disturbed Days Without Magnetic Storms
1964	60	60	33	27
1965	60	60	28	32
1966	60	60	28	32
1967	60	60	32	28
1968	60	60	31	29
1969	60	60	30	30
1970	60	60	29	31
1971	60	60	34	26
1972	60	60	42	18
1973	60	60	39	21
1974	60	60	34	26
1975	60	60	23	37
1976	60	60	26	34

Equation-1.17. Eventhough there exists a large variability in the spectral characteristics of the diurnal anisotropy on a day-to-day basis but the annual average diurnal anisotropy has been observed generally consistent with an energy independent spectra and $R_{max} \simeq 100$ GV. We have determined the spectral exponent, β and upper limiting rigidity, R_{max} of the diurnal anisotropy for different groups (mentioned in Sec. 4.1) using the data from all the available stations for each year during the period 1964-74 by using the method described in Section-3.5. The best fit value of β is one for which the variance among the various values of anisotropy vectors estimated from different stations is minimum.

4.211 On quiet days

The Figure-4.3(a) shows the plots for the variance of the diurnal anisotropy on QD versus the spectral exponent for the period 1964-74. It is quite clear from the Figure-4.3(a) that on QD the variance is minimum for $\beta \simeq 0 \pm 0.2$ with $R_{max} \simeq 100$ GV, during the period 1964-70. Thus, the observed characteristics of the diurnal anisotropy on QD are consistent with the characteristics of the diurnal anisotropy on yearly average basis for the period 1964-70 (Agrawal et al., 1972). These results are in accordance with the predictions of the simple convection-diffusion theory. However, the variance obtained for the period 1971-74 on QD shows that the value of

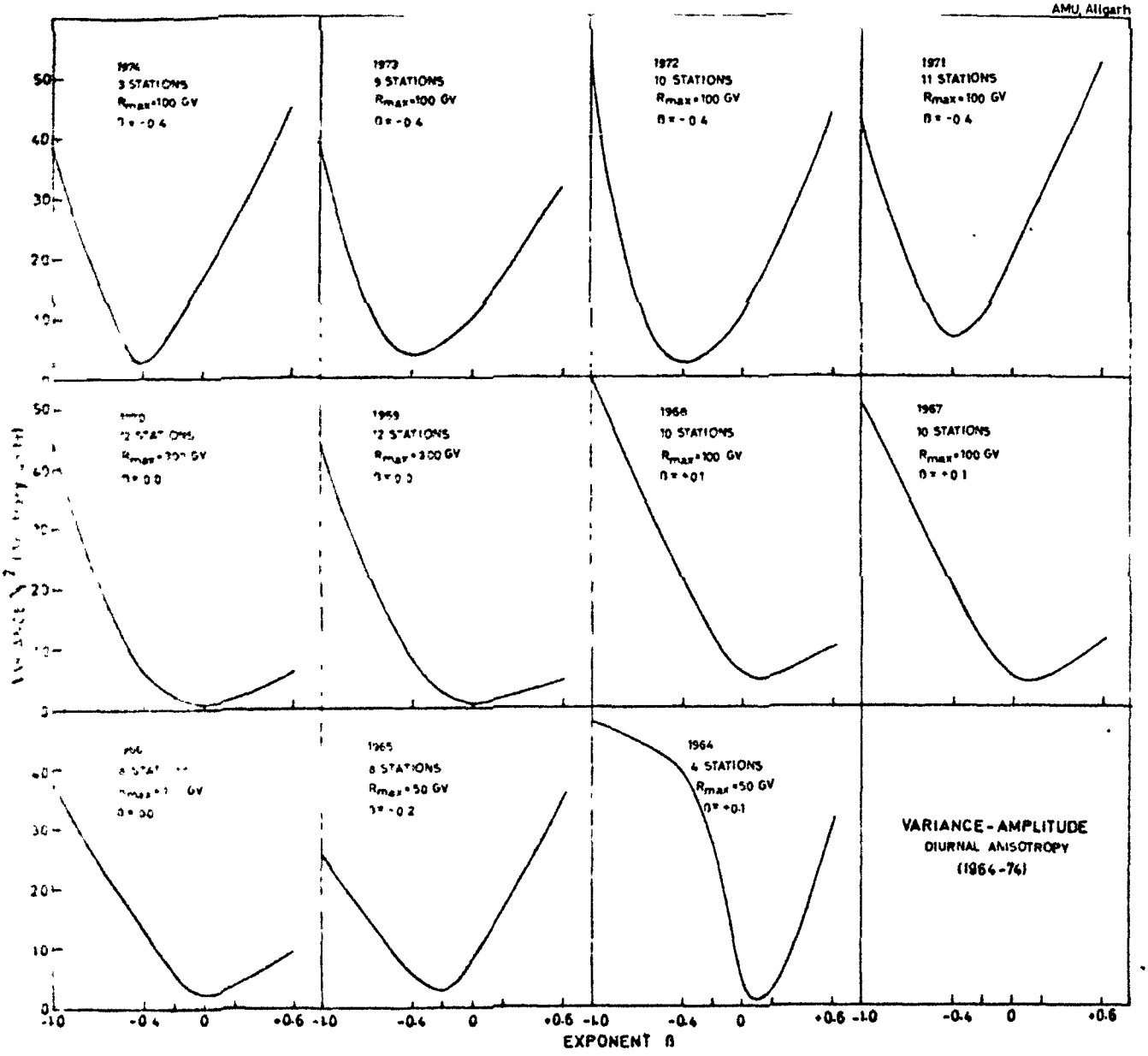

Fig. 4.3 - The observed variance between the diurnal amplitude in space calculated for each station as a function of the exponent β for each year during 1964-74. (a) - QUIET DAYS.

$\beta \simeq -0.4 \pm 0.2$ for the same value of $R_{max} = 100$ GV. This indicates that superimposed on the corotational (also known as azimuthal or tangential) anisotropy, expected from a balance between outward radial convection and inward field alligned diffusion, there is an additional component operating during this period with $\beta \neq 0$.

4.212 On magnetic storms days

Figure-4.3(b) shows that for the diurnal anisotropy on MSD the variance is minimum for the value of $\beta \simeq 0 \pm 0.2$ during the period 1964-74 except during 1966-67 where $\beta \simeq -0.4 \pm 0.2$. In the year 1968, the value of β is indeterminable. Thus, this varying nature of the spectral exponent on MSD indicates that superimposed on corotational anisotropy there is an extra component of the cosmic ray streaming operative on MSD during the entire period 1964-74. It may be outward radial streaming component, which is somewhat smaller, directed along the Earth-Sun line (Quenby and Hashim, 1969). However, the corotational anisotropy is dominating during most of the time.

4.213 On disturbed days and disturbed days without magnetic storms

Figures-4.3(c) and 4.3(d) show the plots for the variance of the diurnal anisotropy on DD and on DDWMS versus the spectral exponent β respectively. It is quite apparent from

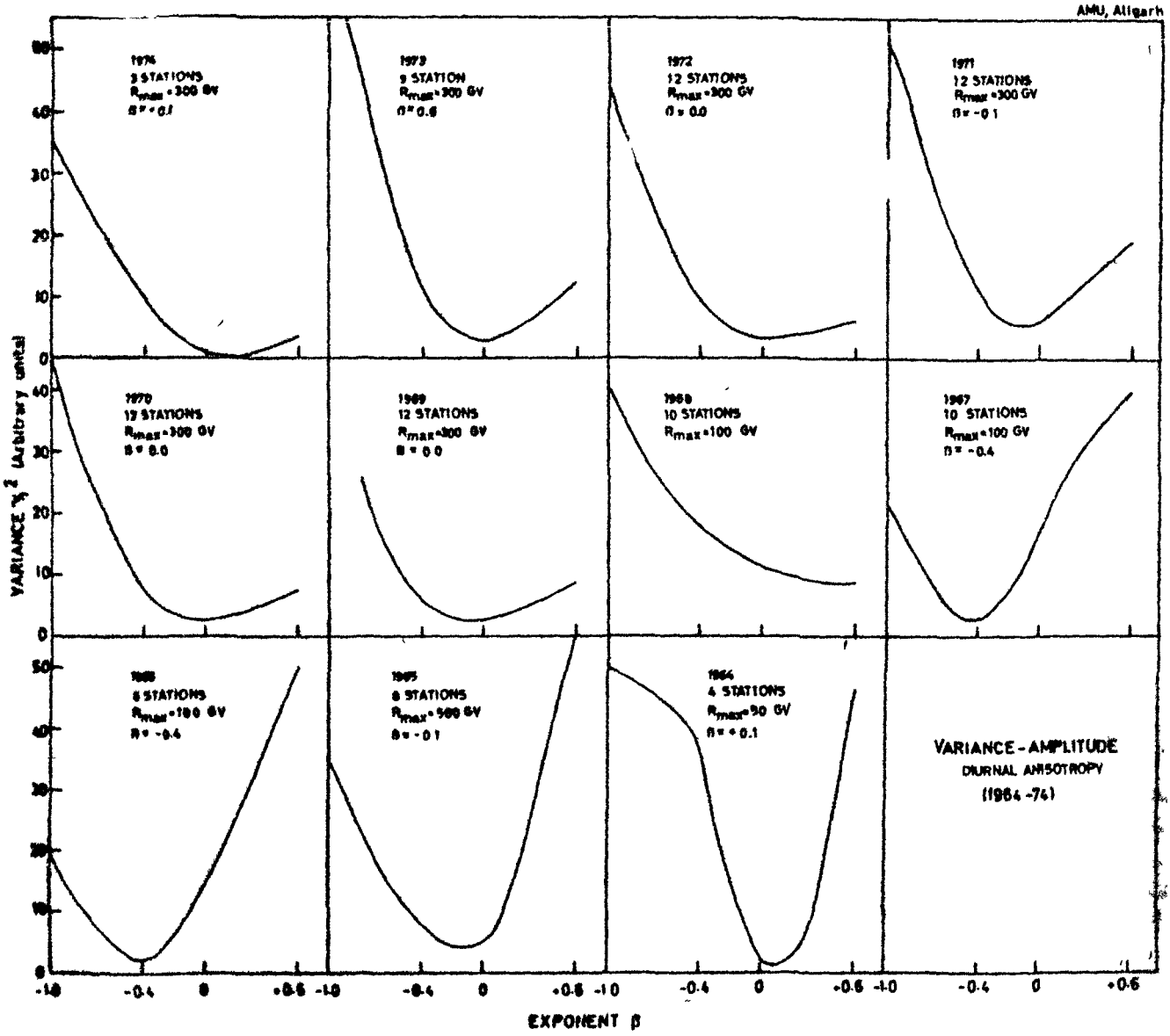

Fig. 4.3(b) - MAGNETIC STORM DAYS

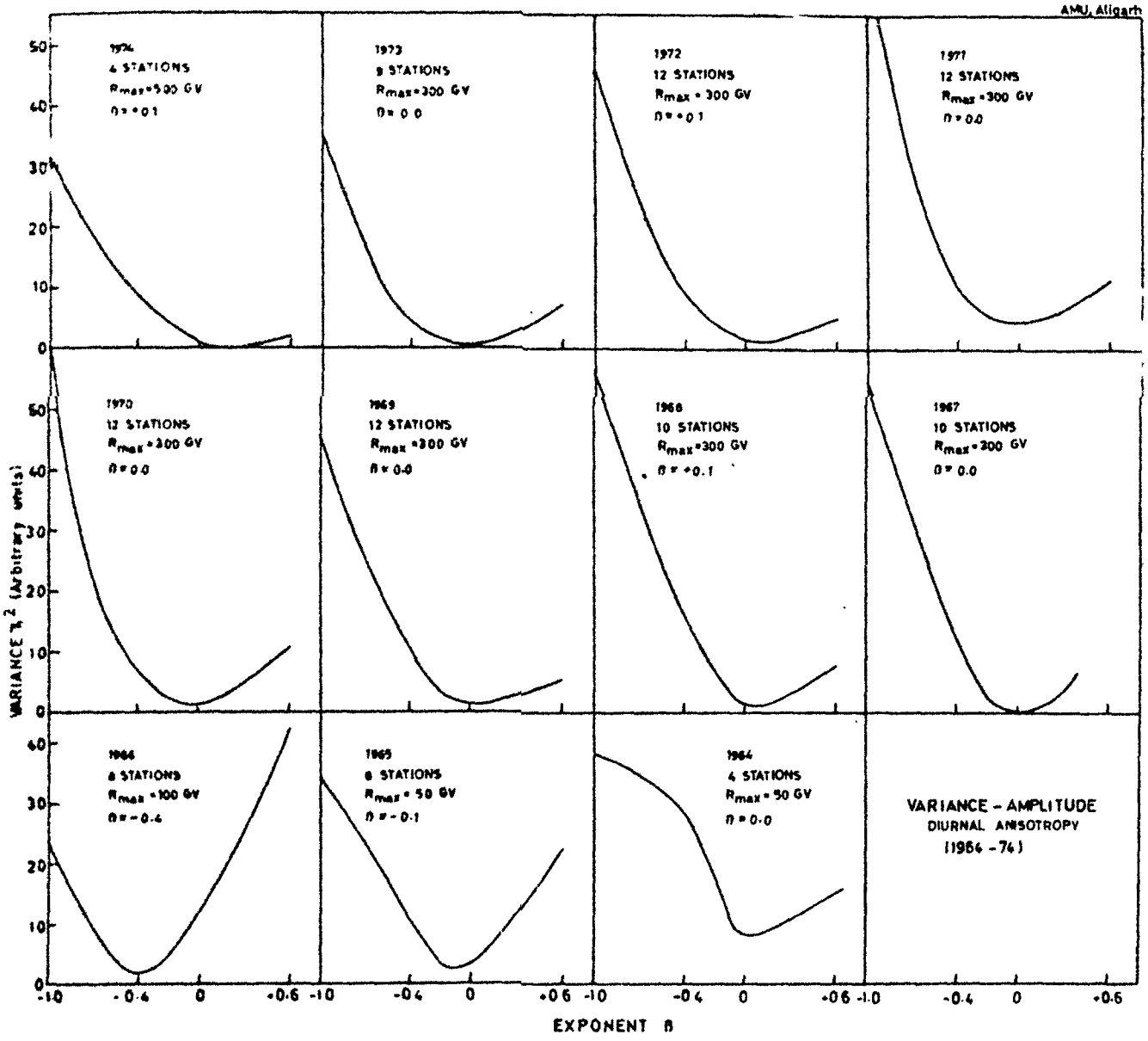

Fig. 4.3(a) - DISTURBED DAYS

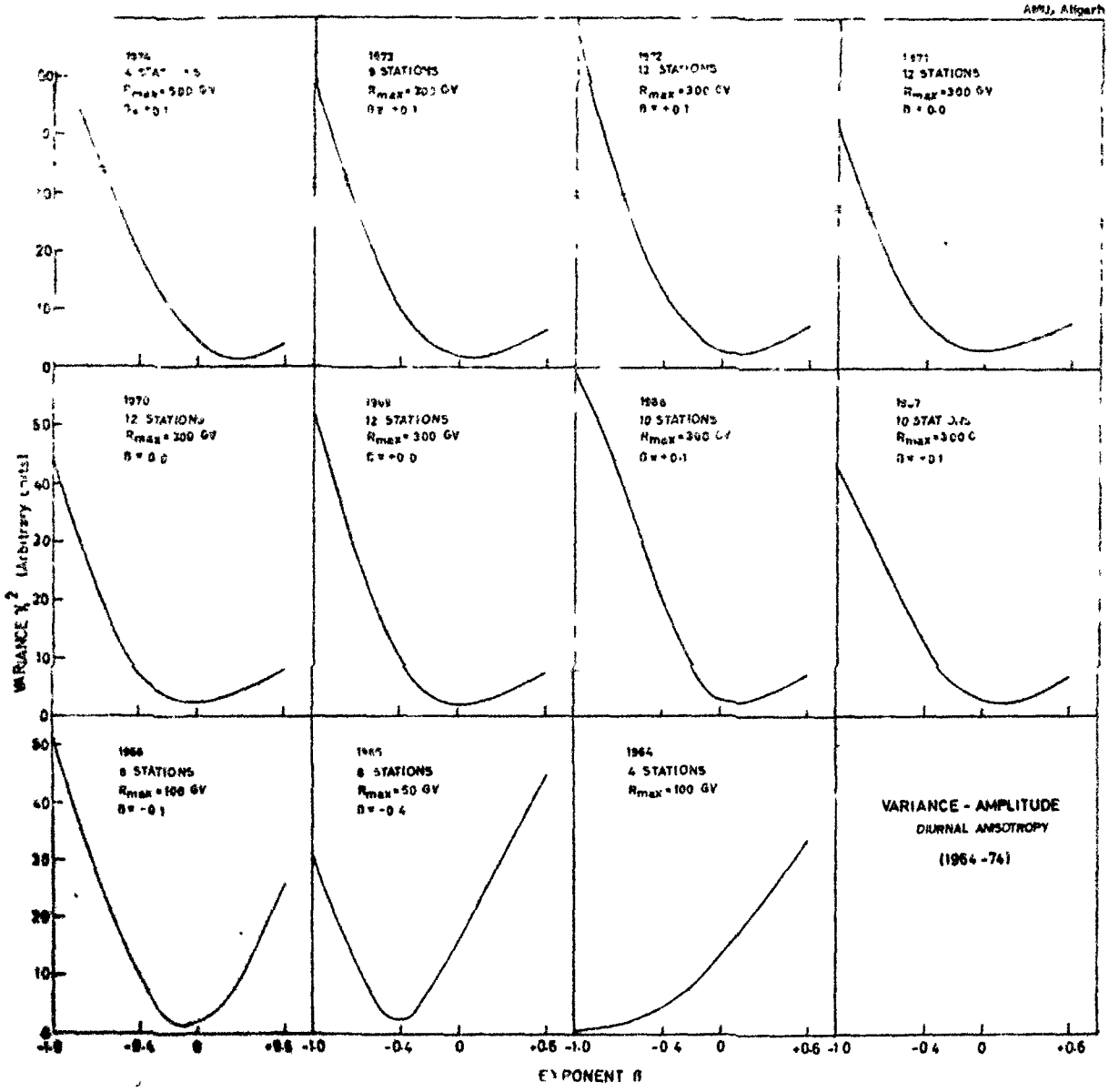

Fig. 4.3(d) - DISTURBED DAYS WITHOUT MAGNETIC STORMS

the Figures-4.3(c) and 4.3(d) that the variance on DD as well as DDWMS is minimum for the value of $\beta \simeq 0 \pm 0.2$ for the entire period 1964-74 except that $\beta \simeq -0.4 \pm 0.2$ during 1966 on DD and during 1965 on DDWMS. This indicates that the corotational anisotropy is more dominant on DD and DDWMS during the period 1964-74.

Thambyahpillai (1975) has estimated the value of R_{max} covering the period mentioned above using the neutron monitor and high energy response detectors. He has reported the long term variation in R_{max} which is in agreement with the results reported by several workers (Jacklyn et al., 1970; Ahluwalia and Ericksen, 1970, 1971; Agrawal et al., 1972). Thus, it has been established that the changes in R_{max} follow the 11-year sunspot cycle with values $\simeq 50$ GV during solar minimum and $\simeq 100$ GV during solar maximum activity periods. However, it may be remarked that the results obtained from meson detectors alone may at best be considered as rough estimates for solar cycle variation in R_{max}. Because for the meson data the temperature correction may not be applied accurately and for underground meson telescopes data it is not possible to apply geomagnetic corrections accurately due to lack of our knowledge of coupling coefficients. Furthermore, Duggal and Pomerantz (1975) suggest that a new approach is essential for determining the upper cut-off rigidity because of energy dependence of the azimuthal anisotropy and the solar magnetic cycle anisotropy (22-year

periodicity) may not be the same. This is also supported from our results on QD (Subsection-4.211) for the period 1971-74.

4.22 Long term variation of diurnal anisotropy

To obtain the anisotropy vector in space, the observed amplitude and phase of the diurnal anisotropy for different groups are corrected for geomagnetic bending and asymptotic cone of acceptance of the detector by taking the value of the exponent of the energy spectrum $\beta = 0 \pm 0.2$ (McCracken et al., 1965; Mori, 1968) as discussed in Section-4.21. Thus, the results obtained for the period 1964-76 on different groups are presented below.

4.221 On quiet days

The values of the amplitude and phase of the diurnal anisotropy on QD for the period 1964-76 are given for few stations in Table-4.3(a). The interstation dispersion and yearly average value of the diurnal amplitude and phase on QD, for the period 1964-76, have also been plotted in Figure-4.4(a). It is determined that on QD the average diurnal amplitude, $r_1^Q \simeq 0.4 \pm 0.01$ % and phase $\phi_1^Q \simeq (19.0 \pm 0.2)$ hrs for the period 1964-70, for all the stations. Further, Figure-4.4(a) also reveals that the phase of the diurnal anisotropy on QD is constant from 1964 to 1970. However, the systematic change in the diurnal phase on QD started since 1971. Thus, the nature of the diurnal phase as observed by us on QD during 1964-70 is

TABLE - 4.3

The observed yearly average diurnal anisotropy vector on different types of days for 6-neutron monitoring stations e.g., Tokyo, Rome, Kiel, Leeds, Calgary and Deep River during the period 1964-76 The standard error in harmonic coefficients for each day is given in Table-4.1

4.3(a) : Quiet Days

Year	Tokyo		Rome		Kiel		Leeds		Calgary		Deep River	
	Amp. (%)	Phase (hrs)	Amp. (%)	Phase (hrs)	Amp. (%)	Phase (hrs)	Amp. (%)	Phase (hrs)	Amp. (%)	Phase (hrs)	Amp. (%)	Phase (hrs)
1964	-	-	-	-	-	-	-	-	.461	17.8	.316	18.6
1965	-	-	-	-	.254	19.7	.284	21.6	.134	19.4	.264	18.8
1966	-	-	-	-	.398	18.9	.470	19.9	.427	18.7	.371	18.6
1967	-	-	.398	19.5	.295	18.7	.312	20.1	.363	19.2	.352	18.7
1968	-	-	.463	18.8	.355	19.1	.442	20.1	.348	18.7	.370	18.6
1969	-	-	.434	20.0	.383	19.6	.457	20.2	.362	19.4	.356	18.9
1970	.352	18.7	.394	18.6	.344	18.7	.383	18.6	.379	18.8	.350	18.1
1971	.295	15.9	.391	17.1	.466	17.5	.478	17.3	.450	17.4	.462	17.2
1972	.281	17.7	.318	17.5	.397	17.7	.408	18.0	.274	16.4	.391	17.1
1973	.284	15.9	.297	15.8	.344	16.7	.371	16.9	.453	16.6	.379	16.6
1974	.413	18.0	.453	17.2	.431	17.8	.561	18.1	-	-	-	-
1975	.237	16.8	.223	15.8	-	-	-	-	-	-	-	-
1976	.149	14.8	-	-	-	-	-	-	-	-	-	-

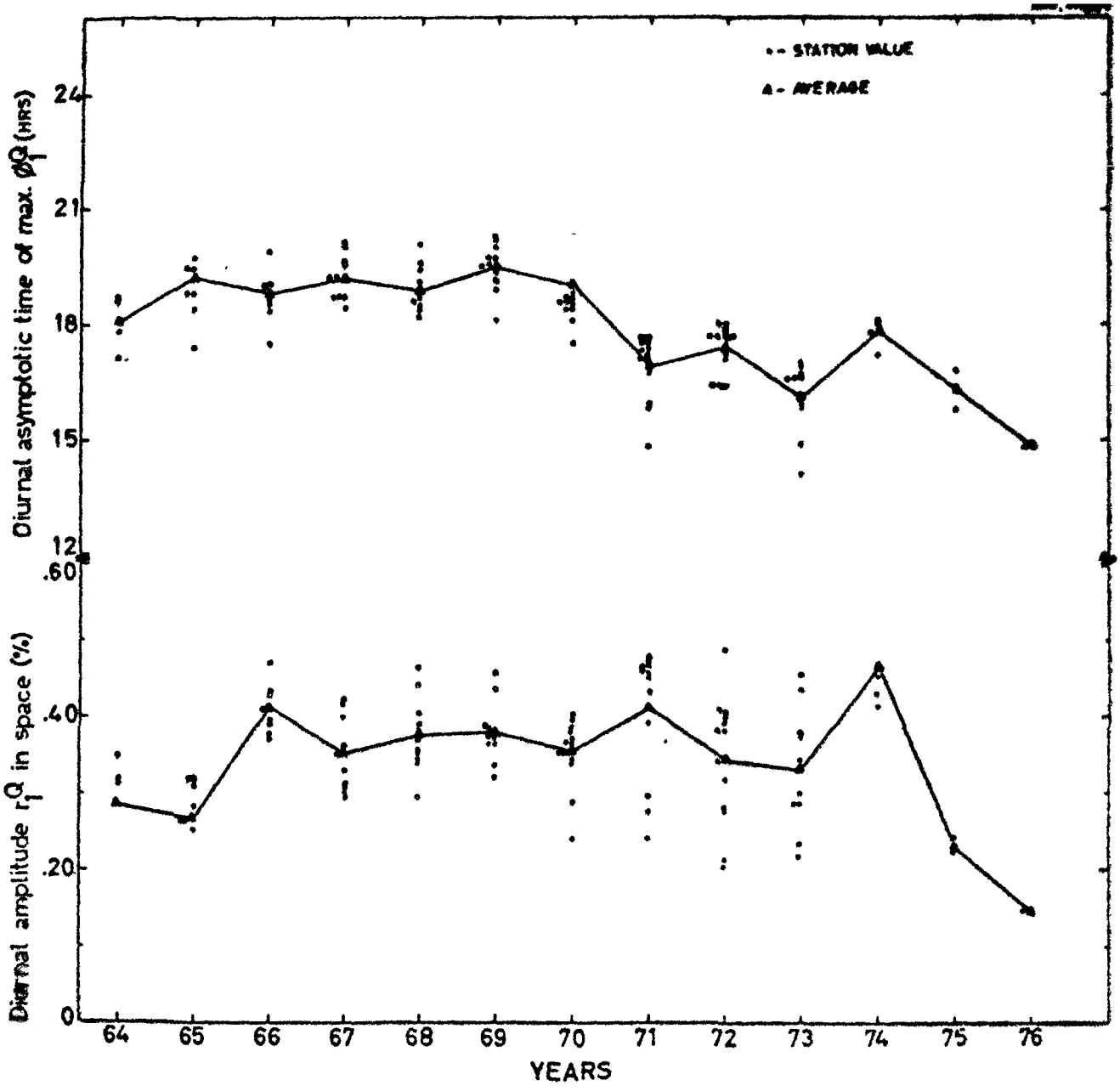

Fig. 4.4 - The interstation dispersion and yearly average value of the diurnal amplitude and phase for the period 1964-76. (a) - QUIET DAYS

in agreement with the time invariant hypothesis on yearly average basis for the period 1957-70 as suggested by earlier workers (Rao, 1972), particularly for neutron monitor observations. But, significant changes have been reported in high energy detectors during the same period 1957-70. It should be noted here that in the year 1954, the amplitude of the diurnal anisotropy has been observed almost insignificant with complete phase reversal at all the neutron monitoring stations operating at that time.

From an examination of Table-4.3(a) and Figures-4.5(a) and 4.6(a), it is observable that the phase of the diurnal anisotropy on QD has shifted towards earlier hours at all the stations from 1970 to 71, the phase shift on QD being larger on equatorial stations having high cutoff rigidity. This trend is also evident from the results on yearly average basis (Agrawal and Ananth, 1975) and from the data of the high energy detectors at surface as well as underground (Thambyahpillai, 1975; Thambyahpillai and Spellar, 1975). The rigidity dependence of the diurnal phase shift on QD may be more easily understood by looking to Figure-4.7, which reveals that the phase of the diurnal anisotropy on QD has further shifted towards earlier hours again in 1975, 1975 and 1976 at all the stations. No significant change is noticeable during the period 1971-72. It is also observable that the phase of the diurnal anisotropy on QD has recovered during 1974 by about 15 - 25^{0} in mid and low latitude stations. Though, this recovery in the phase of the diurnal anisotropy on QD is not very much

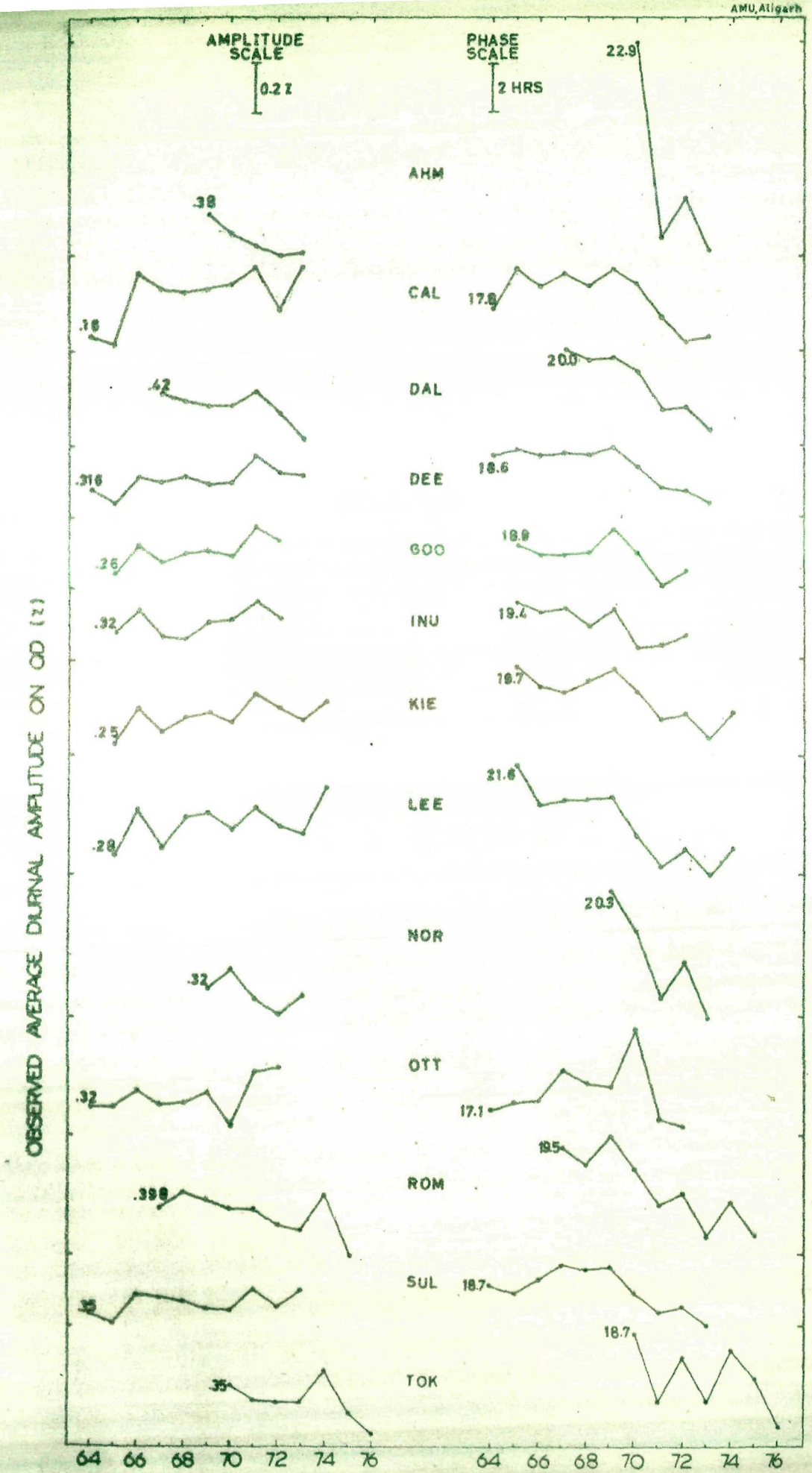

FIG. 4.5(a)

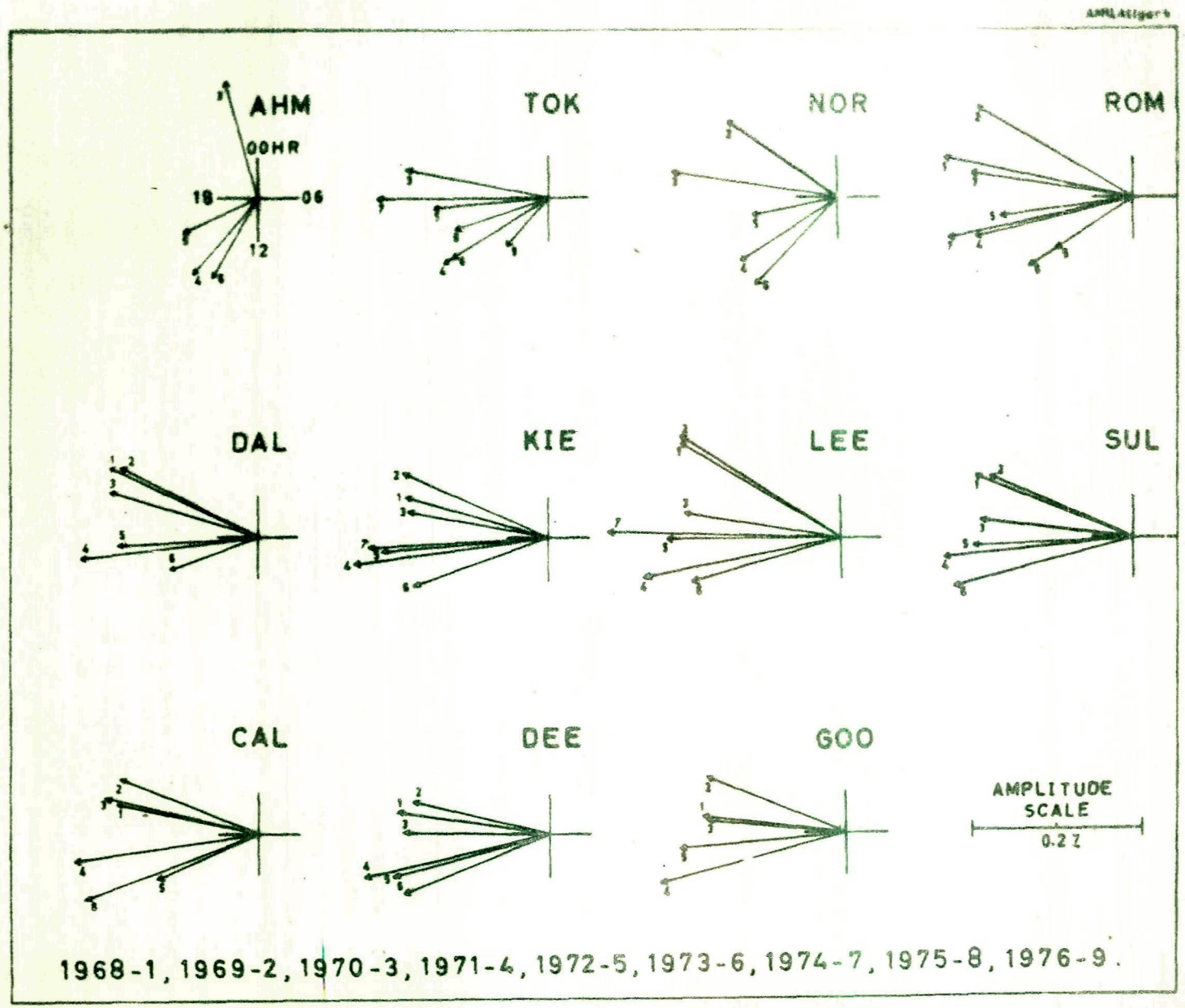

Fig. 4.6 - The observed yearly average diurnal variation for 11 stations plotted on a harmonic dial during 1968-76. The error in the individual daily vectors are given in Table-4.1. (a) - QUIET DAYS.

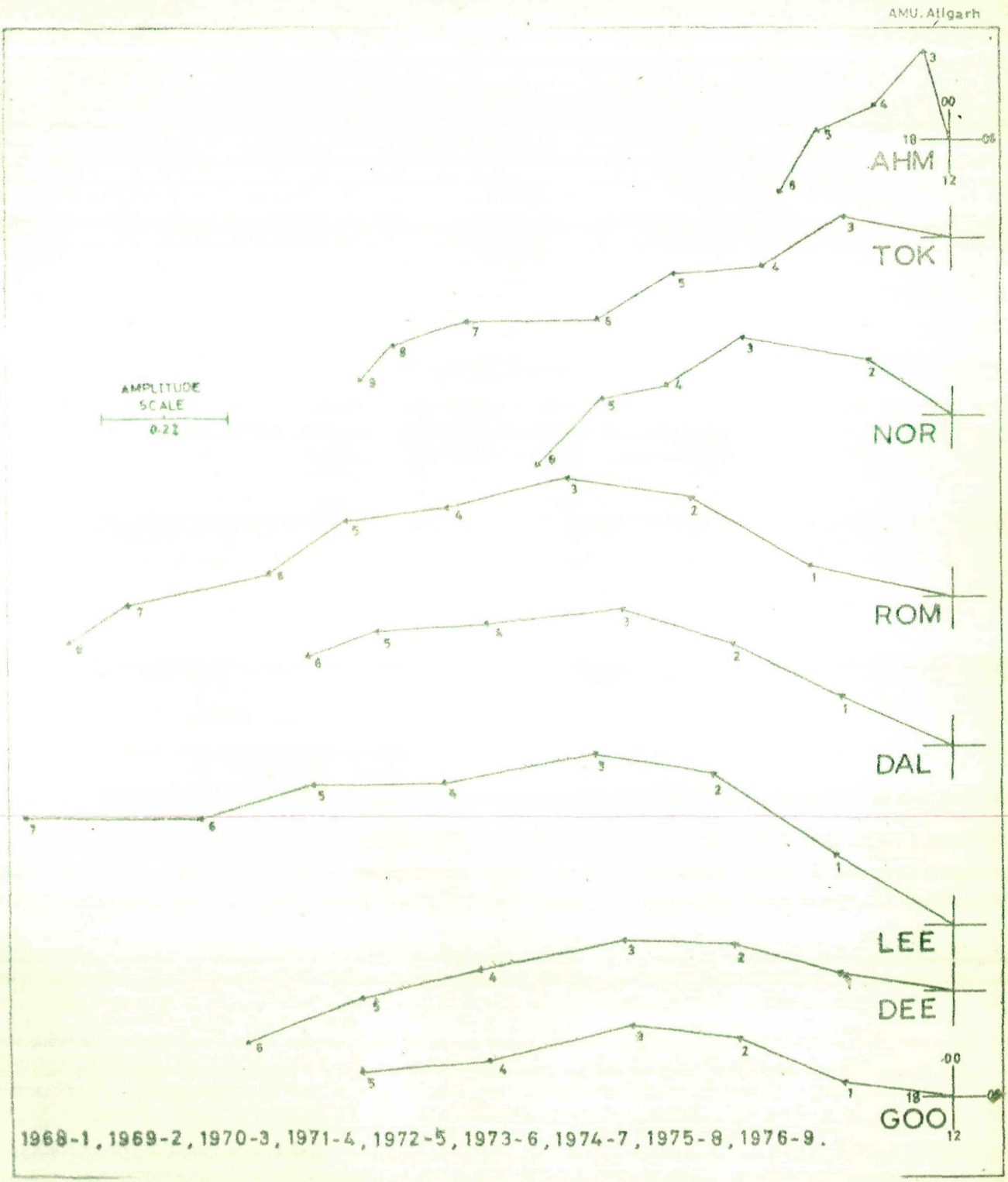

Fig. 4.7 - The observed yearly average diurnal variation on QUIET DAYS for 8 stations plotted as a vector addition diagram during 1968-76. The errors in the individual daily vectors are given in Table-4.1.

significant as compared to the large phase shift during 1970-71, 1972-73 and 1974-75. Once again, a large phase shift towards earlier hours in 1976 is evident, which is found to be maximum $\simeq 45^{\circ}$ as compared to that observed during the period 1970 onwards.

The amplitude of the diurnal anisotropy on QD has not changed so dramatically during 1964-76 as compared to the phase during the same period reported here. Significant changes in the diurnal amplitude on QD may be noticed from Figure-4.4(a). It is observed that during solar minimum period 1964-65 and 1975-76 the diurnal amplitude has decreased but this decrease is more pronounced during 1975-76. It is quite clear from the Figure-4.5(a) that the diurnal amplitude is also decreased during 1971-72 (which is not a period of minimum solar activity) and this decrease is observed by most of the neutron monitoring stations. During 1972-73 the amplitude of the diurnal anisotropy on QD has not changed significantly. However, as reported earlier, there is an associated significant phase shift towards earlier hours during the period 1972-73. The amplitude on QD has decreased in 1975 alongwith large phase shift to earlier hours. During 1976 on QD decrease in amplitude of the diurnal anisotropy is maximum which is approximately half of its value and also the phase shift towards earlier hours is maximum which is $\simeq 45^{\circ}$.

The behaviour of the diurnal anisotropy on QD as observed by neutron monitors during 1970-76 when compared with the meson telescope observations at London and ionisation chamber observations at Carnegie Institution of Washington shows one to one correspondence.

A considerable decrease in β_1 has been observed by underground detectors during 1971 (Thambyahpillai et al., 1975; Murakami et al., 1973; Thambyahpillai and Spellar, 1975) and a small decrease in diurnal amplitude during 1972 has been reported by Murakami et al. (1973), which are in support of our neutron monitor observations on QD.

It will be presented in Chapter-V that for the first time a very significant increase in the amplitude of the semi-diurnal anisotropy on QD at all the stations during 1971 has been noticed, an increase being almost a factor of 2 at most of the stations. The observed increase in the semi-diurnal amplitude at all the stations during 1971 which is not accompanied by any significant increase in the diurnal amplitude on QD has great significance in its production mechanism in terms of the existing models; e.g., the density gradient model proposed by Subramanian and Sarabhai (1967) and Quenby and Lietti (1968) and loss cone or pitch angle distribution model proposed by Nagashima et al. (1972a,b) and Barnden (1973).

4.222 On magnetic storm days

The values of the amplitude and phase of the diurnal anisotropy on MSD obtained for the period 1964-76 are given for few stations in Table-4.5(b). The interstation dispersion and yearly average value of the diurnal amplitude and phase on MSD for the period 1964-76, have been plotted in Figure-4.4(b). The Figure-4.5(b) illustrates the observed yearly average amplitude and phase on MSD, plotted for individual stations. The Figure-4.6(b) shows the harmonic dial representation of the diurnal anisotropy vectors on MSD for the period 1968-76. It is quite clear from these Figures-4.4(b), 4.5(b) and 4.6(b) that the phase as well as the amplitude of the diurnal anisotropy on MSD are not invariant for the period 1964-70, as it is shown on QD. The phase shift to earlier hours for the period 1970-71 is not as prominent as it is observed on QD.

The observed yearly average diurnal phase on QD and MSD have been plotted together for comparison in Figure-4.8, for the period 1965-75. The variation of the A_p-index for the same period 1965-75 has also been shown in the Figure-4.8. The Figure-4.8 reveals that the phase of the diurnal anisotropy on MSD where the A_p-index has higher value is found to shift towards earlier hours in comparison to the phase on QD where A_p-index has lower value for the period 1965-72 except Ahmedabad and Mt. Norikura neutron monitoring equatorial stations which is in agreement with the earlier findings (Sandström, 1965). In contrast, it is observed on all

4.3(b) : Magnetic Storms Days

Year	Tokyo		Rome		Kiel		Leeds		Calgary		Deep River	
	Amp. (%)	Phase (hrs)	Amp. (%)	Phase (hrs)	Amp. (%)	Phase (hrs)	Amp. (%)	Phase (hrs)	Amp. (%)	Phase (hrs)	Amp. (%)	Phase (hrs)
1964	-	-	-	-	-	-	-	-	.203	18.0	.341	18.1
1965	-	-	-	-	.240	15.4	.118	15.9	.109	16.2	.236	14.1
1966	-	-	-	-	.301	18.3	.239	17.9	.474	17.0	.297	16.3
1967	-	-	.262	16.8	.366	16.6	.324	18.7	.194	11.5	.378	15.8
1968	-	-	.449	18.6	.288	17.0	.339	18.6	.362	17.3	.319	17.4
1969	-	-	.276	18.2	.368	16.3	.358	18.6	.253	17.2	.496	15.8
1970	.484	16.9	.465	20.0	.422	18.0	.577	18.4	.443	16.6	.419	16.4
1971	.225	15.1	.496	17.9	.400	17.1	.460	17.2	.418	16.9	.432	15.8
1972	.269	17.3	.359	16.7	.316	16.4	.337	16.5	.253	15.9	.459	15.7
1973	.488	16.8	.430	19.3	.402	17.9	.443	18.0	.393	17.2	.387	16.7
1974	.563	18.6	.522	19.1	.428	18.5	.458	18.0	-	-	-	-
1975	.389	17.1	.479	17.6	-	-	-	-	-	-	-	-
1976	.155	13.2	-	-	-	-	-	-	-	-	-	-

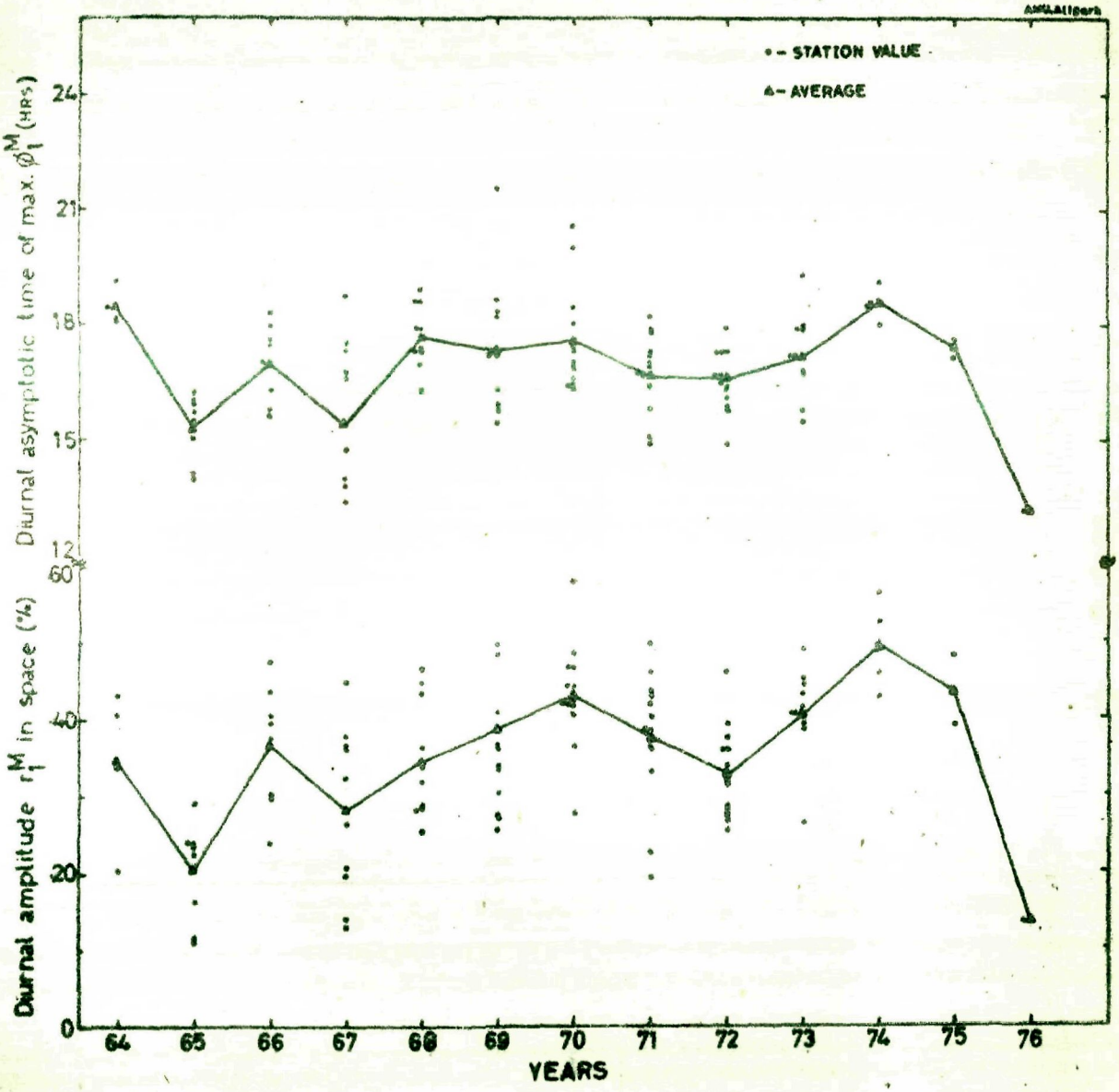

Fig. 4.4(b) - MAGNETIC STORMS DAYS

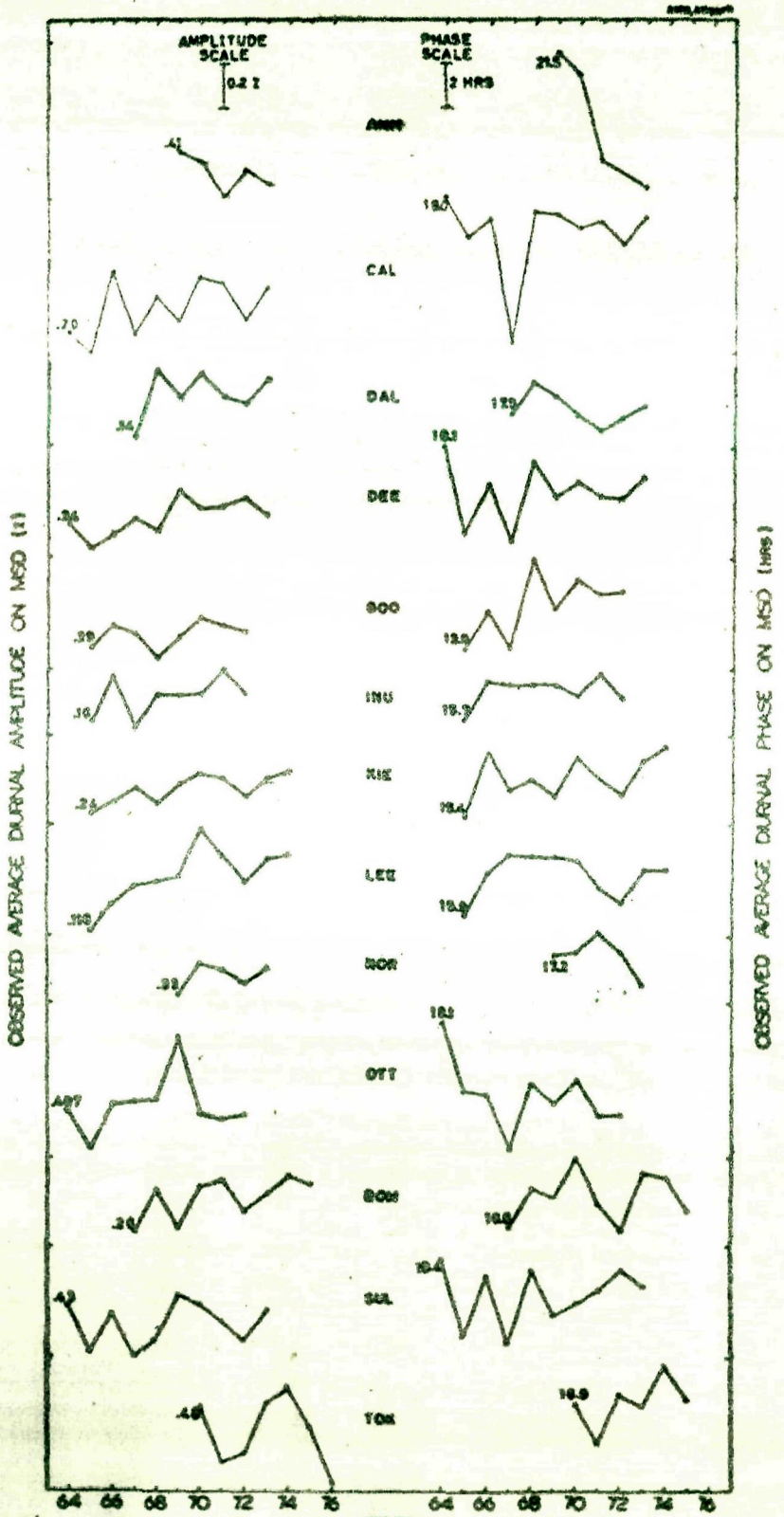
AMPLITUDE SCALE
0.2 I
PHASE SCALE
2 HRS
ABG
CAL
DAL
DEE
GOO
INU
KIE
LER
NOR
OTT
RGM
SUL
TOK
OBSERVED AVERAGE DIURNAL AMPLITUDE ON MSD (I)
OBSERVED AVERAGE DIURNAL PHASE ON MSD (Hrs)
64 66 68 70 72 74 76
YEARS

FIG 45(b)

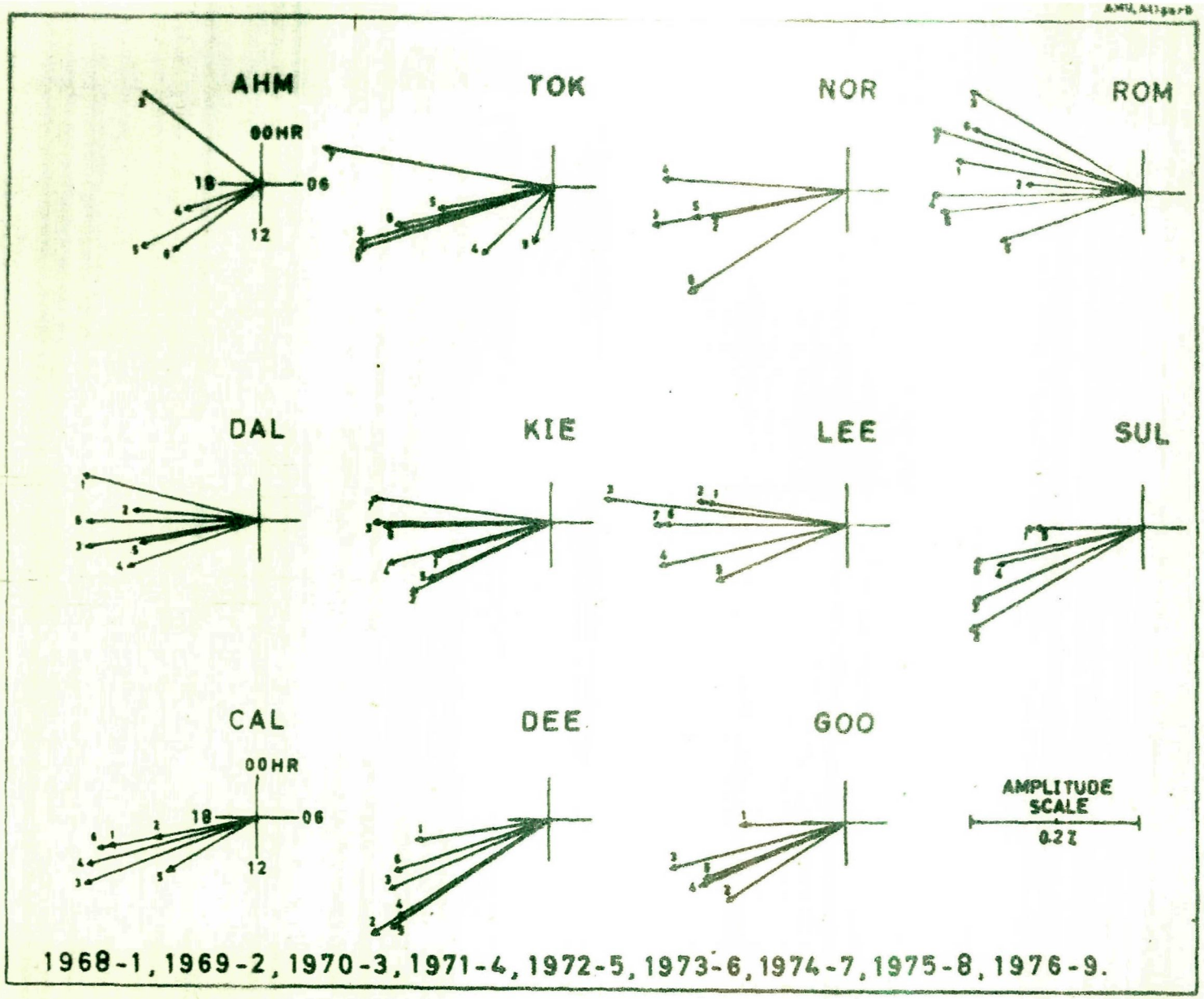

Fig. 4.6(b) - MAGNETIC STORMS DAYS.

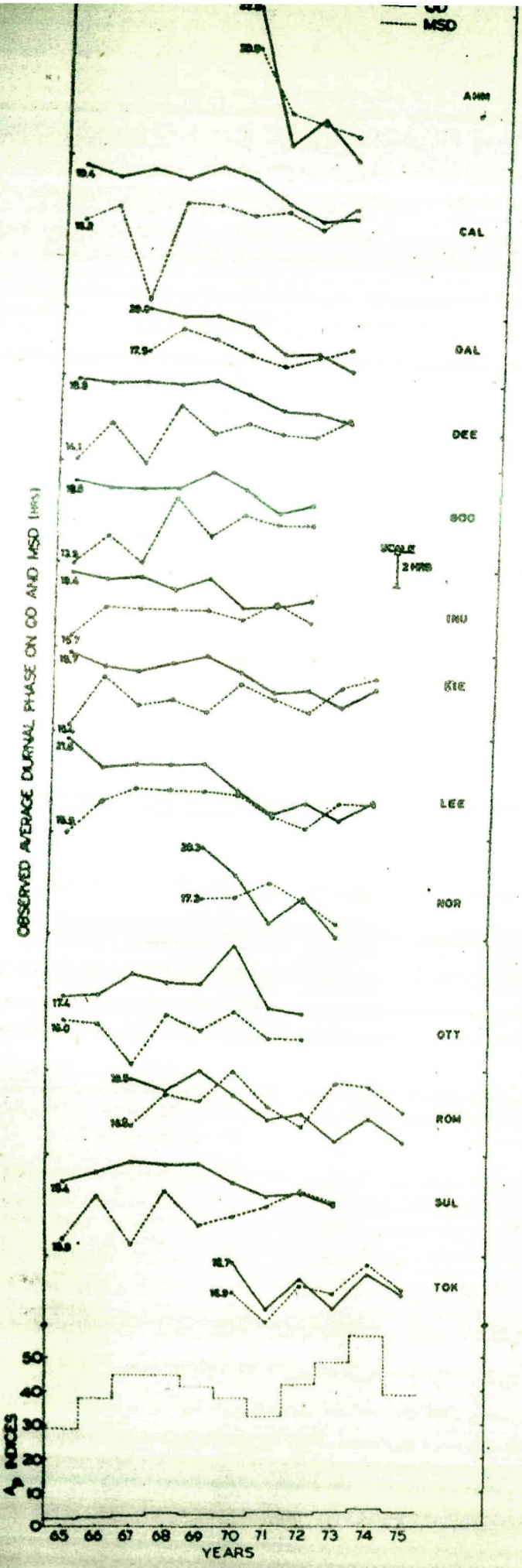
GO
MSD
AMM
CAL
GAL
DEE
BOO
SCALE
2 HRS
INU
KIE
LEE
NOR
OTT
ROM
SUL
TOK
OBSERVED AVERAGE DIURNAL PHASE ON GO AND MSD (HRS)
Ap INDICES
0
10
20
30
40
50
65
66
67
68
69
70
71
72
73
74
75
YEARS

FIG 4 8

the stations for the period 1973-75 that the phase of the diurnal anisotropy on MSD has shifted towards later hours in comparison to the phase on QD, indicating the complete reversal of A_p-ϕ_1 relation during 1973-75. However, Ahmedabad and Mt. Norikura neutron monitoring stations have shown this opposite relationship starting from 1971, as is observable in Figure-4.8. The results showing that there is a complete reversal of A_p-ϕ_1 relation during the period 1969-73, reported by Agrawal and Singh (1975a), are in support of our findings. The exact cause of such drastic change is not known, but it demonstrates very clearly that the inter-planetary conditions which are responsible for both, the diurnal anisotropy of cosmic ray intensity and the geomagnetic A_p-index variation, have drastically changed during the period 1971-75.

4.223 <u>On disturbed days and disturbed days without magnetic storms</u>

The observed values of the amplitude and phase of the diurnal anisotropy for the period 1964-76 on DD and DDWMS are given for few stations in Tables-4.3(c) and 4.3(d) respectively. The interstation dispersion and annual average values of the diurnal amplitude and phase on DD and DDWMS for the period 1964-76 have been plotted in Figures-4.4(c) and 4.4(d) respectively. The Figures-4.4(c) and 4.4(d) reveal that for the period 1964-70, the phase of the diurnal anisotropy on DD and DDWMS remains constant in the azimuthal direction as observed on QD. However, when

4.3(e) : Disturbed Days

Year	Tokyo		Rome		Kiel		Leeds		Calgary		Deep River	
	Amp. (%)	Phase (hrs)	Amp. (%)	Phase (hrs)	Amp. (%)	Phase (hrs)	Amp. (%)	Phase (hrs)	Amp. (%)	Phase (hrs)	Amp. (%)	Phase (hrs)
1964	-	-	-	-	-	-	-	-	.183	18.3	.341	18.2
1965	-	-	-	-	.230	17.1	.199	19.5	.138	17.2	.259	16.5
1966	-	-	-	-	.395	19.0	.413	19.8	.464	17.9	.344	17.6
1967	-	-	.302	18.8	.349	17.8	.428	19.8	.144	16.2	.289	15.7
1968	-	-	.533	19.1	.378	18.0	.414	18.5	.376	18.4	.363	17.8
1969	-	-	.377	18.4	.410	17.7	.428	18.8	.373	17.9	.423	16.9
1970	.348	16.7	.379	19.6	.354	18.2	.441	18.3	.440	16.6	.395	16.6
1971	.283	17.0	.463	17.8	.389	17.0	.425	16.9	.375	17.3	.389	16.1
1972	.271	17.5	.328	17.6	.267	16.9	.290	17.1	.356	17.6	.424	16.2
1973	.459	17.0	.419	18.7	.391	17.9	.426	17.9	.396	17.5	.376	16.9
1974	.516	18.5	.504	18.7	.393	18.2	.409	17.9	-	-	-	-
1975	.406	17.4	.384	17.7	-	-	-	-	-	-	-	-
1976	.240	15.7	-	-	-	-	-	-	-	-	-	-

4.3(d) : Disturbed Days Without Magnetic Storms

Year	Tokyo		Rome		Kiel		Leeds		Calgary		Deep River	
	Amp. (%)	Phase (hrs)	Amp. (%)	Phase (hrs)	Amp. (%)	Phase (hrs)	Amp. (%)	Phase (hrs)	Amp. (%)	Phase (hrs)	Amp. (%)	Phase (hrs)
1964	-	-	-	-	-	-	-	-	.159	18.6	.342	18.2
1965	-	-	-	-	.266	18.7	.321	20.5	.167	17.7	.343	18.0
1966	-	-	-	-	.456	19.2	.551	20.3	.472	18.6	.411	18.5
1967	-	-	.408	20.1	.368	19.0	.504	20.2	.276	18.7	.315	18.4
1968	-	-	.646	19.5	.495	18.7	.501	18.3	.401	19.0	.413	18.2
1969	-	-	.471	18.5	.486	18.7	.489	19.0	.476	18.2	.394	18.2
1970	.220	16.2	.303	19.0	.293	18.5	.315	18.0	.438	16.6	.373	16.8
1971	.425	18.3	.424	17.6	.376	17.0	.386	16.5	.326	17.8	.338	16.7
1972	.280	18.1	.330	20.0	.196	18.8	.217	18.8	.333	17.2	.376	17.6
1973	.405	17.5	.423	17.7	.369	17.8	.396	17.5	.408	18.0	.359	17.3
1974	.448	18.3	.488	18.2	.349	17.9	.347	17.7	-	-	-	-
1975	.417	17.6	.326	17.7	-	-	-	-	-	-	-	-
1976	.341	16.3	-	-	-	-	-	-	-	-	-	-

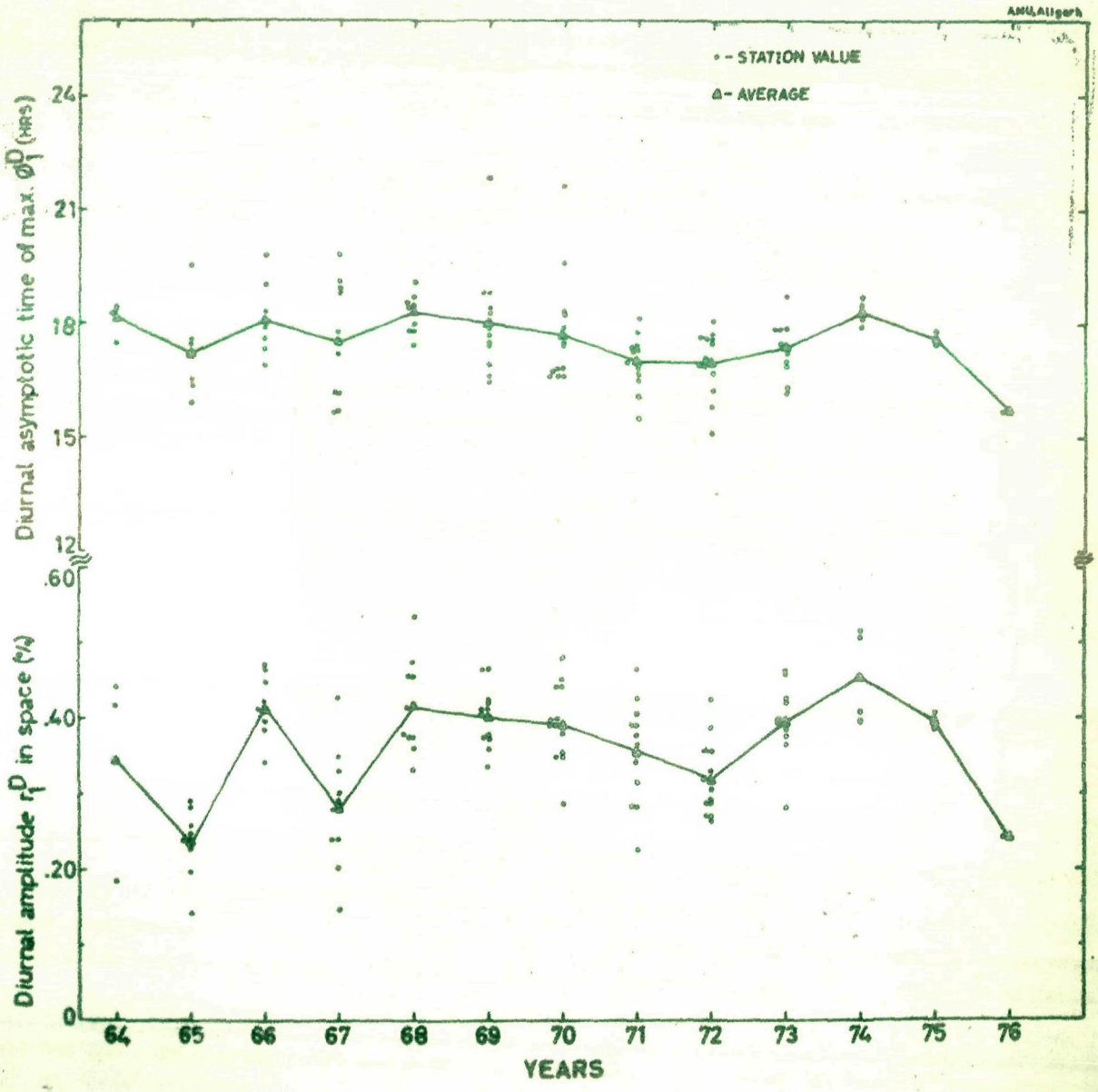

Fig. 4.4(c) - DISTURBED DAYS

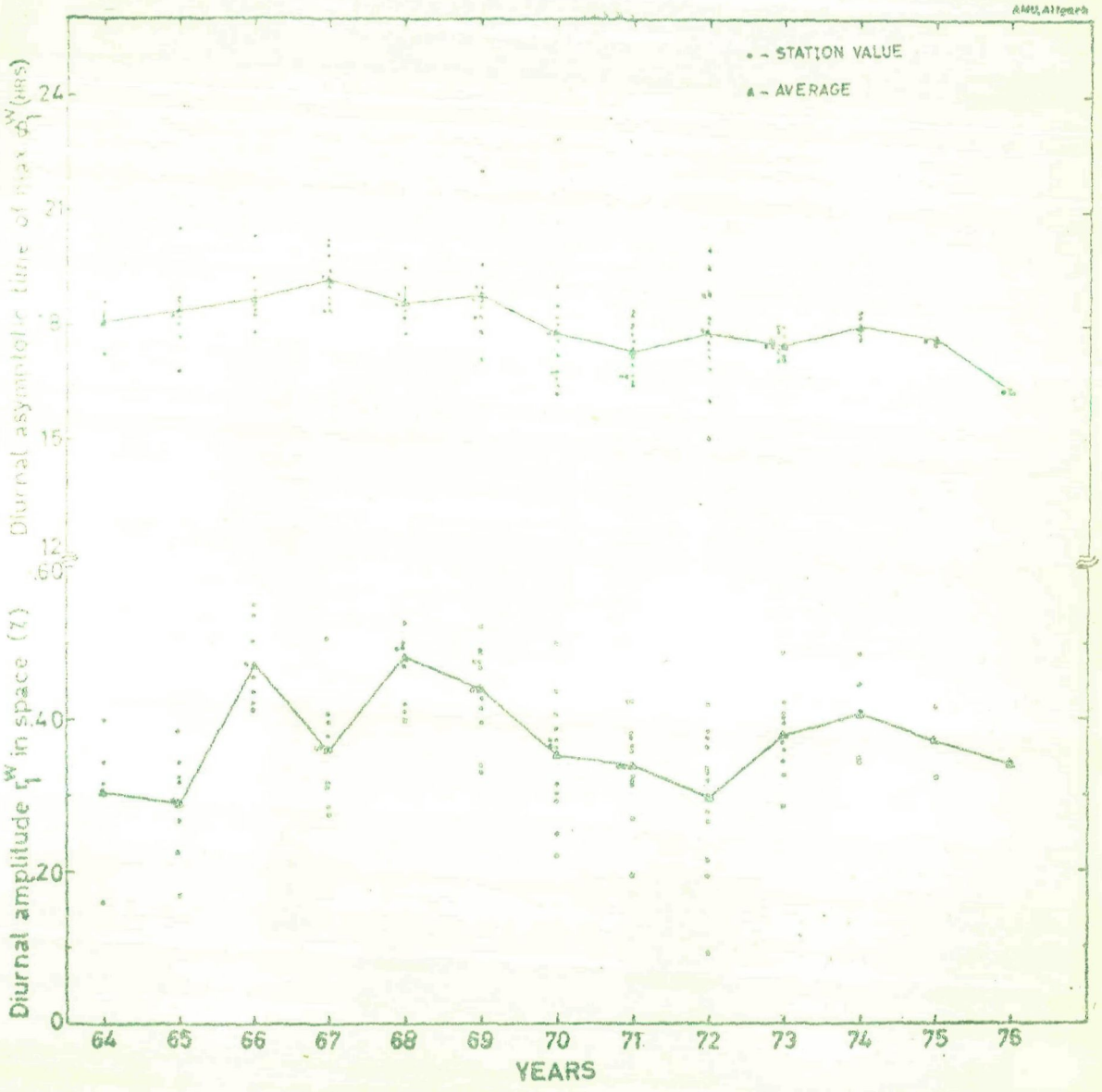

Fig. 4.4(d) - DISTURBED DAYS WITHOUT MAGNETIC STORMS

we look into these Figures-4.4(c) and 4.4(d) for the period 1971-76, we find that unlike as observed on QD, the phase shift towards earlier hours during 1971, 1973 and 1975 is statistically not significant when the average of all the stations is considered. But, the phase shift towards earlier hours in the diurnal anisotropy on DD and DDWMS during 1976, the year of minimum sunspot activity, is quite prominent similar to that as observed on QD.

Significant changes in the diurnal amplitude on DD, r_1^D and DDWMS, r_1^W may also be noticed from Figures-4.5(c) and 4.5(d) respectively, where the plots for individual stations are shown. It appears from these Figures-4.5(c) and 4.5(d) that no definite trend in the amplitude of the diurnal anisotropy on DD and DDWMS may be referred. However, during 1965 there is a decrease in both r_1^D and r_1^W. During 1972, there is no change noticeable in r_1^D whereas statistically significant decrease is shown in r_1^W. Both r_1^D and r_1^W remain constant during 1975. But during 1976, the year of minimum sunspot activity, r_1^D is significantly decreased whereas r_1^W shows no prominent change.

It is quite apparent from the observational results for the characteristics of the diurnal anisotropy on QD, MSD, DD and DDWMS; presented above for the period 1964-76, that the results on monthly/yearly average basis, where all the days in a month/year are considered (Agrawal and Singh, 1975b), are more influenced by the characteristics of the diurnal anisotropy vector on QD.

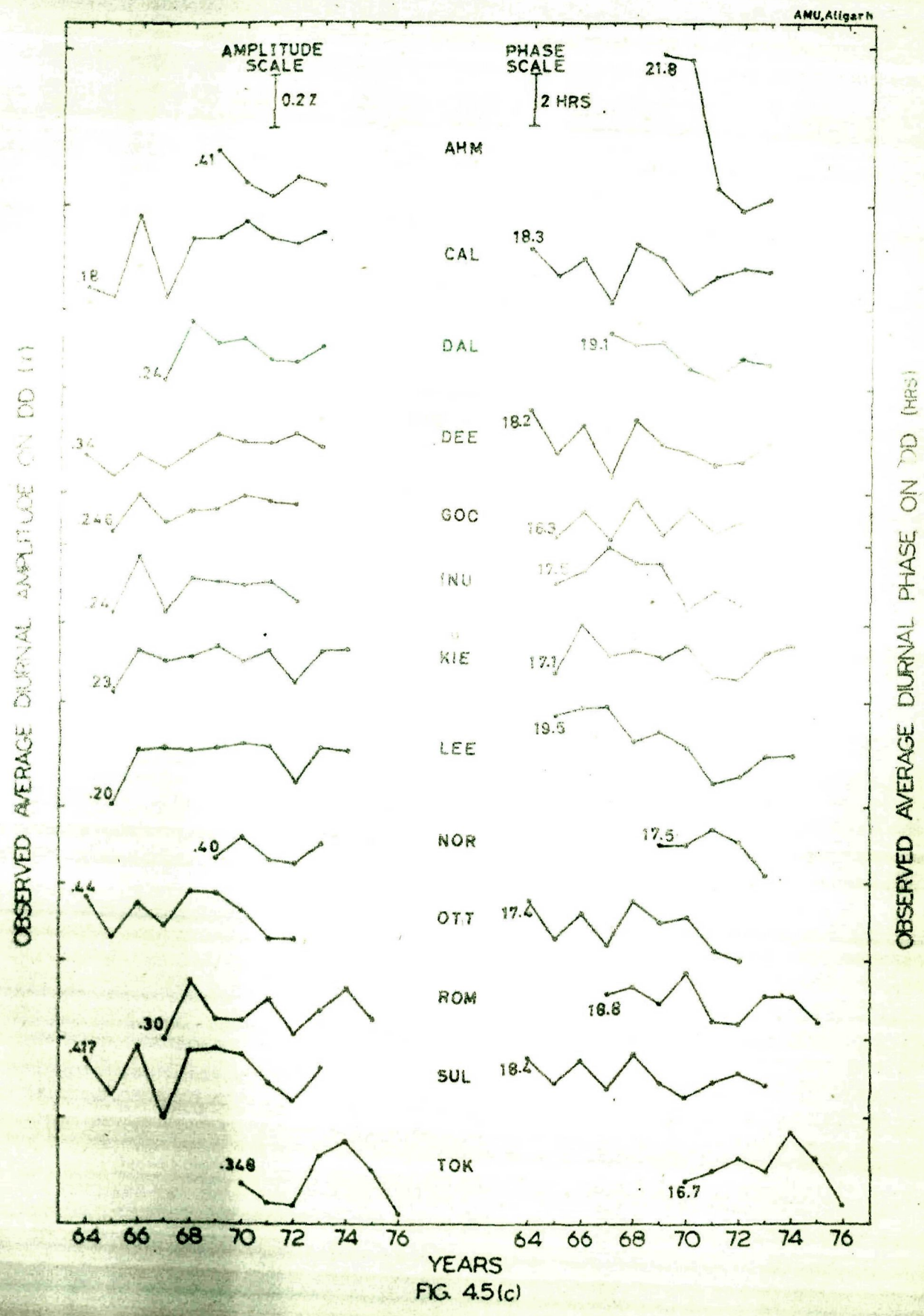
AMU, Aligarh
AMPLITUDE SCALE
0.2 Z
PHASE SCALE
2 HRS
AHM
CAL
DAL
DEE
GOC
INU
KIE
LEE
NOR
OTT
ROM
SUL
TOK
.41
.18
.24
.34
.246
.24
.23
.20
.40
.44
.30
.417
.348
21.8
18.3
19.1
18.2
16.3
17.1
19.5
17.5
17.4
18.8
18.4
16.7
64 66 68 70 72 74 76
YEARS
OBSERVED AVERAGE DIURNAL AMPLITUDE ON DD (Z)
OBSERVED AVERAGE DIURNAL PHASE ON DD (HRS)

FIG. 4.5(c)

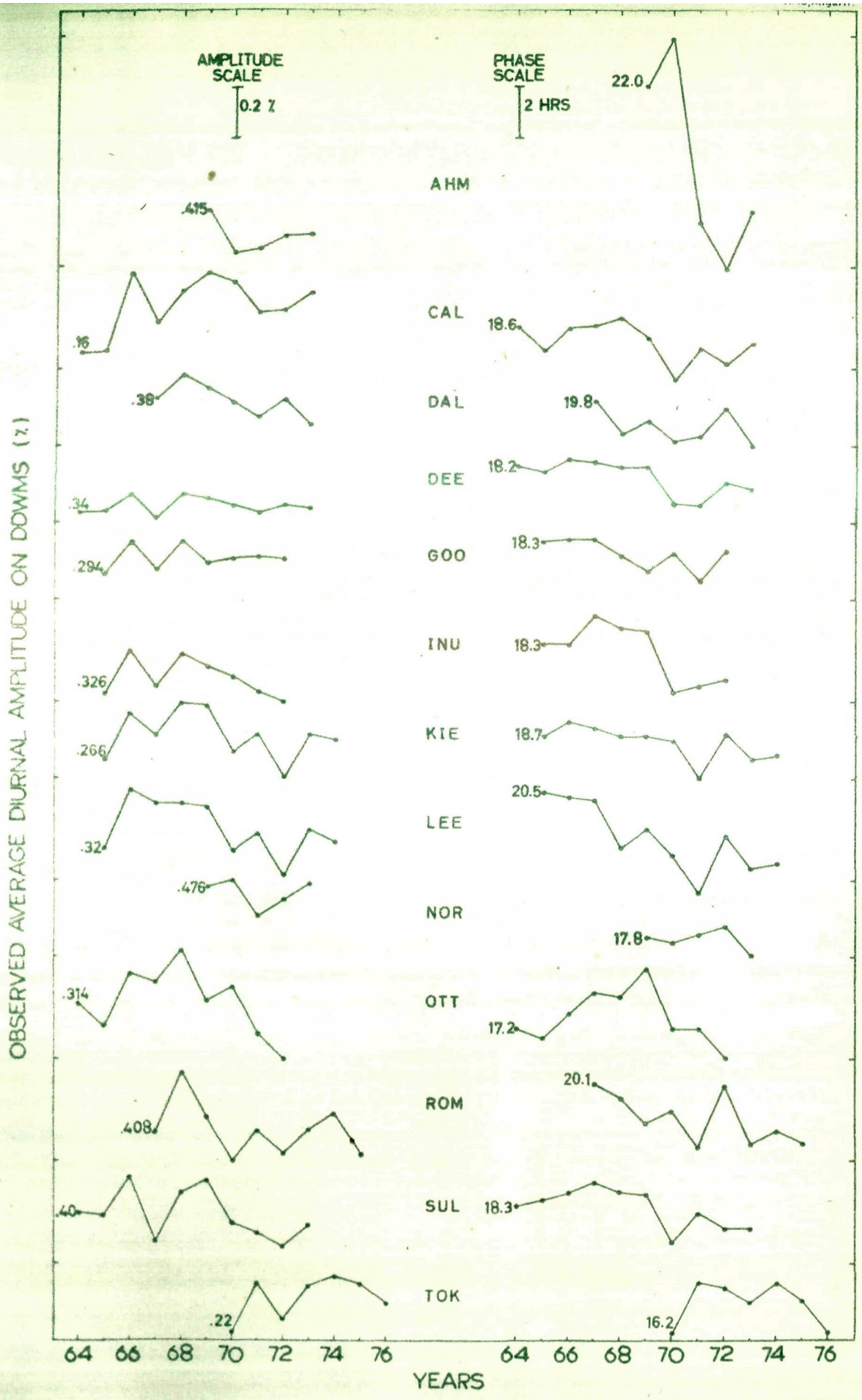
AMPLITUDE SCALE
0.2 %
PHASE SCALE
2 HRS
AHM
CAL
DAL
DEE
GOO
INU
KIE
LEE
NOR
OTT
ROM
SUL
TOK
.415
.16
.38
.34
.294
.326
.266
.32
.476
.314
.408
.40
.22
22.0
18.6
19.8
18.2
18.3
18.3
18.7
20.5
17.8
17.2
20.1
18.3
16.2
64 66 68 70 72 74 76
YEARS
OBSERVED AVERAGE DIURNAL AMPLITUDE ON DDWMS (%)
OBSERVED AVERAGE DIURNAL PHASE ON DDWMS (HRS)

FIG 4.5(d)

4.23 Diurnal anisotropy on a day-to-day basis

It is observed that the amplitude as well as the phase of the diurnal anisotropy change significantly from day-to-day. Rao and Sarabhai (1964) and Patel et al. (1968) have studied the different parameters of the diurnal anisotropy on individual days and they have reported that these parameters are found different on day-to-day basis. We have also studied the day-to-day variation of these parameters particularly during QD and MSD. The results are discussed in the following Sub-sections.

4.231 On quiet days

The amplitude and phase of the diurnal anisotropy on QD as observed on a day-to-day basis for KIE, LEE, SUL and DEE have been plotted in frequency histogram in Figure-4.9(a) for the period from 1968-74. The Figure-4.9(a) shows that there is a variability on a day-to-day basis in the diurnal anisotropy on QD. However, the observed peaks in the diurnal amplitude and phase in the frequency distribution are consistent with the characteristics of the average annual diurnal anisotropy on QD (Figure-4.4(a)). This indicates that the annual average behaviour of the diurnal anisotropy on QD is not a random phenomena.

It is observable from the Figure-4.9(a) that the peak of phase of the diurnal anisotropy on QD occur nearly at the same hour during 1968-70 and it has shifted towards earlier hours

from 1970 to 71 and also from 1972 to 73. This conclusion is also true for periods 1974-75 and 1975-76, which is not shown here. It is also observable from the Figure-4.9(a) that on a day-to-day basis the phase of the diurnal anisotropy on QD has recovered during 1974. The decrease in the amplitude of the diurnal anisotropy on QD during 1972 on a day-to-day basis is also evident from the Figure-4.9(a).

Since the annual average diurnal anisotropy on QD has shown the shift in the phase ϕ_1^0 towards earlier hours after 1970, therefore, we have determined the monthly average diurnal vectors on QD to know the precise period, if any, for which the value of ϕ_1^0 has been largely influenced and thereby affecting the annual average. The Figure-4.10 shows the harmonic dial representation of the monthly average vectors on QD for LEE during 1973. Inspite of large fluctuations from month-to-month, the Figure-4.10 reveals a continuous decreasing trend which is obvious in almost all the stations. Figure-4.10 also illustrates that the phase of the diurnal anisotropy is more influenced during later half of the year, which is found to be true both at low as well as high cutoff rigidity monitors. The cause for such a large phase shift only during the later half of the year in 1971, 1973 and 1975 is not understood presently.

4.232 <u>On magnetic storms days</u>

The amplitude and phase of the diurnal anisotropy on

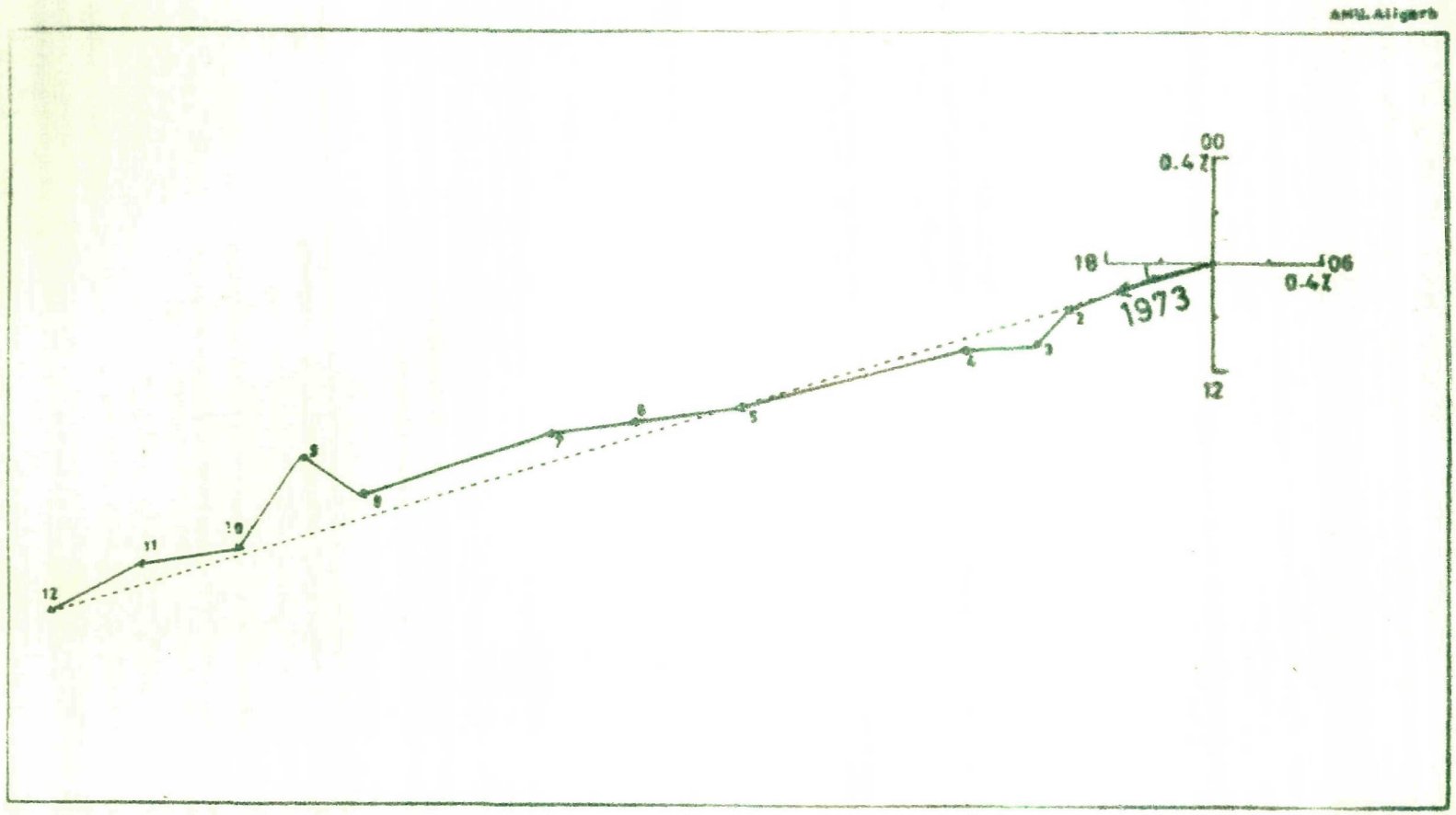

Fig. 4.10 - Monthly average diurnal vectors on OD for LSX during 1973.

MSD as observed on a day-to-day basis for KIE and LEE have been plotted in frequency histogram in Figure-4.9(b) for the period 1968-74. The Figure-4.9(b) illustrates that there is a large variability on a day-to-day basis in the diurnal anisotropy on MSD. The variability in the phase on MSD has been observed more in comparison to that observed on QD. However, the conclusions drawn from the peaks in the histograms of the diurnal anisotropy on MSD (Figure-4.9(b)) are consistent with the results obtained on an annual average basis for the diurnal anisotropy on MSD (Figure-4.4(b)).

4.3 Discussion: long term variation in diurnal anisotropy

The neutron monitor results on different types of days have been presented in the preceding Sections, for the period 1964-76 with a view to discuss them in the light of the results obtained by neutron monitors on yearly average basis where all the days in a year are considered as well as the results based on the observations from other detectors. The importance of the results presented here is that they have allowed us to change the earlier concept of time invariance of diurnal anisotropy particularly on QD and they may also be combined with the results obtained from the high energy detectors to derive meaningful energy spectral characteristics. The results obtained for the diurnal anisotropy on QD, considering 60 days in a year, are as much informative as the results obtained on an yearly average basis, considering

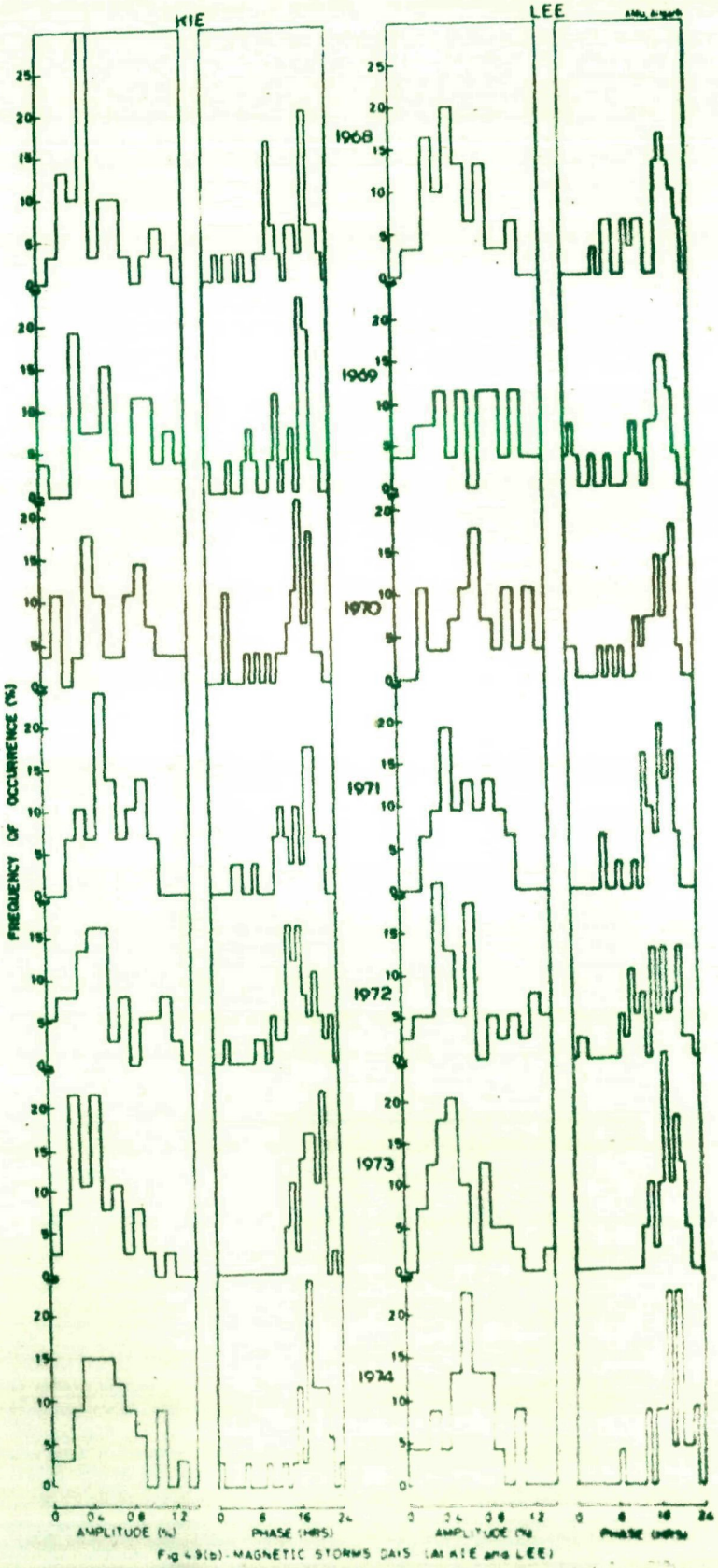

Fig 4.9(b) - MAGNETIC STORMS DAIS (At KIE and LEE)

all the days in a year, for examining the nature of the diurnal anisotropy. The results for the diurnal anisotropy on QD during the period 1957-58 have also been derived (presented in Chapter-VI) and these are found in agreement with the conclusions for the diurnal anisotropy on QD during the period 1964-70. Therefore, this allows us to extend the period 1964-70 to 1957-70 where the invariant nature of the diurnal anisotropy has been observed, for the purpose of discussion. Thus, during the period 1957-70, the neutron monitor observations have shown the invariant nature of the diurnal anisotropy with time, whereas the high energy detectors (meson telescope observations) have always shown large changes in the diurnal anisotropy during the same period 1957-70, which were usually attributed to atmospheric temperature effects. Therefore, the contradiction between the observations performed at neutron and meson monitor energies is only an apparent one and is observed as a consequence of the marked energy dependence of the long term variation.

The neutron monitor observations have shown a significant shift towards earlier hours in the phase of the diurnal anisotropy on QD at all the stations during 1971 for the first time and no significant variation in ϕ_1^0 is observed from 1957-70. Therefore, the observations available for the neutron monitors operated before 1957 are of great significance for deriving any conclusion on the long term variation of the diurnal

anisotropy associated with 22-year solar magnetic cycle and hence it is worthwhile to discuss the results prior to 1957. The average monthly vectors for the period 1953-54 are presented in harmonic dial for Chicago neutron monitoring station in Figure-4.11 (Singh, 1976). It is observable from the Figure-4.11 that both the diurnal amplitude and phase have significantly changed during this period which includes the sunspot minimum year of 1954. The most interesting period is July-September 1954, during which the phase of the diurnal anisotropy has almost reversed ($\sim$03 hours) from its usual 12-18 hours direction (Also see Conforto and Simpson, 1957; Venkatesan and Dattner, 1959; Marsden and Begum, 1959). From these results it is apparent that the neutron monitor observations have shown a significant reduction in the diurnal amplitude as well as large phase shift to earlier hours in ϕ_1 prior to 1957; which is observed again since 1971.

It has been proposed that due to lack of sector structure in the I.M.F., the anomalous diurnal variation with $\phi_1 = 53 \pm 6^{\circ}$ has been caused during July to September 1954. This has been confirmed by Thomson (1971, 1972) from the geomagnetic field derived I.M.F. polarity data showing that the magnetic field pointed constantly 'away' from the Sun during this period. A similar situation has also been reported for the period March 4 to April 11, 1965, period of minimum solar activity, where the I.M.F. showed unidirectional polarity (Antomucci, 1974). However, during this period no significant change in ϕ_1 has been observed.

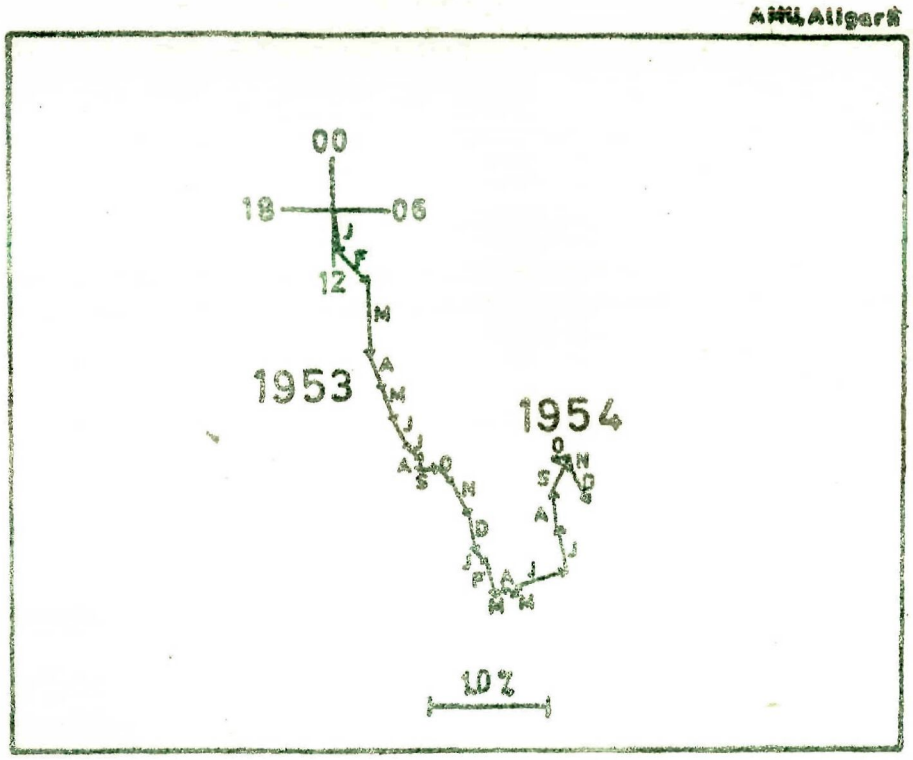

Fig. 4.11 - The monthly diurnal vectors for the period 1953-54 plotted end-to-end for Chicago neutron monitoring station.

been explained due to the existence of southward gradient of cosmic ray particles as the Earth was below the solar equatorial plane during this period. As a consequence of it, cosmic ray streaming should occur, but opposite to that in 1954 and hence can not be easily resolved from the corotational anisotropy. Therefore, the situation similar to 1953-54 should be observed during the present solar minimum period 1975-76 if 22-year wave is present in the anisotropy.

We have, therefore, made an attempt to see whether there is any 22-year periodicity in the diurnal anisotropy. And it has been successfully shown in the following discussion on the basis of the analysis of the data on QD that in fact, a periodicity of 22-year exists in the diurnal anisotropy of cosmic ray intensity.

Agrawal et al. (1977) have investigated that the sector-structure of the I.M.F. derived from polar magnetograms (Svalgaard, 1972) shows the predominance of almost unidirectional sector from July to September, 1976. Leaving aside the mixed polarity days, the predominance of 'away' polarity days has been pointed constantly 'away' from the Sun.

The observed amplitude and phase of the diurnal anisotropy on QD for the years 1975 and 1976 have shown significant decreases in the amplitude and large phase shift to earlier hours. The monthly vectors for the diurnal anisotropy on QD during the period from 1975-76 for Tokyo (Itabashi) neutron monitoring

station have been plotted end to end in Figure-4.12. The Figure-4.12 reveals the extraordinary behaviour of the diurnal anisotropy on QD during 1975-76 for comparison with the monthly vectors during 1953-54 given in Figure-4.11. This is quite apparent from the Figure-4.12 that during July-September, 1976, the amplitude of the diurnal anisotropy on QD has diminished by a factor more than 2 of that in 1970 and also the phase has almost reversed ($\simeq$ 03 hours) from its usual 12 - 18 hours direction. It gives an idea that the situation similar to 1954 has definitely been occurred during 1976, which is observable when a systematic and detailed analysis on long term variation of diurnal anisotropy on QD is performed. Therefore, it clearly emphasizes that the long term variation in the diurnal anisotropy has the 22-year periodicity.

In support of our results on QD, the analysis, where all the days in a month/year are considered, has also indicated that during the period of July-September, 1976, the amplitude has decreased to one third of the average value for the whole year (Agrawal et al., 1977). However, no appreciable change in the value of ϕ_1 is observed during these 3 months and also, the average monthly diurnal phase has never been in the early morning hours during the present solar minimum period of activity e.g., 1975-76, on the basis of the analysis where all the days in a month are considered (Agrawal et al., 1977). This may be due to the fact that days with abrupt fluctuations are quite

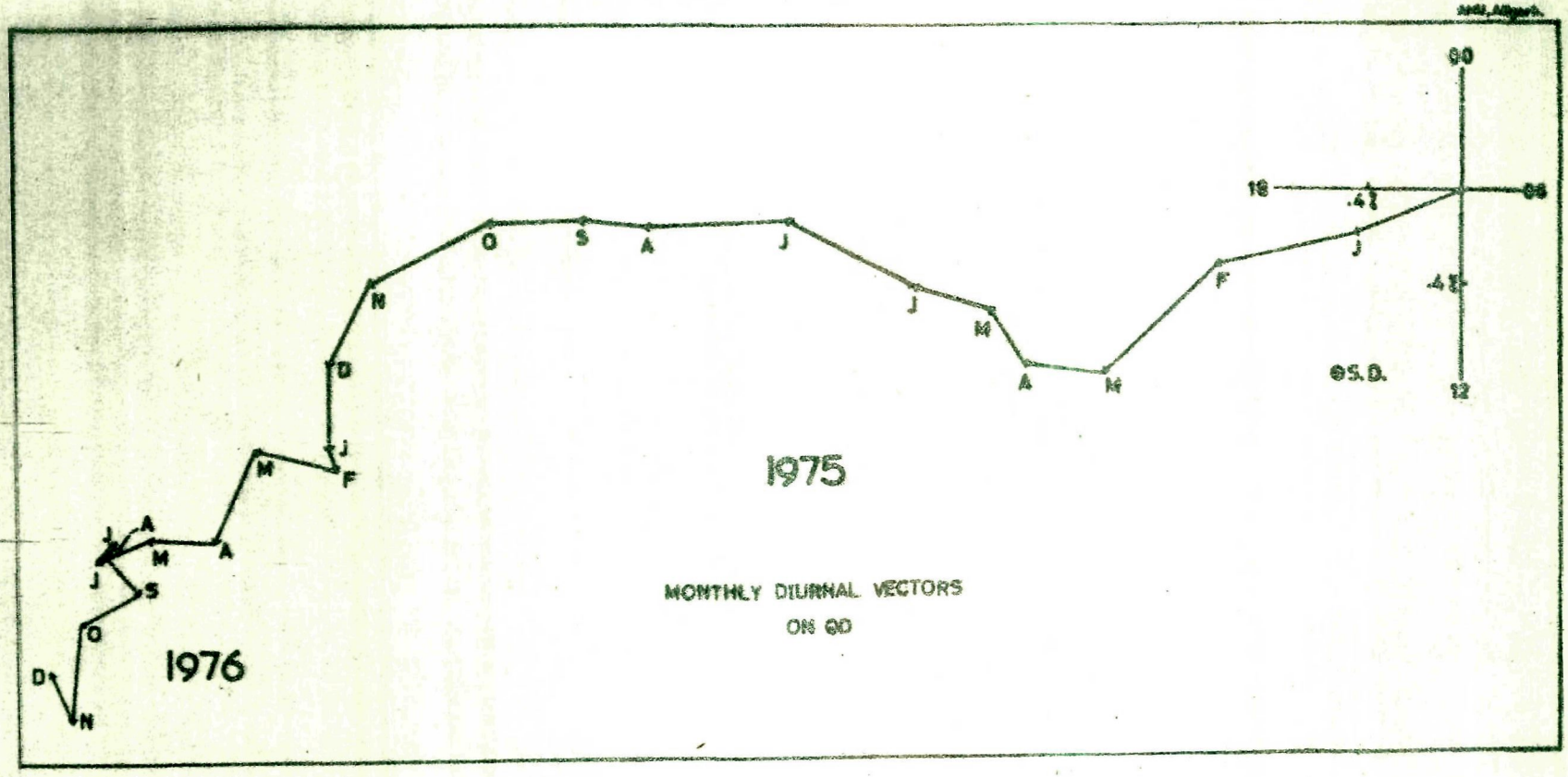

Fig. 4.12 - Shows the vector addition diagram for monthly average diurnal variation on QD for Tokyo (Itabashi) neutron monitor during 1975-76.

frequent especially in the months of July and August, 1976.

Thambyahpillai and Elliot (1953), from the observations of ionisation chamber data recorded at Manchester for the period from 1933 to 1952, for the first time suggested that there exists a 22-year wave in the phase of the diurnal anisotropy, ϕ_1. The systematic and continuous observations made by Carnegie Institution ionisation chambers as well as observations taken at various other places have also supported the existence of 11-year or 22-year periodicity in ϕ_1 (Sarabhai and Kane, 1953; Sarabhai et al., 1954; Stenmaurer and Gheri, 1955). The observed variation in the diurnal anisotropy vector with 11-year periodicity has been generally explained in terms of systematic variation in the upper cutoff rigidity with solar cycle, keeping the free space amplitude almost constant.

4.4 Theoretical models

Gleeson (1969) and Forman and Gleeson (1975) have given the Convection-Diffusion model to explain the cosmic ray diurnal anisotropy. Also, Quenby and Hashim (1969), Forbush (1967, 1969, 1973), Forbush and Beach (1975) and Levy (1976) have theoretically explained these observational results together with those for recent periods from meson detectors. Their models are discussed in detail in the following Sections in the context of the recent variations in the diurnal anisotropy on QD as

observed by neutron monitors.

4.41 Convection-Diffusion model

Gleeson (1969) and Forman and Gleeson (1975) have derived the streaming equation to explain the cosmic ray diurnal anisotropy, $\bar{A}$. It contains the effects due to convection, field aligned diffusion, perpendicular diffusion and the density gradient and may be represented as follows

$$\bar{A} = \bar{A}_c - \frac{3K_{\parallel}}{V}\bar{G}_{\parallel} - \frac{3K_{\perp}}{V}\bar{G}_{\perp} - \frac{3K_T}{V}\frac{\bar{G}\times\bar{B}}{B} \qquad \ldots 4.1$$

where $\bar{A}_c$ is the convective component along the direction of solar wind radially outward from the Sun, $K_{\parallel}$ and $K_{\perp}$ are the diffusion coefficients parallel and perpendicular to the ecliptic component B_{xy} of the magnetic field $\bar{B}$[$B_{xy} = (B_x^2 + B_y^2)^{1/2}$ in the ecliptic plane], V is the particle speed, $\bar{G}$ is the vector density gradient of cosmic rays in the ecliptic plane and K_T is an effective transverse diffusion coefficient.

The contribution of last two terms due to perpendicular diffusion and density gradient is usually small as compared to other terms. The simple convection-diffusion theory where the last two terms in Equation-4.1 are not considered, has been found very successful in explaining the average diurnal anisotropy on 8D for the period from 1957-70 and for majority of days in a year on day-to-day basis (Mathis et al., 1972; Rao et al., 1972;

Ananth et al., 1974; Kane, 1974). The model is depicted in Figure-4.13, to explore the possibilities whether this simple concept of convection and diffusion is also applicable for the period 1971-76 when the characteristics of the diurnal anisotropy on QD have drastically changed.

It has been observed for the period 1970 onwards that neither the solar wind velocity has changed very significantly nor the I.M.F. direction is different from the expected Archimedean spiral as observed earlier during 1957-70. Therefore, in the absence of direct measurements of the diffusion tensor as well as the density gradients both in and out of the ecliptic plane, it is not possible to find the relative contribution of the perpendicular diffusion and density gradient terms to explain the observed variations during 1971-76.

We may deduce the solar wind velocity from the geomagnetic field parameters (K_p - or A_p-index) with the help of the following established expression (Snyder et al., 1963)

$$V(km/sec) = 8.44\ \Sigma K_p + 330 \qquad \text{Eq. 4.2}$$

This may be used to derive the field aligned nature of the diffusion vector on the basis of convection-diffusion model. In this way, the phase shift to earlier hours for the diurnal anisotropy may be understood as due to

(i) the enhancement of the convective vector due to an increase in solar wind velocity accompanied by the increase in

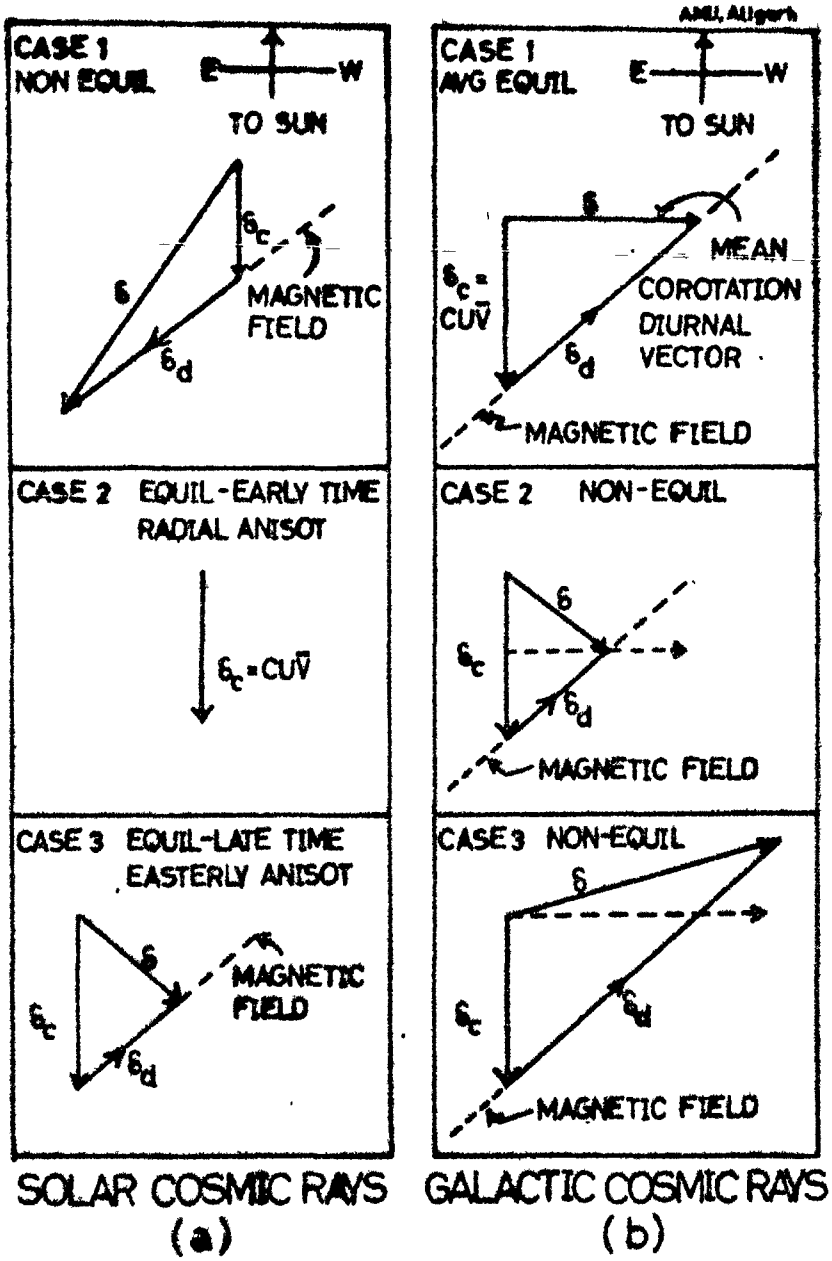

Fig. 4.13 - The proposed unified convection-diffusion model explaining the cosmic ray anisotropies observed at (a) low energies (~ 10 MeV) and (b) high energies (>1 GeV).

A_p-index, which will be accompanied by an increase in the value of r_1 and decrease in ϕ_1,

(ii) as a decrease in the diffusive vector due to an increase in the value of $K_\perp/K_{||}$, which will be accompanied by decrease in r_1 and also decrease in ϕ_1, or

(iii) if both of these operate simultaneously, the amplitude of the diurnal anisotropy may remain constant, shifting ϕ_1 to earlier hours.

However, as is observable in Figure-4.1, which shows the variation of A_p-index on QD supported by the available 'in situ' measurements on solar wind velocity, it is apparent that there is no any significant increase either in the value of A_p-index or the solar wind velocity on QD during 1970-71 and 1972-73. It appears from here that the phase shift towards earlier hours during 1970-71 and 1972-73 is not caused due to the variation in the solar wind velocity. Therefore, the increase in the value of $K_\perp/K_{||}$ may be responsible for causing the large phase shift to earlier hours of the diurnal anisotropy on QD during 1970-71 and 1972-73. This provides the evidence for the significant contribution of the last two terms of the Equation-4.1.

Further, keeping in view the possible relationship between A_p-index and solar wind velocity, as discussed above in (i), it is expected that in any distribution, the increase in A_p-index must reduce the value of ϕ_1. This behaviour has been confirmed

by the observations for the period from 1965-70 for all the neutron monitoring stations (Figure-4.8). However, the opposite relationship between A_p - ϕ_1 is noticed from 1971 on Ahmedabad and Mt. Norikura and from 1973 on all the stations under consideration, i.e., with an increase of A_p-index the value of ϕ_1 increases. Therefore, this behaviour once again shows that the interplanetary conditions have changed drastically for the period 1971-76, indicating that there is better association of the behaviour of the diurnal anisotropy with the $K_\perp/K_{||}$ during 1971-76.

4.42 Other models

(a) Forbush (1967, 1969, 1973) and Forbush and Beach (1975) have explained the long term variations in the diurnal anisotropy as observed by high energy detectors. They have proposed that the total diurnal anisotropy vector is composed of two parts; one component W which is in the direction 128°E from the Sun-Earth line and the other component V at 90°E of the Sun-Earth line. The W component varies with a periodicity of 20-years and passes through its minimum value when Sun's poloidal field changes its direction. This usually occurs during each solar activity maximum. However, according to Forbush (1973), W component passed through zero in the year 1971, three years later than the expected period. This coincides with the Sun's polarity change which occurred in 1971.

when the Sun's north polar field changed from negative to positive values (Howard, 1972). The other component V, varies with the periodicity of one solar cycle ($\simeq$ 10-years). However, this model is not successful in explaining the variations found in the diurnal anisotropy on QD as observed by neutron monitors due to following reasons

(i) the amplitude and phase of the diurnal anisotropy on QD have remained practically constant for the period 1957-70, whereas the model predicts continuous and significant changes in both r_1 and β_1 during this period, even at neutron monitor energies,

(ii) as the component W passes through zero in 1971, the variation in the amplitude and the phase of the diurnal anisotropy on QD in the adjoining years 1970 and 1972 should be of the same order as compared to 1971. However, our analysis shows that for diurnal anisotropy on QD there is large phase shift towards earlier hours at all the neutron monitoring stations supported by the meson monitors associated with significant decrease in amplitude at higher energy range during 1970-1971 with little or no change during 1971-72, and

(iii) the resolution of the diurnal anisotropy vector in two components, i.e., one in the average I.M.F. direction at the Earth's surface, and the other in the corotational direction, is only based on the experimental observations of the

periodicity of long term variation in the diurnal anisotropy for the high energy detectors.

The only justification which is in favour of this model is that W component assumes its mean value of zero during precisely the same year in which the Sun's polar magnetic field reverses its direction. However, this is also not in accordance with our observations and the reasoning given in (ii) above.

(b) Quenby and Hashim (1969), after examining the ionisation chamber data, as Forbush did, and also on the basis of their own observations taken at Manchester, have concluded that the azimuthal streaming from the corotational direction (90^0E of the Sun-Earth line) may be modified by the addition of a heliocentric radial component of streaming always directed away from the Sun. The model suggests that the cosmic ray particles have easy access into the plane of ecliptic from higher heliolatitudes and therefore, an outward radial streaming superimposed on the azimuthal component may result at certain periods of the solar cycle, shifting ϕ_1 to earlier hours and causing an increase in the semi-diurnal amplitude.

Our results (presented in Chapter-V) based on neutron monitor data, for the period 1970-71, show an increase in the value of the amplitude, a_2^0, of the semi-diurnal anisotropy on QD by a factor of two in association with the large phase shift towards earlier hours of the diurnal anisotropy on QD. These results are in qualitative agreement with radial streaming hypothesis.

However, we do not observe any significant increase in the value of r_2^Q associated with the observed decrease in the value of β_1^Q during 1972-73. Further, according to their model the free space amplitude may vary continuously during the solar cycle. Our systematic experimental observations on QD do not support this prediction.

(e) Recently, Levy (1976) has proposed a theoretical model. He has computed the properties of the 22-year wave by assuming the most probable interplanetary parameters. According to this model, an odd symmetry in the I.M.F. about the solar equatorial plane may produce the double solar cycle variation in the diurnal anisotropy. The solar field oscillates by changing its sign in about 11-years so that the full solar magnetic cycle is approximately 22-years. The I.M.F. which is an extension of the solar field through the interplanetary space by its convection through solar wind, reflects the large scale symmetry characteristics of the solar field. By assuming that magnetic field in each hemisphere of the solar magnetic cavity has the same average sense as the magnetic field at the solar pole, the theory predicts a net migration in the direction $\nabla \times \bar{B}$ of positively charged particles with trajectories that cross the reversing layer in the solar equatorial plane. When the north polar fields are directed outward the anisotropy corresponds to a streaming of particles 'away' from the Sun, and the sense reverses when the solar field reverses. This manifests itself as an anisotropy along the

garden hose field direction that varies with the solar magnetic cycle (22-year wave), in accordance with our observations on QD.

Furthermore, the computations indicate that the amplitude of this solar magnetic cycle anisotropy increases with energy. The results from neutron monitor observations for the diurnal anisotropy on QD presented earlier have shown clearly that the shift in the phase of the diurnal anisotropy on QD during 1970-71 is maximum for low latitude neutron monitors like Ahmedabad, Tokyo and Mt. Norikura suggesting that the amplitude of the solar magnetic cycle anisotropy is more for high cutoff rigidity stations as mentioned above as compared to low cutoff rigidity stations.

Our neutron monitor results, for the period 1970 onwards when taken together with the observations prior to 1957, are in qualitative agreement with this model. However, since the systematic neutron observations at widely distributed points are available only through 1957, therefore, a continuous watch for further period is essential, so as to test its validity. Further, the measurements of off-ecliptic interplanetary parameters will also be needed to derive the realistic values for comparison with observations. Qualitatively, the model is able to explain both neutron as well as meson observations.

4.5 Conclusions

On the basis of the neutron monitor observational results and discussion presented in the earlier Sections, the following important conclusions have emerged

1. the amplitude of the diurnal anisotropy of cosmic ray intensity on QD has remained practically invariant during the period 1957-70 ($\sim$0.4 % in space), and the small but significant change in the diurnal amplitude on QD during solar minimum period 1964-65 may be understood in terms of the variation of upper cutoff rigidity, R_{max}, beyond which cosmic ray particles do not corotate.

2. a small decrease in the amplitude of the diurnal anisotropy on QD is also observed on all the latitudes during 1971-72.

3. the decrease in the diurnal amplitude on QD is more pronounced during 1975-76, the period of minimum solar activity. This variation is not accountable by a reasonable change in the value of rigidity spectrum or R_{max}. Further, the diurnal amplitude on QD is very low during July-September, 1976.

4. the phase of the diurnal anisotropy of cosmic ray intensity on QD has remained practically invariant during the period 1957-70 (azimuthal direction or $\sim$ 19 hour in space). Thus, the characteristics of the diurnal anisotropy on QD during the period 1957-70 are in complete agreement with the predictions of convection-diffusion theory.

5. the phase of the diurnal anisotropy has been continuously shifting to earlier hours as we go back to 1954 from 1957. Also, in 1954, the year of minimum solar activity (22-years ago than 1976) the diurnal phase is observed in the $\simeq$ 03 hour direction associated with constantly 'away' interplanetary magnetic field.

6. again, during the declining phase of the present solar cycle 20, the phase of the diurnal anisotropy on QD has steadily advanced to earlier hours since 1971. The phase shift during 1971 is found to be larger at equatorial stations as compared to other stations.

7. the phase shift to earlier hours is more pronounced in the years 1971, 1973, 1975 and 1976. The phase of the diurnal anisotropy on QD, on monthly average basis, has been observed in the early morning hours ($\simeq$ 03 hour) during July-September, 1976; during this period the I.M.F. is almost pointing 'away', leaving aside the mixed polarity days.

8. for the diurnal anisotropy on QD, the rigidity exponent (β) has been estimated to be $\simeq 0 \pm 0.2$ with the upper limiting rigidity $R_{max} \simeq 100$ GV, for the period prior to 1970. For 1971-74, β has been estimated to be $\simeq -0.4 \pm 0.2$ for the same value of the upper limiting rigidity.

9. the phase of the diurnal anisotropy on MSD where the value of A_p-index is higher, is found to shift towards earlier

hours in comparison to the phase of the diurnal anisotropy on QD where the value of A_p-index is lower, on all the stations except Ahmedabad and Mt. Norikura for the period from 1965-72, which is normally expected. For the period from 1973-75, this relationship has become completely opposite on all the stations, i.e., the phase of the diurnal anisotropy on MSD where A_p is higher, has shifted towards later hours in comparison to the phase of the diurnal anisotropy on QD where A_p is lower. However, Ahmedabad and Mt. Norikura neutron monitoring equatorial stations have shown this opposite relationship between A_p - β_1 starting from 1971 onwards. Therefore, the relationship between the A_p-index and the diurnal anisotropy is not invariant during the entire period 1965-75.

10. thus, the variation in the diurnal anisotropy on QD as observed by neutron monitors for the minimum solar activity period 1975-76 is exactly similar to that occurred during the minimum solar activity period 1953-54. Hence, it is quite apparent from here that there is 22-year periodicity in the diurnal anisotropy on QD.

11. the observed variations in the amplitude and phase of the diurnal anisotropy on QD during 1971-76 are not explained by the simple convection-diffusion model due to the probable significant contribution of the perpendicular diffusion and the density gradient terms. Therefore, the knowledge of their relative contribution is of great importance.

suggested to explain the 22-year periodicity in the diurnal anisotropy has been found to be satisfactory to explain the neutron monitor observations on quiet days for the entire period under consideration.

The maiden concept of diurnal anisotropy of cosmic ray intensity proposed here is extremely interesting, since it is quite clear from the results presented here and the conclusions drawn that there is definitely a 22-year periodicity in the diurnal anisotropy, which is observable particularly on QD when a systematic and detailed analysis on long term variation of diurnal anisotropy during different types of days has been performed by the author. Levy's (1976) model has been found satisfactory for understanding the changing behaviour of the interplanetary medium and to explain the variations observed in the diurnal anisotropy. The direct space-craft measurements of the interplanetary magnetic field and plasma together with the cosmic ray flux at various regions would be of great significance in understanding the present behaviour in the diurnal anisotropy and establishing the validity of the proposed model.

CHAPTER - V

CHARACTERISTICS OF THE SEMI-DIURNAL ANISOTROPY

5.1 Introduction

The existence of a significant semi-diurnal anisotropy vector of the cosmic radiation has been proved as early as fifties (Sarabhai and Nerurkar, 1956). However, the observed low amplitude of the semi-diurnal anisotropy and the poor statistics of the observational data had given rise to serious doubt about its presence. As a consequence of it, Katzman and Venkatesan (1960) showed that the semi-diurnal component of the nucleonic intensity is essentially a pressure effect and within the accuracy possible, the existence of a residual vector after correction for pressure can not be established, except at equatorial latitudes. The observed higher amplitude at equatorial stations could not be explained. Since, for a normal type of anisotropy having a negative or zero exponent one expects a smaller amplitude at equatorial stations.

The existence of the semi-diurnal component was strongly indicated from a comparison of the observed variation in the East and West pointing telescope inclined at the same angle to zenith, where the atmospheric contribution to the observed daily variation may be cancelled to a first approximation (Elliot and Bothwell, 1956). The first positive confirmation for the existence of semi-diurnal anisotropy was provided by

Rao and Sarabhai (1961), making use of crossed meson telescope. By using improved numerical filter techniques to obtain better signal to noise ratio with the data from super neutron monitors having high statistical accuracy, Ables et al. (1965) conclusively showed the existence of semi-diurnal component of world wide nature having the phase aligned perpendicular to the I.M.F. direction. The analysis by Ables et al. (1965), Patel et al. (1968) and Lietti and Quenby (1968) have also indicated that the semi-diurnal component has a positive exponent, thus explaining its enhanced presence at equatorial latitudes.

We may derive the following characteristics of the semi-diurnal anisotropy from cosmic ray intensity measured on the Earth

$$\frac{\delta J(R)}{J(R)} = A\, R^{\beta}\, g(\Lambda)\, f(\beta) \qquad \text{for } R_{min} \leqslant R \leqslant R_{max}$$

$$= 0 \qquad \text{for } R_{min} > R > R_{max}$$

where J(R) is the differential rigidity spectrum of primary cosmic ray particles of rigidity R, A represents the magnitude of the anisotropy in space defined in terms of a percent change in the 12 hourly mean intensity of galactic cosmic rays, R^{β} shows the rigidity spectrum of variation of the semi-diurnal anisotropy specified by the exponent β, and limiting rigidities R_{min} and R_{max} in the above relation. The function $g(\Lambda)$ describes the dependence of anisotropy on declination. We have

the directions in space of maximum intensity ϕ_{max}, and of minimum intensity ϕ_{min}.

With the availability of a large amount of data from various super neutron monitors including from equatorial locations, in the last few years, it has now been possible to investigate the semi-diurnal anisotropy characteristics in much greater detail. The author has conducted such a detailed analysis to investigate the characteristics of semi-diurnal anisotropy on different types of days and their long term variation. The results are presented in the following Sections.

5.2 Observational results

Using the results of the theoretical calculation for the relative amplitude and phase of the semi-diurnal variation (McCracken et al., 1965; Agrawal, 1977) for an assumed anisotropy in space, and the observations from a number of neutron monitoring stations given in Table-4.1 and shown in Figure-4.2, the author has attempted for the first time, to derive the detailed characteristics of the semi-diurnal anisotropy of cosmic radiation on different types of days. The number of days used for the analysis on different types of days and for various years are given in Table-4.2. In the following Sections, we first derive the characteristics of the semi-diurnal anisotropy on different types of days and then compare the results with the theoretical predictions.

5.21 Spectral exponent of semi-diurnal anisotropy

The spectral index may be determined by an intercomparison of either the semi-diurnal amplitude, r_2 or the semi-diurnal phase in space, ϕ_2 as observed at a number of stations. The value r_2 and ϕ_2 has been derived for each station and each year for different values of β from -1.5 to +2.0 and for various values of R_{max} from 60 to 500 GV. The variance, χ^2 in the value of r_2 or ϕ_2 determined for different stations are evaluated for different values of β for each year during 1964-74. The best fit value of β is obtained by imposing the condition that the variance at that value should be a minimum (Rao et al., 1963). Such type of calculations are performed separately on quiet days, magnetic storms days, disturbed days, and disturbed days without magnetic storms. The analysis has been extended for the entire period to derive the best fit values of β for each year during 1964-74, using both the semi-diurnal amplitude and phase.

5.211 On quiet days

Figure-5.1(a) shows the plot of variance in the values of amplitudes of the semi-diurnal component on QD as observed at different stations calculated for each value of β during the period 1964-74. The curves clearly show that the minimum variance is observed for values of $\beta \simeq +0.6 \pm 0.2$.

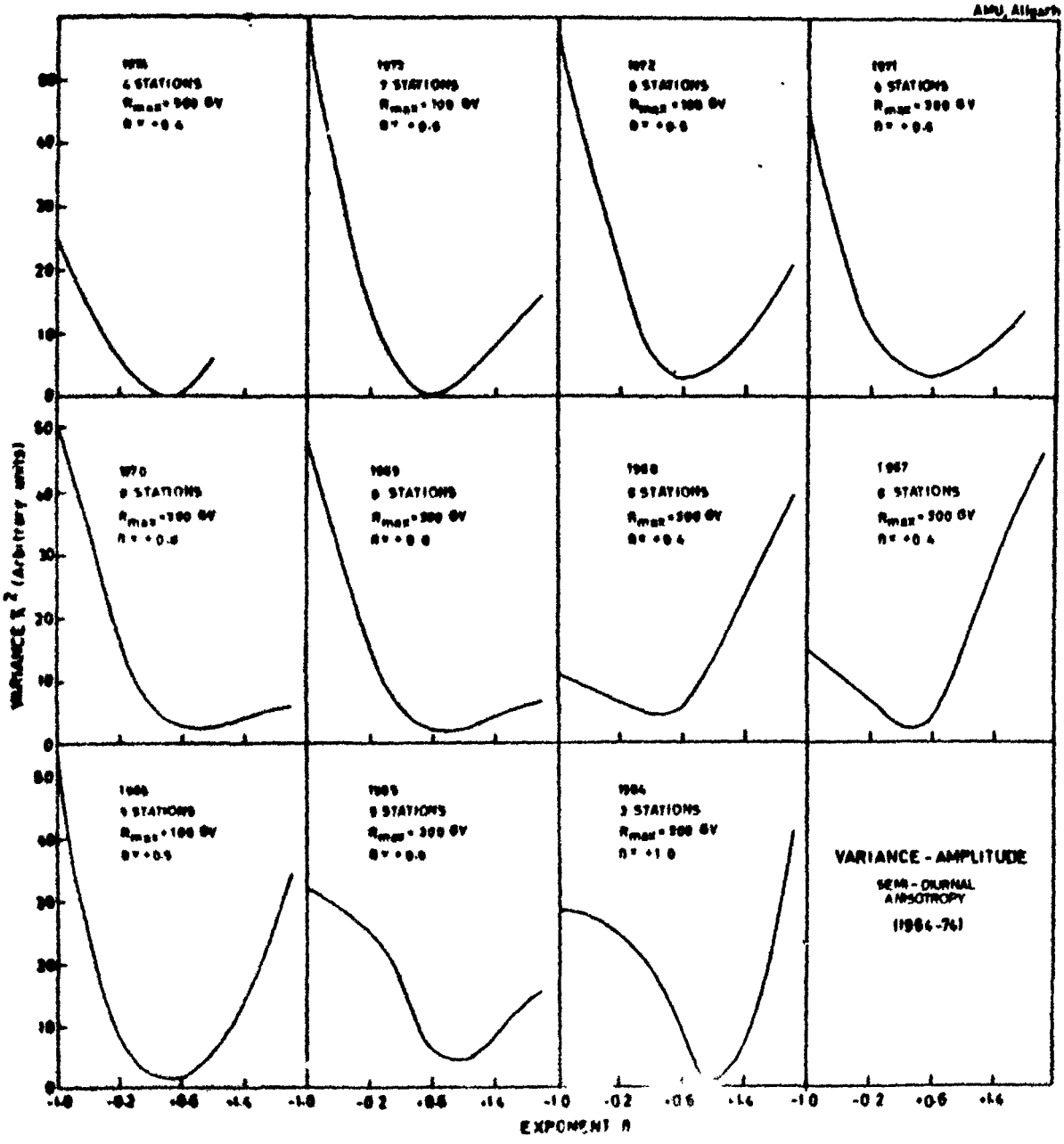

Fig. 5.1 - The observed variance between the semi-diurnal amplitude in years calculated for each station as a function of the exponent n for each year during 1964-74. (a) - (k)

5.212 On magnetic storms days

Figure-5.1(b) shows the plot of variance in the values of amplitudes of the semi-diurnal component on MSD as observed at different stations, calculated for each value of β during the period 1964-74. It is apparent from the Figure-5.1(b) that the minimum variance is observed for the positive value of β upto $\simeq + 0.7 \pm 0.2$.

5.213 On disturbed days and disturbed days without magnetic storms

The plots of variance in the values of amplitudes of the semi-diurnal anisotropy on DD and DDWMS, as observed at different stations, calculated for each value of β during the period 1964-74 are illustrated in Figures-5.1(c) and 5.1(d) respectively. It is observable from the Figure-5.1(c) that β on DD may have either positive or negative value during the period 1964-74 but not zero. Also, from Figure-5.1(d), it is observable that β on DDWMS is positive for the entire period 1964-74, extending upto the value $\simeq + 1.4 \pm 0.2$.

5.22 Long term variation of semi-diurnal anisotropy

To obtain the anisotropy vector in space, the observed amplitude and phase of the semi-diurnal anisotropy for different types of days are corrected for geomagnetic bending and asymptotic cone of acceptance of the detector by taking the value of

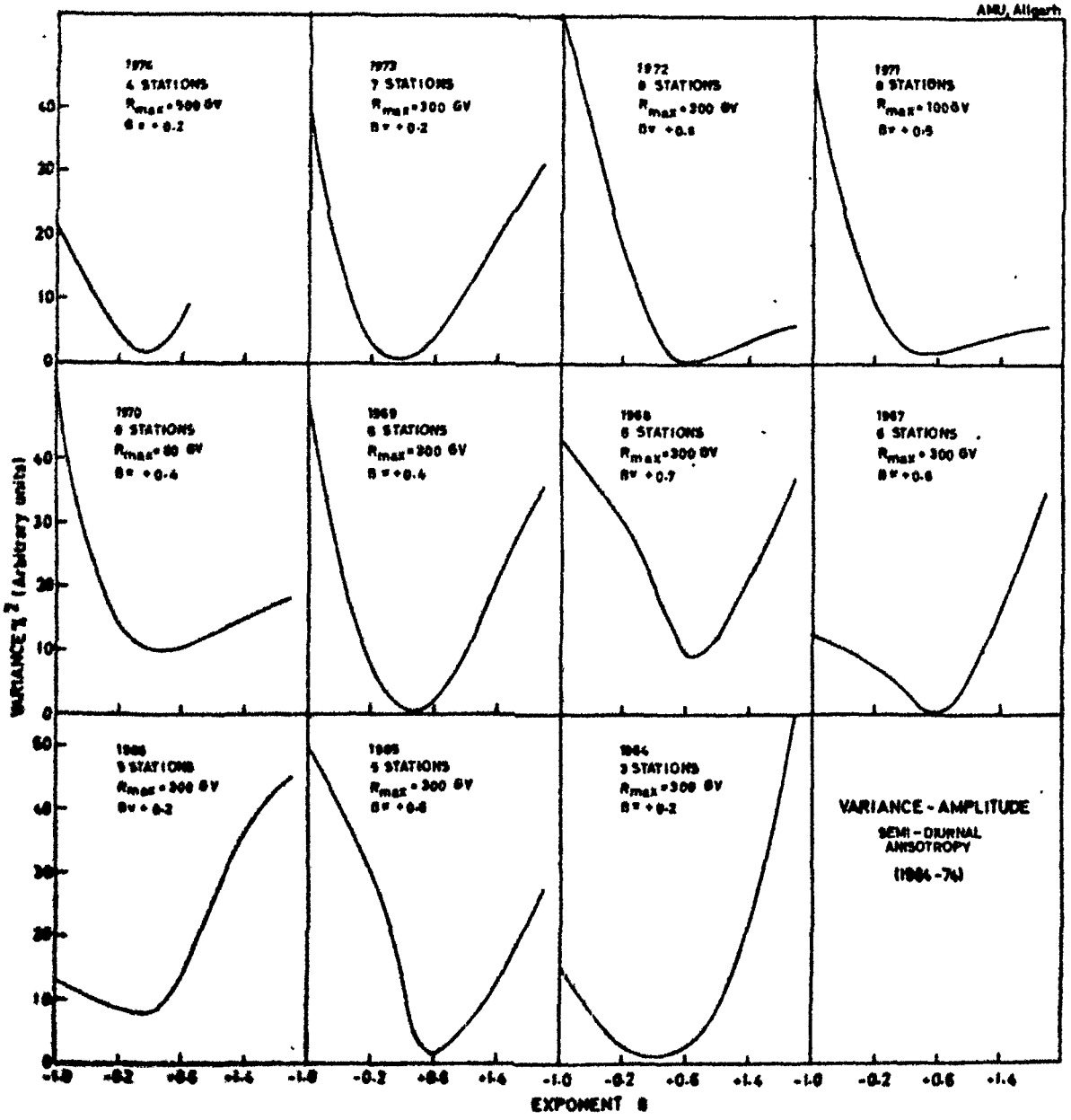

Fig. 5.1(b) - MAGNETIC STORMS DATA.

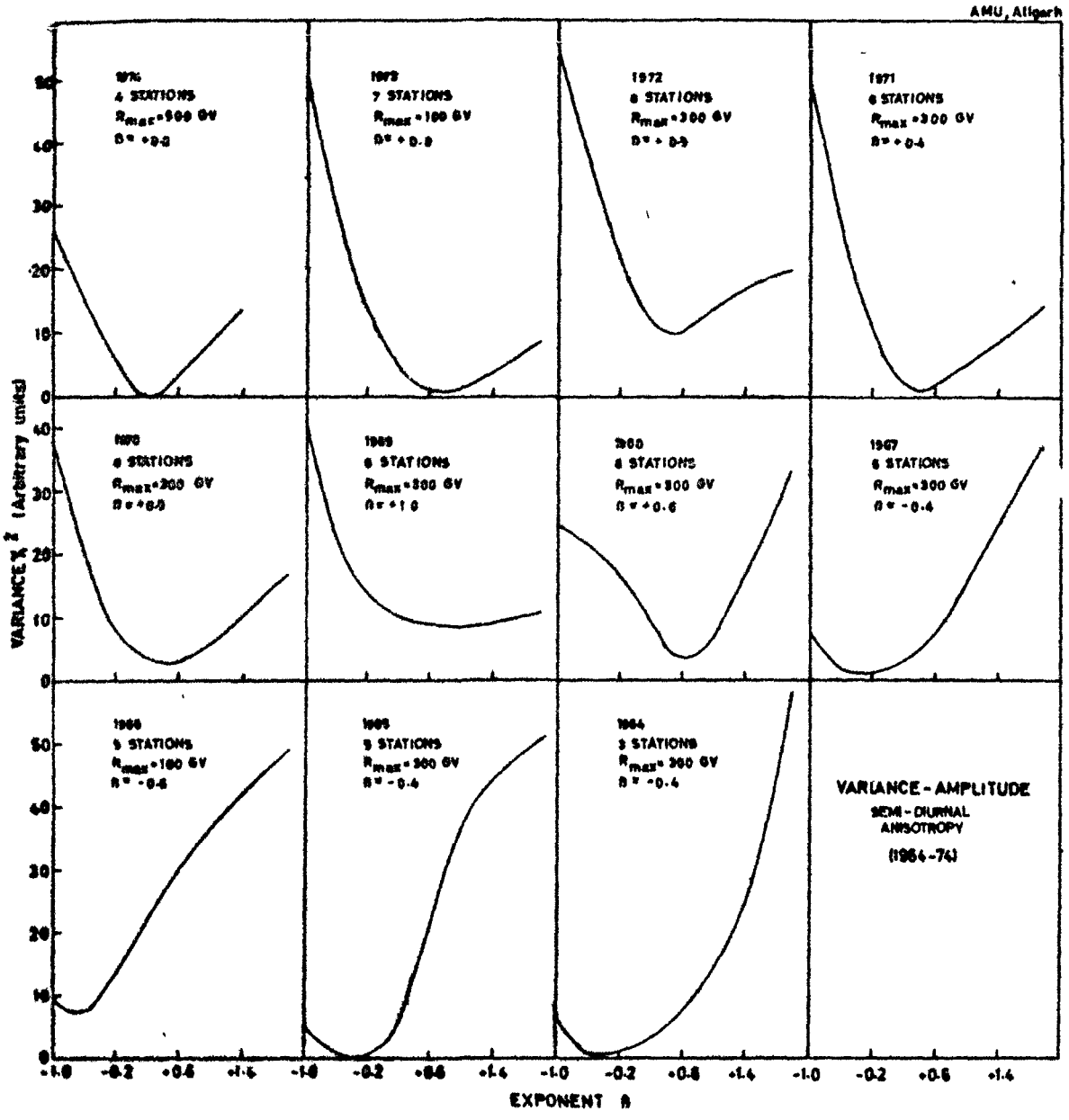

Fig. 5.1(a) - DISTURBED DAYS.

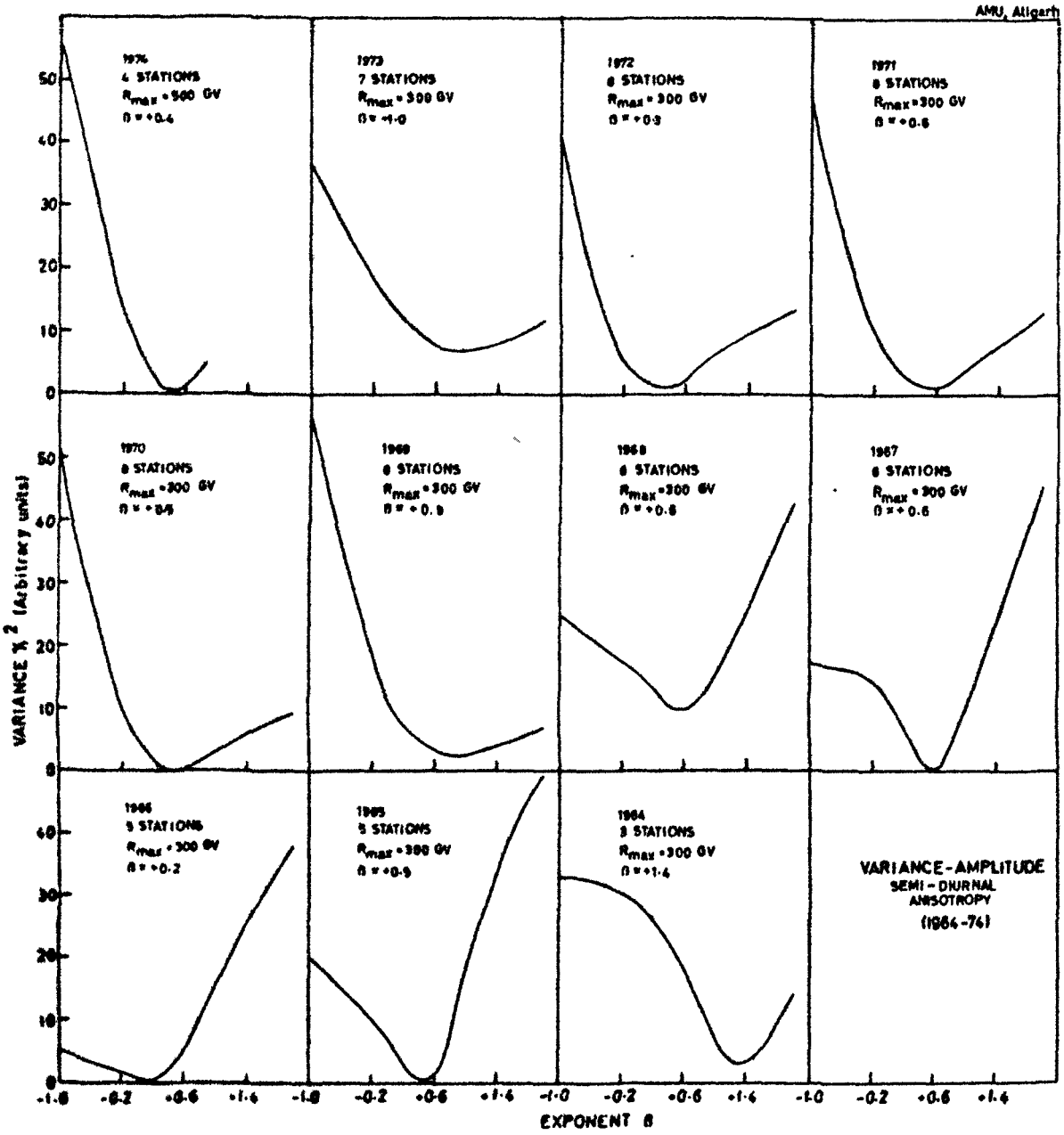

Fig. 5.1(a) - DISTURBED DAYS WITHOUT MAGNETIC STORMS.

the exponent of the energy spectrum $\beta = +0.6 \pm 0.2$ (McCracken et al., 1965; Agrawal, 1977) as discussed in Section-5.21. Thus, the results obtained for the period 1964-76 on different types of days are given below.

5.221 On quiet days

The values of the amplitude and phase of the semi-diurnal anisotropy on QD for the period 1964-76 are given for few stations in Table-5.1(a). The interstation dispersion and yearly average value of the semi-diurnal amplitude and phase on QD, for the period 1964-76, have also been plotted in Figure-5.2(a). It is determined that on QD the average semi-diurnal amplitude, $r_2^Q \simeq 0.08 \pm 0.01$ % and phase, $\phi_2^Q \simeq 3.5 \pm 0.5$ hours for the period 1964-70, for all the stations. Further, Figure-5.2(a) also illustrates that the amplitude and the phase of the semi-diurnal anisotropy on QD remain statistically invariant during 1964-70.

It is also observable from the Figure-5.2(a) that after 1970, the semi-diurnal amplitude on QD has shown an increasing trend, unlike to its behaviour during the period 1964-70 and there is a significant increase in the semi-diurnal amplitude on QD during 1970-71 and 1973-74 at all the stations under consideration. This increase in the semi-diurnal amplitude on QD during 1970-71 by almost a factor of 2 at most of the stations together with the shift of the phase of diurnal anisotropy on QD

TABLE - 5.1

The observed yearly average semi-diurnal anisotropy vector on different types of days for 6-neutron monitoring stations e.g., Tokyo, Rome, Kiel, Leeds, Calgary and Deep River during the period 1964-76. The standard error in harmonic coefficients for each day is given in Table-4.1.

5.1(a) : Quiet Days

Year	Tokyo		Rome		Kiel		Leeds		Calgary		Deep River	
	Amp. (%)	Phase (hrs)	Amp. (%)	Phase (hrs)	Amp. (%)	Phase (hrs)	Amp. (%)	Phase (hrs)	Amp. (%)	Phase (hrs)	Amp. (%)	Phase (hrs)
1964	-	-	-	-	-	-	-	-	.070	4.9	.091	4.1
1965	-	-	-	-	.171	3.1	.050	5.8	.055	5.2	.088	3.8
1966	-	-	-	-	.077	1.6	.017	8.8	.115	3.2	.069	3.1
1967	-	-	.090	8.6	.094	1.2	.093	0.9	.102	2.4	.080	1.2
1968	-	-	.132	2.8	.118	4.2	.029	4.8	.061	4.6	.110	3.4
1969	-	-	.095	3.7	.090	4.3	.050	3.0	.089	3.7	.110	2.4
1970	.099	4.8	.075	0.4	.081	2.9	.022	1.0	.106	3.8	.116	2.4
1971	.138	4.2	.094	1.1	.214	3.2	.175	3.1	.140	3.1	.152	2.6
1972	.087	3.4	.093	0.3	.176	2.1	.175	1.6	.062	5.4	.096	3.1
1973	.164	2.9	.084	10.8	.072	1.6	.069	2.3	.104	3.4	.125	2.3
1974	.130	4.1	.121	0.8	.165	3.0	.158	4.0	-	-	-	-
1975	.163	3.2	.027	1.2	-	-	-	-	-	-	-	-
1976	.097	3.6	-	-	-	-	-	-	-	-	-	-

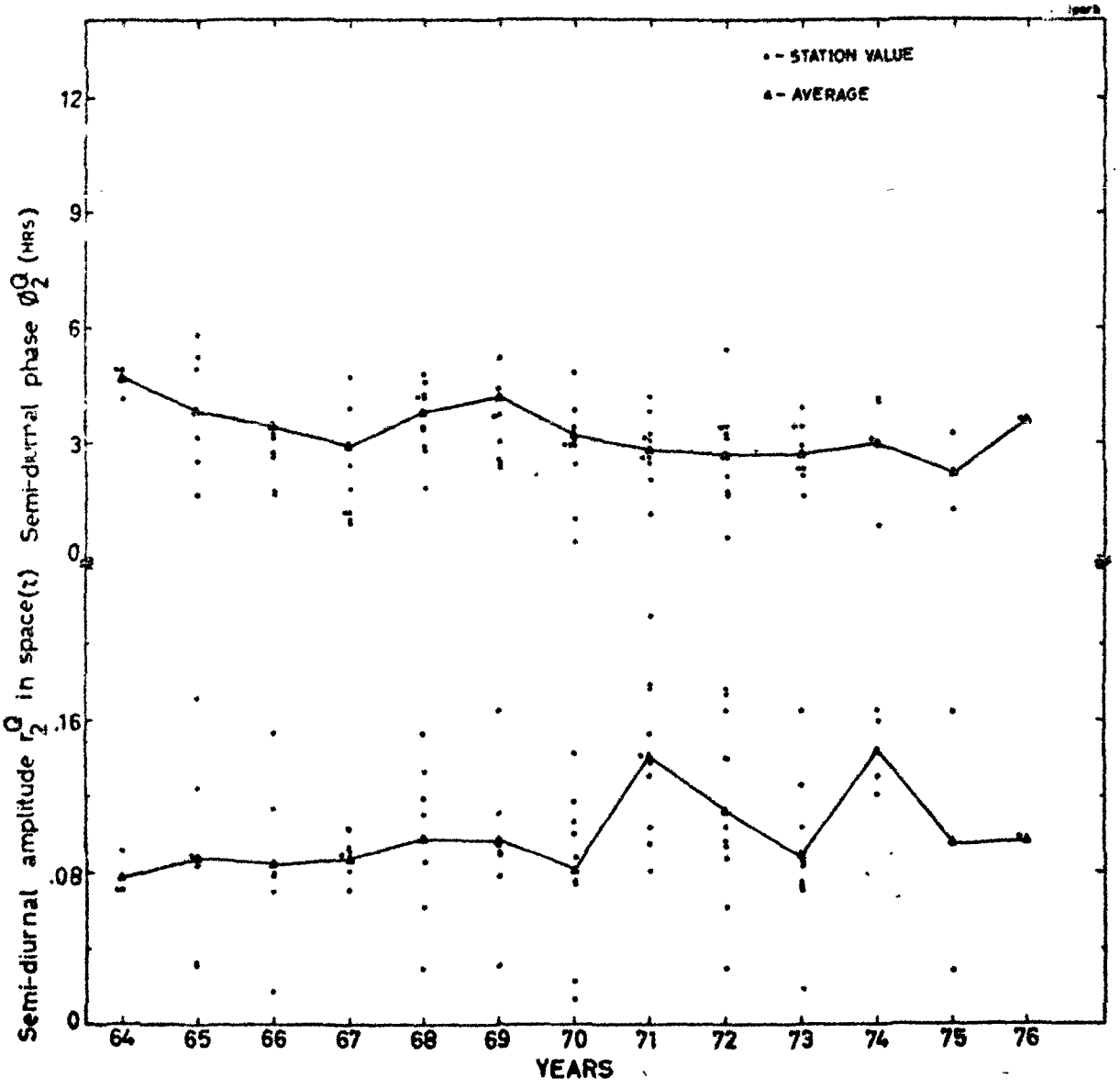

Fig. 5.2 - The interstation dispersion and yearly average value of the semi-diurnal amplitude and phase for the period 1964-76. (a) - QUIET DAYS.

towards earlier hours and not accompanied by any significant increase in the diurnal amplitude on QD during 1970-71 (as discussed in Chapter-IV) has great significance in its production mechanism in terms of the existing models, e.g., this is in qualitative agreement with radial streaming hypothesis. However, we do not observe any significant increase in the value of r_2^Q associated with the observed decrease in the value of ϕ_1^Q during 1972-73 (as discussed in Chapter-IV).

As regards the phase of the semi-diurnal anisotropy on QD, it remains statistically constant during the period 1971-76, as it is observed for the period 1964-70. These view points are demonstrated in Figure-5.3(a) where the observed semi-diurnal amplitude and phase on QD during the period 1964-76 have been plotted for the individual stations separately and also shown on harmonic dial in Figure-5.4(a) for the period 1968-73.

5.222 <u>On magnetic storms days</u>

The values of the amplitude and phase of the semi-diurnal anisotropy on MSD obtained for the period 1964-76 are given for few stations in Table-5.1(b). The interstation dispersion and yearly average value of the semi-diurnal amplitude and phase on MSD for the period 1964-76 have been plotted in Figure-5.2(b). The Figure-5.3(b) illustrates the observed yearly average semi-diurnal amplitude and phase on MSD, plotted for individual stations. The Figure-5.4(b) shows the harmonic

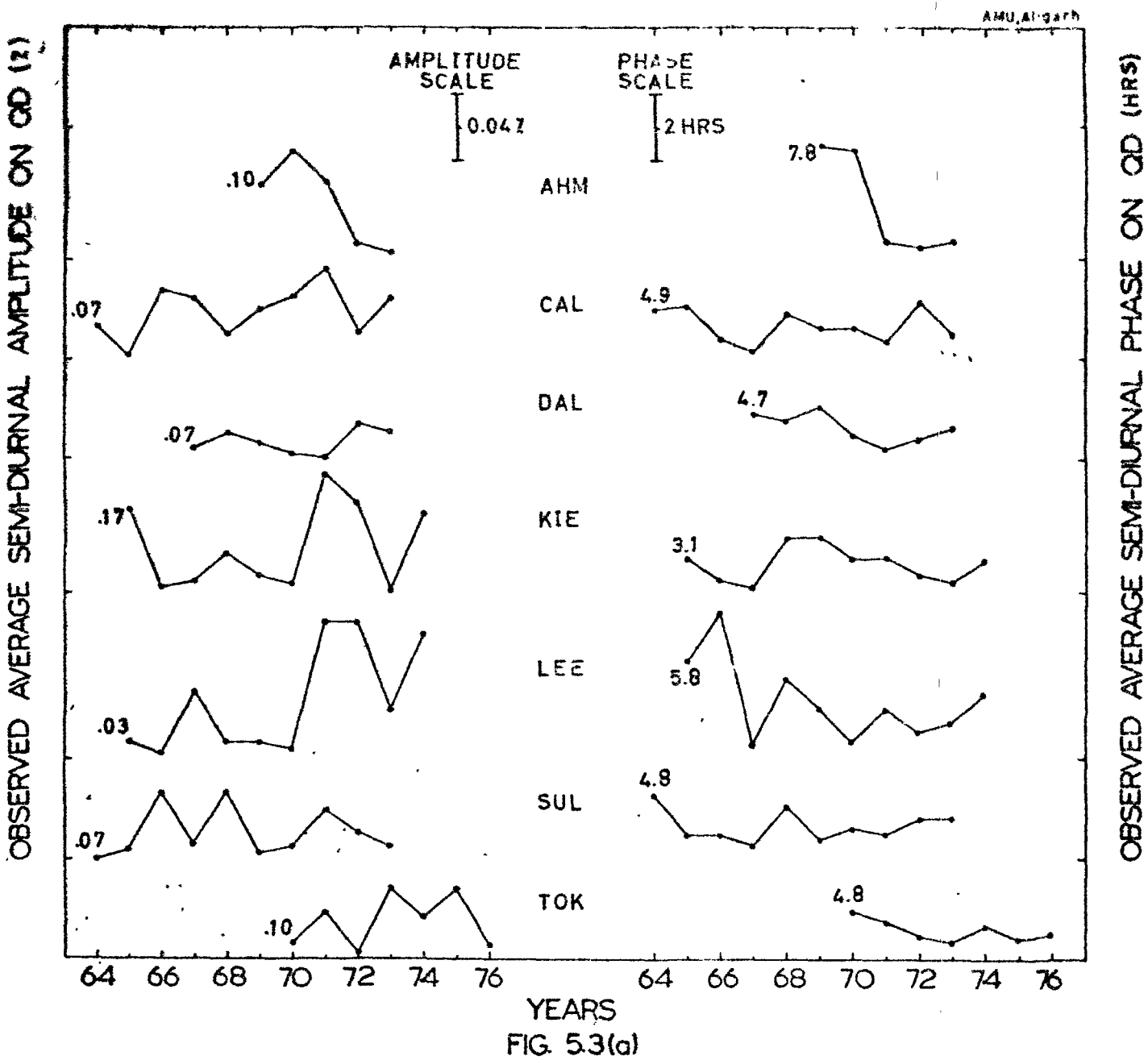
AMU, Aligarh
AMPLITUDE SCALE
0.04 γ
PHASE SCALE
2 HRS
AHM
CAL
DAL
KIE
LEE
SUL
TOK
.10
7.8
.07
4.9
.07
4.7
.17
3.1
.03
5.8
.07
4.8
.10
4.8
64 66 68 70 72 74 76
64 66 68 70 72 74 76
YEARS
OBSERVED AVERAGE SEMI-DIURNAL AMPLITUDE ON QD (γ)
OBSERVED AVERAGE SEMI-DIURNAL PHASE ON QD (HRS)

FIG. 5.3(a)

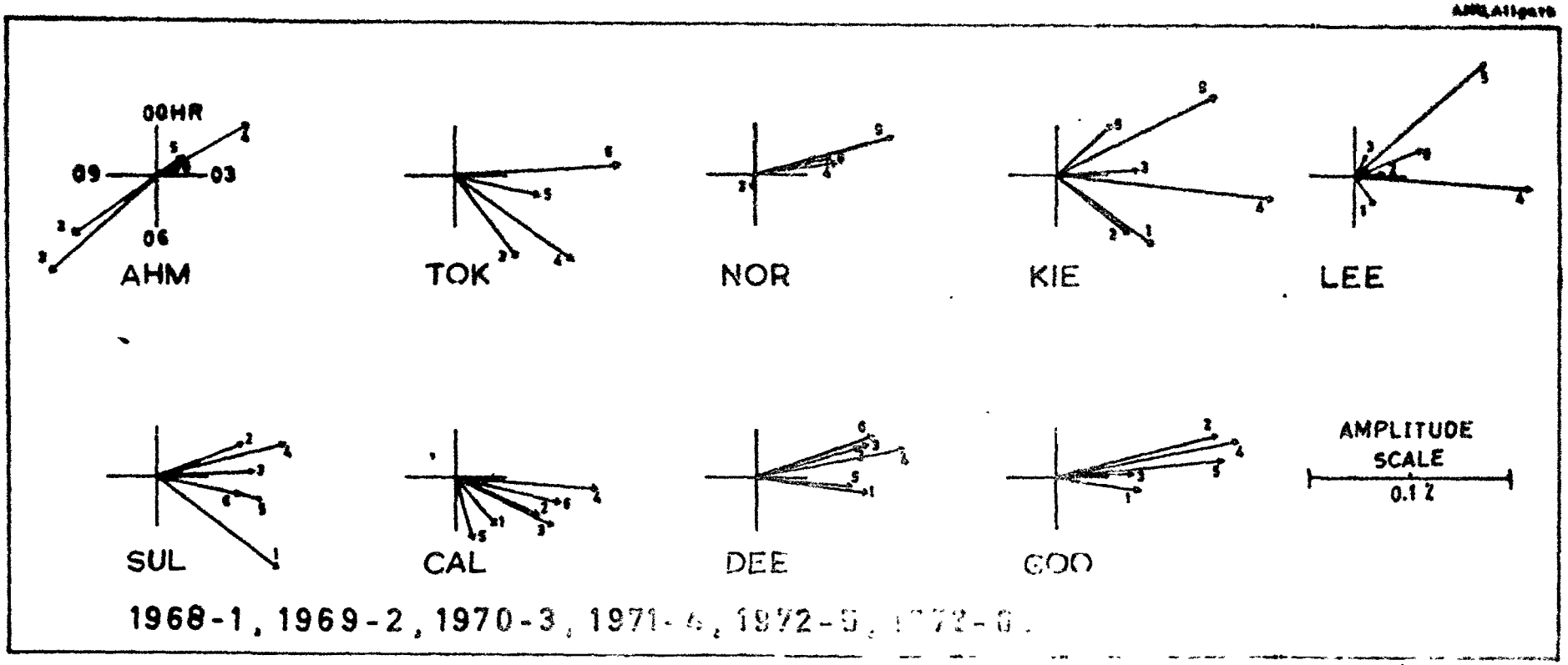

Fig. 5.4 - The observed yearly [illegible] plotted for 9 stations plotted on a harmonic dial during 1968 [illegible]. The [illegible] in the individual daily vectors are given in Table-4.[illegible] (a). [illegible].

5.1(b) : Magnetic Storms Days

Year	Tokyo		Rome		Fiel		Leeds		Calgary		Deep River	
	Amp. (%)	Phase (hrs)	Amp. (%)	Phase (hrs)	Amp. (%)	Phase (hrs)	Amp. (%)	Phase (hrs)	Amp. (%)	Phase (hrs)	Amp. (%)	Phase (hrs)
1964	-	-	-	-	-	-	-	-	.047	5.9	.130	4.8
1965	-	-	-	-	.104	0.2	.182	9.5	.055	7.1	.128	5.0
1966	-	-	-	-	.132	0.5	.079	11.0	.169	4.9	.081	5.4
1967	-	-	.298	7.6	.188	9.1	.254	9.9	.008	1.6	.122	5.1
1968	-	-	.041	1.0	.156	4.6	.050	4.7	.121	3.9	,102	3.8
1969	-	-	.151	3.4	.086	5.8	.061	0.2	.185	2.5	.096	4.3
1970	.115	4.6	.138	3.0	.074	5.7	.138	6.1	.116	7.4	.053	10.2
1971	.129	4.7	.102	2.7	0.35	4.7	.019	10.4	.057	1.8	.193	2.0
1972	.132	2.3	.058	2.1	.122	3.0	.135	3.1	.047	5.6	.193	2.5
1973	.193	3.2	.054	1.3	.199	2.0	.167	2.7	.211	4.5	.247	3.2
1974	.204	4.6	.163	1.3	.095	4.0	.204	4.6	-	-	-	-
1975	.122	1.7	.184	2.7	-	-	-	-	-	-	-	-
1976	.121	3.2	-	-	-	-	-	-	-	-	-	-

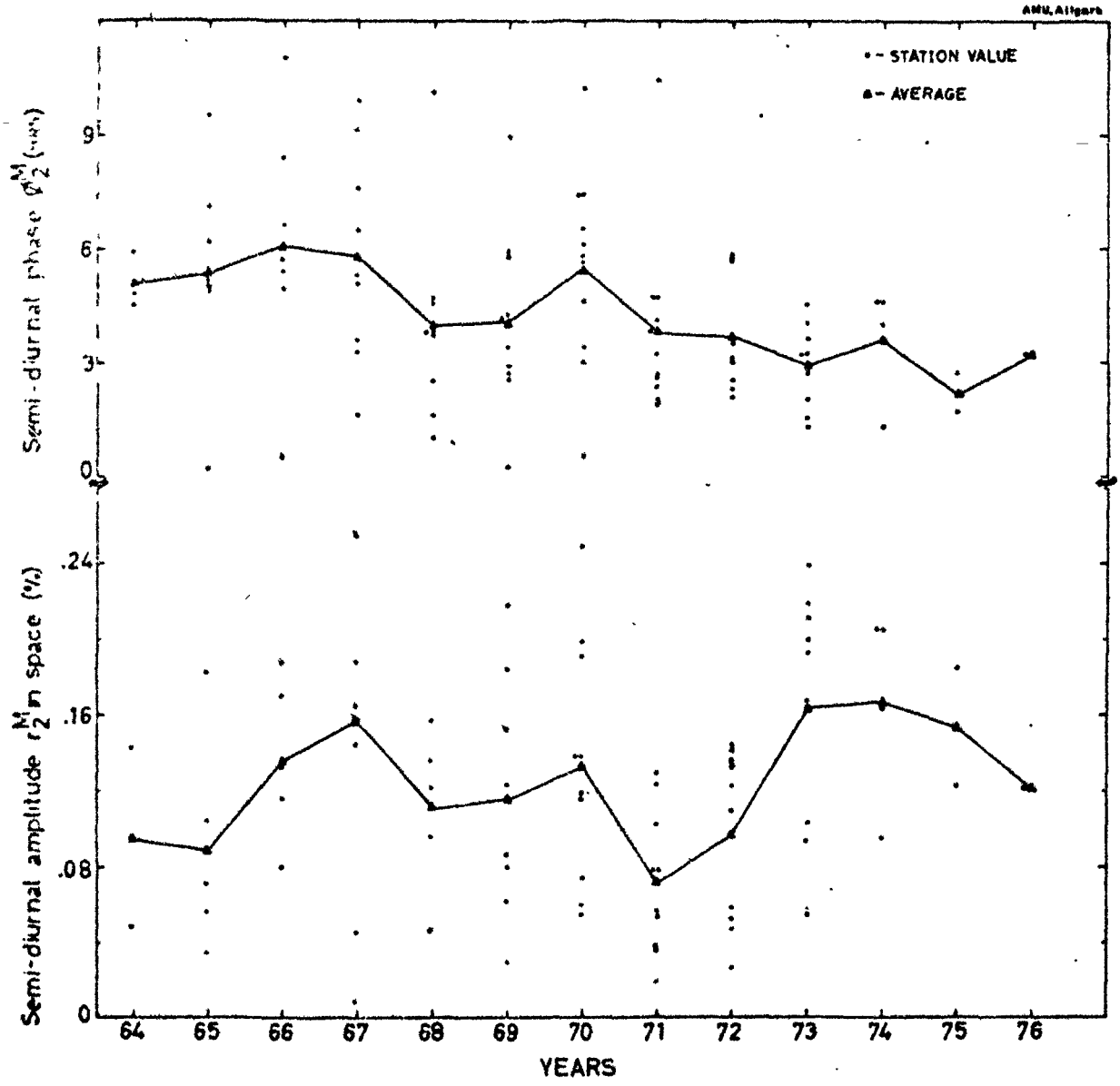

Fig. 5.2(b) - MAGNETIC STORMS DAYS.

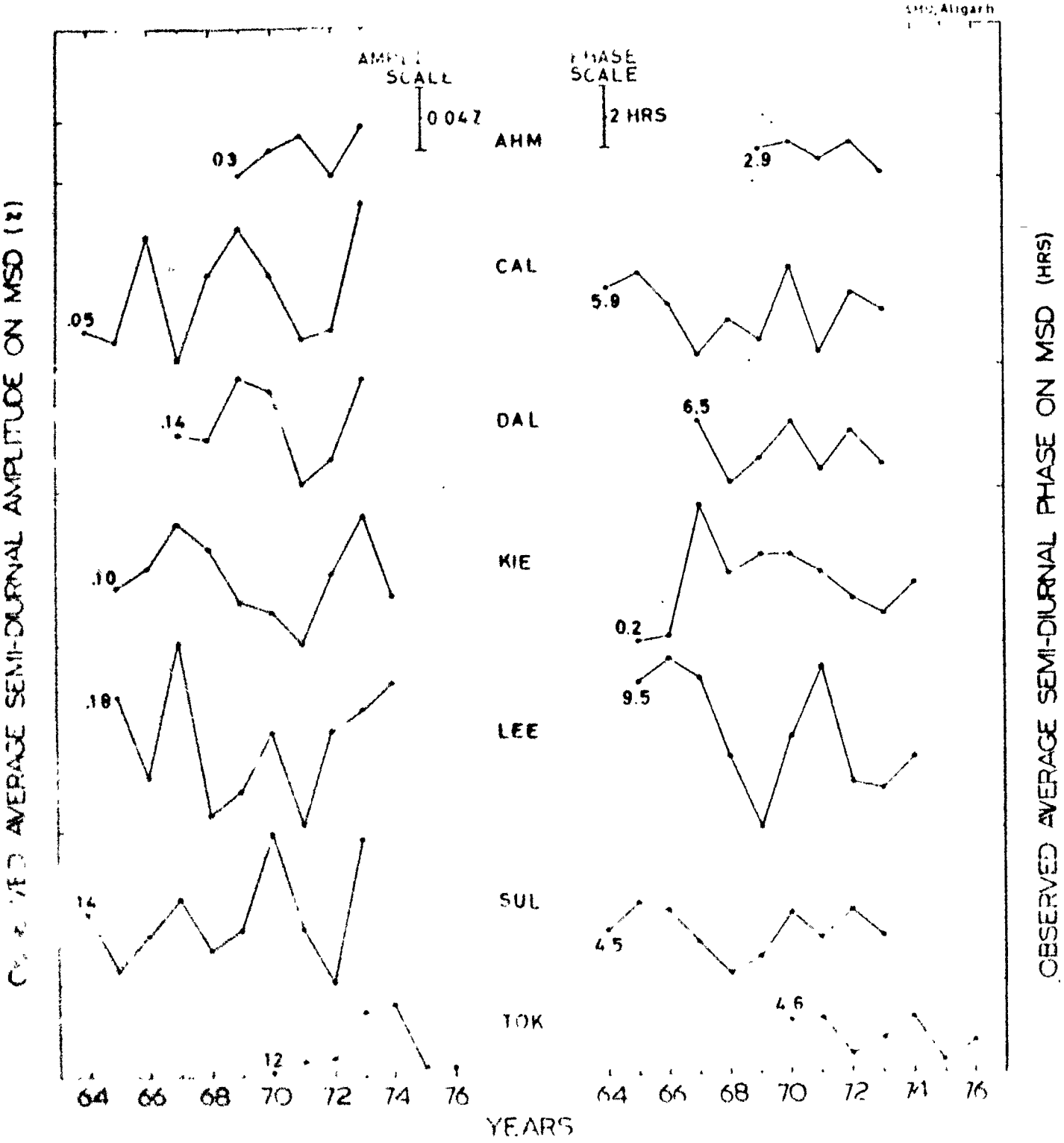
AMPLITUDE SCALE
0.047
PHASE SCALE
2 HRS
AHM
CAL
DAL
KIE
LEE
SUL
TOK
.03
2.9
.05
5.9
.14
6.5
.10
0.2
.18
9.5
.14
4.5
4.6
12
64
66
68
70
72
74
76
YEARS
OBSERVED AVERAGE SEMI-DIURNAL PHASE ON MSD (HRS)

FIG 5.3(b)

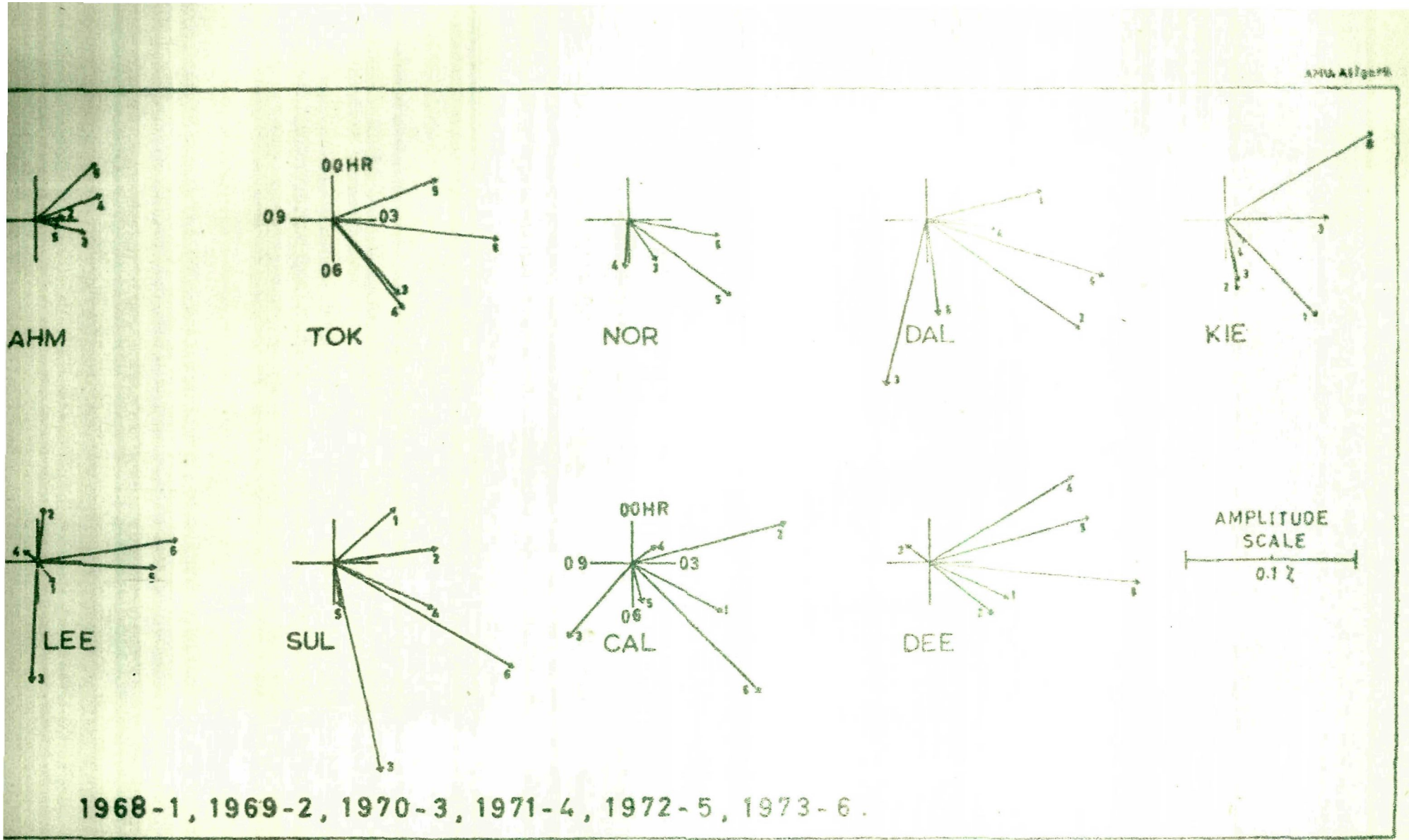

Fig. 5.4(b) - MAGNETIC STORMS DAYS.

dial representation of the semi-diurnal anisotropy vectors on MSD for the period 1968-73.

It is observable from these illustrations that the average semi-diurnal amplitude on MSD shows a slight random variation during the period 1964-70, unlike as shown for QD. However, an increasing trend of the semi-diurnal amplitude is observable on MSD in comparison to that observed on QD during 1964-70. In support of our findings, Agrawal and Singh (1975a) have also reported an increase in semi-diurnal amplitude with the increasing value of A_p-index. Again, opposite to that shown for QD, the semi-diurnal amplitude on MSD during 1970-71 has decreased and during 1972-73 it has increased at most of the stations. The average semi-diurnal phase on MSD shows no definite trend for the entire period 1964-76.

5.223 <u>On disturbed days and disturbed days without magnetic storms</u>

The observed values of the amplitude and phase of the semi-diurnal anisotropy for the period 1964-76 on DD and DDWMS are given for few stations in Tables-5.1(c) and 5.1(d) respectively. The interstation dispersion and annual average values of the semi-diurnal amplitude and phase on DD and DDWMS for the period 1964-76 have been plotted in Figures-5.2(c) and 5.2(d) respectively.

5.1(c) : Disturbed Days

Year	Tokyo		Rome		Kiel		Leeds		Calgary		Deep River	
	Amp. (%)	Phase (hrs)	Amp. (%)	Phase (hrs)	Amp. (%)	Phase (hrs)	Amp. (%)	Phase (hrs)	Amp. (%)	Phase (hrs)	Amp. (%)	Phase (hrs)
1964	-	-	-	-	-	-	-	-	.039	5.3	.105	3.4
1965	-	-	-	-	.039	1.7	.077	8.9	.023	6.0	.103	4.8
1966	-	-	-	-	.077	3.2	.089	5.0	.174	4.5	.128	3.9
1967	-	-	.140	7.3	.097	0.9	.044	0.2	.116	3.1	.116	3.5
1968	-	-	.131	3.7	.179	4.5	.111	4.7	.107	4.2	.158	3.0
1969	-	-	.070	4.1	.054	5.0	.057	0.6	.090	2.3	.061	5.0
1970	.151	5.4	.102	1.9	.056	3.3	.113	5.0	.062	5.2	.045	1.2
1971	.128	4.7	.122	3.5	.086	2.7	.052	3.7	.064	3.0	.147	2.6
1972	.133	2.2	.056	1.2	.128	3.3	.151	3.2	.110	4.2	.182	2.6
1973	.196	3.4	.063	3.0	.155	2.5	.178	3.0	.172	4.7	.210	3.2
1974	.196	4.7	.110	2.6	.151	4.1	.212	4.3	-	-	-	-
1975	.179	2.8	.106	0.6	-	-	-	-	-	-	-	-
1976	.113	3.0	-	-	-	-	-	-	-	-	-	-

5.1(d) : Disturbed Days Without Magnetic Storms

Year	Tokyo		Rome		Kiel		Leeds		Calgary		Deep River	
	Amp. (%)	Phase (hrs)	Amp. (%)	Phase (hrs)	Amp. (%)	Phase (hrs)	Amp. (%)	Phase (hrs)	Amp. (%)	Phase (hrs)	Amp. (%)	Phase (hrs)
1964	-	-	-	-	-	-	-	-	.039	4.2	.155	2.0
1965	-	-	-	-	.112	3.7	.045	5.8	.025	4.7	.083	4.6
1966	-	-	-	-	.165	4.0	.188	5.0	.180	4.3	.199	3.4
1967	-	-	.094	7.0	.303	1.9	.148	3.0	.213	3.1	.186	2.4
1968	-	-	.220	3.9	.204	4.3	.197	4.7	.098	4.4	.232	2.7
1969	-	-	.048	6.5	.043	3.7	.057	0.2	.019	0.7	.044	6.3
1970	.190	5.3	.109	0.9	.107	2.1	.131	3.9	.113	3.5	.092	1.8
1971	.127	4.8	.163	4.1	.165	2.3	.136	3.8	.110	3.5	.125	3.8
1972	.139	2.1	.079	0.0	.143	2.8	.190	3.3	.096	5.3	.157	2.9
1973	.206	3.6	.124	4.0	.118	4.1	.217	3.6	.107	5.4	.138	3.4
1974	.187	4.8	.137	4.1	.217	4.2	.229	4.1	-	-	-	-
1975	.221	3.1	.088	1.6	-	-	-	-	-	-	-	-
1976	.108	2.9	-	-	-	-	-	-	-	-	-	-

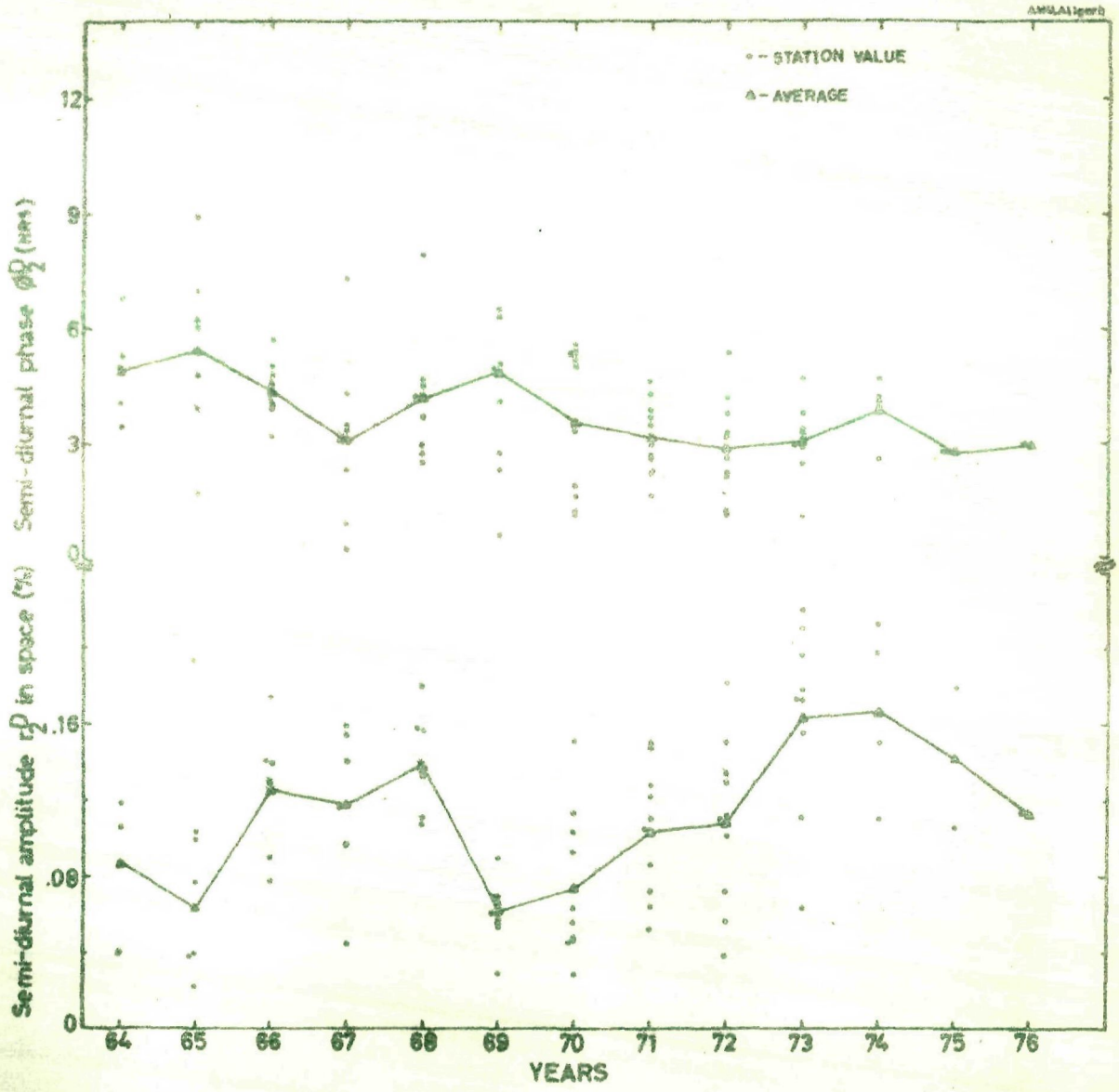

Fig. 5.2(e) - DISTURBED DAYS

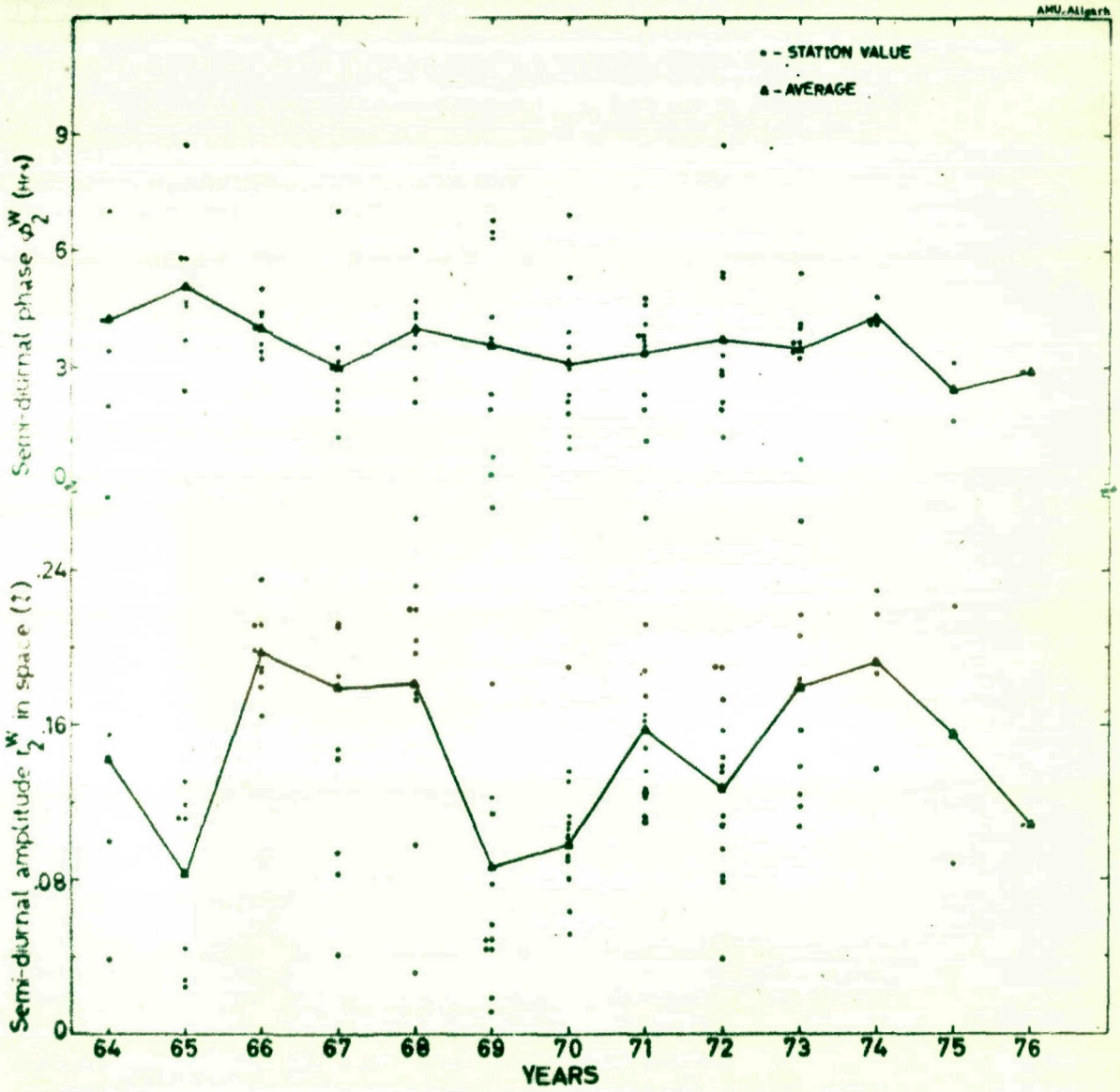

Fig. 5.2(a) - DISTURBED DAYS WITHOUT MAGNETIC STORMS.

It is observed that the semi-diurnal amplitude on DD as well as on DDWMS shows a very random behaviour during the entire period 1964-76. Also, the semi-diurnal phase on DD and DDWMS shows large fluctuations during the entire period 1964-76. Therefore, this allows us for taking no definite conclusion for the semi-diurnal anisotropy behaviour on DD and DDWMS for the period 1964-76 with the presently available neutron monitor data.

5.23 Upper cutoff rigidity of semi-diurnal anisotropy

Since the solar modulation effects which essentially depend on the electromagnetic conditions in space are the main resources to give rise to both the diurnal as well as the semi-diurnal anisotropies in the interplanetary medium, therefore, it is expected that there must exist an upper cutoff rigidity, R_{max}, above which the particles are not affected and lower cutoff rigidity, R_{min}, below which the particles are not affected.

Figure-5.5 shows the variance, χ^2 of the amplitude and phase of the semi-diurnal anisotropy on QD as a function of R_{max}, for $\beta = + 0.6$ and for the year 1972. It is seen from the Figure-5.5 that both the amplitude and phase of the semi-diurnal anisotropy on QD show a minimum variance for R_{max} = 100 - 300 GV. This suggests that we may write $R_{max} = 200 \pm 100$ GV which shows that the present set of data is not

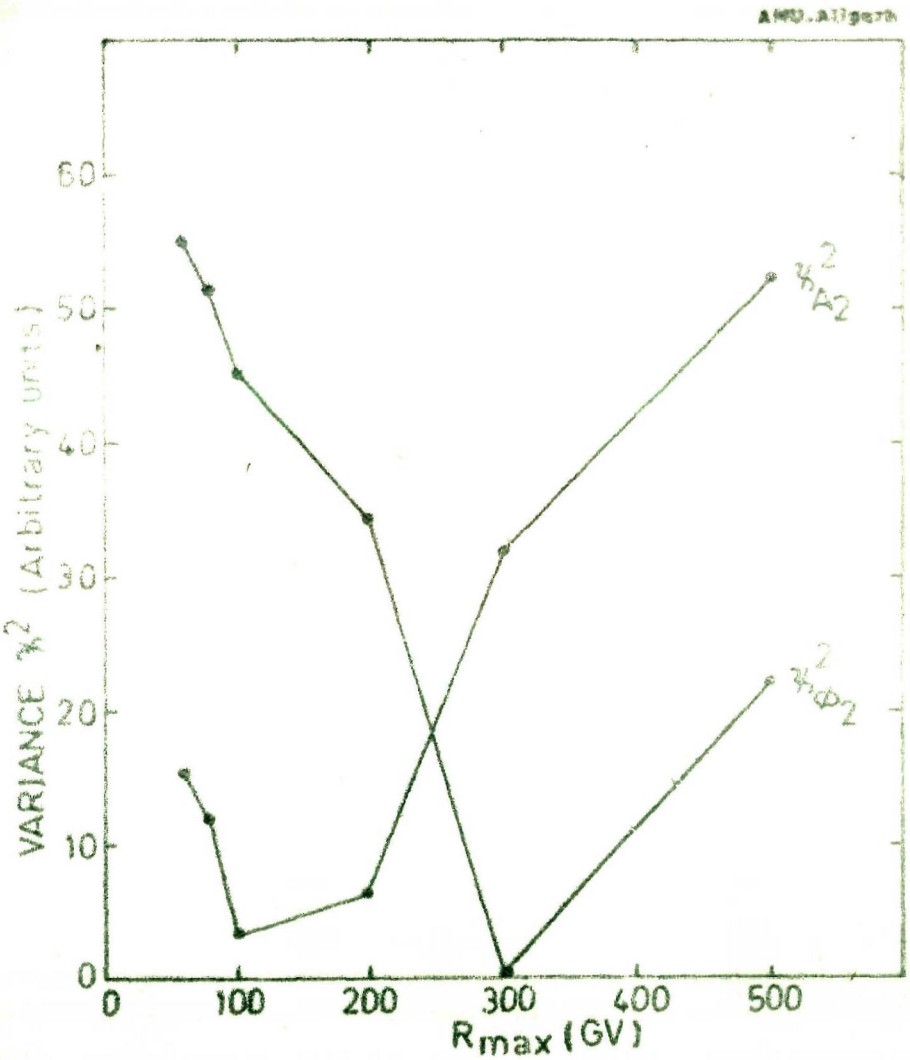

Fig. 5.5 - The variance in amplitude and phase of semi-diurnal anisotropy plotted as a function of R_{max} for β= +0.6 for the year 1972.

sufficient for determining an unambiguous value of R_{max}. A similar analysis for all the years during 1964-74 and on other types of days shows that presently available data is consistent with a time invariant R_{max} of 200 ± 100 GV. For a more accurate estimate of R_{max} and its secular change, it is obvious that we need data from more equatorial stations.

In Figure-5.6, variance for the amplitude on QD of the semi-diurnal anisotropy for the year 1969 has been plotted for different values of β and for various R_{max}. It is observable from the Figure-5.6 that the semi-diurnal anisotropy depends on R with $R^{+1.4}$ upto 60 GV above which the value of the exponent decreases.

5.3 Theoretical interpretation of semi-diurnal anisotropy

To explain the observed semi-diurnal anisotropy, Subramanian and Sarabhai (1967) and Quenby and Lietti (1968) have independently proposed that it may arise due to the particle density gradient in the plane perpendicular to the plane of ecliptic (Section-1.5). The basic difference between the two models however, is in the assumption of the nature of the perpendicular density gradient profile. The essential requirement of both the models is the existence of the increasing density of cosmic ray particles, both above and below the equatorial plane of the Sun. The presence of such a gradient may be indirectly inferred from the observations of the cosmic ray

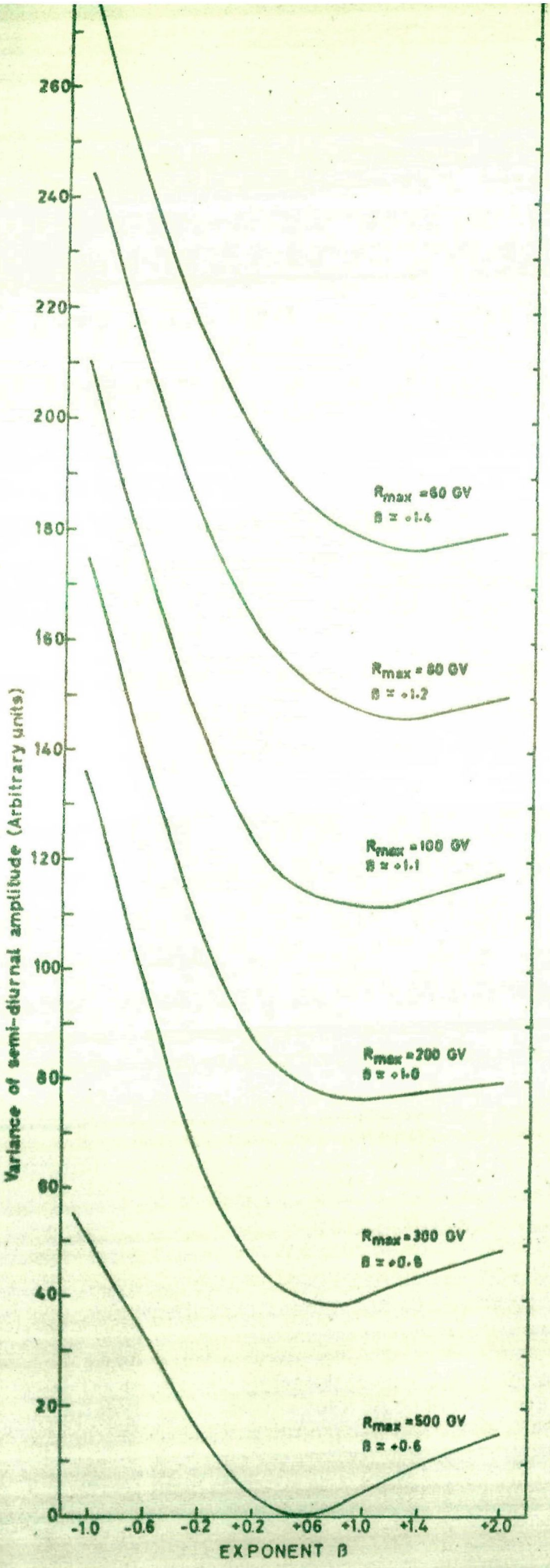

Fig. 5.6 - The variance in amplitude of semi-diurnal anisotropy on quiet days plotted as a function of β for the year 1963 and for different R_{max} and β (8 Stations).

intensity variation during the course of one year, when the Earth's position changes by $\pm 7.25^{0}$ in heliographic latitude. Comparison of cosmic ray intensities, after proper normalisation, observed when the Earth is in different heliolatitude position with respect to Sun, should provide a direct measure of the perpendicular density gradient. Even though the results from such an analysis are not conclusive, Subramanian (1971b) has shown that observed cosmic ray intensity variation does not provide necessary density gradients to explain the observed semi-diurnal anisotropy of cosmic rays.

Nagashima et al. (1972a,b) and Barnden (1973) have attempted to refine the convection-diffusion theory by invoking the hypothesis of 'pitch angle distribution' in the I.M.F. irregularities. In particular the model presented by Barnden (1973), makes use of the 'origin of scatter coefficients' technique, which involves the theoretical computation of the trajectories of the particle in the realistic configuration of the I.M.F., to obtain the hour by hour profile of the daily variation as observed at the Earth, associated with any arbitrary radial cosmic ray density gradient when the mean-free-paths are specified. The approach, in many respects is similar to the trajectory tracing of the cosmic ray particle in the simulated geomagnetic field (McCracken et al., 1965). With this refinement the semi-diurnal component comes out as a natural consequence of pitch angle scattering.

The presence of the semi-diurnal anisotropy may be due to two reasons, e.g., (i) the density decreases more sharply towards the Sun from a given point than it increases away from the Sun as a result of radial dependence of the density gradient, and (ii) the two mean sampling points parallel to the I.M.F. are not equispaced relative to the perpendicular viewing points. In essence, the density variation along the field line due to density gradients is the same as the 'sink' proposed earlier by Rao and Sarabhai (1964), with the result that such a profile contains both diurnal and semi-diurnal variation components (Sarabhai and Subramanian, 1966). The agreement of the theory with experimental results is not very satisfactory. However, since the theoretical predictions are sensitive to the initial assumptions concerning the mean-free-paths and radialy density gradient profile, a more rigorous analysis with a better understanding of the mean-free-path is necessary to have agreement between the theoretically predicted and experimentally observed results.

5.4 Conclusions

On the basis of the detailed observational evidence presented above, the following important conclusions may be derived

1. the semi-diurnal amplitude in space on QD for cosmic ray particles in the range 1 - 200 GV is $\simeq 0.03 \pm 0.01$ % during the period 1964-70. The amplitude of the semi-diurnal anisotropy

on QD has increased by a factor of 2 in all the stations during 1970-71. Also, the amplitude of the semi-diurnal anisotropy on QD shows a significant increase during 1974.

2. the phase of the semi-diurnal anisotropy on QD during the period 1964-76 is $\simeq 3.3 \pm 0.5$ hours which is along a direction essentially perpendicular to the interplanetary magnetic field direction.

3. the properties of the semi-diurnal anisotropy of cosmic ray intensity on QD in the rigidity range 1 to 200 GV are found to be rigidity dependent with a spectral exponent of + 0.6.

4. thus, the semi-diurnal variation on QD is consistent with an anisotropy which could be expressed by

$$\frac{\delta J(R)}{J(R)} = K\, R^{+0.6}\, \mathrm{Cos}^2 \wedge\, \mathrm{Cos}2(\theta - 49.5)\ \%$$

$$\text{for } R_{min} \leqslant R \leqslant R_{max}$$

$$= 0 \qquad \text{for } R_{min} > R > R_{max}$$

where K is a constant, R is rigidity and $\wedge$ is declination.

5. the systematic behaviour as observed on QD has not been observed in the characteristics of the semi-diurnal anisotropy on ND and [illegible] during the entire period 1964-76.

C H A P T E R - VI

SOLAR FLARE LOCATION EFFECT ON DAILY VARIATION OF COSMIC RAY INTENSITY

6.1 Introduction

During last few years, our knowledge of solar flare production of cosmic rays has increased largely. The effects, associated with the solar flares, observed at ground, e.g., large solar flux increases, Forbush decreases etc. have been studied from time to time by several workers (Pomerantz and Potnis, 1960; Yadav, 1964a; Bo Östman et al., 1969; Agrawal et al., 1974). It has been observed that those solar flares which occur on, or near the western limb of the solar disc show the following effects

(i) the most rapid rise to maximum intensity,

(ii) the most intense anisotropies,

(iii) on the average, the greatest particle fluxes,

(iv) very short flight times for the cosmic rays from the Sun to Earth, and

(v) on those occations for which the data have been good enough, the cosmic rays have been observed to arrive at the Earth from a direction roughly in the ecliptic plane.

All these facts have led to the picture that lines of force of the interplanetary magnetic field stretch in a relatively well ordered fashion from a sunspot which is near

the western limb to the vicinity of the Earth. This provides an easy route for the cosmic rays to follow in order to reach the Earth, which is in general agreement with the concept that the solar wind will stretch out the solar magnetic fields to form lines of force in the form of an Archimedes spiral. However, the solar flare location effect on the daily variation of cosmic ray intensity has not been given any attention so far. Therefore, the author has analysed the data of the ground based neutron and meson monitors to study the solar flare location effect on the diurnal anisotropy of the cosmic ray intensity.

6.2 Analysis of the data

The stations, whose neutron and meson monitor data is used in the analysis for studying the solar flare location effect for the periods 1957-58 (period of maximum sunspot activity) and 1973 (year of the declining phase of the sunspot activity), are given in Table-6.1. The total number of days used in different groups are given in Table-6.2. Solar flares with importance greater than two have not been considered because of the fact that during the period under consideration there is only one flare with importance greater than two. And if it is considered, it will influence the results towards the side in which it has occurred.

The pressure corrected data after applying trend correction has been analysed harmonically as discussed in Section-3.3.1

TABLE - 6.1

List of stations whose data have been used for studying the solar flare location effect on daily variation of cosmic ray intensity.

S.	Station Name	Type of the Monitor *	Vertical Cutoff Rigidity (in GV)	Geographic Coordinates Latitude (in deg)	Geographic Coordinates E.Longitude (in deg)	Period of use
1	Kodaikanal, India	N	17.47	10.23	77.46	1957-58
2	Ahmedabad, India	N	15.94	23.01	72.61	1957-58,73
3	Lae, New Guinea	N	15.52	- 6.73	147.00	1957-58
4	Makapuu pt., USA	N	13.23	21.30	202.35	1957-58
5	Tokyo-Itabashi, Japan	N	11.61	35.75	139.72	1973
6	Mt.Norikura, Japan	N	11.39	36.12	137.56	1973
7	Seoul, Korea	N	10.79	37.58	127.05	1973
8	Athens, Greece	N	8.72	37.97	23.72	1973
9	Alma Ata, USSR	N	6.69	43.25	76.92	1957-58
10	Rome, Italy	N	6.32	41.90	12.52	1957-58,73
11	Pic-du-Midi, France	N	5.36	42.93	0.25	1973
12	Hermanus, South African	N	4.90	-34.42	19.22	1957-58
13	Berkeley, USA	N,M	4.50	37.86	237.70	1957-58
14	Dallas, USA	N	4.35	32.78	263.20	1973
15	Hugspitze, FRG	N,M	4.24	47.42	10.98	1957-58
16	Climax, USA	N	3.03	39.37	253.85	1957-58
17	Gottingen, FRG	N	3.00	51.52	9.93	1957-58
18	Kiel, FRG	N	2.29	54.33	10.13	1973
19	Lincoln, USA	N	2.22	40.82	269.32	1957-58
20	Leeds, England	N	2.20	53.83	358.42	1957-58,73
21	Mt.Wellington, Australia	N	1.89	-42.92	147.23	1957-58
22	Chicago, USA	N	1.72	41.83	272.33	1957-58
23	Yakutsk, USSR	N	1.70	62.02	129.72	1957-58
24	Uppsala, Sweden	N	1.45	59.85	17.58	1957-58
25	Mt.Washington, USA	N	1.24	44.28	288.70	1957-58
26	Sulphur Mt., Canada	N,M	1.14	51.20	244.39	1957-58,73
27	Calgary, Canada	N	1.09	51.08	245.91	1973
28	Ottawa, Canada	N,M	1.08	45.40	284.40	1957-58
29	Deep River, Canada	N	1.02	46.10	282.50	1957-58,73
30	Macquarie Island	N	0.55	-54.48	158.97	1957-58
31	Kiruna, Sweden	N	0.34	67.83	20.45	1957-58
32	Mawson, Antarctica	N,M	0.22	-67.60	62.88	1957-58
33	Churchill, Canada	N,M	0.21	58.75	265.91	1957-58
34	Resolute, Canada	N,M	0.05	74.69	265.09	1957-58

* N = Neutron, M = Meson.

TABLE - 6.2

Total number of days used in different groups for the period 1957-58 and 1973.

Group / Period	Quiet days	Western limb Solar flare days	Eastern limb Solar flare days
1957-58	75	69	66
1973	60	22	27

(data is not corrected for temperature effect). Thus, the values of the amplitude and phase of the first harmonic component of the neutron and meson intensities for different stations are obtained. Days of large solar flux increases, large Forbush decreases etc., if any, are excluded from the analysis. The amplitude and phase of the diurnal anisotropy obtained at ground are corrected for the geomagnetic effects as discussed in Section-3.4 to obtain the anisotropy vector in space. The analysis has been extended on quiet days for the comparison among the anisotropy vectors on quiet days and the days where solar flares have occurred on the western and the eastern limb of the solar disc.

6.3 Observational results

The average amplitude and the phase of the diurnal anisotropy of cosmic ray intensity as observed with the neutron and meson monitors have been plotted in Figures-6.1(A) and 6.1(B) respectively for the period 1957-58, for the QD and for the days where the solar flares have occurred on the western and the eastern limbs of the solar disc. The one sigma standard errors have been shown by circles in the same Figures-6.1(A) and 6.1(B). It is apparent from the Figure-6.1(A) that the average amplitude of the diurnal anisotropy, for nucleonic component on the days where solar flares have occurred on the western limb of the solar disc is larger in comparison to the

FIG. 6.1(A)

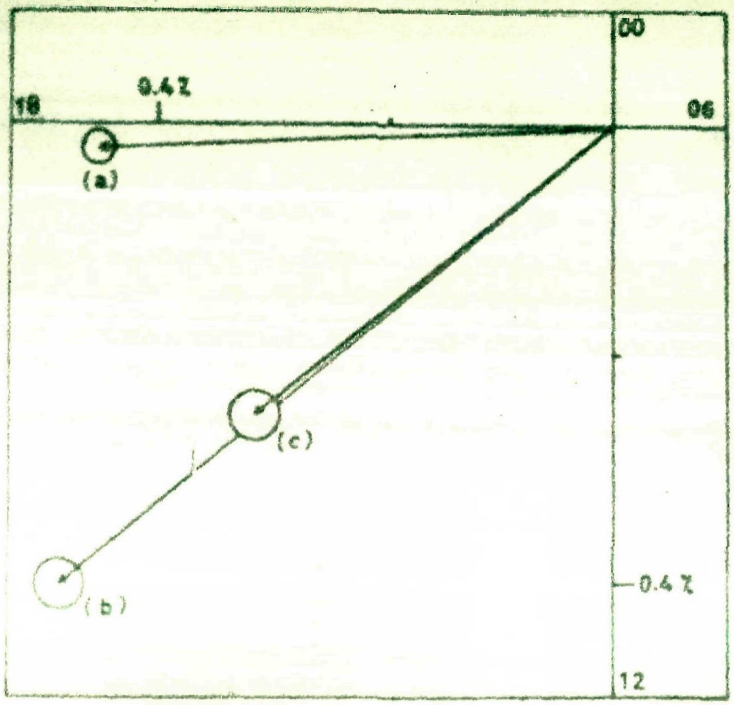

FIG. 6.1(B)

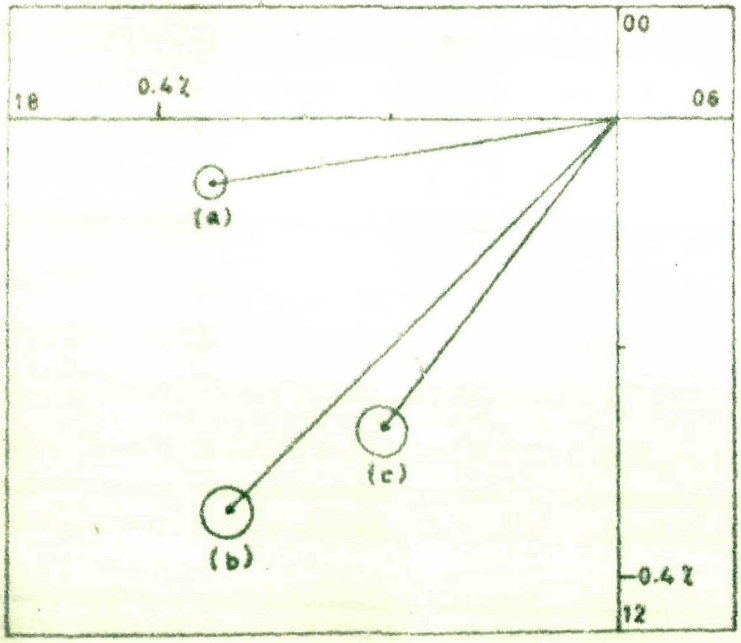

Fig. 6.1 - Diurnal anisotropy vectors on (a) QUIET DAYS, (b) WESTERN LIMB SOLAR FLARE DAYS, (c) EASTERN LIMB SOLAR FLARE DAYS for NEUTRON MONITORS (6.1 A) and MESON MONITORS (6.1 B) during 1957-58.

days where solar flares have occurred on the eastern limb of the solar disc. However, the amplitude of the diurnal anisotropy on the days for which the solar flares have occurred on the eastern limb of the solar disc is of the same order as it is observed on QD. These results are also supported by Yadav and Sud (1972).

It is also apparent from the Figure-6.1(A) that for the nucleonic component the average direction of the diurnal anisotropy in space in local asymptotic time is almost same on the days where the solar flares have occurred on the western as well as eastern limbs of the solar disc. However, if these results are compared with the direction of the diurnal anisotropy in space on QD, it is found that the direction of the diurnal anisotropy on days where solar flares have occurred on the western limb as well as eastern limb of the solar disc is earlier in comparison to QD. This phase shift towards earlier hours has been observed about three hours for the nucleonic component.

The above results for the amplitude and the phase of the diurnal anisotropy on QD and the days where the solar flares occur on the western and the eastern limbs of the solar disc are also supported by the meson monitor observations, as is apparent from the Figure-6.1(B). These results are true to a large extent for the individual stations, given in Table-6.1, as well, which have not been illustrated here.

The nature of the diurnal anisotropy vector on QD and on days where the flares have occurred on the western limb and the eastern limb of the solar disc, based on the neutron monitor observations, has also been studied during 1973 in addition to the period 1957-58 as mentioned above. Figure-6.2 illustrates the diurnal anisotropy vector for neutron monitors during the years 1957-58 (Figure-6.2(A)) and during the year 1973 (Figure-6.2(B)) on QD, western limb solar flares, and eastern limb solar flares. It is quite clear from the Figure-6.2 that during 1957-58, the phase of the diurnal anisotropy on QD, $\phi_1^Q \simeq 18.00$ hrs and during 1973, $\phi_1^Q \simeq 16.00$ hrs. It shows that there is a phase shift of about two hours towards earlier hours for the diurnal anisotropy on QD during 1973 in comparison to the phase observed during 1957-58 which is true for all the individual stations as well. This is in accordance with the results presented in Section-4.221. The observational results based on meson monitor data for the period 1957-58 by Yadav (1964b) are in support of our findings.

Further, for the year 1973, the phase of the diurnal anisotropy for the days where the flares have occurred on the western limb of the solar disc is same as it is observed for the days where the flares have occurred on the eastern limb of the solar disc. This result is similar to the result observed during 1957-58 for the days where the flares have occurred on the western and the eastern limbs of the solar disc. But, during 1973, the

FIG·6.2(A)

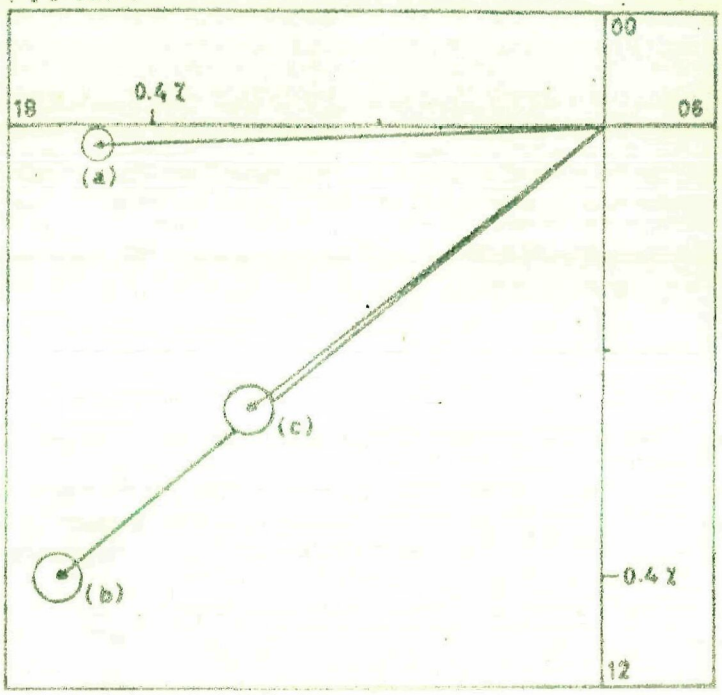

FIG·6.2(B)

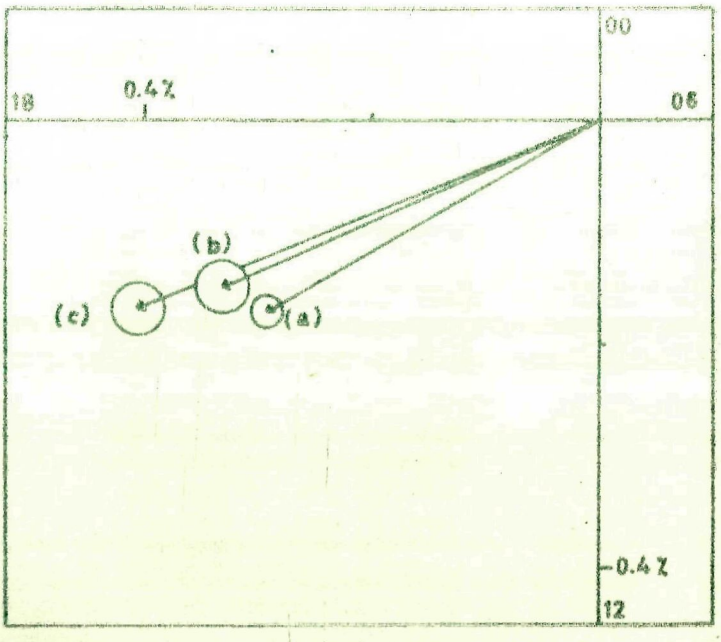

Fig. 6.2 - Diurnal anisotropy vectors on (a) QUIET DAYS, (b) WESTERN LIMB SOLAR FLARE DAYS, (c) EASTERN LIMB SOLAR FLARE DAYS for neutron monitors during 1957-58 (6.2 A) and 1973 (6.2 B).

amplitude of the diurnal anisotropy for the days where the flares have occurred on the western limb of the solar disc is less in comparison to the amplitude of the diurnal anisotropy for the days where the flares have occurred on the eastern limb of the solar disc. This result for the amplitude of the diurnal anisotropy during 1975 on western and eastern limb solar flare days is opposite to that observed during 1957-58. This may be due to the fact that the period 1957-58 is the period of maximum solar activity and the year 1975 is the declining phase of the solar activity. The study of the solar flare location effect on spectral characteristics of the diurnal as well as semi-diurnal anisotropy during the different phases of the solar activity e.g., maximum solar activity period, minimum solar activity period and the transition period of the solar activity is in progress and will be reported shortly.

6.4 Conclusions

On the basis of the neutron monitor and meson telescope observational results presented in this Chapter, the following important conclusions may be drawn

1. the results obtained for the amplitude and phase of the diurnal anisotropy on QD during 1957-58 are in accordance with the results for the diurnal anisotropy on QD during 1964-70 (presented in Chapter-IV). This indicates that the

nature of the diurnal anisotropy vector on QD may be regarded as invariant during the entire period 1957-70.

2. the amplitude of the diurnal anisotropy for western limb solar flare days is larger than the eastern limb solar flare days, during 1957-58. This relationship between the amplitude of diurnal anisotropy for western limb and for eastern limb solar flare days is opposite during 1973.

3. the phase of the diurnal anisotropy for western as well as eastern limb solar flare days shows a shift towards earlier hours by about three hours in comparison to the phase of the diurnal anisotropy on QD during 1957-58. Whereas, during 1973, the phase of the diurnal anisotropy for western as well as eastern limb solar flare days remains almost in the same direction as it is observed on QD.

REFERENCES

Ables, J.G.; McCracken, K.G. and Rao, U.R.	1965	Proc. 9th Int. Conf. Cosmic Rays, London, 1, 208.
Ables, J.G.; Barouch, E. and McCracken, K.G.	1967	Planet. Space Sci., 15, 547.
Agrawal, S.P.	1973	Ph.D. Thesis, Gujrat University.
Agrawal, S.P.	1977	Unpublished (Private communication).
Agrawal, S.P. and Ananth, A.G.	1973	Proc. 13th Int. Conf. Cosmic Rays, Denver, 2, 1005.
Agrawal, S.P. and Singh, R.L.	1975a	Proc. 14th Int. Conf. Cosmic Rays, Munich (West Germany), 4, 1253.
Agrawal, S.P. and Singh, R.L.	1975b	Proc. 14th Int. Conf. Cosmic Rays, Munich (West Germany), 4, 1193.
Agrawal, S.P.; Ananth, A.G. and Rao, U.R.	1972	Can. J. Phys., 50, 1323.
Agrawal, S.P.; Ananth, A.G.; Bemalkhedkar, M.M.; Kargathra, L.V.; Rao, U.R. and Ramdan, H.	1974	Pre-print, India-CR-74-02.
Agrawal, S.P.; Singh, R.L.; Nigam, S.K. and Sharma, R.M.	1977	Proc. 15th Int. Conf. Cosmic Rays, Plovdiv (Bulgaria), 1 26.
Ahluwalia, H.S.	1962	Proc. Phys. Soc., 80, 472.
Ahluwalia, H.S. and Dessler, A.J.	1962	Planet. Space Sci., 9, 195.
Ahluwalia, H.S. and Brieksen, J.H.	1970	Acta Physica Hung., 29, Supp. 2, 159.
Ahluwalia, H.S. and Brieksen, J.H.	1971	J. Geophys. Res., 76, 6613.

Ahluwalia, H.S. and Singh, S.	1973	Proc. 13th Int. Conf. Cosmic Rays, Denver, 2, 948.
Alfven, H.	1950	Cosmical Electrodynamics, Oxford Press (London).
Alfven, H.	1954	Tellus, 6, 232.
Allum, F.R.; Palmeira, R.A.R.; McCracken, K.G.; Rao, U.R.; Fairfield, D.H. and Gleeson, L.J.	1974	Solar Phys., 38, 327.
Ananth, A.G.	1975	Ph.D. Thesis, Gujrat University.
Ananth, A.G.; Agrawal, S.P. and Rao, U.R.	1974	Pramana, 3, 74.
Antonucci, E.	1974	Euro-Cess Scient. and Tech. Rev., 6, 17.
Axford, W.I.	1965a	Planet. Space Sci., 13, 115.
Axford, W.I.	1965b	Planet. Space Sci., 13, 1301.
Axford, W.I.	1968	Space Sci. Rev., 8, 331.
Bachelet, F.; Balata, P.; Dyring, E. and Iucci, N.	1965	Nuovo Cimento, 35, 25.
Bachelet, F.; Dyring, E.; Iucci, N. and Villoresi, G.	1967	Nuovo Cimento, 52B, 106.
Bachelet, F.; Iucci, N.; Villoresi, G. and Sperre, B.	1972a	Nuovo Cimento, 7B, 17.
Bachelet, F.; Iucci, N.; Villoresi, G. and Zangrilli, M.	1972b	Nuovo Cimento, 11B, 1.
Ballif, J.R.; Jones, D.E. and Coleman, P.J.	1969	J. Geophys. Res. 74, 2289.
Barker, M.C. and Hatton, C.J.	1970	Acta Physica Hung., 29, Supp. 2, 177.
Barker, M.C. and Hatton, C.J.	1971	Planet. Space Sci., 19, 549.
Barnden, L.R.	1973	Proc. 13th Int. Conf. Cosmic Rays, Denver, 2, 1277.

Baroueh, E.	1974	Solar Wind, III, Pub. by Institute of Geophys., U.S.A., 206.
Baroueh, E. and Burlaga, L.F.	1975	J. Geophys. Res., 80, 649.
Bemalkhedkar, M.M.	1974	Ph.D. Thesis, Gujrat University.
Bercovitch, M.	1965	Proc. 8th Int. Conf. Cosmic Rays, Jaipur, 332.
Bercovitch, M.	1967	Proc. 10th Int. Conf. Cosmic Rays, Calgary, Part A, 269.
Biermann, L.	1951	Z. Astrophys., 29, 274.
Biermann, L.	1957	Observatory, 77, 109.
Bland, C.J.	1962	Phil. Mag., 7, 1487.
Blenford, G.E., Jr.; Friedlander, M.W.; Klarman, J.; Domeroy, S.S.; Walker, R.M.; Wefel, J.P.; Fowler, P.H.; Kidd, J.M.; Kobetich, E.J.; Moses, R.T. and Throne, R.T.	1973	Phys. Rev. D, 8, 1707.
Bo Östman; Shutrasakul, Likit and Yadav, R.S.	1969	Arkiv For Geofysik, Bd. 5 nr 36, 529.
Brunberg, E.A. and Dattner, A.	1954	Tellus VI, 1, 73.
Bukata, R.P.; McCracken, K.G. and Rao, U.R.	1968	Can. J. Phys., 46, 5994.
Burlaga, L.F.	1967	J. Geophys. Res., 72, 4449.
Burlaga, L.F.	1971	Space Sci. Rev., 12, 600.
Burlaga, L.F. and Ness, N.F.	1968	Can. J. Phys., 46, 5962.
Carmichael, H.	1964	Cosmic Rays IQSY Instruction Manual No. 7 (London).
Carmichael, H. and Bercovitch, M.	1969	Can. J. Phys., 47, 2073.

Carmichael, H. and Peterson, R.W.	1971	Proc. 12th Int. Conf. Cosmic Rays, Hobart, 3, 887.
Carmichael, H.; Bercovitch, M.; Shea, M.A.; Magidin, M. and Peterson, R.W.	1968	Can. J. Phys., 46, S1006.
Carmichael, H.; Shea, M.A. and Peterson, R.W.	1969	Can. J. Phys., 47, 2057.
Chapman, S. and Bartels, J.	1940	Geomagnetism, II, Oxford University Press.
Coleman, P.J.Jr.; Davis, L.Jr.; Smith, E.J. and Jones, D.E.	1966	J. Geophys. Res., 21, 2831.
Compton, A.H. and Getting, I.A.	1935	Phys. Rev., 47, 817
Conforto, A.M. and Simpson, J.A.	1957	Nuovo Cimento, 5, 1052.
Crowden, J.B. and Marsden, P.L.	1962	J. Phys. Soc. Japan, 17, 484.
De Brunner, H. and Flueckiger, E.	1971	Proc. 12th Int. Conf. Cosmic Rays, Hobart, 3, 911.
Dessler, A.J.	1967	Rev. Geophys., 5, 1.
Dhanju, M.S. and Sarabhai, V.A.	1967	Phys. Rev. Letters, 19, 252.
Dorman, L.I.	1957	Cosmic Ray Variations, State Pub. House, Moscow.
Dorman, L.I.	1963	Prog. Elem. Particle and Cosmic Ray Phys., 7, North Holland Pub. Co.
Dorman, L.I.	1974	Cosmic Rays, North Holland Pub. Co.
Duggal, S.P. and Pomerantz, M.A.	1962	Phys. Rev. Letters, 8, 215.
Duggal, S.P. and Pomerantz, M.A.	1975	Proc. 14th Int. Conf. Cosmic Rays, Munich, 4, 1299.

Duggal, S.P.; Forbush, S.E. and Pomerantz, M.A.	1967	Nature, 214, 154.
Duggal, S.P.; Forbush, S.E. and Pomerantz, M.A.	1970	J. Geophys. Res., 75, 1150. 455.
Elliot, H.	1952	Prog. in Cosmic Ray Phys., I 455.
Elliot, H. and Dolbear, D.W.N.	1950	Prog. Phys. Soc., 63, 137.
Elliot, H. and Dolbear, D.W.N.	1951	J. Atmo. Terr. Phys., 1, 205.
Elliot, H. and Rothwell, P.	1956	Phil. Mag., 1, 699.
Fairfield, D.H. and Ness, N.F.	1974	J. Geophys. Res., 79, 5089.
Faller, A.M. and Marsden, P.L.	1965	Proc. 9th Int. Conf. Cosmic Rays, London, 1, 231.
Fenton, A.G.; McCracken, K.G.; Rose, D.C. and Wilson, B.G.	1959	Can. J. Phys., 37, 970.
Fisk, L.A. and Axford, W.I.	1969	J. Geophys. Res., 74, 4973.
Fisk, L.A. and Axford, W.I.	1970	Solar Phys., 12, 304.
Forbush, S.E.	1938	J. Geophys. Res., 43, 203.
Forbush, S.E.	1954	J. Geophys. Res., 59, 525.
Forbush, S.E.	1958	J. Geophys. Res., 63, 651.
Forbush, S.E.	1967	J. Geophys. Res., 72, 4937.
Forbush, S.E.	1969	J. Geophys. Res., 74, 3451.
Forbush, S.E.	1973	J. Geophys. Res., 78, 7933.
Forbush, S.E. and Venkatesan, D.	1960	J. Geophys. Res., 65, 2213.
Forbush, S.E. and Beach, L.	1975	Proc. 14th Int. Conf. Cosmic Rays, Munich, 4, 1204.

Forman, M.A. and Gleeson, L.J.	1970	Preprint, Nanash Univereity.
Forman, M.A. and Gleeson, L.J.	1975	Astrophys. and Space Sci., 32, 77.
Fowler, I.L.	1963	Rev. Sci. Instr., 34, 731.
Fujii, Z.; Fujimato, K.; Veno, H.; Kondo, L. and Nagashima, K.	1970	Acta Physica Hung., 29, Supp. 2, 83.
Fulks, G.J.	1975	J. Geophys. Res., 80, 1701.
Girgis, A.H.; Tolba, M.F.; Wahab, S.A. and Salem, A.M.	1977	Planet. Space Sci., 25, 39.
Gleeson, L.J.	1969	Planet. Space Sci., 17, 31.
Gleeson, L.J.	1971	Astrophys. Space Sci., 10, 471.
Gleeson, L.J.	1973	Proc. Solar Terr. Conf. Calgary, 79.
Gleeson, L.J. and Axford, W.I.	1967	Astrophys. J., 149, L.115.
G Gleeson, L.J. and Axford, W.I.	1968a	Astrophys. Space Sci., 2, 431.
Gleeson, L.J. and Axford, W.I.	1968b	Astrophys. J., 154, 1011.
Gleeson, L.J. and Urch, I.H.	1973	Astrophys. Space Sci., 25, 387.
Gold, T.	1959	J. Geophys. Res., 64, 1665.
Gosling, J.T.; Hansen, R.T. and Bame, S.J.	1971	J. Geophys. Res., 76, 1811.
Harman, C.V. and Hatton, C.J.	1968	Can. J. Phys., 46, S1052.
Hashim, A. and Thambyahpillai, T.	1969	Planet. Space Sci., 17, 1879
Hashim, A. and Bercovitch, M.	1972	Planet. Space Sci., 20, 791.
Hashim, A.; Bercovitch, M. and Steljes, J.F.	1972	Solar Phys., 22, 220.

Hatton, C.J.	1971	Prog. Elem. Particle and Cosmic Ray Phys., X, North Holland Pub. Co., 1.
Hatton, C.J.; Marsden, P.L. and Willetts, A.C.	1968	Can. J. Phys., 46, S915.
Hedgecock, P.C.	1963	Proc. 8th Int. Conf. Cosmic Rays, Jaipur.
Hedgecock, P.C.; Quenby, J.J. and Webb, S.	1972	Nature, 240, 173.
Hess, V.F.	1912	Phys. S., 13, 1084.
Howard, R.	1972	Solar Phys., 25, 5.
Hughes, E.B. and Marsden, P.L.	1966	J. Geophys. Res., 71, 1455.
Hughes, E.B.; Marsden, P.L.; Brooke, G.; Meyer, M.A. and Wolfendale, A.W.	1964	Proc. Phys. Soc. London, A83, 239.
Hundhausen, A.J.	1968	Space Sci. Rev., 8, 690.
Hundhausen, A.J.	1970	Rev. Geophys. Space Phys., 8, 729.
Hundhausen, A.J.	1972	Coronal Expansion of Solar Wind.
Intriligator, D.S.	1974	App. J. Letters, 188, L 23.
Intriligator, D.S.	1975	Proc. 14th Int. Conf. Cosmic Rays, Munich, 2, 1033.
Jacklyn, R.M.; Duggal, S.P. and Pomerantz, M.A.	1970	Acta Physica Hung., 29, Supp. 2, 47.
Jokipii, J.R.	1966	Astrophys. J., 146, 480.
Jokipii, J.R.	1967	Astrophys. J., 149, 405.
Jokipii, J.R.	1971	Rev. Geophys. Space Phys., 9, 27.
Jokipii, J.R. and Parker, E.N.	1967	Planet. Space Sci., 15, 1375.
Jokipii, J.R. and Coleman, P.J.Jr.	1968	J. Geophys. Res., 73, 5495.
Jokipii, J.R. and Parker, E.N.	1969	Astrophys. J., 155, 777.

Jokipii, J.R. and Parker, E.N.	1970	Astrophys. J., 160, 735.
Kaminer, N.S.; Ilgach, S.P. and Khadakhanova, T.S.	1964	Geomagnetism i aehronomya, 4, 653.
Kane, R.P.	1962	J. Phys. Soc. Japan, 17, 468.
Kane, R.P.	1966	Nuovo Cimento, 45, 8.
Kane, R.P.	1968	Nuovo Cimento, B57, 36.
Kane, R.P.	1972	J. Geophys. Res., 77, 5573.
Kane, R.P.	1974	J. Geophys. Res., 79, 1321.
Kane, R.P.	1975	J. Geophys. Res., 80, 470.
Kargathra, L.V.	1972	Ph.D. Thesis, Gujrat University.
Katzman, J. and Venkatesan, D.	1960	Can. J. Phys., 38, 1011.
Kodama, M. and Inoue, A.	1970	JARE, Scientific Reports Series A, No. 9, 1.
Krymskiy, G.F.	1964	Geomag. and Aeronomy, 4, 765.
Lapointe, S.M. and Rose, D.C.	1962	Can. J. Phys., 40, 687.
Lemaitre, G. and Vallarta, M.S.	1933	Phys. Rev., 43, 87.
Levy, E.H.	1976	J. Geophys. Res., 81, 2082.
Lietti, B. and Quenby, J.J.	1968	Can. J. Phys., 46, 8942.
Lindgren, S.	1970	Acta Physica Hung., 29, Supp. 2, 345.
Lockwood, J.A.	1971	Space Sci. Rev., 12, 658.
Lockwood, J.A. and Webber, W.R.	1967	J. Geophys. Res., 72, 3395.
Lockwood, J.A. and Webber, W.R.	1968	Can. J. Phys., 46, 8903.
Lust, R	1967	Solar Terr. Phys. Ed. King and Newman, Academic Press, 1.
Marsden, P.L. and Begum, S.N.	1959	Phil. Mag., 4, 1247.

Mathews, T.; Mercer, J.B. and Venkatesan, D.	1968	Can. J. Phys., 46, 8854.
Mathews, T.; Venkatesan, D. and Wilson, B.G.	1969	J. Geophys. Res., 74, 1218.
Mathews, T.; Quenby, J.J. and Sear, J.	1971	Nature, 229, 246.
McCracken, K.G.	1962	J. Geophys. Res., 67, 447.
McCracken, K.G. and Rao, U.R.	1965	Proc. 9th Int. Conf. Cosmic Rays, London, 1, 215.
McCracken, K.G. and Ness, N.F.	1966	J. Geophys. Res., 71, 3315.
McCracken, K.G.; Rao, U.R. and Shea, M.A.	1962	M.I.T. Tech. Rep. No. 77.
McCracken, K.G.; Rao, U.R.; Fowler, B.C.; Shea, M.A. and Smart, D.F.	1965	IQSY Instruction Manual No. 10.
McCracken, K.G.; Rao, U.R. and Bukata, R.P.	1966	Phys. Rev. Letters, 17, 928.
McCracken, K.G.; Rao, U.R. and Ness, N.F.	1968	J. Geophys. Res., 73, 4159.
McCracken, K.G.; Rao, U.R.; Bukata, R.P. and Keath, E.P.	1971	Solar Phys., 18, 100.
Mercer, J.B. and Wilson, B.G.	1968	Can. J. Phys., 46, 8849.
Michel, F.C.	1967	J. Geophys. Res., 72, 1917.
Montgomery, M.D.	1973	Space Sci. Rev., 14, 559.
Neri, S.	1968	Nuovo Cimento, B58, 1.
Nori, S.; Yamue, S. and Iehinose, M.	1971	Rep. Ionosphere Space Res., 25, 271.
Morrison, P.	1956	Phys. Rev., 101, 1397.

Murakami, K.; Wada, M.; Miyasaki, Y. and Mishima, Y.	1973	Proc. 13th Int. Conf. Cosmic Rays, Denver, 2, 1028.
Nagashima, K.; Potnis, V.R. and Pomerantz, M.A.	1961	Nuovo Cimento, 19, 292.
Nagashima, K.; Ueno, H.; Fujimoto, K.; Fujii, Z and Kondo, I.	1972a	Rep. Ionosphere Space Res., 26, 1.
Nagashima, K.; Fujimoto, K.; Fujii, Z.; Ueno, H. and Kondo, I	1972b	Rep. Ionosphere Space Res., 26, 31.
Neher, H.V.	1952	Prog. in Cosmic Ray Phys., I, Interscience Pub.
Ness, N.F.	1967	Solar Terr. Phys. Ed. King and Newman, Academic Press, 57.
Ness, N.F.; Seeares, C.S. and Seek, J.B.	1964	J. Geophys. Res., 69, 3531.
Newkirk, G.Jr.	1973	Proc. 14th Int. Conf. Cosmic Rays, Munich, 11, 3594.
Nicolsen, P. and Sarabhai, V.	1948	Proc. Phys. Soc., 60, 509.
O'Gallagher, J.J.	1967	Astrophys. J., 150, 675.
O'Gallagher, J.J. and Simpson, J.A.	1967	Astrophys. J., 147, 819.
Orpen, J.F. and Webber, W.R.	1968	Can. J. Phys., 46, S883.
Parker, E.N.	1958a	Astrophys. J., 128, 664.
Parker, E.N.	1958b	Phys. Rev., 110, 1445.
Parker, E.N.	1963	Interplanetary Dynamical Processes, Interscience, New York.
Parker, E.N.	1964	Planet. Space Sci., 12, 735.
Parker, E.N.	1965	Planet. Space Sci., 13, 9.
Parker, E.N.	1967	Planet. Space Sci., 15, 1723.

Parker, E.N.	1969	Space Sci. Rev., 9, 325.
Patel, D.; Sarabhai, V. and Subramanian, G.	1968	Planet. Space Sci., 16, 1131.
Pathak, P.N. and Sarabhai, V.	1970	Planet. Space Sci., 18, 81.
Phillips, J. and Parsons, N.R.	1962	J. Phys. Soc. Japan (Supp. A II), 17, 519.
Pomerantz, Martin A. and Potnis, Vasant R.	1960	J. Franklin Institute, 270, 227.
Pomerantz, M.A. and Duggal, S.P.	1971	Space Sci. Rev., 12, 75.
Pomerantz, M.A. and Duggal, S.P.	1974	Rev. Geophys. Space Phys., 12, 343.
Pomerantz, M.A.; Agarwal, S.P. and Potnis, V.R.	1958a	Phys. Rev., 109, 224.
Pomerantz, M.A.; Agarwal, S.P. and Potnis, V.R.	1958b	Phys. Rev. Letters, 1, 65.
Pomerantz, M.A.; Agarwal, S.P. and Potnis, V.R.	1960	J. Franklin Institute, 269, 235.
Quenby, J.J.	1965	Proc. 9th Int. Conf. Cosmic Rays, London, 1, 3.
Quenby, J.J. and Lietti, B.	1968	Planet. Space Sci., 16, 1209.
Quenby, J.J. and Hashim, A.	1969	Planet. Space Sci., 17, 1121.
Rao, U.R.	1972	Space Sci. Rev., 12, 719.
Rao, U.R. and Sarabhai, V.	1961	Proc. Roy. Soc., A263, 101.
Rao, U.R. and Sarabhai, V.	1964	Planet. Space Sci., 12, 1055.
Rao, U.R. and Agrawal, S.P.	1970	J. Geophys. Res., 75, 2391.
Rao, U.R.; McCracken, K.G. and Venkatesan, D.	1963	J. Geophys. Res., 68, 345.

Rao, U.R.; McCracken, K.G. and Bartley, W.C.	1967	J. Geophys. Res., 72, 4345.
Rao, U.R.; McCracken, K.G.; Allum, F.R.; Palmeira, R.A.R.; Bartley, W.C. and Palmer, I.	1971	Solar Phys., 19, 209.
Rao, U.R.; Ananth, A.G. and Agrawal, S.P.	1972	Planet. Space Sci., 20, 1799.
Rau, W.	1939	Z. Phys., 114, 482.
Rasdan, H. and Bemalkhedkar, M.M.	1971	Proc. 12th Int. Conf. Cosmic Rays, Hobart, 2, 697.
Rasdan, H. and Bemalkhedkar, M.M.	1972	Cosmic Electro dynamics, 3, 297.
Roelof, E.C.	1968	Can. J. Phys., 46, S990.
Ryan, M.J.; Ormes, J.F. and Balasubrahmanyan, V.K.	1972	Phys. Rev. Letters, 28, 295.
Ryder, P. and Hatton, C.J.	1968	Can. J. Phys., 46, S999.
Sandstrom, A.E.	1955	Tellus, 7, 204.
Sandstrom, A.E.	1965	Cosmic Ray Phys., North Holland Pub. Co., 201.
Sarabhai, V.A. and Kane, R.P.	1953	Phys. Rev., 90, 204.
Sarabhai, V. and Nerurkar, N.W.	1956	Ann. Rev. Nucl. Sci., 6, 1.
Sarabhai, V. and Subramanian, G.	1965	Proc. 9th Int. Conf. Cosmic Rays, London, 1, 204.
Sarabhai, V. and Subramanian, G.	1966	Astrophys. J., 145, 206.
Sarabhai, V.A.; Desai, U.D. and Venkatesan, D.	1954	Phys. Rev., 96, 469.
Sarabhai, V.; Pai, G.L. and Wada, M.	1965	Nature, 206, 703.
Sawyer, C.	1974	Geophys. Res. Letters, 1, 295.

Sekido, Y. and Yoshida, S.	1950	Rep. Iono. Res. Japan, 4, 57.
Sekido, Y.; Yoshida, S. and Kamiya, Y.	1952	Rep. Iono. Res. Japan, 6, 195.
Shea, M.A.	1972	Ground-based Cosmic Ray Inst. Catalogue, AFCRL-72-0411.
Shea, M.A.; Smart, D.F.; McCracken, K.G. and Rao, U.R.	1968	Supp. IQSY Instruction Manual No. 10, AFCRL-68-0030.
Shen, M.L.	1968	Supp. Nuevo Cimento, 4, 1177.
Simpson, J.A.	1948	Phys. Rev., 73, 1389.
Simpson, J.A.	1954	Phys. Rev., 94, 426.
Simpson, J.A.	1957	Ann. I.G.Y. (London Pergamon Press) Part VII.
Simpson, J.A.; Fonger, W. and Treiman, S.B.	1953	Phys. Rev., 90, 934.
Singer, S.F.	1958	Prog. in Elem. Particle and Cosmic Ray Phys., IV, 203.
Singh, R.L.	1976	Ph.D. Thesis, A.P.S. University, Rewa.
Snyder, C.W.; Neugebauer, M. and Rao, U.R.	1963	J. Geophys. Res., 68, 6361.
Sternsurer, R. and Gheri, H.	1955	Naturuissens Chaften, 42, 294.
Stern, D.	1964	Planet. Space Sci., 12, 973.
Steker, F.B.; Rambenheimer, B.C. and Vander Walt, A.J.	1971	Proc. 12th Int. Conf. Cosmic Rays, Hobart, 3, 87.
Steshkov, Y. and Charakhchyan, T.N.	1968	Can. J. Phys., 46, 8927.
Strong, I.B.; Ashridge, J.R.; Barne, S.J. and Hundhausen, A.J.	1967	Zodiacal Light and the Interplanetary Medium, NASA SP-150 (ed. by J. Weinberg).
Subramanian, G.	1971a	J. Geophys. Res., 76, 1693.

Subramanian, G.	1971b	Can. J. Phys., 49, 34.
Subramanian, G. and Sarabhai, V.	1967	Astrophys. J., 149, 417.
Suga, K.; Sakuyama, H.; Kavaguchi, S. and Hara, T.	1971	Phys. Rev. Letters, 27, 1604.
Svalgaard, L.	1972	J. Geophys. Res., 78, 2064.
Swann, W.F.G.	1933	Phys. Rev., 44, 224.
Tanskanen, P.J.	1968	Can. J. Phys., 46, S819.
Thambyahpillai, T.	1975	Proc. 14th Int. Conf. Cosmic Rays, Munich, 4, 1221.
Thambyahpillai, T. and Elliot, H.	1953	Nature, 171, 918.
Thambyahpillai, T. and Spellar, R.D.	1975	Planet. Space Sci., 23, 961.
Thambyahpillai, T.; Spellar, R.D. and Peacock, D.S.	1973	Proc. 13th Int. Conf. Cosmic Rays, Denver, 2, 1045.
Thomson, D.M.	1971	Planet. Space Sci., 19, 1169.
Thomson, D.M.	1972	Planet. Space Sci., 20, 2196.
Trieman, S.B.	1952	Phys. Rev., 86, 917.
Venkatesan, D. and Dattner, A.	1959	Tellus, 11, 116.
Venkatesan, D. and Mathews, T.	1968	Can. J. Phys., 46, S794.
Wainio, K.M.; Gelvin, T.N.; Mere, K.A. and Tiffany, O.L.	1968	Can. J. Phys., 46, S1048.
Webber, W.R.	1962	Prog. in Elem. Particle and Cosmic Ray Phys., 6, 224.
Webber, W.R. and Quenby, J.J.	1959	Phil. Mag., 4, 654.
Wibberentz, G.	1974	J. Geophys. Res., 79, 667.

Wilcox, J.M. and Ness, N.F.	1965	J. Geophys. Res., 70, 5793.
Wilcox, J.M. and Colburn, D.S.	1969	J. Geophys. Res., 74, 2388.
Wilcox, J.M. and Colburn, D.S.	1970	J. Geophys. Res., 75, 6366.
Wilcox, J.M. and Colburn, D.S.	1972	J. Geophys. Res., 77, 751.
Wolfe, J.H.; Silva, R.W.; McKibbin, D.D. and Mason, R.H.	1966	J. Geophys. Res., 71, 5329.
Yadav, R.S.	1964a	Proc. Nat. Acs. Sci., India, 34(A), IV, 567.
Yadav, R.S.	1964b	Proc. Nat. Acs. Sci., India, 34(A), I, 55.
Yadav, R.S. and Sud, L.V.	1972	Proc. Nat. Acs. Sci., India, 42(B), I, 28.
Yadava, R.S. and Naqvi, T.H.	1973	Tech. Note No. 1, A.M.U., Aligarh.
Yoshida, S.	1955	Proc. Int. Conf. Cosmic Rays, Guanaguato, 358.

Reprinted from the *Journal of the Institution of Electronics & Telecom. Engrs.*, 1975 Vol. 21, No. 12, pp. 653-657

Instrumentation for Continuous Monitoring of Low Energy Cosmic Ray Intensity

S. KUMAR*, R. PRASAD*, R. S. YADAV*, T. H. NAQVI** AND RAIS AHMED*** (Member)

(*Manuscript received on 27 November* 1974)

This paper describes a high counting rate Neutron Monitor developed at Aligarh for continuous monitoring of low energy nucleonic component of cosmic rays. Transistorized electronic circuits used are described.

COSMIC ray research offers the promises of being able to investigate phenomena inaccessible to any other experimental discipline in solar-physics and Geophysics. International Geophysical Year (Simpson et al., 1953; Simpson, 1957) [1957-58] was the important period for the systematic development in the field of the cosmic ray research, because it led to the world-wide distribution of standardized cosmic ray intensity detecting apparatus including Neutron Monitor (Simpson, 1957). This provided the research workers in the field an unprecedented array of solar, geophysical and cosmic ray intensity data, enabling them to develop physical understanding of the nature of the magnetic field of the earth, sun and interplanetary space, and interaction of the galactic cosmic rays and solar particles with the interplanetary magnetic field (Webber, 1962; McCracken, 1962; Carmichael, 1962; Rao et al., 1963).

Cosmic ray data from stations situated at different geographic coordinates and at sea and mountain levels, is useful to perform systematic studies of some of the problems which are yet to be studied properly. Such a study may, obviously, give a better understanding of the modulating mechanism of cosmic-ray intensity and also throw light on various controversies existing about various aspects of the time variation problems studied in the past years. The fine features of the variations of cosmic ray intensity may be measured with a detector that yields a high counting rate, such as NM-64 monitor developed by Carmichael (1964). We have designed a similar equipment which gives a high counting rate and provides low background counts.

DESCRIPTION OF THE NEUTRON MONITOR

A neutron monitor is a combination of the local neutron producer, moderator, neutron detector and reflector. The geometry of the Aligarh neutron monitor is shown in Figures 1, 2 & 3. BF_3 proportional counters with diameter 2 inches, active length 36 inches and filled with enriched BF_3 gas (90% B^{10}) at 60 cm of Hg pressure are used to detect the thermal neutrons. The 2 inch thick lead Blocks are placed above, below and in between the neutron counters. Evaporation neutrons are produced by interactions of the nucleonic component with lead

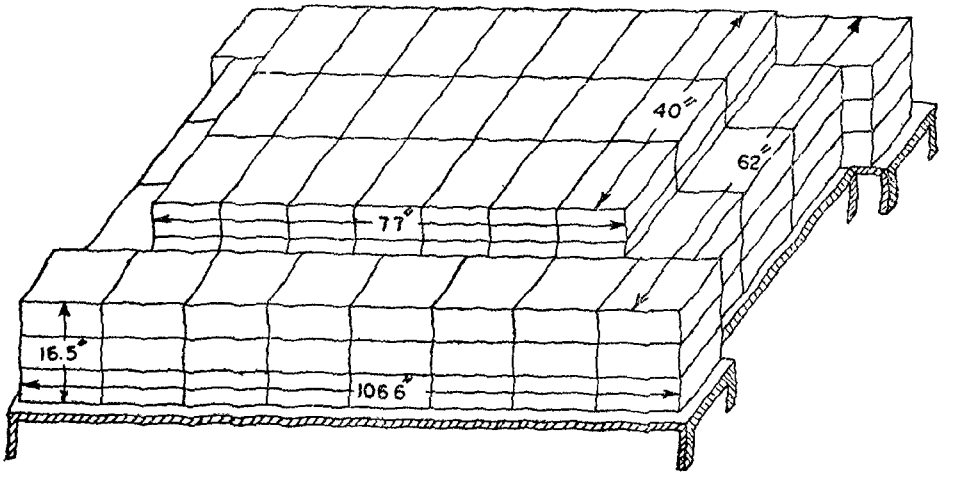

Fig. 1. Exterior view of the Neutron Monitor.

*Dept. of Physics, Aligarh Muslim University, Aligarh 202 001
**Applied Physics Section, Z.H. Engg. College, Aligarh 202 001
***Director, NCERT, Sri Aurovindo Marg, New Delhi 110 016

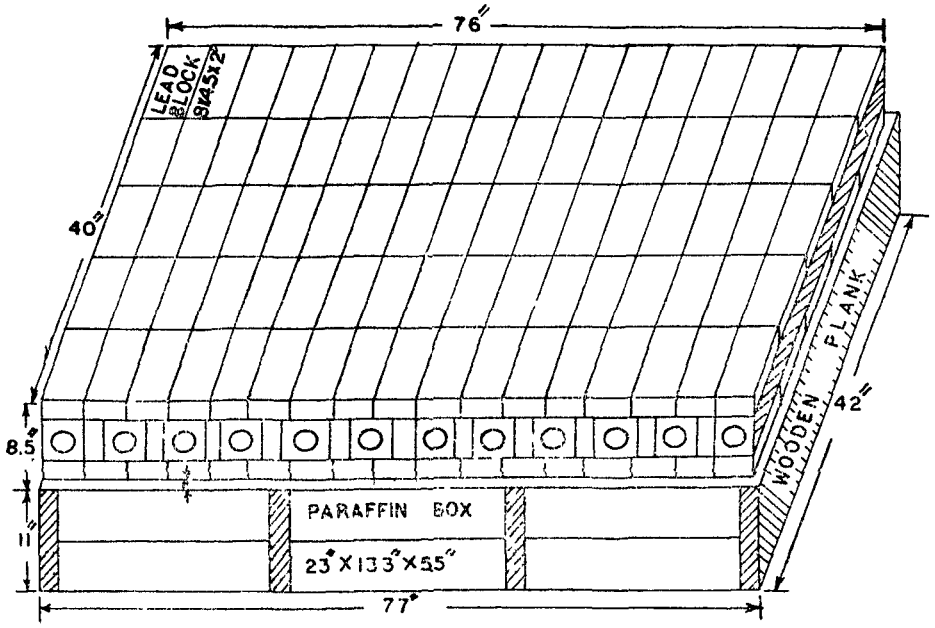

Fig. 2. Interior view of the Neutron Monitor.

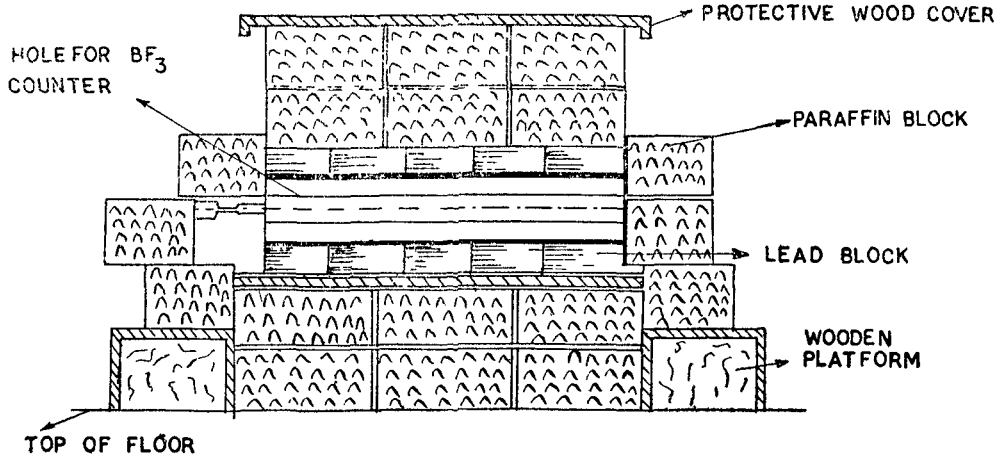

Fig. 3. Lateral view of the Neutron Monitor.

nuclei (Weisskopf, 1937). These locally produced evaporation neutrons are thermalized by 1.25 inch thick layer of paraffin placed around each counter as inner moderator. The 11 inch thick layer of paraffin surrounding the lead blocks and the counter assembly is used as a reflector to exclude the atmospheric neutrons from detection. The reflector also acts as scatterer for unwanted low energy neutrons produced in materials close to the neutron monitor.

ELECTRONIC CIRCUITRY

One module of the Neutron Monitor (Fig. 1) consists of 12 BF_3 counters. The output from 12 counters is divided into two sections each containing six counters. Each section is associated with its own independent electronic circuits. The block diagram of the whole electronic arrangement is shown in Fig. 4. The division of counters into two half sections provides a check on performance of the detecting system by comparing the counting rate from two half sections.

The amplitude of the output α-pulses from BF_3 counters is of the order of a millivolt. These pulses are amplified by a pre-amplifier whose gain is 10. In each section the output of two counters is connected to the input of a pre-amplifier. The output of 3-pre-amplifiers in each section, is fed to a pulse mixer circuit, the output of the pulse mixer is fed to a linear amplifier (ECIL Model No. 521). After sufficient amplification, the α-pulses are separated from much smaller background pulses by adding a discriminator in the output of the linear amplifier. The alpha-pulses obtained from the output of the discriminator circuit are scaled down with the help of a scaler and registered by an electromechanical recorder. Finally the cosmic ray nucleonic compo-

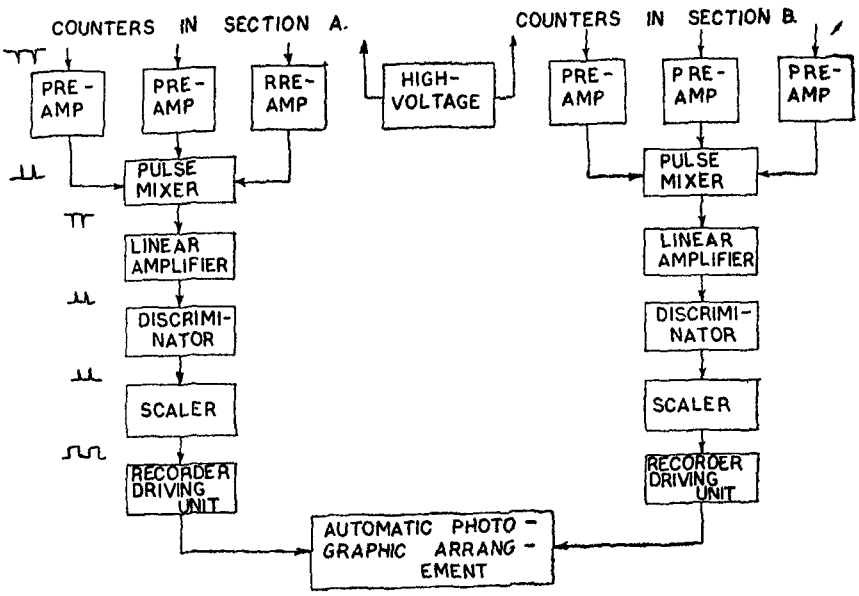

Fig. 4. Block diagram of the electronic apparatus.

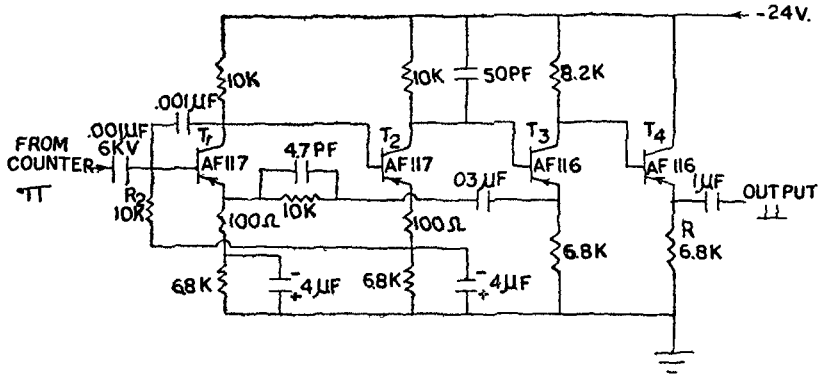

Fig 5. Pre-amplifier.

nent is photographed on 35 mm. film at an hourly interval by an automatic photographic arrangement. The properties and general description of the pre-amplifier, pulse mixer, discriminator, and scaling circuits are given below.

Pre-amplifier

The detailed diagram of the pre-amplifier with typical values of components used is shown in Fig. 5. The first two stages of this circuit have a feedback bias arrangement for current stabilization of both the stages. Resistance R_2 provides dc current feedback from emitter of transistor T_2 to the base of transistor T_1. The ac negative current feedback from the emitter of transistor T_3 to the emitter of Transistor T_1 provides wide frequency response and low distortion. We have used a fixed resistance R of value 6.8KΩ in the emitter follower for the last stage. This value of the resistance R provides minimum noise and distortion in the circuit.

Pulse Mixer Unit

The circuit diagram of the pulse mixer unit with the values of components used is shown in Fig. 6. Transistor T_1 and T_2 form an OR-gate with three inputs and one output. When a pulse of positive polarity exists at one or more of the inputs of the OR-gate, an output of the same polarity is obtained. This output-pulse of the OR-gate is amplified through a one stage common emitter amplifier T_3. The output stage T_4 is an emitter follower.

Discriminator Unit

Discriminator Unit, shown in Fig. 7, is employed to cut-off the pulses having height less than a preset discriminator bias voltage. It gives positive pulses at the output for all input pulses of positive polarity exceeding the present discriminator bias. The bias may be varied from 0.6 to 5.0 volts, by means of a panel mounted helical potentiometer.

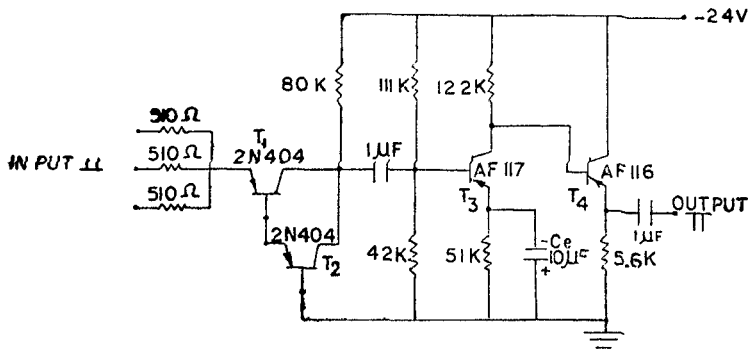

Fig. 6 Pulse mixer unit.

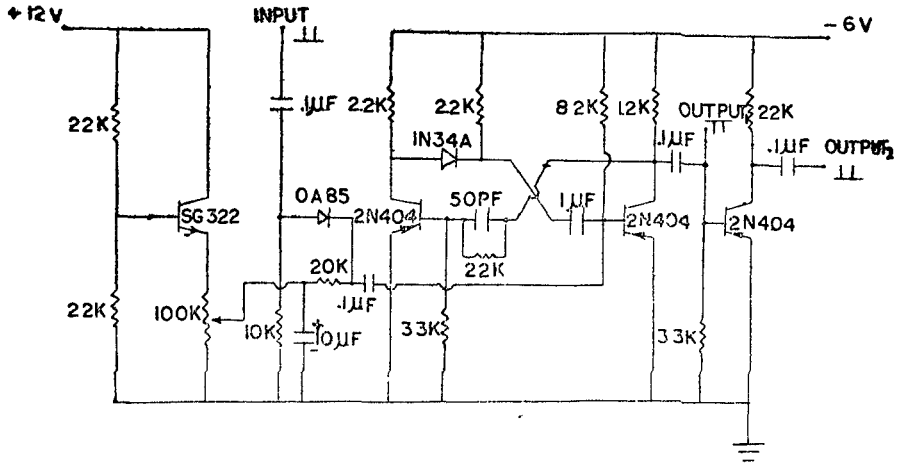

Fig. 7. Discriminator unit.

Scaling Unit

Scaling unit consists of eight binaries, which are identical. The detailed circuit diagram of a binary with typical values of the components used is shown in Fig. 8. The binary has facility of symmetric triggering by positive pulses at the bases of transistors T_1 and T_2.

All components in this scaling unit are very critical. The components which are to be given extra special consideration are the collector resistors which have to be within 5% of each other and the base and feedback resistors which have to be within less than 3% of each other.

The circuit can handle approximately 10^6 evenly spaced pulses per sec.

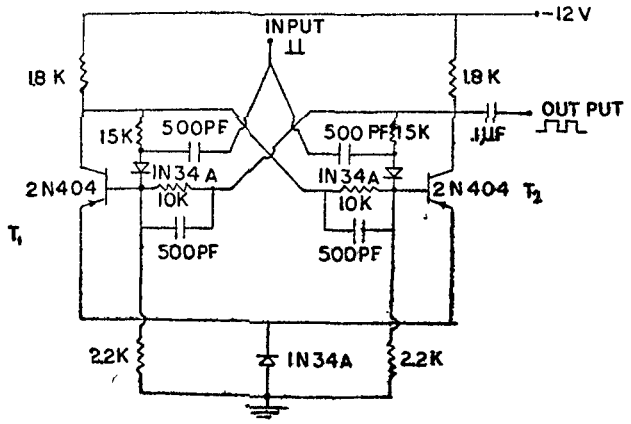

Fig. 8. Scaling binary.

Recorder Driving Unit

The circuit diagram of the recorder driving unit is shown in Fig. 9. In recorder driving unit, the output pulses of the last stage of the scaling unit are first fed to a monostable multivibrator (T_1 & T_2). The output pulses of the monostable multivibrator are used to operate the relay of electromechanical recorder connected in the collector arm of the power amplifier.

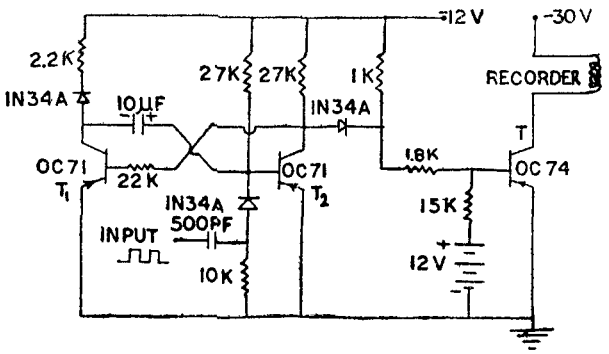

Fig. 9. Recorder driving unit.

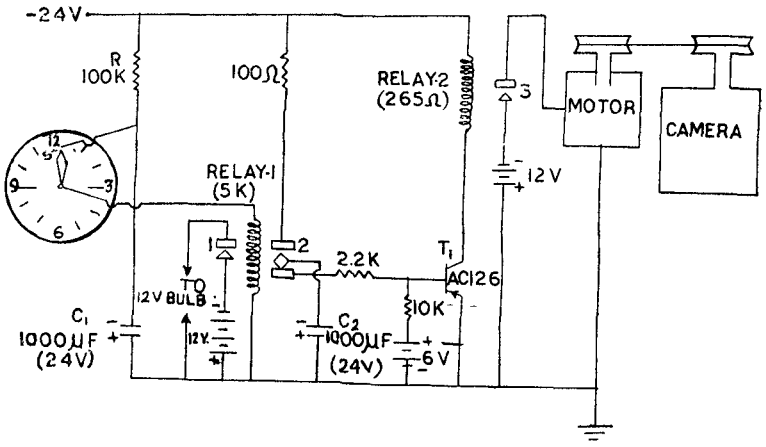

Fig. 10. Automatic photographic recording system.

Automatic Photographic Recording System

An automatic photographic recording system is shown in Fig. 10. It consists of a transistorized wall clock, an electronic circuit, a 1/20 HP motor and a 35 mm camera. The transistorized clock gives regular contacts after each hour. When the clock makes the contact S, the condenser C_1, which is initially charged, gets discharged through relay-1 making contacts 1 and 2. Contact 1 lights the bulbs (12 V DC) for 3 seconds and during this time the contact 2 charges the condenser C_2. Three seconds is the discharge time of the condenser C_1. When the condenser C_1 has been fully discharged, the contacts 1 and 2 break and the condenser C_2 now gets discharged giving negative pulse to the transistor T_1. This takes the transistor into conduction activating relay-2 and making the contact 3 which runs the motor for 12 secs., which is the discharge time of the condenser C_2.

When the bulbs light for 3 seconds a photograph of the reading of the electromechanical recorder showing the number of counts of the cosmic ray intensity, time, and date is taken by the 35 mm camera. Then, the motor runs for 12 seconds to roll the exposed part of the film and brings a fresh frame of the film in its position for the next exposure. This whole process is separated at hourly intervals and hourly data are preserved on the 35 mm films.

ACKNOWLEDGEMENT

The authors are grateful to Prof. M. S. Swami for his interest and extend their thanks to Dr. G. C. Upreti, Z. H. Engg. College, AMU, Aligarh, Dr. L. V. Sud, Department of Physics, Regional Engg. College, Kurukshetra, and Mr. S. K. Gupta for their helpful discussions. The authors wish to thank the Department of Atomic Energy, Government of India for grants which made this work possible.

REFERENCES

1. SIMPSON (JA) et al. Phys. Rev. **90**; 1953; 44-50 and 934-50.
2. SIMPSON (JA). Ann. I. G. Y. **4**, Part 4; 1957. Pergamon Press, London, P 351-73.
3. WEBBER (WR). Prog. in Elem. Particles and Cosmic Ray Physics. **4**, 1962. North-Holland Publ. Co., Amsterdam. P 77-237.
4. MCCRACKEN (KG). J. Geophys. Res. 67; 1962; 423-58.
5. CARMICHAEL (H). Space Sci. Rev. **1**; 1962; 28-35.
6. RAO (UR), MCCRACKEN (KG) and VENKATESAN (D). J. Geophys. Res. **68**; 1963; 345-69.
7. CARMICHAEL (H). Cosmic Rays, IQSY Instruction Manual No. 7; 1964. IQSY Secretariat, London.
8. WEISSKOPF (VF). Phys. Rev. **52**, 1937; 295-303.

REPRINTED FROM
PROCEEDINGS OF THE NATIONAL ACADEMY OF SCIENCES, INDIA
SECTION A, VOL. XLVII. PART II. 1977

Solar Flare Location Effect on the Spectral Characteristic of the Diurnal Anisotropy of Cosmic Ray Intensity

R. S. Yadava, Santosh Kumar and T. N. Naqvi

NATIONAL ACADEMY OF SCIENCES, INDIA
ALLAHABAD

PROC. NAT. ACAD. SCI. INDIA, 47(A), II, 1977

SOLAR FLARE LOCATION EFFECT ON THE SPECTRAL CHARACTERISTICS OF THE DIURNAL ANISOTROPY OF COSMIC RAY INTENSITY

R. S. YADAVA, SANTOSH KUMAR, *Cosmic Rays and Space Physics Group, Physics Department, A. M. U., Aligarh*

AND

T. H. NAQVI, *Applied Physics Section, Z. H. College of Engg. and Technology, A. M. U., Aligarh*

ABSTRACT

The spectral parameter of the diurnal anisotropy of cosmic ray intensity are studied separately for days where the solar flares have occurred on the western limb as well as on the eastern limb of the solar disc for both nucleonic as well as mesonic components of the cosmic rays. It is observed that the diurnal amplitude of the cosmic ray intensity in space is larger for days where solar flares have occurred on the western limb of the solar disc as compared to the days where solar flares have occurred on the eastern limb of the solar disc. This is true in both nucleonic as well as mesonic components of the cosmic ray intensity.

The average value of the direction in space, of diurnal anisotropy in local asymptotic time for various stations is almost same and is observed at around the same hours for flares which occur on the western as well as eastern limb of the solar disc. When these results are compared with the direction of the diurnal anisotropy in space on quiet days, it is found that the direction of the diurnal anisotropy on days where solar flares have occurred on the western limb as well as eastern limb of the solar disc, is earlier in comparison to quiet days. This phase shift towards earlier hours is about three hours for nucleonic as well as mesonic components of the cosmic ray intensity. The variation of the rigidity exponent β observed on different types of days for the nucleonic component has also been discussed.

INTRODUCTION

During last few years, our knowledge of solar flare production of cosmic rays has increased largely. The effects, associated with the solar flares, observed at ground *e.g.* large solar flux increases and large increase in cosmic ray intensity have been studied from time to time by several workers. It has been observed that those solar flares which occur on, or near the western limb of the solar disc show the following effects.

(*i*) the most rapid rise to maximum intensity,

(*ii*) the most intense anisotropies,

(*iii*) on the average, the greatest particle fluxes,

(*iv*) very short flight times for the cosmic rays from the sun to earth and,

(*v*) on those occasions for which the data have been good enough, the first cosmic rays have been observed to arrive at the earth from a direction roughly in the plane of the ecliptic.

TABLE 1

List of stations whose data have been used

S. No.	Station	Type of the Monitor*	Geographic Coordinates Latitude (in deg.)	Longitude (in deg,)	Cut-off rigidity (in GV)
1	Alma Ata	N	43.20	76.94	6.69
2	Berkeley	N, M	37.86	237.70	4.50
3	Chicago	N	41.83	272.33	1.72
4	Churchill	N, M	58.75	265.91	0.21
5	Climax	N	39.37	253.82	3.03
6	Deep River	N	46.10	282.50	1.02
7	Gottingen	N	51.52	9.93	3.00
8	Hermanus	M	-34.42	19.22	4.90
9	Kiruna	M	67.83	20.43	0.54
10	Kodaikanal	N	10.23	77.46	17.47
11	Lae	M	-6.73	147.00	15.52
12	Leeds	N	53.82	358.45	2.20
13	Lincoln	N	40.82	263.32	2.22
14	Macquarie	M	-54.50	158.90	0.55
15	Makapuu pt.	M	21.30	202.35	13.23
16	Mawson	N, M	-67.60	62.88	0.22
17	Mt. Washington	N	44.30	288.70	1.24
18	Mt. Wellington	N	-42.92	147.24	1.89
19	Ottawa	N, M	45.40	284.40	1.08
20	Resolute	N, M	74 69	265.09	<0.05
21	Rome	N	41.90	12 52	6.31
22	Sulphur Mt.	N, M	51.20	244.39	1.14
23	Uppsala	N	59.85	17.92	1.43
24	Yakutask	N	62.02	129.72	1.70
25	Zugspitze	N, M	47.42	10.98	4.24

*N = Neutron, M = Meson.

All these facts have led to the picture that lines of force of the interplanetary magnetic field stretch in a relatively well ordered fashion from near a sunspot which is near the western limb to the vicinity of the earth. This provides an easy route for the cosmic rays to follow in order to reach the earth, which is in general agreement with the concept that the solar wind will stretch out the solar magnetic fields to form lines of force in the form of an Archimedes spiral. However, the solar flare location effect on the daily variation of cosmic ray

intensity has not been given any attention so far. Therefore, we have analysed the data of the ground based neutron and meson monitors to study the solar flare location effect on the diurnal anisotropy of the cosmic ray intensity.

TABLE 2

The total number of days used in different groups.

	Group	Number of days
(a)	Quiet Days	75
(b)	Western Limb Solar Flare Days	69
(c)	Eastern Limb Solar Flare Days	66

EXPERIMENTAL DATA AND ANALYSIS

The stations, whose neutron and meson monitor data is used in the analysis for the period 1957–58, are given in table 1. The pressure corrected data of the neutron and meson have been used in the present analysis. The data is not corrected for the temperature effect. Data for days where the solar flares have occurred on the western limb and those on which they are observed on the eastern limb are averaged separately after having applied the trend correction. Solar flares with importance greater than two have not been considered because of the fact that during the period under consideration there is only one flare with importance greater than two. And if it is considered, it will influence the results towards the side in which it has occurred. The averaged data is subjected for the harmonic analysis (Yadava and Naqvi, 1973) and the values of the amplitude and phase of the first harmonic component of the neutron and meson intensities for different stations are analysed. Days of large worldwide variations, large solar flux increases and large Forbush decreases are excluded from the analysis. The amplitude and phase of the diurnal anisotropy obtained at ground are corrected for the geomagnetic effects (McCracken *et al.*, 1965) using the method developed by Rao *et al.* (1963), to obtain the anisotropy vector in space. The analysis has been extended on quiet days for the comparison among the anisotropy vectors on quiet days and the days where solar flares have occurred on the western and the eastern limb of the solar disc. Finally, the rigidity exponent, β has been calculated by imposing the condition that the variance among the various values of anisotropy vectors estimated from observations at different stations is minimum.

RESULTS AND DISCUSSION

The average amplitude and the direction of the diurnal anisotropy of cosmic ray intensity as observed with the neutron and meson monitors has been plotted in figs. 1(A) and 1(B) respectively for the period 1957–1958, for the quiet days and for the days where the solar flares have occurred on the western and the eastern limbs of the solar disc. The one sigma standard errors have been shown by circles in the figures. It is apparent from the figure 1(A) that the average amplitude of the diurnal anisotropy, for nucleonic component on the days where solar flares have

occurred on the western limb of the solar disc is larger in comparison to the days where solar flares have occurred on the eastern limb of the solar disc. However, the amplitude of the diurnal anisotropy on the days for which the solar flares have occurred on the eastern limb of the solar disc is of the same order as it is observed on quiet days.

It is also apparent from the figure 1(A) that for the nucleonic component the average direction of the diurnal anisotropy in space in local asymptotic time is almost same on the days where the solar flares have occurred on the western as well as eastern limbs of the solar disc. However, if these results are compared with the direction of the diurnal anisotropy in space on quiet days, it is found that the direction of the diurnal anisotropy on days where solar flares have occurred on the western limb as well as eastern limb of the solar disc is earlier in comparison to quiet days. This phase shift towards earlier hours has been observed about three hours for the nucleonic component.

The above results for the amplitude and the direction of the diurnal anisotropy on quiet days and the days where the solar flares occur on the western and the eastern limbs of the solar disc are also supported by the meson monitor observations, as is apparent from the figure 1(B). These results are true to a large extent for the individual stations, given in table 1, as well, which have not been illustrated here.

Apart from the amplitude and hour of maximum, the source of diurnal variation is also characterised by the rigidity spectrum. In case of the corotational mechanism, no rigidity dependence is expected. Thus, a study of the rigidity dependence may yield valuable extra information.

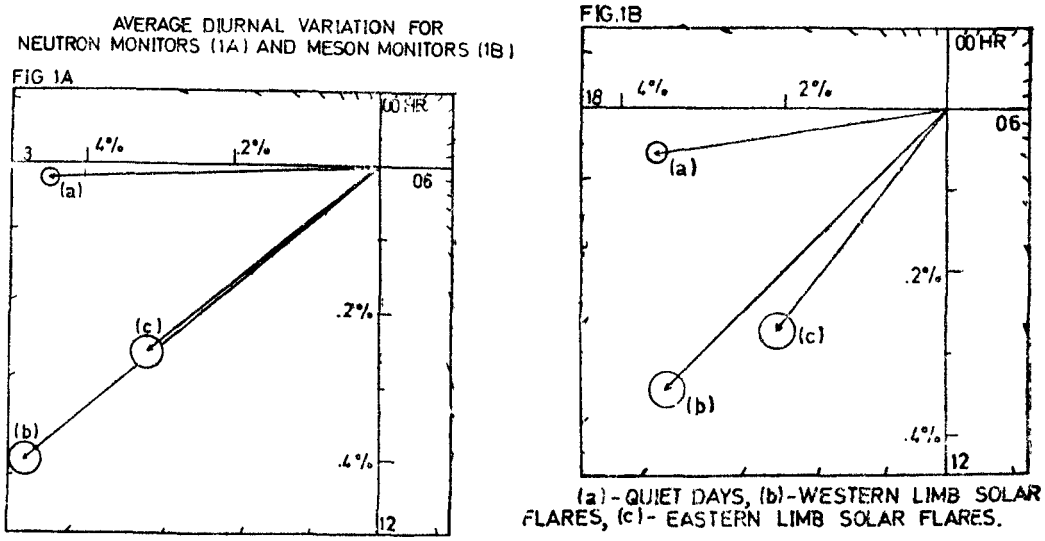

Fig. 1. The diurnal vectors along with their one sigma error circle, observed with the neutron monitors (A) and meson monitors (B) on quiet days and days where the solar flares occur on the western and the eastern limbs of the solar disc.

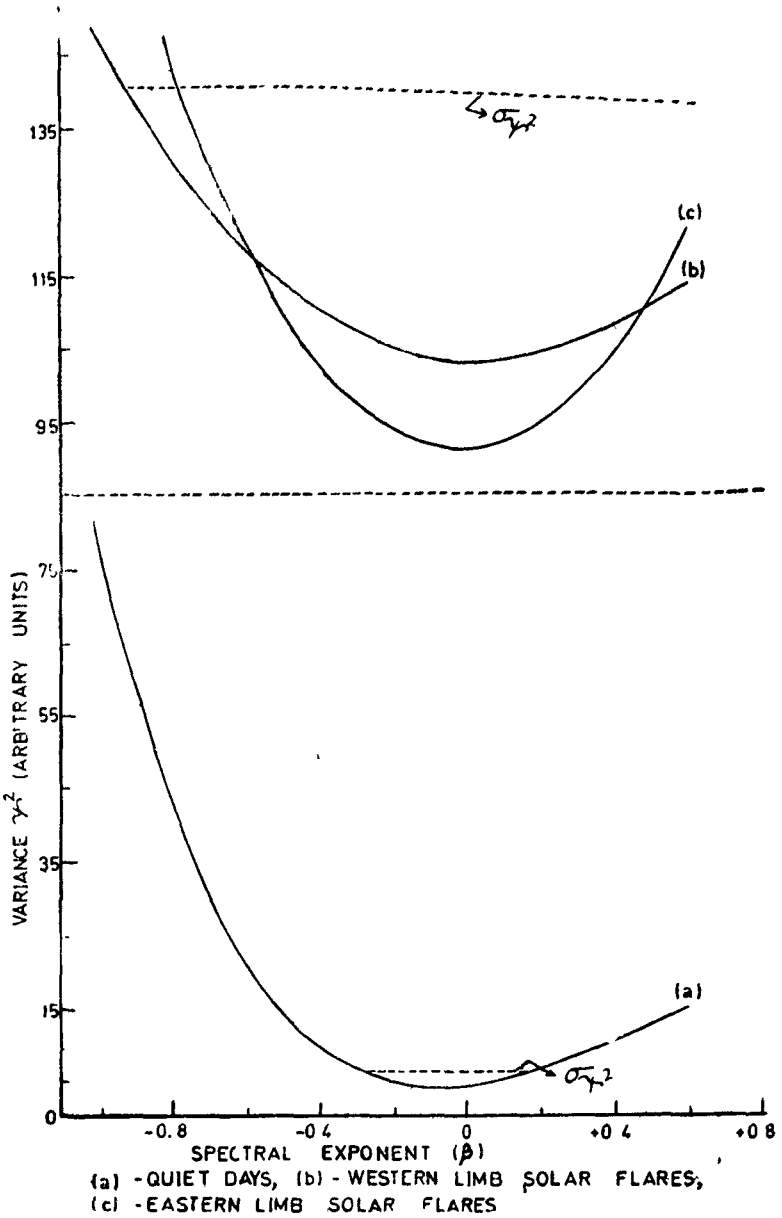

Fig. 2. The variance (ψ^2) versus β. The dashed lines show one sigma standard error of the minimum variance.

We have calculated the variance (ψ^2) among the various observed diurnal vectors in space using the neutron monitors data for the available stations, separately for the quiet days and the days where the solar flares have occurred on the western and the eastern limbs of the solar disc. Figure 2(a) shows that the minimum variance for quiet days occurs for $\beta \simeq 0 \pm 0.2$ (corresponding space values of R_1 and ϕ_1 are equal to $0.45 \pm 0.01\%$ and 17.8 ± 0.2 hours respectively). These characteristics of the corotational anisotropy are in agreement with the predictions of the simple convection-diffusion theory. However, the variation in the values of the variance obtained for the days where the solar flares have occurred on the western and the eastern limbs of the solar disc is very large (fig. 2b and c) which shows that β is indeterminable on these days. Therefore, the analysis indicates that superimposed on corotational anisotropy there is an additional component operating during the days of solar flares with $\beta \neq 0$. The characteristics of this superimposed anisotropy is expected to be defined by carrying a rigorous analysis with the data of larger number of stations and for the flares occurred during different periods of solar activity. Thus, the exact mechanism causing these needs to be further explored.

Acknowledgements

The authors are grateful to Prof. M. Z. Rahman Khan, Head, Physics Department, A.M.U, Aligarh-202001, for providing facilities during this work and extend their thanks to Prof. S. P. Agrawal, Vikram Space Physics Centre, A.P.S. University Rewa (M.P.)-486001 for his exceedingly helpful discussions. The financial support rendered by D. A. E., Government of India is gratefully acknowledged.

References

McCracken, K. G., Rao, U. R., Fowler, B. C., Shea, M. A. and Smart, D. F. (1965). *IQSY Inst. Manual* No. 10.

Rao, U. R., McCracken, K. G. and Venkatesan, D. (1963). *J. Geophys. Res.*, **68**, 345.

Yadava, R. S. and Naqvi, T. H. (1973). *Technical Note* 1. (A. M. U., Aligarh), **14**.

REPRINTED FROM
PROCEEDINGS OF THE NATIONAL ACADEMY OF SCIENCES, INDIA
SECTION A, VOL. XLVII PART IV, 1977

DAILY VARIATION OF COSMIC RAY INTENSITY

Santosh Kumar and R. S. Yadava

NATIONAL ACADEMY OF SCIENCES, INDIA
ALLAHABAD

PROC. NAT. ACAD. SCI., INDIA, 47(A), IV, 1977

DAILY VARIATION OF COSMIC RAY INTENSITY

SANTOSH KUMAR AND R. S. YADAVA, *Cosmic Rays and Space Group*
Physics Deptt., A. M. U., Aligarh

ABSTRACT

The characteristics of the daily variation of cosmic ray intensity on different types of days has been studied by using the data of neutron monitors. It is observed that the phase of the diurnal anisotropy is invariant on quiet days and disturbed days without magnetic storms during the period from 1957-1970. Its direction in space is observed as (18 ± 1) hr. local asymptotic time. However, the phase of the diurnal anisotropy has been found to shift towards earlier hours on magnetic storms days with the increased value of the A_p - index in comparison to quiet days and disturbed days without magnetic storms. The behaviour of A_p - index, definitive sunspot numbers and solar flux at 2800 MH_z is studied during the same period. It is found that A_p - index has the better correlation with the different spectral parameter of the diurnal anisotropy.

INTRODUCTION

McCracken and Rao (1965) showed an impressive agreement between the observed diurnal variation of the cosmic radiation derived from neutron monitor data and that predicted by the Axford (1965), Parker (1964) model. They concluded that on yearly average basis the diurnal anisotropy during the period 1957-65, was invariant. However, the results of Duggal *et al.* (1967), based on neutron monitor data for the same period, indicated that the mean diurnal anisotropy was not invariant. On yearly average basis, relatively large variations of the diurnal anisotropy are observed by Forbush and Venkatesan (1960) in the ionization chamber data for the period 1937 to 1959. Similarly, a large variability in various spectral parameters of the diurnal anisotropy on day-to-day basis has also been reported by other workers (Patel *et al.* (1968), Pomerantz and Duggal (1971)).

The study of various spectral parameters of the daily variation on magnetically quiet and disturbed days during period of different solar activity provides a way for understanding the mechanisms that produce the diurnal anisotropy. In this paper, the characteristics of the diurnal anisotropy on magnetically different types of days is studied. The basic choice for the selection of days is being A_p - index and other indices have been taken on those particular days. An attempt has been made to establish the relationship among the parameters of the diurnal anisotropy and the solar geomagnetic activity parameters.

EXPERIMENTAL DATA AND ANALYSIS

The data of the neutron monitors, corrected for the meteorological effects, for the stations which are given in table 1 are used for the analysis. The period 1957-70 is divided mainly into three categories, (*i*) minimum solar activity period (1964-65) ; (*ii*) maximum solar activity periods (1957-58 and 1968-70) ; and (*iii*) transition period of solar activity (1966-67). For every month five most quiet days and five disturbed days (Pandey *et al.* (1971) are selected separately. The disturbed days are further divided into two groups. First—the disturbed days with magnetic storms

TABLE 1

List of stations used to derive diurnal anisotropy vectors

Station Name	Geomagnetic Coordinates		Geographic Coordinates		Altitude H (Meters)	Vertical Cutoff Rigidity (GV)
	N. Latitude	E. Longitude	N. Latitude	E. Longitude		
Ottawa	56°.8	351°.1	45°24′	284°.4	57*	1.08
Deep-River	57°.5	358°	46°06′	282°.5	145	1.02
Sulphur-Mountain	58°.2	300°.3	51°.2	244°.39	2283	1.14
Resolute	82°.9	289°.3	74°.43′	265° 02	17	0.00

*Before December 1960, H = 101 M

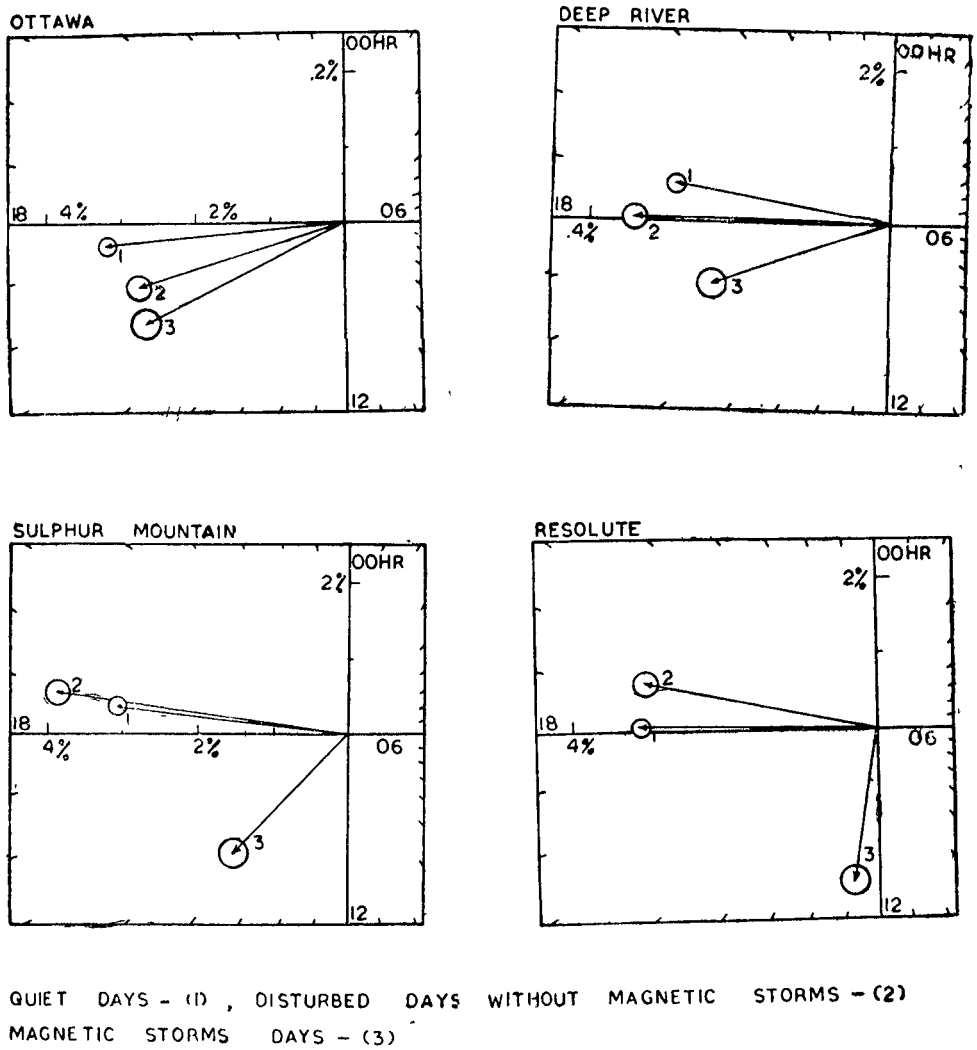

Fig. 1. The observed average diurnal vectors along with their one sigma error circle for the minimum solar activity period from 1964-65.

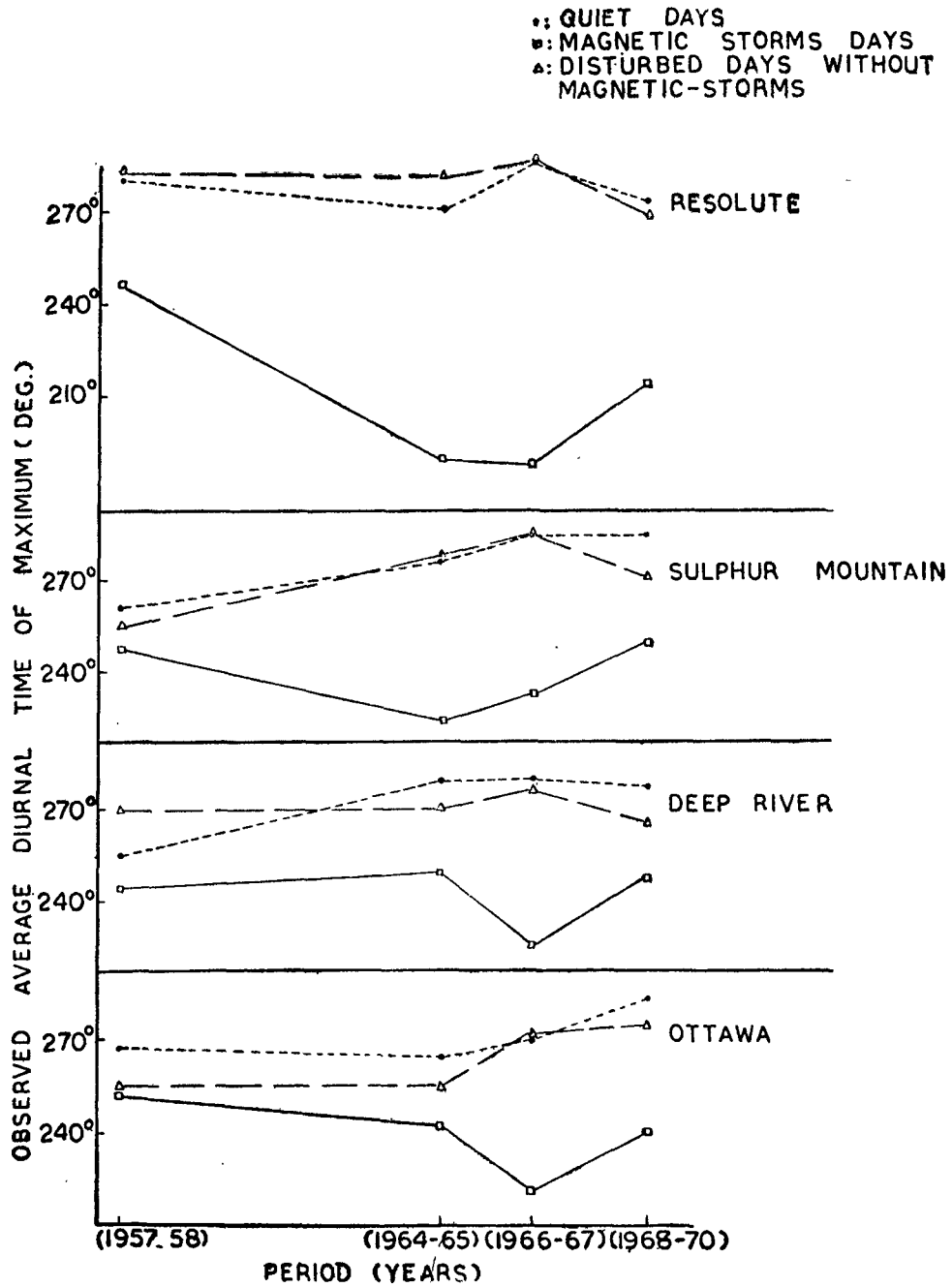

Fig. 2. The observed average diurnal time of maximum (ϕ_1) in deg. plotted for different periods of solar activity from 1957-70.

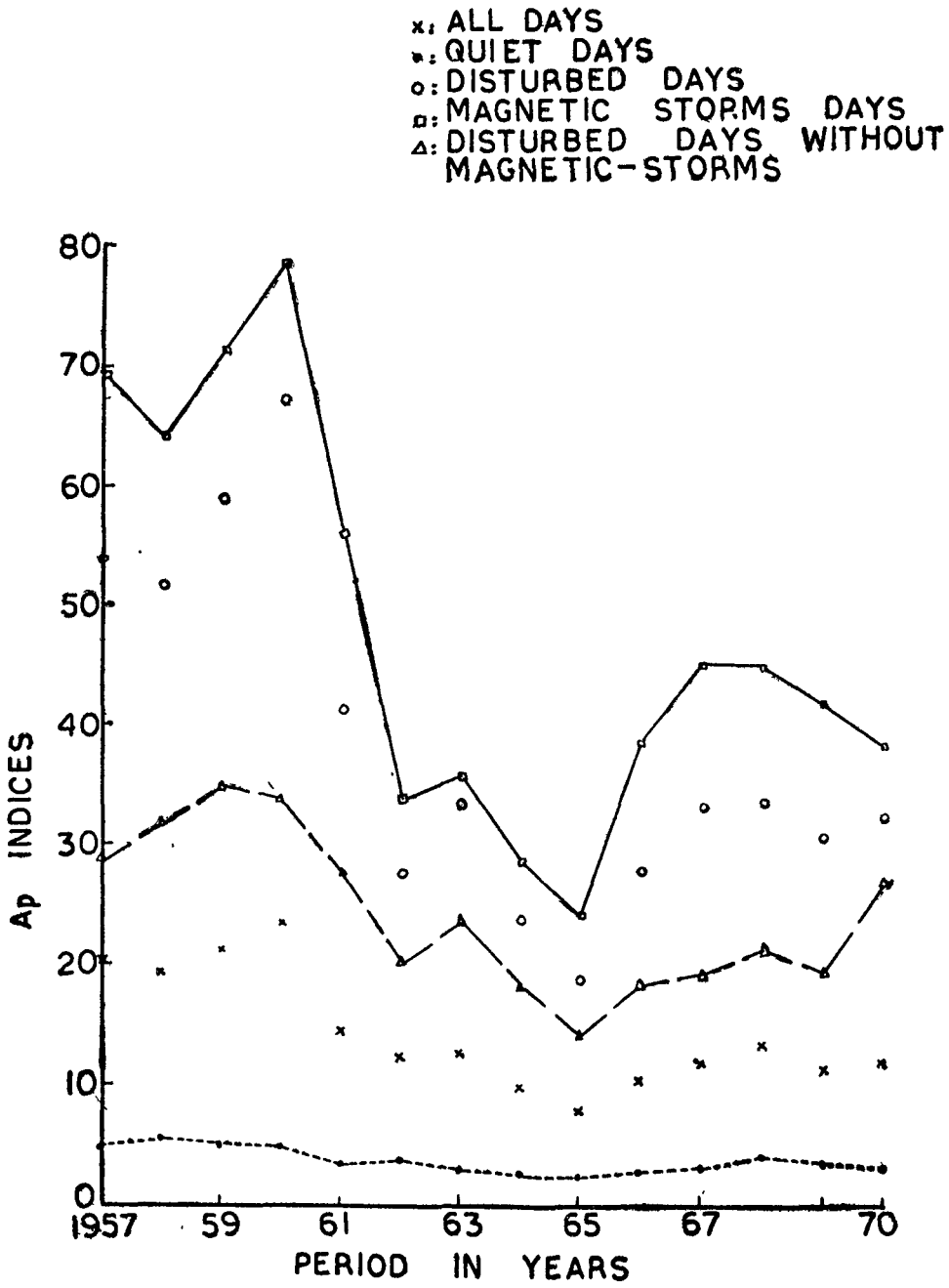

Fig. 3. (*a*) The yearly average values of A_p - indices for different types of days plotted for each year from 1957-70.

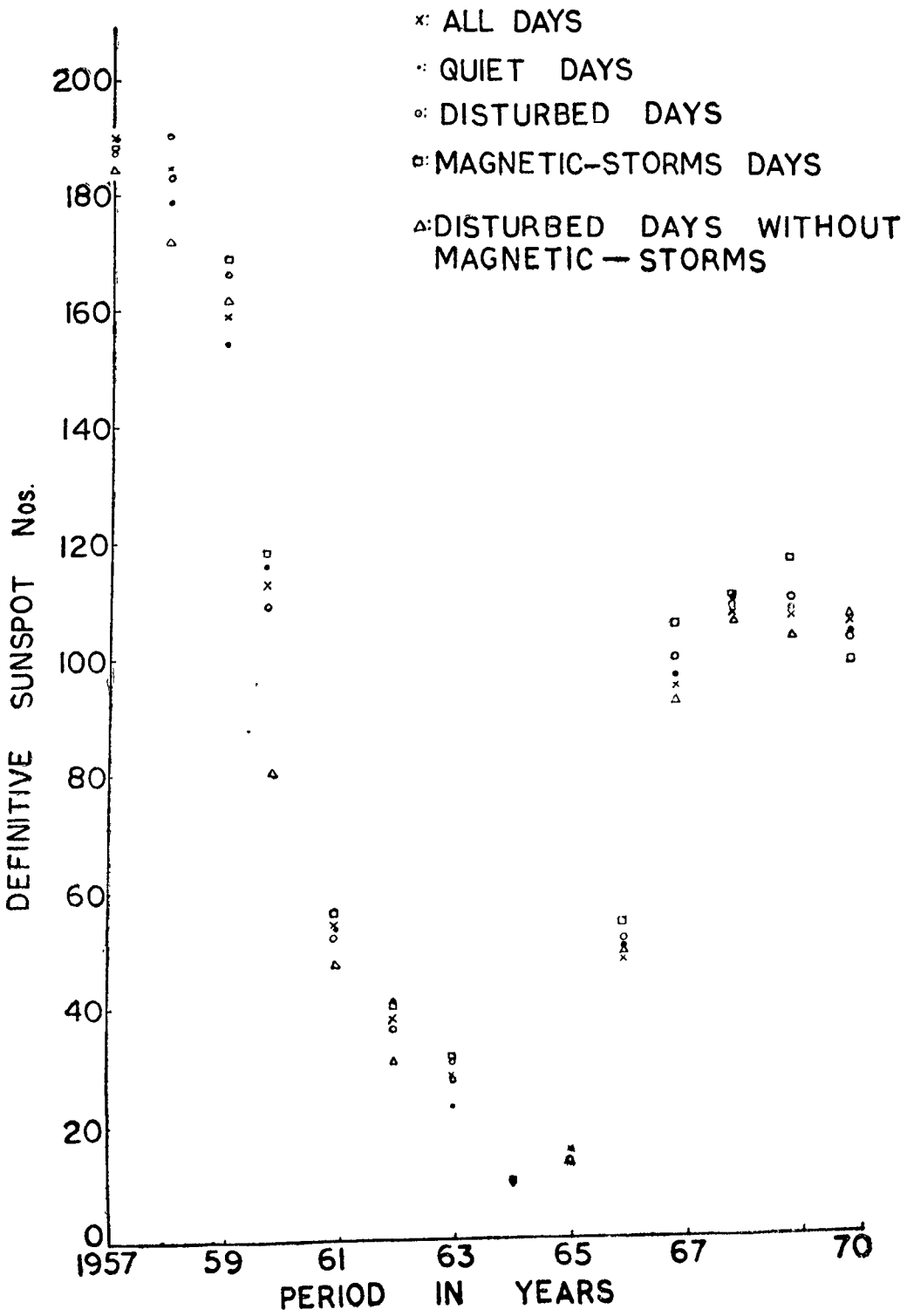

Fig. 3. (*b*) The yearly average values of definitive sunspot numbers for different types of days plotted for each year from 1957-70.

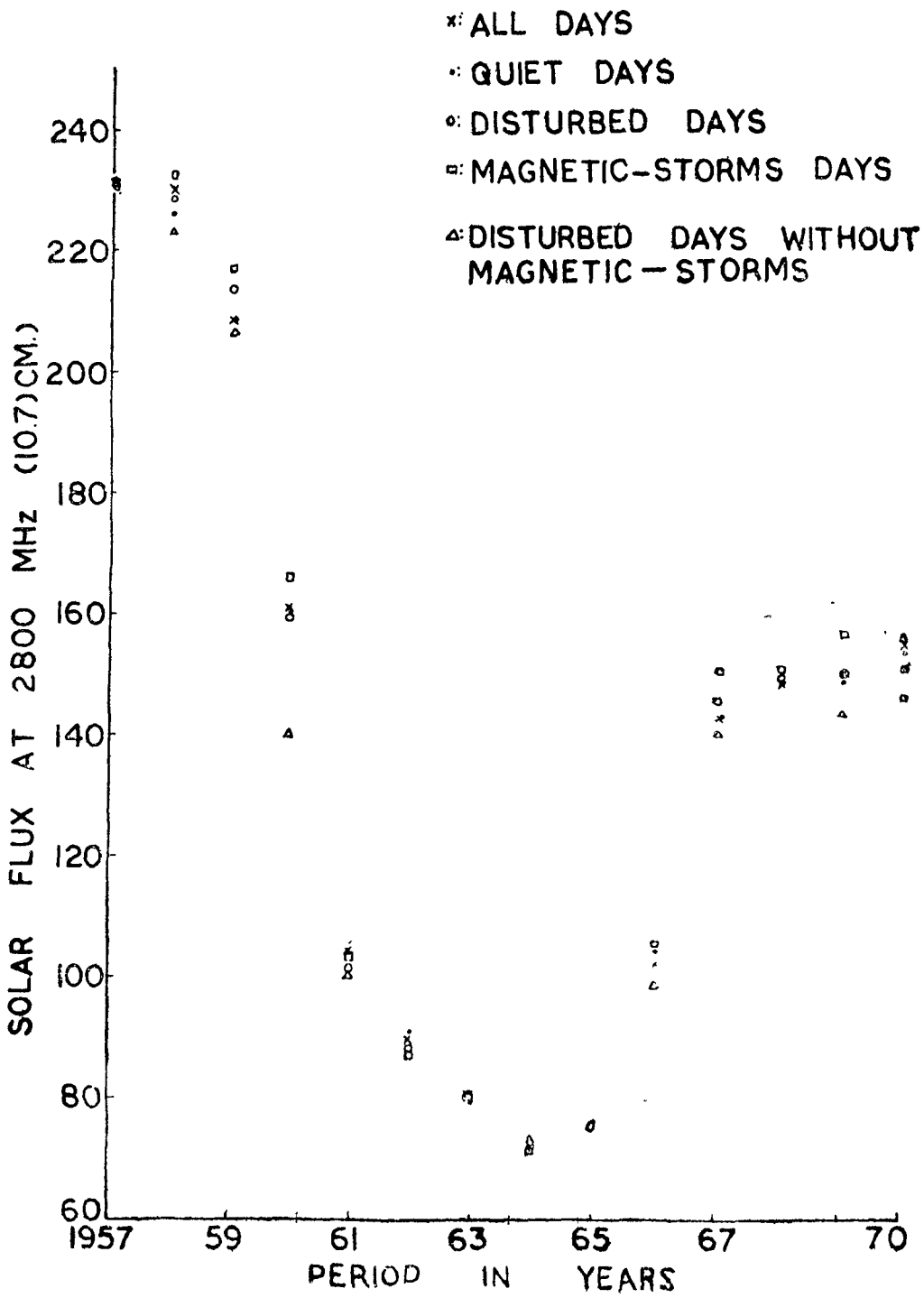

Fig. 3. (c) The yearly average values of solar flux at 2800 MHz for different types of days plotted for each year from 1957-70.

with different degree of the activity (or magnetic storms days), and second—the disturbed days without magnetic storms. The Forbush decrease days are removed from the analysis. The long term trend has been removed by the method of trend correction (Yadava and Naqvi, 1973). The trend corrected data is subjected for harmonic analysis and the average values of the amplitude and phase of the first harmonic component of the neutron intensity for different stations are analysed. To obtain the anisotropy vector in space, the observed daily variation parameters for different stations are corrected for the effect of the geomagnetic bending and the width of the asymptotic cone of a detector (Rao, *et al.*, 1963) for an energy independent spectrum, $\beta=0.0$ (McCracken *et al.*, 1965). Finally, A_p - indices, definitive sunspot numbers (Pandey *et al.*, 1971) and solar flux at 2800 MH_z for the period 1957–70 have been plotted to observe their relationship with the various spectral parameters of the diurnal anisotropy.

Results and Discussion

The average diurnal variation of cosmic ray intensity for minimum solar activity period has been plotted in figure 1 along with their one sigma standard errors which are shown by circles. From the figure 1, it is apparent that the diurnal time of maximum has significantly changed to earlier hours in all the stations on magnetic storms days in comparison to quiet days and disturbed days without magnetic storms during this period. This is found to be true also during the period of maximum solar activity and the transition period, as illustrated in figure 2. These results are in complete agreement with the earlier findings (Sandstrom, 1965).

From the figure 2, it is apparent that the phase of the diurnal anisotropy is invariant, on quiet days and disturbed days without magnetic storms, during the maximum solar activity periods, minimum solar activity period and the transition period of solar activity, and it is in the direction of $(270 \pm 15°)$ or (18 ± 1) hr local asymptotic time. This result is in accord with the findings of McCracken and Rao (1965) on yearly average basis.

It is also apparent from the figure 1 that the diurnal amplitude on quiet days and disturbed days without magnetic storms is almost the same during the minimum solar activity period. But the result of significance is that the diurnal amplitude is smaller on the magnetic storms days, except Ottawa where it is almost same, in comparison to quiet days and disturbed days without magnetic storms.

From the pattern of the curves in figures 3 (*a*), 3 (*b*) and 3 (*c*), presenting the data of A_p - indices, sunspot numbers and solar flux at 2800 MH_z for the period 1957–70 for all days and on different types of days discussed earlier, it is observed that the magnitude and the nature of the behaviour of solar activity in terms of sunspot numbers and solar flux at 2800 MH_z is almost similar on different types of days throughout the period under consideration. While, in case of A_p - index, the nature of the behaviour of A_p - indices is almost similar on different types of days, and its magnitude is large both on magnetic storms days and disturbed days without magnetic storms as compared to the quiet days. But the magnitude at magnetic storms days is very large as compared to quiet days as well as disturbed days without magnetic storms.

An attempt has been made to establish the validity of the convection-diffusion theory for the period under consideration In the absence of the solar wind velocity and interplanetary magnetic field direction data, the problem has been approached indirectly. Agrawal and Singh (1975) have pointed out the likely association of

A_p - index with the convective and diffusive vectors. It is expected that the distribution of diurnal vectors for various values of A_p will remain the same, if the interplanetary conditions do not change drastically.

The long term change in the diurnal variation of the cosmic ray intensity has been explained by Forbush (1973) as due to the superposition of a 20-year wave on the corotational anisotropy. It is therefore, expected to observe a continuous and systematic change in the diurnal time of maximum. Our results based on the neutron monitor observations with constant diurnal time of maximum during the period 1957-70, on quiet days and disturbed days without magnetic storms, completely disagree with the above expectation.

On the other hand, Quenby and Hashim (1969) have suggested the possibility of outward radial streaming (from 12-hour direction) in the solar system by assuming a symmetrical rising density gradient away from the plane of ecliptic. This will effectively change the corotational streaming from 18-hour direction to the earlier hours, for example, in case of magnetic storms days in comparison of quiet days and disturbed days without magnetic storms.

From the present set of the observed average diurnal vectors and with the increasing trend in the value of A_p - index from 1957-70 on magnetic storms days in comparison to quiet days and disturbed days without magnetic storms, it may be speculated that an increase in the average value of A_p - index might have increased the interplanetary magnetic field fluctuations thereby increasing (K_1/K_{11}) which reduces the diffusive vector accompanied by a decrease in diurnal amplitude on magnetic storms days. An increase in the average value of A_p - index may also increase the solar wind velocity thereby increasing the convective vector which increases the value of diurnal amplitude. It may also be noted that if both of them operate simultaneously, the diurnal amplitude may remain constant.

Conclusion

From the foregoing observational results and discussion it is concluded that—

(*a*) the phase of the diurnal anisotropy has been found to shift towards earlier hours on magnetic storms days with the increased value of the A_p - index in comparison to quiet days and disturbed days without magnetic storms, during the period from 1957-70.

(*b*) the phase of the diurnal anisotropy is invariant on quiet days and disturbed days without magnetic storms during the period from 1957-70. Its direction in space is observed as (18 ± 1) hr local asymptotic time. This is in complete agreement with the predictions of convection diffusion theory.

(*c*) during the minimum solar activity period, the diurnal amplitude in observed to be smaller on magnetic storms days in comparison to quiet days and disturbed days without magnetic storms.

(*d*) out of the three geophysical parameters, *viz.*, A_p - index, definitive sunspot numbers, and solar flux at 2800 MH_z ; the A_p - index is expected to have the better correlation with the different spectral parameters of the diurnal anisotropy.

Acknowledgements

The authors are grateful to Prof. M. Z. Rahman Khan, Head, Physics Department, A.M.U., Aligarh, for providing facilities during this work and extend their thanks to Prof. S. P. Agrawal, Vikram Space Physics Centre, A.P.S. University, Rewa (M. P.) and Dr. G. Subramanian, P.R.L., Ahmedabad, for their exceedingly helpful discussions. The financial support rendered by D.A.E., Government of India is gratefully acknowledged.

References

Agrawal, S. P. and Singh, R. L. (1975). *Time variation of the characteristics of the diurnal anistropy of cosmic radiation*, Paper presented to the 14th Inter. Conf. on Cosmic Rays, Munich, West Germany.

Axford, W. I. (1965). *Planetary Space Sci.*, **13**, 115.

Duggal, S. P., Pomerantz, M. A. and Forbush, S. E. (1967). *Nature*, **214**, 154.

Forbush, S. E. and Venkatesan, D. (1960). *J. Geophys. Res.*, **65**, 2213.

Forbush, S. E. (1973). *J. Geophys. Res.*, **78**, 7933.

McCracken, K. G. and Rao, U. R. (1965). *Proc. 9th Inter. Conf. on Cosmic Rays (London)* **1**, 213.

McCracken, K. G., Rao, U. R., Fowler, B. C., Shea, M. A. and Smart, D. F. (1965). *IQSY Inst. Manual* No. 10.

Parker, E. N. (1964). *Planetary Space Sci.*, **12**, 735.

Patel, D., Sarabhai, V. and Subramanian, G. (1968). *Planetary Space Sci.*, **16**, 1131.

Pomerantz, M. A. and Duggal, S. P. (1971). *Space Sci. Rev.*, **12**, 75.

Pandey, V. K., Aggarwal, S. and Mahajan, K. K. (1971). *A catalogue of Solar Geophysical Data from* 1957-70 (N. P. L., New Delhi).

Quenby, J. J. and Hashim, A. (1969). *Planetary Space Sci.*, **17**, 1121.

Rao, U. R., McCracken, K. G. and Venkatesan, D. (1963). *J. Geophys. Res.*, **68**, 345.

Sandstrom, A. E. (1965). *Cosmic Ray, Physics* (North Holland Pub. Co., Amsterdam), 240.

Yadava, R. S., and Naqvi, T. H. (1973). *Technical Note* No. 1 (A. M. U., Aligarh), 14.